THE UNIVERSITY OF BRIGHTON, SCHOOL OF PHARMACY AND BIOMOLECULAR SCIENCES

HIGHLY-EFFICIENT MORPHOGENS FOR GUIDED ANGIOGENESIS

Maria Elena Verdenelli

A thesis submitted in partial fulfillment of the
requirements of the University of Brighton
for the degree of Doctor of Philosophy

January 2018

In conjunction with

ABSTRACT

Coronary artery disease and stroke are leading causes of mortality in Europe, resulting in a loss of function of the affected tissue. One of the challenges is to restore the myocardium tissue functionality using growth-factors mimicking peptides to stimulate the development of pre-existing blood vessels to enhance tissue regeneration and ensure tissue viability. In this research, hyperbranched peptides based on poly (ε-lysine) (i.e. dendrons) of different branching generations (Gx) were used as protein scaffolds to present, at their uppermost branching generation, peptide analogues for key growth factors such as the Angiopoietin-1 (Ang-1), the Vascular Endothelial growth factor (VEGF) or the Platelet Derived growth factor (PDGF-BB). The resulting dendritic angiogenic peptides have been designed specifically to target myocardial ischemic tissue starting from a molecular root [di-phenilalanine (FF)] capable of being retained for longer times within the target tissue by interacting with the extracellular matrix (ECM) through hydrophobic interactions and being decorated with the specific angiogenic bioactive peptide analogues capable of inducing a precise biological response in targeting cells.

Synthesis of the dendritic angiogenic peptides was performed using an established solid phase method by a manual method and characterised by analytical HPLC, Mass Spectrometry and FT-IR. The angiogenic potential of dendritic angiogenic peptides has been evaluated by a 2D *in vitro* model where the human umbilical vein endothelial cells (HUVECs) were spiked with the soluble linear and dendritic analogues resulting in an endothelial sprouting. Successively, dendritic angiogenic peptides have been used as functionalisation molecules for collagen type I engineered as either injectable biomaterials (beads) or cardiac patches (scaffolds). The potential of these novel synthesised molecules in inducing angiogenesis *in vitro* when covalently grafted to the biomaterial surfaces also showed an angiogenic potential demonstrating that the bioactivity is not confined to their soluble form. However, their bioactivity in both soluble and grafted form was shown to depend on the molecular branching of the dendron and relative availability of the bioactive sequences. Indeed, the present study for the first time unveils a novel biomaterial approach to stimulate angiogenesis through nano-structured biomaterials and emphasise the need for a finely spaced presentation of the relevant peptide sequence to obtain established endothelial sprouting.

Table of Contents

List of Figures

List of Tables

List of Abbreviation

Generation zero dendron	FFgen0K (G0)
Generation one dendron	FFgen1K (G1)
Generation two dendron	FFgen2K (G2)
Functionalised dendron with QHREDGS sequence	FFgen0K $(QHREDGS)_{2,4,8}$
Functionalised dendron with WQELYQLKY sequence	FFgen0K$(WQELYQLKY)_2$
Functionalised dendron with RKIEIVRKK sequence	FFgen0K$(RKIEIVRKK)_2$
Vascular Endothelial growth factor	VEGF
Angiopoietin-1	Ang-1
Platelet Derived Growth Factor	PDGF-BB
Extra cellular matrix	ECM

Acknowledgements

I would like to Acknowledge my supervisors, Prof. Matteo Santin, Dr. Steve Meikle and Dr. Gary Phillips who gave me the opportunity to work on this interesting research project and giving me constantly support and good advice.

I would like to thanks also all the supervisors and fellows that have participated in the Angiomattrain project under the Marie Curie fellowship for sharing with me knowledge and friendship.

A special thanks to Dr. Valeria Perugini and Dr. Maria Gemiliana Dessi for helping me in the biological part of this project and supporting me in these past years away from home.

Finally, but not less important, I would like to thanks my family and my boyfriend that enable me to complete this project providing me love and support even with miles and miles of distance.

This thesis is dedicated to Cecilia and Ennio,

your souls remain with me.

Declaration

I declare that the research contained in this thesis, unless otherwise formally indicated within the text, is the original work of the author. The thesis has not been previously submitted to this or any other university for a degree, and does not incorporate any material already submitted for a degree.

Signed

Date

28/02/2018

1.INTRODUCTION

Diseases of the heart and circulatory system (cardiovascular disease or CVD) are the main cause of mortality in Europe, accounting for over 4 million deaths each year or 46% of all deaths in Europe. Indeed, CVD causes more deaths among Europeans than any other pathology: almost 1.8 million of these deaths were due to coronary heart disease (CHD) (20% of all deaths), and close to a further 1.1 million due to stroke (12% of all deaths). Cardiovascular disease causes a greater proportion of deaths among women (51%) than men (42%) overall, however, among women, these deaths are more likely to be in old age. During the past five years, there was a decrease in the CVD mortality rates on patients over 65 years. Despite this reduction in mortality, the morbidity has increased in the majority of the European countries for patients who have been hospitalized after acute episodes or treated for chronic CVD (Nichols, 2014). It is clear that in many countries of Europe a large proportion of the populations will lose their lives prematurely to heart disease and strokes.

1.1 OVERVIEW OF THE HUMAN HEART

1.1.1 ANATOMY OF THE HEART

The heart is the central organ of the circulatory system and is placed in the thoracic cavity (Mohrman, 2013). Precisely, the heart is located between the two lungs and is covered by the pericardium, a double-layered membrane sac that secures it to the diaphragm and isolates it from the other organs. The heart has a muscular framework and on its inside presents four cavities: the upper cavities are called the left and right atria, and the lower cavities are called the left and right ventricles (Fig.1.1). A wall of muscle called the septum separates the left and right atria and the left and right ventricles. These four cavities disclose in their inner surface unique features strictly related to their specific role.

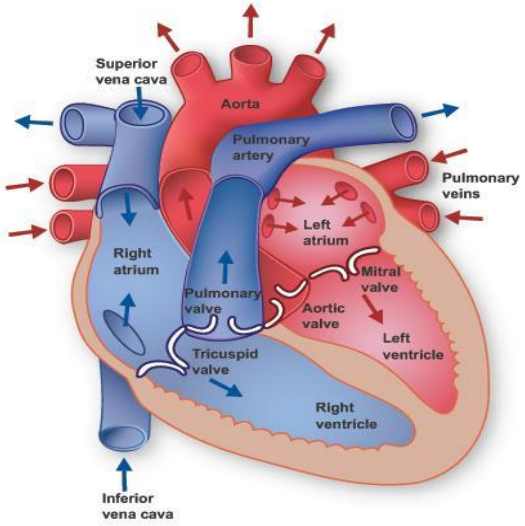

Fig.1.1 Anatomy of the heart (Adapted from an illustration in http://www.texasheart.org).

The atria inner surface appears smooth and regular in proximity of the veins outlet, whereas it is trabecular laterally and anteriorly. Each atrium has an opening, a valve, through which the atrium is capable of pushing the blood into the underlying ventricle. Ventricles have a rough conic shape and on their inner walls they present irregular muscular columns called trabecular carneae which cover all of the inner ventricular surfaces.

The heart muscular component is constituted by myocardium and this tissue is more developed in ventricles than in atria. Myocardium fibres tend to assemble into bundles of different size and these bundles are immersed in a highly vascularised stroma (Maciejko, 2004). The heart wall is composed by three different layers that are epicardium, myocardium and endocardium (Fig.1.2).

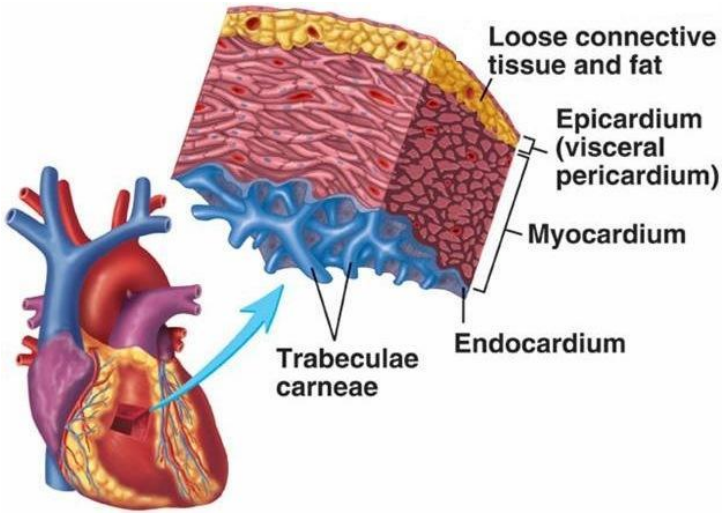

Fig.1.2 Layers of the heart wall: from the bottom to the top it is possible to recognise the endocardium (a membrane that wraps the cardiac cavities), the myocardium, (the thicker layer of the cardiac wall) and the epicardium (the protective membrane that isolates the heart from the other organs) (Adapted from an illustration in Mohrman, 2013).

The epicardium covers the entire external heart surface and continues until the beginning of the big vessels. The myocardium represents the thicker layer of the cardiac wall and is made up of a peculiar striated muscular tissue. Myocardium has two main purposes: it guarantees the hearts contractile activity and represents the specific conduction system that executes the pacemaker function and the transmission of the contractile impulse. Lastly, the endocardium is the membrane that covers all the cardiac cavities (Mohrman, 2013).

1.1.2 PHYSIOLOGY OF THE HEART

As stated previously, the heart is composed by four separate chambers. The upper chamber on each side of the heart is called atrium that receives and collects the blood coming to the heart. The atrium then delivers blood to the lower chambers, called ventricles, which pump blood away from the heart through powerful, rhythmic contractions. The human heart is actually two pumps in one. The right side receives oxygen-poor blood from the various regions of the body and delivers it to the lungs where oxygen is absorbed in the blood. The left side of the heart receives the oxygen-rich blood from the lungs and delivers it to the rest of the body (Fig.1.3) (Ferrari, 1998).

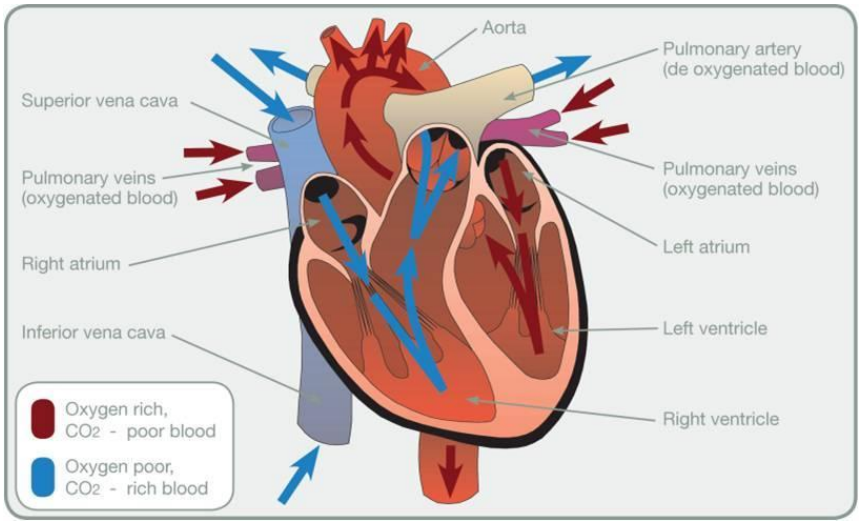

Fig.1.3 Physiology of the heart: The heart works like a suction and pressure pump: drawing in its cavities venous blood and sends it to the lungs through the pulmonary artery. From there the pulmonary veins bring it back again to the heart, which, through the aorta, comes in all capillary networks (Adapted from an illustration in Ferrari, 1998).

The cardiac cycle is made up of all the phenomena that take place from the beginning of one heartbeat to the start of another. Every cycle starts with the spontaneous onset of an action potential in the sinoatrial node, located in the upper vena cava outlet. The action potential, that is a short-lasting event in which the electrical membrane potential of a cell rapidly rises and falls, following a consistent trajectory, has been originated there and it propagates then throughout the atria and in the ventricles. In this way the atria work as a trigger pump for the ventricles that generate the strength able to push the blood in the vascular system. The cardiac cycle is made up of a relaxation period of the cardiac muscle tissue, diastole, and a contraction period, systole.

When the ventricles relax, they make room to accept the blood from the atria; when the ventricles contract, they force the blood from their chambers into the arteries leaving the

heart. The left ventricle empties into the aorta and the right ventricle into the pulmonary artery (Cooper, 2007).

1.2 CORONARY ARTERY DISEASE

The main forms of CVD are coronary heart disease (CHD) and stroke (Nichols, 2014). Heart Ischemia is part of the CHD that results in a reduced blood flow to the heart leading to a lack of oxygen and other nutrients in the heart tissue. Mostly, this is caused by shrinkage of the hearts arteries due to the formation of a plaque (Fig.1.4). This plaque is called atheroma and is formed by fats, proteins and fibrous tissue that forms in the wall of the arteries resulting in a narrowed blood vessel lumen. Fibrin can be deposited on the atheroma surface as well, thus facilitating the formation of thrombi (Liao, 2011). A chronic inflammation of the intima is the main cause of the atheroma formation: the process begins with an accumulation of lipid cells below the endothelium where the majority of these cells are macrophages and T cells (Hansson, 2006). The inner part of the atheroma is formed by foam cells surrounded by a layer of smooth-muscle cells in a collagen matrix. The deposition of calcium salts makes the atheroma very fragile developing the possibility of rupture, aneurysms and thromboembolism. Therefore, MI arises when the atheroma becomes big enough to obstruct coronary artery (Stary, 1995).

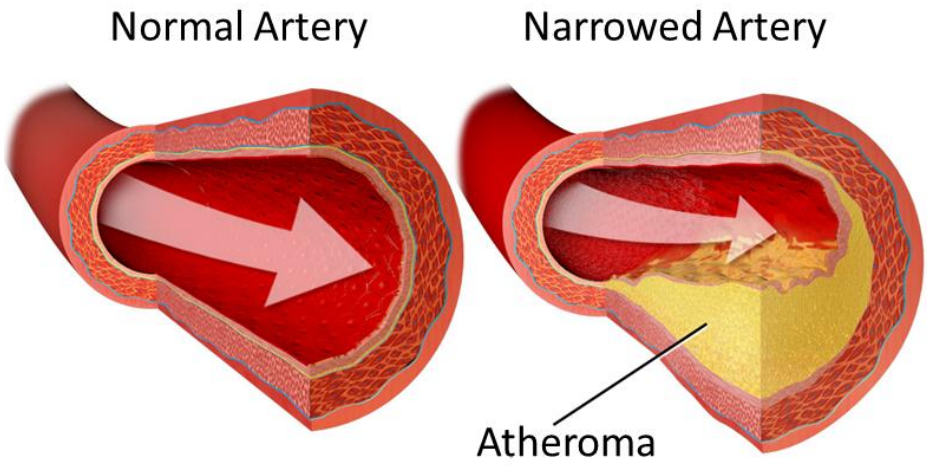

Fig.1.4 Occlusion in the coronary artery results in a lack of oxygen to cardiomyocytes, cells necrosis subsequent to inadequate myocardial perfusion and imbalance between demand and supply of oxygen (Adapted from Liao, 2011).

Theoretically, a heart attack can occur at any age but its frequency significantly increases with age and when there are risk factors involved (e.g. smoking, lack of exercise, high cholesterol) that can lead easily to arteriosclerosis. Arterial coronary obstruction compromises the blood flow to a specific myocardium region, causing ischemia,

myocardial dysfunction and potentially the death of the cardiac muscular cells. The first biochemical consequence of the myocardium ischemia is the arrest of the aerobic metabolism that lead in few seconds to a cascade of potentially detrimental metabolites. Nevertheless, this initial physiological alteration can be reversible, but it has been already demonstrated that a sever ischemia with duration of more than 20-30 minutes can lead to irreversible cardiomyocytes death (necrosis) (Linkermann, 2013).

In most cases of acute myocardium infarction, permanent heart damage is shown when myocardium perfusion is highly reduced for a long period of time (2-4 hours).

For this reason, a prompt myocardium reperfusion can restore normal organ physiology and functionality (Sell, 2009). Reducing the effects of ischemic heart disease is an important area of research because it would improve the quality of life of those people affected by cardiovascular disease and could reduce healthcare costs related to their treatment.

1.2.2 CURRENT TREATMENTS FOR CVD

Current treatments for cardiovascular disease allow surgical reperfusion strategies, pharmacological therapies and, for end-stage patients, full heart transplantation. The goals of current treatment are to relieve the symptoms and to reduce the risk factors in order to slow, stop or reverse the build-up of the plaque and to bypass plaque-clogged coronary arteries (Mahla, 2016).

1.1.2.1 Surgical Reperfusion Strategies

Surgical treatments include both percutaneous coronary intervention (PCI) and coronary artery bypass grafting (CABG) (Devlin, 2014).

Percutaneous coronary intervention (Fig.1.5) is a non-invasive procedure where coronary arteries, blocked or narrowed by plaque, are made pervious again. A device, made of a thin flexible tubular mesh is positioned at the site of blockage with a balloon or through mesh self-expansion to re-open the coronary artery lumen; once in position, the expansion system is inflated to compress the plaque, to deploy the stent thus restoring the blood flow through the artery.

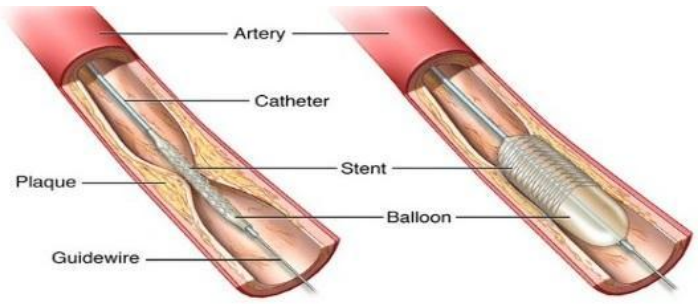

Fig.1.5 Diagram of PCI: a flexible tube with an expansion system is inserted through a blood vessel in order to compress the plaque and restore blood flow. To help to keep the vessel opened a stent is used (Adapted from www.elcaminohospital.org).

CABG is a non-specific surgical procedure (Fig.1.6) used when there is the need to bypass blocked blood vessels: artery or vein segments are removed from an healthy area of the patient's body and used to bypass the narrowed or blocked coronary artery thus restoring blood flow to the heart (Devlin, 2014).

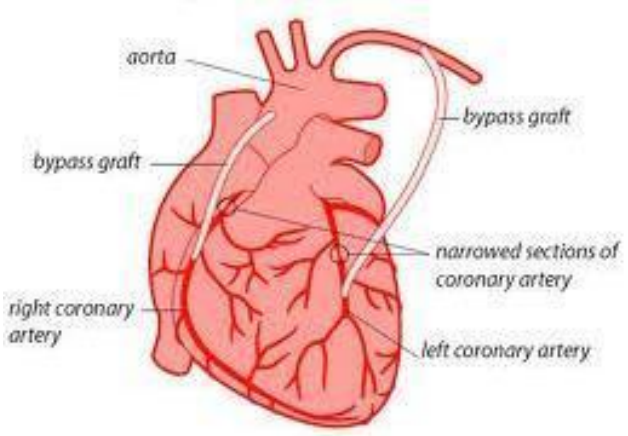

Fig.1.6 CABG procedure: a segment of a blood vessel is removed and used to bypass narrows coronary arteries in order to improve blood flow to the heart (Adapted from Devlin, 2014).

1.1.2.2 Pharmacological Therapies

In general, drugs (e.g. aspirin, nitrates, beta blockers) are used to relieve CVD symptoms and prevent heart failure (Ridker, 2003).

In particular, drugs can be used to lower LDL cholesterol, blood pressure and other CHD risk factors that contribute to the blood clots formation resulting in a loss of functionality of the heart tissue.

Certainly, the use of these treatments have faced a great deal of problems related to patients' individuality, drug resistance, restenosis and the possibility of scar tissue formation, even after reperfusion strategies (Baig, 1999). Given the problems with existing

treatments, there is a need to provide alternative strategies for the treatment of hypoxic tissue like the infarcted myocardium. One such approach is the stimulation of cells or tissue to artificially induce new vessels formation that may provide an innovative and alternative method to enhance the regeneration of the damaged myocardium leading to an improved patients' recovery.

1.2 ANGIOGENESIS PROCESS

The formation of new blood vessels is essential for organogenesis and successful embryonic and foetal development (Carmeliet, 2000). However, in an adult organism the angiogenesis process, that is the formation of new blood vessels from pre-existing vasculature, is limited and occurs only in association with repair process such as wound and fracture healing (Clapp, 2009).

Angiogenesis is regulated by a balance between endogenous pro- and anti-angiogenic factors that are involved in a multi-step process.

The angiogenesis process consists of four main steps: destabilisation, sprouting, branching and stabilisation (Fig.1.7) (Adams, 2007).

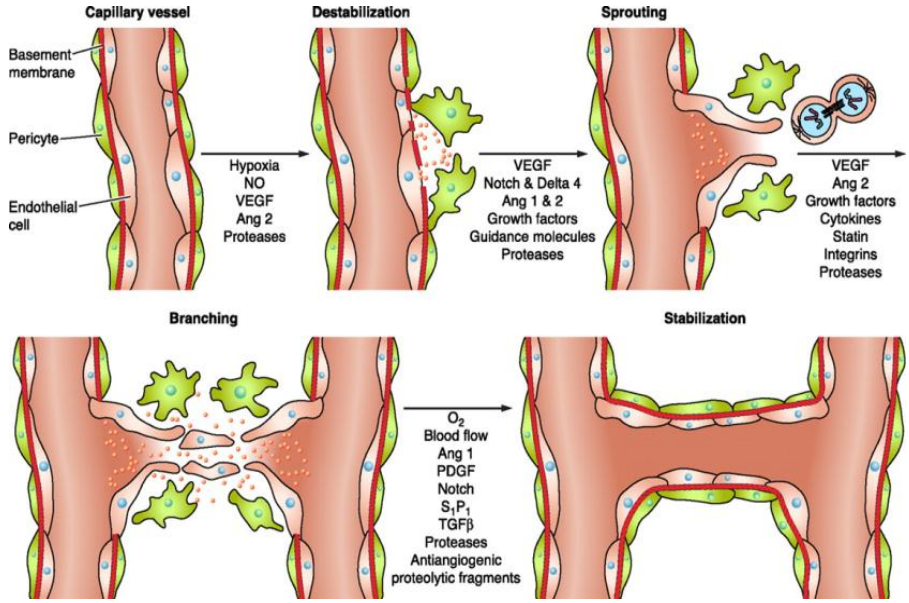

Fig. 1.7 It is possible to consider several stages in the angiogenic process: - Destabilization of pre-existing vessels following an increase in vascular permeability and the loss of connections between endothelial cells; - Migration and proliferation of endothelial cells in a tissue area where the formation of new vessels is needed; - Differentiation of endothelial cells characterised by an arrest of cell proliferation and the formation of primitive capillaries. (Adapted from Clapp, 2009).

The initial impulse that triggers the process is given by hypoxia (low oxygen environment, < 20%), which induces the production of nitric oxide (NO) and the expression of several growth factors such as vascular endothelial growth factor (VEGF), angiopoietin -1 and -2;

NO interacts ECM proteases to increase the permeability of the capillary vessel wall through the disruption of endothelial cell contacts that leads to the destabilisation of the blood vessel (Fig.1.7, destabilisation). At this stage, endothelial cells are free to migrate out of the basement membrane and proliferate. The main growth factors involved in this process are VEGF, angiopoietins and basic fibroblast growth factor (bFGF) that guide the directional migration of endothelial cells. Moreover, several proteases (e.g. matrix metallo-proteases (MMPs), heparinases, chymases, tryptases), secreted by endothelial cells, degrade and change the ECM composition, allowing a sufficient support and guidance for endothelial cell migration. The formation of the newly formed blood vessel is induced primarily by VEGF with the consequent formation of sprout extension (Fig.1.7, branching panel). In addition, proteases enhance vessel sprouting by releasing angiogenic molecules of the ECM. The onset of blood flow after the maturation stage decreases VEGF expression, thereby reducing endothelial proliferation. Stabilisation of the newly formed vessel is followed by an increase expression of anti-angiogenic factors in order to avoid uncontrolled vessel growth (Clapp, 2009).

Platelet Derived Growth Factor (PDGF) is the major signalling factor involved in the final step of angiogenesis providing the recruitment of mural cells (pericytes); this action is crucial for vessel stabilisation because an insufficient recruitment could lead to vessel regression and lack of functionality (Adams, 2007).

1.2.1 Main Growth Factors Involved in the Angiogenesis Process

As described in Section 1.2, angiogenesis is regulated by a number of growth factors and proteins belonging to the extra-cellular matrix (ECM). Growth factors involved in the angiogenic process regulate the formation of new blood vessels and prevent their regression (Nakamura, 2009). Efforts have been made to take advantage of the potential of angiogenic growth factors to help induce vascular formation and to promote it.

1.2.1.1 Vascular endothelial growth factor

Vascular endothelial growth factor (VEGF) is a crucial regulator of normal and abnormal angiogenesis. The loss of a single VEGF allele results in a deficient vascularisation and early embryonic death (Ferrara, 2003).

In 1989, the purification of an endothelial cell-specific mitogen led to the discovery of vascular endothelial growth factor (Herttuala, 2007), highlighting the potential of this molecule to have a crucial role in the regulation of physiological and pathological growth of blood vessels (Lu, 2003).

VEGF is a highly specific mitogen for vascular endothelial cells and is a homodimeric protein belonging to the cysteine knot growth factor family (Chan, 2011). The alternative splicing from a single VEGF gene generates four different isoforms ($VEGF_{121}$, $VEGF_{165}$, $VEGF_{189}$ and $VEGF_{206}$) of this growth factor. These isoforms have peculiarities in terms of molecular mass and biological properties that make them unique (Lu, 2003). The most abundant isoform, that is present in the human body, is the $VEGF_{165}$: a glycoprotein with high affinity to bind heparin. VEGF carries out its biological function by binding to two tyrosine kinase receptors (Fig.1.8), the kinase domain receptors (KDR) and the Fms-like tyrosine kinase (Flt-1), both localised on the cell surface of various endothelial cell types (Gupta, 2009). VEGF induces receptors dimerization that stimulates endothelial cells mitogenesis.

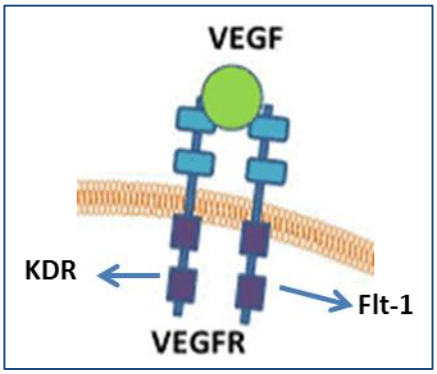

Fig.1.8 VEGF binding sites are identified on cell surface. VEGF binds to two different receptors (KDR and Flt-1) dimerising them and resulting in the VEGFR receptor (Adapted from Herttuala, 2007).

VEGF receptor expression increases in response to several stimuli and it results in endothelial cells proliferation, migration and angiogenesis (Su, 2009). VEGF is highly expressed in response to hypoxia. Indeed, VEGF is involved in the system that restores the oxygen supply to tissue when blood circulation is inadequate (Chan, 2011).

1.2.1.2 Angiopoietin-1

Angiopoietin-1 (Ang-1) belongs to the family of the vascular growth factors and it plays a critical role in mediating interactions between the endothelium and the surrounding matrix and mesenchyme (Rask, 2010). Ang-1 has a high affinity to its receptor, Tie-2. This receptor is a transmembrane tyrosine kinase uniquely expressed by endothelial cells (Fig.1.9) capable of autophosphorylation after binding (Deli, 2013).

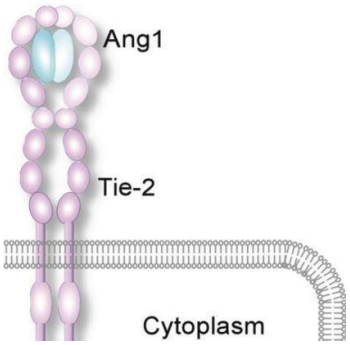

Fig.1.9 Ang-1 binds Tie-2 resulting in the autophosphorylation of the receptor and the consequently binding to two downstream proteins (GRB-2 and SH-PTP2) involved in the alteration process in cellular morphology and differentiation (Adapted from Deli, 2013).

Studies performed on knockout animals suggest that Tie-2 expression is crucial for the preservation and development of the primitive capillary network. Therefore, Ang-1/Tie-2 system is involved in the regulation of capillary tube formation and is indispensable for the survival of endothelial cells but it has no effect on cells proliferation (Falkman, 1996). Ang-1 has a central role in preserving the existing vessels enhancing contacts between endothelial cells and mural cells (Puig-Sanvincens, 2013). Lastly, Ang-1 interacts directly with cardiomyocytes via integrins to encourage adhesion, viability, specific cardio-protective signalling and prevent induced apoptosis (Rask, 2010).

1.2.1.3 Platelet Derived Growth Factors

Platelet derived growth factors (PDGF-BB) is a dimeric glycoprotein composed of two A (-AA) or two B (-BB) chains or a combination of the two (-AB) (Fig.1.10).

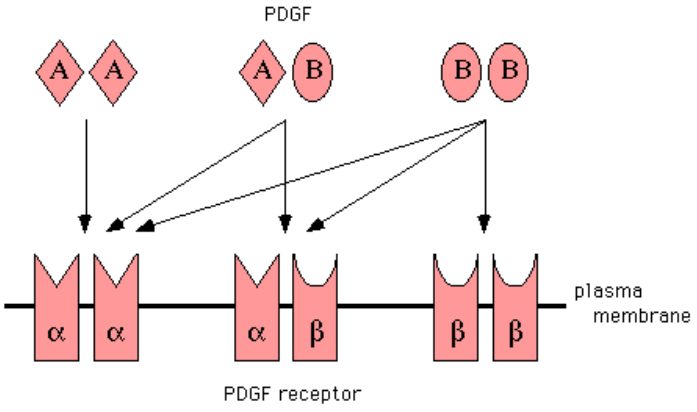

Fig.1.10 PDGF is a glycoprotein composed of different chains that create different isoforms (Adapted from Hsieh, 2014).

The isoforms of PDGF have different receptors resemblance and thus, different role in biological activities. PDGF-BB plays an important role in the recruitment of perivascular

cells to endothelium. Moreover, PDGF-BB has been implicated in the angiogenesis process being the most relevant growth factors involved in the maturation and stabilization steps of the process.

Studies conducted on knockout mice have shown how PDGF-BB expression is knocked out specifically in endothelial cells and has a crucial role in the formation of mature vessels during development; whilst, before the knockout, vessels were hemorrhagic and show a smaller number of perivascular cells (Hsieh, 2014).

1.2.1.3 Angiogenic Growth Factors as Pharmaceutical treatment for ischemic diease

Different growth factors serve as stimuli for endothelial cells proliferation and migration and induce new vessels formation (Clapp, 2009). Indeed, there have been several clinical trials (phase II or phase III) on therapeutic angiogenesis for the treatment of ischemic heart and peripheral disease involving the main growth factors acting in the angiogenesis process (VEGF, Ang-1, PDGF-BB) with a particular attention on VEGF (Zachary, 2010). Therefore, Henry *et al*. (2001) have been demonstrated how intracoronary and intravenous recombinant VEGF-A_{165} infusion improve myocardial perfusion in patients with stable angina (phase I trial) that are not suitable for established reperfusion methods. Similar results have been obtained by Laham *et al*. (2000) with an intracoronary infusion of FGF-2 (Fibroblast growth factor 2) that shows signs of therapeutic efficacy.

Despite good results achieved in the early phase of clinical trials, protein therapy seems to be ineffective for most of the trials after phase III (Zachary, 2010). These disappointing outcomes were related to the placebo effect, targeting of the damaged area, optimal dose concentration and time points of administration (Annex, 2005). However, the main limitation of protein therapy is due to the short half-life of angiogenic growth factors in blood that, added to the dose-limiting hypotension issue, may result in an ineffective treatment.

1.3 REGENERATIVE MEDICINE

Regenerative medicine can be defined as the science that "regenerates human cells, tissue or organs, to restore or establish normal function" (Lee, 2005). Therefore, regenerative medicine merges the field of biology and engineering with the aim of guiding body regeneration by specifically controlling the biological environment. This novel science is a promising therapeutic approach in place of organ transplantation, which is limited due to immune response against allografts and the limited number of donor organs available (Lanza, 2007).

Tissue regeneration strategies can be divided into three categories: (i) direct injection of cells into the damage tissue or in the systematic circulation, (ii) implantation of cells after they have been expanded and guided to form a 3D tissue structure in a bioreactor and (iii) scaffold-based delivery of signalling molecules such as growth factors, drugs or oligonucleotides that stimulate cell migration, growth and differentiation (Cross, 1991).

The use of combination of cells, engineering knowledge and materials method in union with suitable biochemical and physico-chemical factors capable of improving or replacing biological functions, are promising therapeutic approaches to reactivate blood flow through angiogenesis to support tissue regeneration when myocardium is damaged (Bussolati, 2001).

1.3.1 Novel approach for Myocardial Infarction (MI) injury

The human heart is composed of adult cardiac myocytes, cells that are completely differentiated and cannot proliferate or regenerate after injury; that is the reason why the heart cannot regenerate after a myocardial infarction (MI) (Dallabrida, 2005). The seriousness of myocardial damage depends on the duration of vessel occlusion (Clapp, 2009). Therefore, blood vessels formation is crucial in the healing of the infarcted myocardium in order to restore normal organ physiology and functionality.

Reducing the effects of ischemic heart disease is an important area of research because it would improve the quality of life of those patients affected by cardiovascular disease and could reduce the healthcare costs. As a result, alternative treatment strategies have been investigate to reverse this frequently and deadly disease.

1.2.3.1 Myocardial Repair

One of the standard tissue engineering approaches consists of the isolation of specific cells through a biopsy from a patient, to seed them on a 3D biomimetic construct under precise environmental conditions and to implant/deliver the novel designed construct into the desire site in the patient's body aiming at new tissue formation (Fig.1.11) (Novosel, 2011).

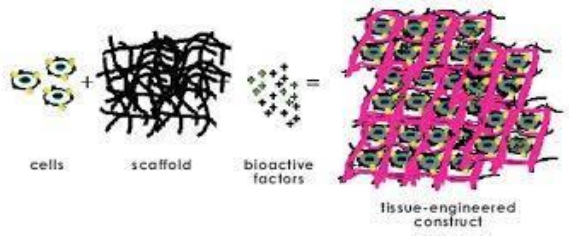

Fig.1.11 Principles underlying scaffold-based tissue engineering. A scaffold or matrix, living cells, and biologically active molecules are used in variable strategies to form a "tissue-engineered construct (TEC)" to promote the repair and regeneration of the tissue (Adapted from Novosel, 2011).

Tissue regeneration can be achieved either *in vitro* or *in vivo*. The *In vitro* approach maintains good control over physical, chemical and mechanical properties of the construct, on seeded cells and function but it is limited by the capability to create a strong tissue and the possibility of tissue necrosis after transplantation (Timar, 2001). The *in vivo* approach is simpler and feasible compared to the *in vitro* and aims to create new tissue directly *in situ*. However, the critical element to consider is the perfusion of the construct and so, vascularisation is compulsory in order to achieve complete tissue regeneration (Rivron, 2008). Indeed, the most important requirements from tissue engineering scaffold are its ability to support vascular infiltration (Zisch, 2003). Thus, a myocardial tissue engineered graft requires angiogenesis for its growth and survival. The occurrence of angiogenesis is driven by regulating molecules that influence cells behavior.

1.3.2 Natural biomaterials for angiogenic growth factor delivery

1.3.2.1 Alginate

Alginate is an anionic polysaccharide composed of beta-D-mannuronic acid and alpha-L-guluronic acid (Fig.1.12) and it derives from the marine brown algae. When alginate is conjugated with divalent cations, it forms a hydrocolloid gel (Draget, 1997).

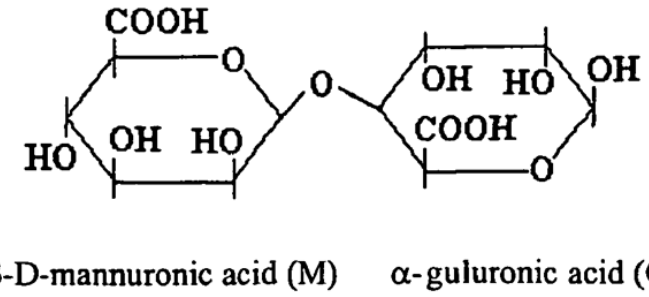

Fig.1.12 Chemical structure of alginate: it is a block polymer composed by beta-D-mannuronic acid and alpha-L-guluronic acid (Penman,1972).

Alginate hydrogels are widely used in wound healing and food additives (Gombotz, 2010) and because of its biocompatibility and the ease with which it can be gelled, alginate is widely used in the immobilisation and encapsulation of cells (Smidsrod, 1990). Indeed, because gelation happens in an aqueous environment, alginate microspheres are a promising system to entrap either angiogenic molecules like VEGF (Schuch, 2002) or cells (Peters, 1998).

1.3.2.2 Chitosan

Chitosan is a linear polysaccharide composed of N-acetyl-D-glucosamine units and is obtained from the crustacean shells in basic aqueous solution (Fig.1.13) (Rinaudo, 2006).

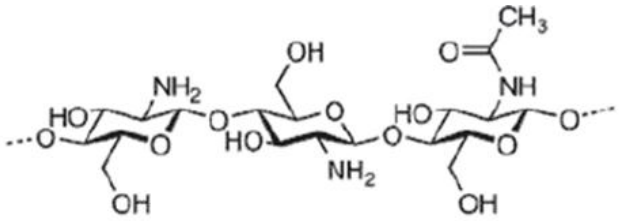

Fig.1.13 Chitosan structure (Rinaudo, 2006).

Derivatives of chitosan have been produced for the prolonged release of basic fibroblast growth factor (bFGF) (Kikuchi, 2002). Moreover, chitosan-albumin microspheres and fibres have been assembled for the release of acid fibroblast growth factor (aFGF) and result in the stimulation of neovascularisation in rat (Lee, 2000). Furthermore, a cross-linked version of chitosan with collagen has been used to produce a scaffold used to investigate the growth of endothelialised human skin replacement (Ma, 2003).

1.3.2.3 Fibrin

Fibrin is a protein used in blood coagulation. It is a fibrillar protein that is polymerised to form a "mesh" (together with platelets) over the wound site. Fibrin derived from fibrinogen, a plasma protein synthesised by the liver. In the coagulation process thrombin is activated and is responsible for the conversion of fibrinogen to fibrin. Then, fibrin is transversely connected to the factor XIII to form a clot (Shireman, 1998).

Indeed, fibrin clots follow every step of blood vessel formation, starting from the migration of endothelial cells to the maturation and stabilisation of a vessel network (Vasita, 2006). ′Fibrin glue′ can be found in the market as a mixture of concentrated fibrinogen and thrombin and it is widely use in surgery as sealants (Fasol, 1994). Moreover, fibrin clots can be produced from the patient′s blood and use as temporary delivery matrix for therapeutics protein, cells or DNA genes that may enhance healing (Bach, 2001). Indeed, fibrin is gradually resorbed and permits the growth of new tissue.

Regarding ischemic tissue, fibrin glue can be used as temporary scaffold to enhance the formation of granulation tissue that is composed by a high level of vascularity (Sahni, 1999). Furthermore, fibrin glue was found to stimulate capillary ingrowth without the help of added growth factors when injected subcutaneously (Kipshidze, 2000).

Studies using fibrin glue as a delivery matrix for Fibroblast Growth Factors (aFGF and bFGF) have shown to improve perfusion of ischemic rat myocardium and tracheal rabbit autografts, respectively (Sakiyama-Elbert, 2000). The positive outcome of these experiments appears to validate fibrin glue as an efficient vehicle for local release as well. Indeed, fibrin matrix tethered with bFGF showed to be able to improve endothelial proliferation (Hinsberg, 2001). Moreover, clinical studies on VEGF therapy of critical limb ischemia results in an increase of the patient's limb blood supply while has been treated with an intramuscular deposition of VEGF coupled to fibrin glue (Kipshidze, 2000). Additionally, other clinical applications of fibrin glue include the formation of a complete endothelium on the luminal surface of prosthetic bypass grafts (Currie, 2001) or to re-establish vessel surface endothelium damaged by angioplasty (Spicer, 2010). However, the release kinetics of these growth factors remain a huge issue despite the positive results mentioned above. For example, release of growth factors from fibrin glue results in an uncontrolled released of the 70-100 % of the molecules just after injection and consequently the potential of the factor to produced adverse effects on healing (Shireman, 1999).

1.3.2.4 Collagen and Gelatine

Since 1988, hydrogels made from collagen or gelatine have been used as scaffolds for the release of angiogenic molecules (Thompson, 1988).

Gelatine is obtained by selective hydrolysis and denaturation of collagen from skin, bone or tendon. After purification by filtration, gelatine is concentrated by evaporation and sterilized at 138 °C, gelled by a cooling process and finally dried in order to obtain a solid final product, that is stable and easy to store. The main features that make gelatine a good candidate for the release of angiogenic molecules and as a scaffold for tissue engineering are the inherent adhesiveness for cells and the proteolytic degradability (Tabata, 2000).

Collagen is one of the most important proteins in vertebrates and represents one third of the total protein of the human body, where it plays a key role in the structure and function of organs and tissues, such as skin, cartilage and muscle. Collagen fibres are the main components of connective tissue forming the bulk of soft tissues including skin, ligament, tendons and cartilage (L'Heureux, 1993). According to the sequence of amino acids that constitute the collagen polypeptide chains and to the structure of the chains themselves, 28 types of collagen have been identified, among which the most important are:

- type I collagen, which is located especially in the skin and blood vessels, where it is the main structural component of the extracellular matrix of the dermis;

- type II collagen, which is an essential element of the cartilage and plays a key role in the joints and intervertebral discs;
- type III collagen, present in the walls of blood vessels (Auger, 1995).

Collagen type I is the most abundant protein in native blood vessels and in combination with smooth muscle cells (SMCs) is able to provide wall strength and resistance to vessel damage in physiological conditions (Buttafoco, 2006). Indeed, collagen type I has a predominant role in the field of injectable biomaterials for the treatment of MI. Collagen type I is made of two αI chains and one α2 chain (Fig.1.14) that form fibrils of 50nm in diameter.

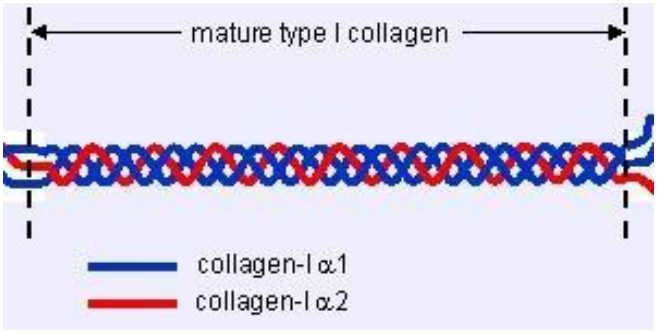

Fig. 1.14 Schematic representation of Collagen type I: in blue the two αI chains and in red the one α2 chain (Adapted from Perruccio, 2008).

It is possible to find this particular type of collagen in bone, skin, blood vessels and tendon (Sell, 2009). Collagen type I is widely used in cardiovascular tissue engineering not only because it is the predominant protein of the ECM but also for its relatively low immunogenicity, good mechanical properties and ability of providing biological signals to cells hence regulating their functional response (Barnes, 2007). Furthermore, collagen type I is a resorbable biopolymer (Kolacna, 2007). Because of these characteristics, collagen type I has been used in this project as a biomaterial platform for the exposure of dendritic angiogenic peptides. Type I collagen scaffold can be produced as highly porous interconnecting systems with suitable properties to enhance cell adhesion and migration (Albes, 1994). Indeed, type I collagen has been widely studied and used as tissue engineered scaffold for skin, bone and blood vessels replacement and regeneration (Wissink, 2000; Gautam, 2014; Matthews, 2001; Yoshimoto, 2003). However, collagen scaffold has been shown to have very poor loading capacities for growth factors. Indeed, different methods have been used to modify and improve the entrapment of angiogenic factors into collagen matrices (Sell, 2009). The results is a collagen coating prepared by

cross-linking of type I collagen and heparin that is able to bind and retain angiogenic factors through molecular affinity thus creating a specific target to the tissue to repair (Gerber, 1999). Moreover, the addition of bFGF enhanced human umbilical vein endothelial cell (HUVEC) adhesion and proliferation (Wissink, 2000).

1.4.1 Synthetic biomaterials for angiogenic growth factor delivery

Due to the problem related to the risk of infectious pathogens and immunogenicity of natural biomaterials, the demand for synthetic replacements has opened a wide range of studies investigating novel classes of synthetic materials able to have the same features of the natural matrices described above.

The basic properties that a synthetic material should have in order to be a suitable candidate for tissue engineering applications are their ability to control degradation and be resorbed completely by the body while acting as a structural support to let cells grow into a three-dimensional organisation (Hubbell, 1999). Indeed, the synthetic substitute should be assembled to form a highly porous internal structure in order to have an adequate cell seeding density *in vitro*, enough space to let blood vessels invade the synthetic replacement *in vivo* and to permit oxygen and nutrients to reach cells (Griffith, 2002).

The main synthetic materials that have been used for delivery of angiogenic growth factors in tissue engineering application are poly(lactic-*co*-glycolic acid) (PLGA) and polyethylene glycol (PEG) (Sheridan, 2000; Lee, 2017;Phelps, 2013).

1.4.1.1 Poly(lactic-co-glycolic acid)

PLGA is a copolymer approved by the Food and Drug Administration (FDA) for the manufacturing of medical devices due to its biodegradability and biocompatibility properties (Peters, 2002). PLGA is synthesised by means of ring-opening co-polymerisation of two different monomers, the cyclic dimers (1,4-dioxane-2,5-diones) of glycolic acid and lactic acid (Fig.1.15).

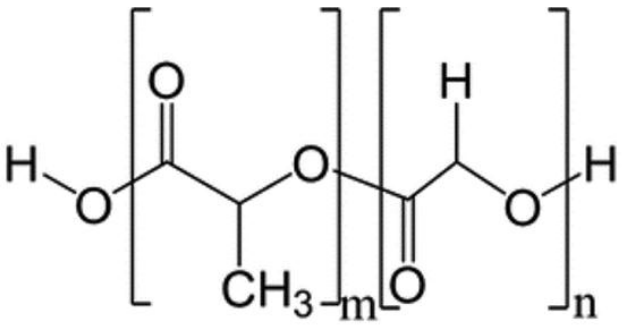

Fig.1.15 Chemical structure of PLGA.

Polymers can be synthesised as either random or block copolymers thereby tuning the polymer properties. Depending on the ratio of lactide to glycolide used for the polymerisation, different forms of PLGA can be obtained: these are usually identified on the basis of the molar ratio of the monomers used (Arras, 1998). PLGAs will vary from fully amorphous to fully crystalline polymers depending on block structure and molar ratio. PLGA degrades by hydrolysis of its ester linkages in the presence of water. PLGA has been successful as a biodegradable polymer because it undergoes hydrolysis in the body to produce CO_2 and water easily cleared by the body. There is minimal systemic toxicity associated with using PLGA for drug delivery or biomaterial application, but it has been shown that intermediate fragments of the polymer causes inflammatory reactions that can lead to unwanted tissue resorption (Cleland, 2001).

Specifically, PLGA scaffold are able to adsorb proteins, after implantation, from body fluid and produce a layer of these adsorbed protein that is responsible for the cell adhesiveness property of the material (Kim, 2002). PLGA scaffold can be functionalised with growth factors and ECM components as well as with autologous cells (Richardson, 2001). Regarding therapeutic angiogenesis has been demonstrated that Dermagraft (PLGA scaffold for commercial use) can induce angiogenesis *in vivo* in a mice cardiac ischemia model (Kellar,2001).

In addition, clinical and pre-clinical studies have demonstrated the potential of complementary delivery of different angiogenic growth factors in order to obtain mature and stable vascular networks: PLGA matrices were produced adding VEGF and microspheres containing PDGF. This system is able to control the faster release of VEGF by surface erosion and slower release of PDGF by bulk erosion (Han, 2013).

1.4.1.2 Polyethylene glycol

Polyethylene glycol (PEG) or Polyethylene oxide (PEO) is a polymer prepared by the polymerisation of ethylene oxide (Fig.1.16).

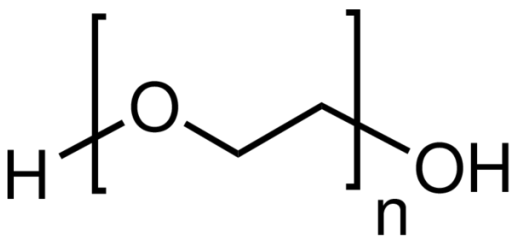

Fig.1.16 Chemical structure of PEG.

PEG scaffolds are obtained from aqueous solutions in which linear and branched PEG macromers are dissolved. These polymer chains have reactive groups that can be cross-linked to form hydrogels using two different methods: light-induced free radical reactions and chemical Michael-type addition reactions (Sawhney, 1993). PEG macromers are characterised by hydrophilic properties, large size that do not permit the polymer to cross the cell membrane and they are non-adhesive to proteins or cells (Sawhney, 1994). PEG intrinsic non-adhesive properties have been used in applications such as the control of postoperative tissue adhesion as well as to release of drugs able to prevent these adhesions (Landeen, 2001).

More recently, the idea of an engineered PEG capable of delivering biological signalling hence able to interact with cells has been developed. PEG hydrogels have been designed with the incorporation into the polymer chain of bioactive sites that let a direct molecular interaction between material and cells to occur (West, 1995).

In particular, VEGF has been conjugated to the PEG hydrogel during the matrix formation using a cysteine residue present in the VEGF structure. The strength of the covalent bond between the polymer and the growth factor allows the release of the molecule only after the degradation of the PEG matrix due to proteolytic degradation. Results showed how the functionality of VEGF is maintained and even crucial for endothelial cell survival (Leslie-Barbick, 2011). Moreover, when the PEG hydrogel tethered with VEGF is implanted in rats, it induces the complete regeneration of the damaged tissue (Zisch, 2003; Garcìa, 2015).

The high demand for structures capable of interacting with the surrounding healthy tissue of a damaged tissue area and to encourage tissue regeneration has focussed the attention on a new class of hyperbranched biomaterials, i.e. dendrons, able to mimic the ECM at molecular level and have biological effects as the natural ECM (Lloyd, 2007). Indeed, materials supplied with specific cues involved in the structure or in the function of natural ECM have been designed and investigated in the last few years (Wang, 2013).

Specifically in this project, these dendrons have been chosen to be the "support materials" to these mimicking molecules and they will be widely discussed in the following chapters.

1.5 DENDRIMERS AND DENDRONS

A dendrimer is a polymeric molecule composed of multiple branched monomers that originate radially from a central core, reminiscent of a tree structure, from which

dendrimers derive their name (Greek, *dendron=tree)* (Bosman, 1999). A typical dendrimer is composed by three different topological parts (Fig.1.17):

(a) Focal core

(b) Interior shells composed of repeating units

(c) Multiple peripheral functional groups

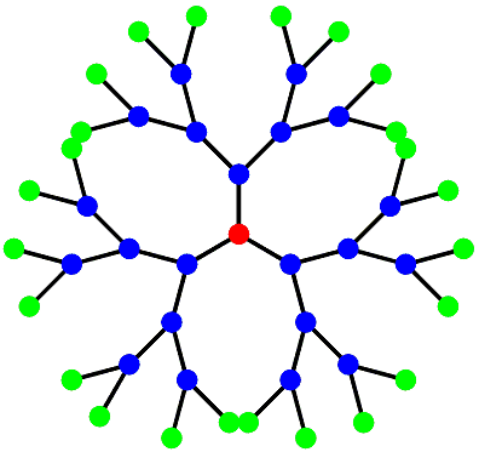

Fig.1.17 A typical dendrimer structure: in red is highlighted the core, in blue the branch points that define the number of repeating units and in green the peripheral functional groups.

The focal core, can encapsulate various chemical species, with specific properties, that can be positioned in a special nano-environment that is surrounded by extensive branching arms. The interior layers are composed of repeating units that define the dendrimer branching generations and provide a flexible space created within the empty areas of the dendritic building blocks; these voids can be exploited to encapsulate various small guest molecules. Finally, the third part of a dendrimer is the multivalent surface, which can expose a large number of functionalities that can interact with the external environment (Cloninger, 2002).

When the core of a dendrimer is removed, a number of identical fragments called dendrons remain. A Dendron can be divided into three different regions: the core, the branched units and the periphery (Fig.1.18) (Tomalia, 1985). The number of branched points, assembled upon moving outward from the core of the dendron to its periphery, defines its generation (G0, G1, G2); dendrons of higher generations are larger, more branched and have more end groups than the dendrons of lower generations (Lee, 2005).

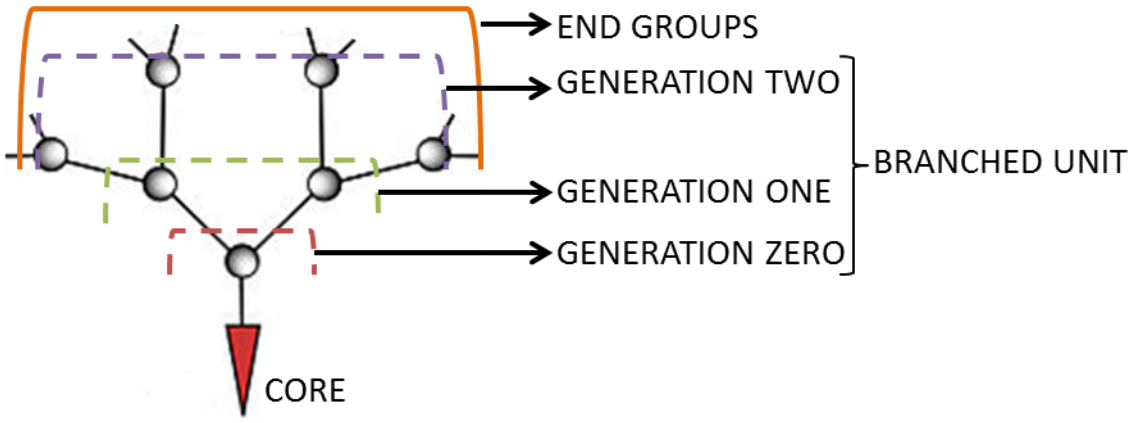

Fig.1.18 Anatomy of a dendron: the red triangle identifies the core of the molecule; the broken lines identify the various regions of the dendrons and the different generations (G0, G1 and G2) and the solid orange line that marks the periphery with the end groups.

1.5.1 DENDRON SYNTHESIS

Unlike the conventional synthesis of linear polymers where a mixture of materials with different molecular weight is produced, the synthesis of dendrons is obtained by a multistep process of organic synthesis that leads to a mono-disperse polymeric product (Crampton, 2007). Dendrons are widely used as protein scaffolds due to their specific and defined structure offering technological advantages when compared to linear polymers of the same molecular weight. Indeed, dendrons have a higher solubility than linear polymers and they also show a very low intrinsic viscosity (Grayson, 2001).

Dendrons can be synthesised either using a divergent or convergent method:

- the divergent approach leads to the final dendron starting from the core of the molecule and adding outward the building blocks by repetitions of coupling and activations steps (Fig.1.19) until the desired product is obtained.

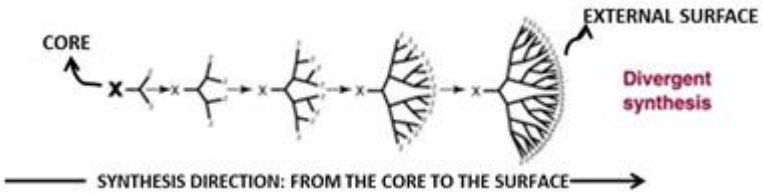

Fig.1.19 Divergent method for constructing dendritic macromolecules: the synthesis begins from a core and continues radially outwards by consequential reaction of activation and condensation (Adapted from Grayson, 2001).

Certainly, the coupling and activation steps increase exponentially as the dendron increases its size and therefore large excess of reagent is essential to complete this type of synthesis.

The interesting characteristic that makes this method the chosen one for the synthesis of dendrons is the ability of the peripheral functionalities to avoid chemical reaction with the core monomer thus preventing an uncontrolled hyperbranched polymerisation (Grayson, 2001). Moreover, the divergent approach is recommended when a large quantity of dendrons is required because dendrons obtained with this method is doubled with each step of the reaction. At the same time, the side effect of producing dendrons with the divergent method is the possibility of having incomplete branches or side reactions that increase exponentially during the synthesis of the molecule (Tomalia, 1984).

- The convergent approach begins the synthesis starting from the end groups (external surface) and continues inwards by activation and condensations reactions adding monomers (Fig.1.20) (Grayson, 2001).

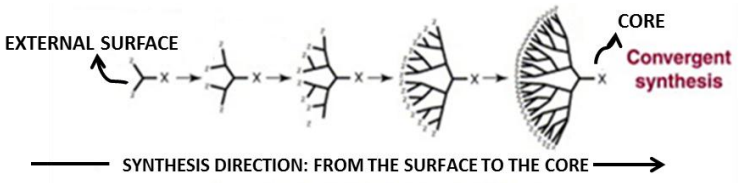

Fig.1.20 Convergent method for dendrons production: the synthesis begins at the external surface of the final macromolecule and continues inward reaching the core (Adapted from Grayson, 2001).

The convergent approach has an opposite development if compared to the divergent one. Moreover, the convergent methods required just few chemical reactions to reach the core of the molecule and then no reagents excess is needed to complete the synthesis. However, the first coupling step occurs on the external surface where the end groups are positioned, and so the monomers, increase exponentially with the increase of the generations leading to a higher probability of steric inhibition and lower yields. For this reason, convergent approach is not recommended in the production of highly branched molecules (Bracci, 2003). Moreover, the divergent approach can be used to produce dendrimers and dendrons in a short time, often within a week. Indeed, the divergent approach is widely used in biological research in which dendrimers and dendrons are employed for achieving different biochemical effects (Bosman,1999). Several other methods can be used in the synthesis of branched structures, but they are only combinations or adaptations of the two approaches described above (Touzani, 2011). Synthesis of hyperbranched molecules can be conducted either in liquid or solid phase depending on the molecule structure required: if the desired product is a spherical structure (e.g. dendrimer) the synthesis should be performed in liquid

phase. Otherwise, solid phase can provide the formation of a tree-like structure like the dendrons.

1.6 AIMS OF THE THESIS

Myocardium tissue regeneration, using therapeutic angiogenesis, tries to treat ischemic disease by generating new blood vessels from the existing vasculature. Therapeutic angiogenesis takes advantage of specific biomolecules that have angiogenic potential (VEGF, Ang-1, PDGF-BB) to enhance new blood vessel formation and reactivate the normal function of the myocardium. There are many problems related to the use of these particular angiogenic growth factors including: (i) controlled targeting and release of the specific biomolecules, (ii) susceptibility to denaturation and bioavailability, (iii) tissue retention (Post, 2001). Indeed, a particular system able to control bioactive factors delivery while providing them with conformational stability has not been found during the extended literature review of this thesis.

Clearly, the first contribution to knowledge of the present project is the integration into a dendrimeric structure of known short amino acids sequences found in growth factors involved in angiogenesis. Previous studies have shown that the linear forms of these peptides analogues preserve the intrinsic function of the growth factors while being less susceptible to conformational changes. At the same time, these peptide analogues have disadvantages related to the limited utility due to their poor stability under storage, short in vivo life span and lack of precise targeting and release to the target tissue (Miklas, 2012).

Here, the integration of these peptide sequences at the outermost branching generation of dendrimers enhances their stability through the role of protein scaffold played by the dendron, offers a precise spatial orientation to the bioactive molecules due to the well-defined distance between molecular branches and enable a design that can improve the correct exposure of these macromolecules from the surface of the biomaterial scaffolds and their retention within the target tissue when delievered as free, soluble macromolecules. Moreover, dendrons are able to present multiple functionalities to the living cells depending on the therapeutic needs . Therefore, dendrons functionalised with pro-angiogenic peptides could improve the spatial temporal delivery of pro-angiogenic factors in the field of myocardium regeneration overcoming problems related to targeting and release. Finally, these novel dendritic angiogenic peptides can be used in conjunction with biomaterials implants as cardiac patches either being released from them or being integrated as stable surface functionalisation moieties.

For these reasons, the project aims to: (i) design novel protein scaffolds called dendrons, capable of exposing angiogenic peptide analogue sequences; (ii) characterise and evaluate the efficacy of the new molecules to modulate angiogenic stimuli *in vitro* in a 2D model as "free drugs"; (iii) demonstrate the efficacy of bioactive angiogenic peptide analogues as functionalisation tool both for injectable materials as well as for cardiac patches.

2. POLY (Ɛ-LYSINE) DENDRONS AS A NOVEL CLASS OF PROTEIN SCAFFOLD FOR THE SPACED EXPOSURE OF ANGIOGENIC PEPTIDE ANALOGUES

2.1 INTRODUCTION

2.1.1 BIOLOGICAL APPLICATION FOR DENDRIMER AND DENDRONS

The design of specific therapeutics and diagnostics systems with well-defined sizes and shapes is of great interest in several medical applications such as drug delivery, gene transfection and imaging (Tomalia, 2002). The high level of control possible over the architectural design of dendrimers, their size, shape, branching units/density and their surface functionality, clearly outlines these macromolecules as exclusive and ideal carriers in those applications (Tomalia, 1984).

Dendrimers structure permits the encapsulation of bioactive agents in the voids created by the branched units or chemically attached onto the dendrimer surface. In this regard, the high density of exposed surface groups allows the grafting of functionalities that may alter the solubility or the toxicity of dendrimers (Fields, 1990). Indeed, the surface of dendrimers provides an excellent platform for the attachment of cell-specific ligands, solubility modifiers, specific amino acids sequences and imaging tags. The ability to covalently bind any or all of these molecules in a well-defined and controllable manner onto a dendritic surface clearly differentiates dendrimers from other carriers such as micelles, liposomes and engineered particles (Lee, 2005).

One example of cell-specific dendron carriers is a dendron modified with RGD (Arg, Gly, Asp) peptide sequence that mediates cell attachment (Forget, 2007). This dendron has been used in order to multiply the presence of the bioactive RGD peptide sequence, to investigate tissue-implant interaction and to favour osteoblast-adhesion. Another example of cell-specific dendritic carrier is a dendron modified with phosphoserine, the most effective functional group in inducing biomineralization in living tissue (Meikle, 2013). This functionalised dendron also acts as a stimulus for the activation of specific signal cascades and promotes the differentiation of adhering progenitor cells into an osteoblastic phenotype. Moreover, dendrons have been functionalised with a VEGF blocker peptide sequence able to inhibit HUVECs proliferation and angiogenesis in the treatment of cancer and avascular tissue (eg. Cartilage, cornea) (Meikle, 2011).

2.1.2 BIOACTIVE LINEAR ANGIOGENIC PEPTIDES

Peptide sequence, or amino acid sequence, is the order in which amino acid residues, connected by peptide bonds, lie in the peptides and proteins chain. The sequence is generally reported from the C-terminal end containing free amino group to the N-terminal end containing free carboxyl group. Bioactive angiogenic peptides that have been already

reviewed in the first chapter and are used to mimic growth factors in their stimulation of the angiogenesis process are:

1) Gln-His-Arg-Glu-Asp-Gly-Ser (Fig.2.1):

Angiopoietin-1 mimicking bioactive peptide is based on the fibrinogen domain of Ang-1 and is identified as the integrin binding site inside the growth factor. Linear peptide derived from this sequence (-QHREDGS) is sufficient to promote cardiomyocyte survival (Rask, 2010). Moreover, Ang-1 mimicking peptide is able to enhance tube formation and assist endothelial cells survival (Dallabrida, 2005).

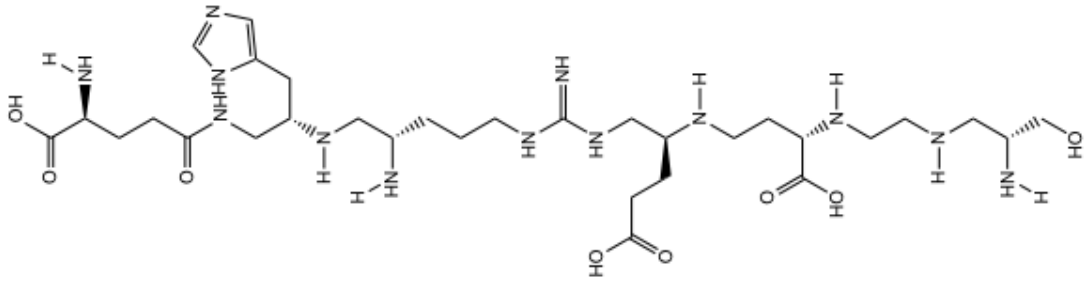

Fig.2.1 Chemical structure of Ang-1 bioactive angiogenic peptide. The synthesis starts from the C-terminal (left side) and continues linearly until the N-terminal (right side).

2) Trp-Gln-Glu-Leu-Tyr-Gln-Leu-Lys-Tyr (Fig.2.2):
VEGF mimicking-peptides is based on a nine amino acids sequence derived from a region of the VEGF binding interface showing similar bioactivity to that of the VEGF. This peptide originates from the region of the VEGF that binds to VEGFR-1 domain 2 and is stabilised by alteration in the amino acids sequence in order to maintain its own bioactivity (D'Andrea, 2005). Regarding its function, VEGF mimicking peptides stimulates blood vessels formation and triggered angiogenic process (Leslie-Barbick, 2011).

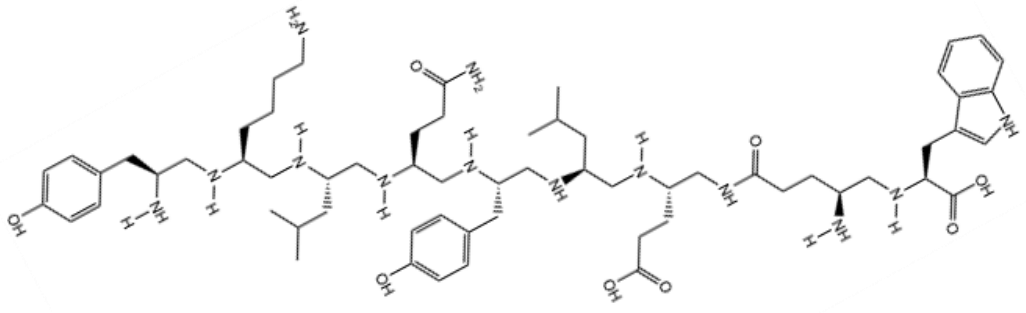

Fig.2.2 Chemical structure of VEGF bioactive angiogenic peptide. The synthesis starts from the C-terminal (left side) and continues linearly until the N-terminal (right side).

3) Arg-Lys-Ile-Glu-Ile-Val-Arg-Lys-Lys (Fig.2.3):

PDGF-BB mimicking bioactive peptide derived from residues in loops I and III of PDGF-BB. This peptide has been identified as the one who is able to maintain the same bioactivity of PDGF-BB (Brennand, 1997). Indeed, PDGF-BB mimicking peptide stabilises blood vessels through mural cells recruitment (Zisch,2003).

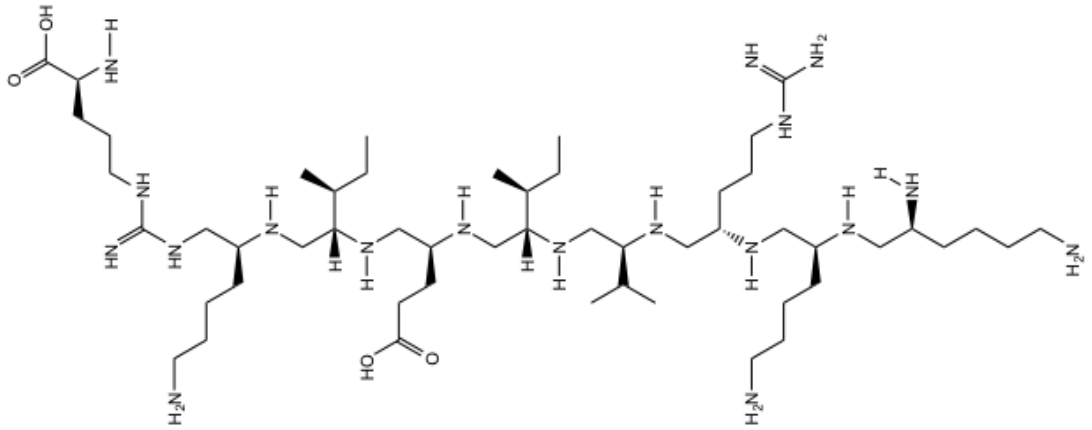

Fig.2.3 Chemical structure of PDGF-BB bioactive angiogenic peptide. The synthesis starts from the C-terminal (left side) and continues linearly until the N-terminal (right side).

Bioactive linear angiogenic peptides have been used widely as linear peptides in order to enhance angiogenesis and myocardial repair (Shim, 2006; Rask, 2010; Chan, 2011). In this project for the first time, bioactive linear angiogenic peptides have been used in conjugation with dendrons in order to create novel macromolecules able to mimic growth factors behaviour and support myocardial regeneration aided by angiogenesis *in vitro*.

2.1.3 AIMS OF THE CHAPTER

The aim of this chapter is to present a general methodology for the synthesis, characterisation and functionalisation of a well-defined class of poly (ε-lysine) dendrons of different generations starting with a diphenylalanine (FF) root. The design of this novel class of branched molecules increases the interaction with the tissue ECM due to the FF molecular root that enhances hydrophobic interactions, whereas the hyperbranched structure acts as a protein scaffold giving the bioactive peptides conformational stability, precise spatial orientation to enhance receptor interaction and capacity to prolong peptide efficiency. Poly (ε-lysine) dendrons have been synthesised through a manual solid-phase peptide synthesis method on a solid resin support using a cleavable linker allowing the easy detachment of the obtained molecules at completion of the synthesis. The same method has been used to functionalised poly (ε-lysine) dendrons with angiogenic peptide analogues. The novel designed molecules have been then characterised by high performance liquid chromatography (HPLC), mass spectrometry (MS) and Fourier transform infrared spectroscopy (FT-IR).

2.2 MATERIALS & METHODS

2.2.1 SOLID-PHASE PEPTIDE SYNTHESIS (SPPS)

Synthesis of all poly (ε-lysine) dendrons of various generations (genX, X=number of branching units) was carried out using a process of solid-phase peptide synthesis designed by our group. This method involves linking various amino acids to a solid resin starting from the carboxyl group terminal and reaching the amino group terminal by repetitions of coupling and deprotection reactions. The process is outlined in Fig.2.4.

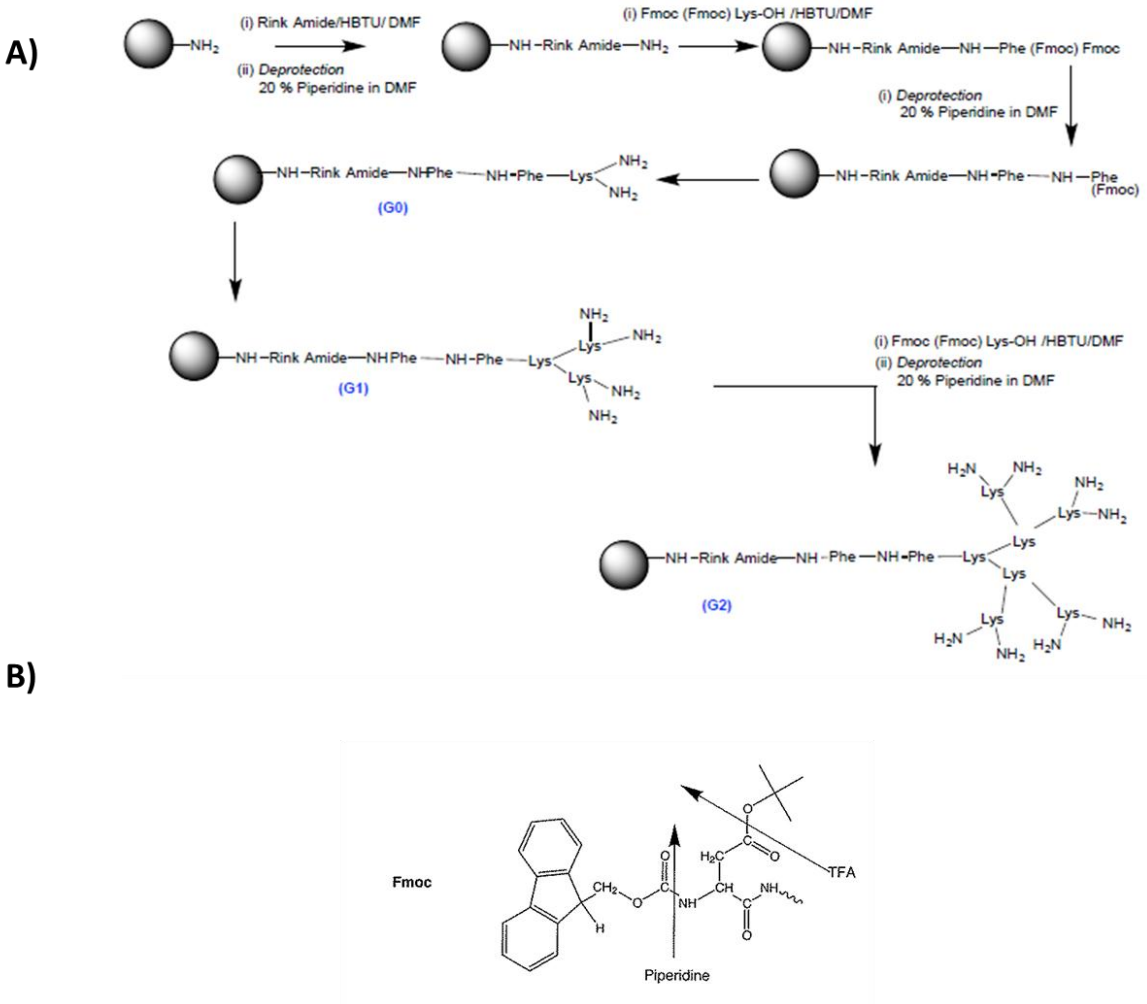

Fig.2.4 SPPS is performed on a Tenta Gel NH_2 resin using Fmoc-α-amine protected amino acids. Resin is swollen to expose functional groups. Then an amino acid is attached to the resin via a linker (Rink Amide), the blocking group is removed during the deprotection step (panel B) and the next amino acid is then coupled to the amino acid-linker-support. These coupling-deprotection steps are repeated until the desired peptide is produced.

In this work, poly (ε-lysine) dendrons were synthesised starting from a Tenta Gel S ($-NH_2$) resin (Iris Biotech GmbH, UK) consisting of polystyrene beads which are 90 μm in diameter. Resin (0.5 g) was swollen by the addition of 3 mL of N,N-dimethylformamide

(DMF, (AGTC Bioproducts, Hessle, UK) in a 10 mL syringe to increase the availability of amine groups on the surface of the resin particles. Separately, a coupling mixture of 3 mL of DMF, 140 µL of N,N-diisopropyl ethylamine (DIPEA, (Iris Biotech GMbH, Germany)), 0.4 mmol of 2-(1H- O-benzotriazole-N,N,N',N'-tetramethyluronium hexafluorophosphate (HBTU) (Novabiochem, Germany) and 0.4 mmol of Rink Amide linker (Iris Biotech GMbH , Germany) was combined and briefly dissolved using a ultrasonicating water bath (Fischerbrand FB11002). DMF was then expelled from the syringe and the Rink Amide coupling mixture was added, briefly shaken and left to react for 30 minutes. During this coupling reaction amide bonds are formed between the carboxyl groups of the Rink Amide linker and the amine groups present on the resin beads. Importantly, the amine groups present on the Rink Amide linker are protected with Fmoc groups, to stop formation of amide bonds between Rink Amide linker molecules. Therefore, due to Fmoc protecting groups, the reaction mixture must then be deprotected after each coupling step, in order to remove these groups and allow amine groups to become available for the next coupling step. After 30 minutes the coupling mixture was removed from the reaction vessel and the resin was washed with 3 mL of DMF; this step was repeated three times. For the first deprotection step, a solution of 20% piperidine (Fisher Scientific, Loughborough, UK) in DMF was prepared and 3 mL were added to the reaction vessel, left for 2 minutes and then expelled. This deprotection step was repeated three times in total, followed by five washes with DMF. This process of one coupling reaction followed by three deprotection steps, was repeated for each coupling reaction, except each consecutive coupling mixture contained 0.4 mmol of an amino acid instead of Rink Amide linker.

Therefore, SPPS method allows the production of a specific sequence of Fmoc-amino acids as summarised in Table 2.1.

Table 2.1 Assembly sequence of FFgen0K, FFgen1K and FFgen2K.

Coupling Step	No. Coupling	Amino Acid (0.4 mmol)	Reactive Sites at Start/ End of synthesis process (mmol)	Molar Excess	Suppliers
Rink Amide	1	Fmoc Rink Amide linker	0.1 / 0.1	4	Iris Biotech GmbH UK
FF	2	Fmoc-Phe- OH	0.1 / 0.1	4	Novabiochem UK
FFgen0K	1	Fmoc-Lys(Fmoc)- OH	0.1 / 0.2	4	Novabiochem UK
FFgen1K	2	Fmoc-Lys(Fmoc)- OH	0.2 / 0.4	4	Novabiochem UK
FFgen2K	4	Fmoc-Lys(Fmoc)- OH	0.4 / 0.8	4	Novabiochem UK

After the formation of the branched structures (Fig.2.5), the synthesis has moved forward in order to form the bioactive linear angiogenic peptides.

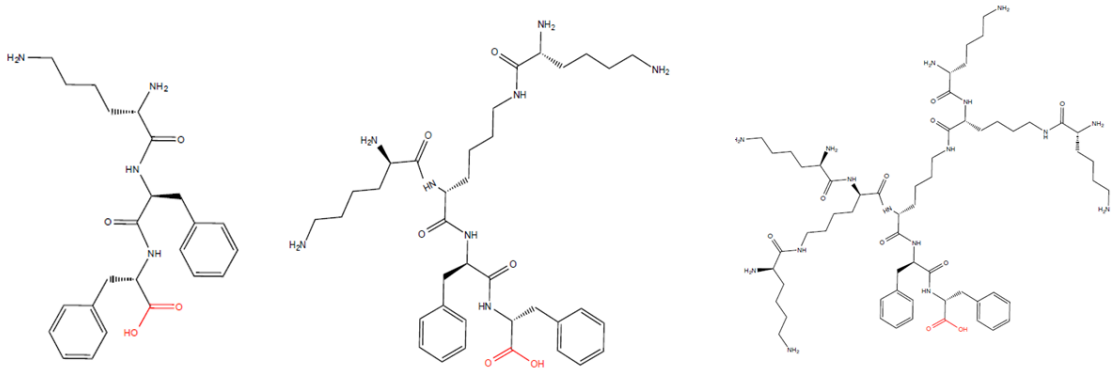

Fig.2.5 Chemical structure of generation 0 (left side), generation 1 (middle) and generation 2 (right side) dendrons. C-terminal is indicated in red.

Therefore, each generation was functionalised with the Ang-1 peptide analogue (-QHREDGS-NH_2) and generation 0 was functionalised with the VEGF (-WQELYQLKY-NH_2) and the PDGF-BB (-RKIEIVRKK-NH_2) peptide analogue building up the peptide directly on the dendrons following the same SPPS method used previously.

The different assembled dendrons tethered bioactive linear angiogenic peptides are listed in the tables below with their consequential assembly steps (Table 2.2 - 2.6).

Table 2.2 Assembly steps of FFgen0K(QHREDGS)$_2$

Coupling Step	No. Coupling	Amino Acid (0.4 mmol)	Molar Excess	Suppliers
FFgen0K	1	Fmoc- Lys(Fmoc)- OH	4	Novabiochem UK
Q (Gln)	1	Fmoc- Gln(Fmoc)- OH	4	Novabiochem UK
H (His)	1	Fmoc- His(Fmoc)- OH	4	Novabiochem UK
R (Arg)	1	Fmoc- Arg(Fmoc)- OH	4	Novabiochem UK
E (Glu)	1	Fmoc- Glu(Fmoc)- OH	4	Novabiochem UK
D (Asp)	1	Fmoc- Asp(Fmoc)- OH	4	Novabiochem UK
G (Gly)	1	Fmoc- Gly(Fmoc)- OH	4	Novabiochem UK
S (Ser)	1	Fmoc- Ser(Fmoc)- OH	4	Novabiochem UK

Table 2.3 Assembly of FFgen1K(QHREDGS)$_4$

Coupling Step	No. Coupling	Amino Acid (0.4 mmol)	Molar Excess	Suppliers
FFgen1K	2	Fmoc- Lys(Fmoc)- OH	4	Novabiochem UK
Q (Gln)	1	Fmoc- Gln(Fmoc)- OH	4	Novabiochem UK
H (His)	1	Fmoc- His(Fmoc)- OH	4	Novabiochem UK
R (Arg)	1	Fmoc- Arg(Fmoc)- OH	4	Novabiochem UK
E (Glu)	1	Fmoc- Glu(Fmoc)- OH	4	Novabiochem UK
D (Asp)	1	Fmoc- Asp(Fmoc)- OH	4	Novabiochem UK
G (Gly)	1	Fmoc- Gly(Fmoc)- OH	4	Novabiochem UK
S (Ser)	1	Fmoc- Ser(Fmoc)- OH	4	Novabiochem UK

Table 2.4 Assembly of FFgen2K(QHREDGS)$_8$.

Coupling Step	No. Coupling	Amino Acid (0.4 mmol)	Molar Excess	Suppliers
FFgen2K	4	Fmoc- Lys(Fmoc)- OH	4	Novabiochem UK
Q (Gln)	2	Fmoc- Gln(Fmoc)- OH	4	Novabiochem UK
H (His)	2	Fmoc- His(Fmoc)- OH	4	Novabiochem UK
R (Arg)	2	Fmoc- Arg(Fmoc)- OH	4	Novabiochem UK
E (Glu)	2	Fmoc- Glu(Fmoc)- OH	4	Novabiochem UK
D (Asp)	2	Fmoc- Asp(Fmoc)- OH	4	Novabiochem UK
G (Gly)	2	Fmoc- Gly(Fmoc)- OH	4	Novabiochem UK
S (Ser)	2	Fmoc- Ser(Fmoc)- OH	4	Novabiochem UK

Table 2.5 Assembly of FFgen0K(WQELYQLKY)$_2$.

Coupling Step	No. Coupling	Amino Acid (0.4 mmol)	Molar Excess	Suppliers
FFgen0K	1	Fmoc- Lys(Fmoc)- OH	4	Novabiochem UK
W (Trp)	1	Fmoc- Trp(Fmoc)- OH	4	Novabiochem UK
Q (Gln)	1	Fmoc- Gln(Fmoc)- OH	4	Novabiochem UK
E (Glu)	1	Fmoc- Glu(Fmoc)- OH	4	Novabiochem UK
L (Leu)	1	Fmoc- Leu(Fmoc)- OH	4	Novabiochem UK
Y (Tyr)	1	Fmoc- Tyr(Fmoc)- OH	4	Novabiochem UK
Q (Gln)	1	Fmoc- Gln(Fmoc)- OH	4	Novabiochem UK
L (Leu)	1	Fmoc- Leu(Fmoc)- OH	4	Novabiochem UK
K (Lys)	1	Fmoc- Lys(Fmoc)- OH	4	Novabiochem UK
Y (Tyr)	1	Fmoc- Tyr(Fmoc)- OH	4	Novabiochem UK

Table 2.6 Assembly of FFgen0K(RKIEIVRKK)$_2$.

Coupling Step	No. Coupling	Amino Acid (0.4 mmol)	Molar Excess	Suppliers
FFgen0K	1	Fmoc- Lys(Fmoc)- OH	4	Novabiochem UK
R (Arg)	1	Fmoc- Arg(Fmoc)- OH	4	Novabiochem UK
K (Lys)	1	Fmoc- Lys(Boc)- OH	4	Novabiochem UK
I (Ile)	1	Fmoc- Ile(Fmoc)- OH	4	Novabiochem UK
E (Glu)	1	Fmoc- Glu(Fmoc)- OH	4	Novabiochem UK
I (Ile)	1	Fmoc- Ile(Fmoc)- OH	4	Novabiochem UK
V (Val)	1	Fmoc- Val(Fmoc)- OH	4	Novabiochem UK
R (Arg)	1	Fmoc- Arg(Fmoc)- OH	4	Novabiochem UK
K (Lys)	1	Fmoc- Lys(Boc)- OH	4	Novabiochem UK
K (Lys)	1	Fmoc- Lys(Boc)- OH	4	Novabiochem UK

Once all functionalised dendrons were synthesised, each sample was washed eight times with 5 mL of dichloromethane (Fisher Scientific, Loughborough, UK), then eight times with 5 mL of methanol (Fisher Scientific, Loughborough, UK) and finally eight times with 5 mL of diethyl ether (Fisher Scientific, Loughborough, UK).

2.2.2 CLEAVAGE OF DENDRON AND FUNCTIONALISED DENDRON FROM RESIN

The completed dendrons were detached from the Tentagel resin via the addition of TFA (trifluoroacetic acid) to break down the Rink Amide linker bonding the peptide to the resin. Two different cleavage solutions (Table 2.7) were used for detaching the produced molecules from the Tentagel resin:

Table 2.7 Composition of the two different cleavage solution used in this work.

CLEAVAGE SOLUTION 1	CLEAVAGE SOLUTION 2
95% TFA	95% TFA
5% Water	2.5% Water
n/a	2.5% TIPS (triisopropylsilane)

Initially, the cleavage solution 1 containing 95% TFA and 5 % of water (HPLC grade, Fisher Scientific, Loughborough, UK) was prepared. Each completed peptide was then weighed and added to a glass-dropping vial and approximately 1 mL of cleavage mixture was added for every 50 mg of peptide mixture. Glass stoppers were then secured onto each vial and these were left for 3 hours. Approximately 1 hour before the completion of this reaction, a plastic centrifuge tube (one for each dendrons type) was weighed (empty) and placed in a box of ice, and 20 mL of diethyl ether was added to each. At this time, a Pasteur pipette was also filled with glass wool and secured over each centrifuge tube with a clamp. Upon completion of the cleavage reaction, each peptide mixture was carefully Pasteur pipetted into the clamped pipettes and filtered into each respective centrifuge tube. This allowed for the resin particles to become trapped in the glass wool and the peptide to precipitate out of cleavage solution.

Samples were centrifuged at 3500 rpm for 5 minutes (Denley BS400, UK). After centrifugation, excess liquid was carefully poured away, to leave a functionalised dendron pellet in the bottom of each tube. These were then, topped up to 20 mL with more diethyl ether, vortexed (Stuart Scientific, Autovortex SA5, UK) and centrifuged again. This step was repeated three times to allow the maximum amount of functionalised dendrons to be removed from the cleavage solution; finally leaving the small pellet at the bottom of each tube. These samples were then left overnight to allow any residual diethyl ether to evaporate off.

At the end of cleavage process, each centrifuge tube was weighed again and the original weights of the empty tubes were subtracted to give the final weight of each functionalised dendrons produced.

The same cleavage method described above has been used also with the cleavage solution 2 (95% TFA, 2.5% water and 2.5% TIPS) in order to verify any differences in dendrons collection.

In conclusion, in this project different dendrons generations have been designed, synthesised and functionalised.

2.2.3 DENDRONS CHARACTERISATION BY HPLC, MS and FT-IR

Every macromolecule produced (dendrons and dendrons tethered bioactive linear angiogenic peptide) was characterised using high performance liquid chromatography (HPLC), mass spectrometry (MS) and Fourier transform infrared spectroscopy (FT-IR).

2.2.3.1 HIGH PERFORMANCE LIQUID CHROMATOGRAPHY (HPLC)

HPLC is an analytical chemistry technique used to separate, identify, and quantify each component in a mixture. It relies on pumps to pass a pressurised liquid solvent containing the sample mixture through a column filled with a solid adsorbent material. Each component in the sample interacts differently with the adsorbent material (solid phase), causing different flow rates for the different components and leading to the separation of the components as they flow out the column. The separation of a mixture of peptides and proteins during an HPLC run is the culmination of two events that occur during the chromatographic process. The first deals with solute retention and has its foundation in the concept of mass distribution along the solid (stationary) phase. Specifically, as solute move down the length of column, carried by a controlled solvent flow rate that is delivered by the HPLC pumps, the individual components of the mixture interact with the mobile phase and stationary phase to different extents (Fig.2.6). The second event involves band (or peak) broadening as the solutes travel down and through the chromatographic matrix. Together, these effects lead to band broadening which progressively increases during the transit through the column (Islam, 2005).

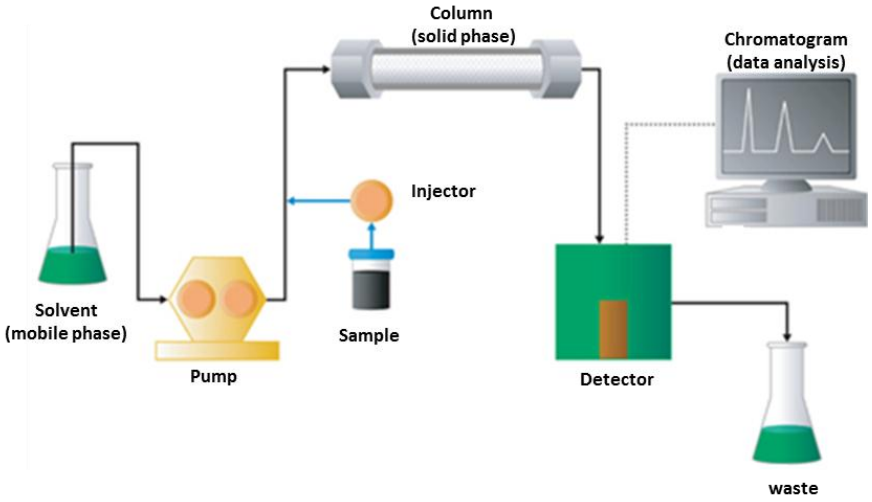

Fig.2.6 Diagram of typical components of HPLC: A solvent is pressurised and pumped in combination with the sample into a column containing a solid material. The sample interacts with this material and the detector records the different flow rate generated by the different interaction sample/solid phase. Data obtained are then analysed and plot in a chromatogram. (Adapted from www.waters.com).

A typical chromatogram is represented in Fig.2.7: here, the concentration of two generic solutes (A and B) eluting from the column, based on the response of the detector, is plotted against time.

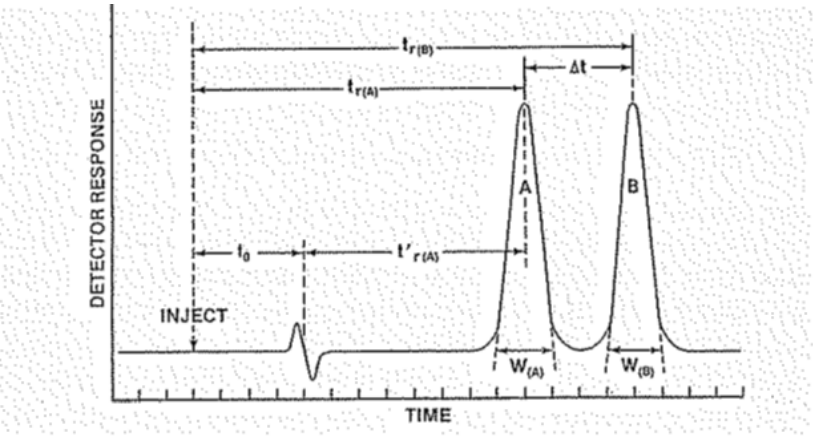

Fig.2.7 Example of chromatogram with most important chromatographic parameter: A and B represent two peaks of two different compounds, t_0 is the elution starting time, $t_{r(A)}$ and $t_{r(B)}$ the retention times. (Adapted from Matsudaira, 1993).

After injection onto an HPLC column, any sample components that do not interact with the stationary phase would elute at time t_0 in the void volume (v_0) which is characteristic for that column. The retention times, $t_{r(A)}$ and $t_{r(B)}$, for the two sample components (Fig.2.7) are the times from injection to the times of maximum concentration in the eluted peaks. Similarly, the retention volumes are the amounts of solvent required for their elution.

The chromatography technique used to analyse dendrons was a reverse phase chromatography (RPC) where the stationary phase used was silica support modified with alkyl chains which provide the hydrophobic surface where separation can take place. Indeed, in this HPLC mode the retention of peptides (dendron in our case) has traditionally been considered to be a function of their relative hydrophobicity. Consequently, the molecule adsorbs onto the hydrophobic surface and remains bound until a sufficiently-high concentration of organic solvent flows through and displace it from the solid support. For the analysis of gen0, gen1 and gen2 the produced dendrons were separated by a standard analytical HPLC method (Waters^{TM} 717 plus Autosampler) performed on a hydrophobic RP 18 column (150 x 4.60 mm, Luna 3u C18 100A, Phenomenex) at 25˚C (Column chiller Model 7955, Jones Chromatography). Chromatograms were recorded on UV detector (SPO-84 6A, Shimadzu) using conditions listed in Table 2.8 and analysed by HPLC software, Total Chrom-TC Navigator.

Table 2.8 HPLC conditions used to analysed FFgen0K, FFgen1K and FFgen2K.

Solvents	Solvent A: deionised water + 0.1% v/v TFA Solvent B: acetonitrile + 0.1 % v/v TFA
Gradient	15 min 20% A and 80% B 3 min 20% A and 80% B 1 min 20% A and 80% B 1 min 0% A and 100% B
Flow rate	1 mL/min
UV-Detection Wavelength	223 nm

2.2.3.2 MASS SPECTROMETRY (MS)

Mass spectrometry and tandem mass spectrometry (MS/MS) analysis are widely used as a technique in protein identification (Wysocki, 2005). Mass spectrometers measure the mass/charge ratio of compounds. The information produced by the mass spectrometer, plots of peak intensities against mass-to-charge (m/z) values, can be analysed and compared with lists generated from "theoretical" digestion of a protein or "theoretical" fragmentation of a peptide. The major tool that enabled examination of protein structure is the soft ionisation techniques in order to 'scatter' biomolecules, in particular electrospray ionisation (ESI) and matrix assisted laser desorption/ionization (MALDI) (Wysocki, 2005). The mass analyser used in this project is a Time -of-flight (TOF) analyser that accelerates the ions by using a short voltage gradient and measure the time ions take to pass through a field free flight tube (Fig.2.8) (Wysocki, 2005).

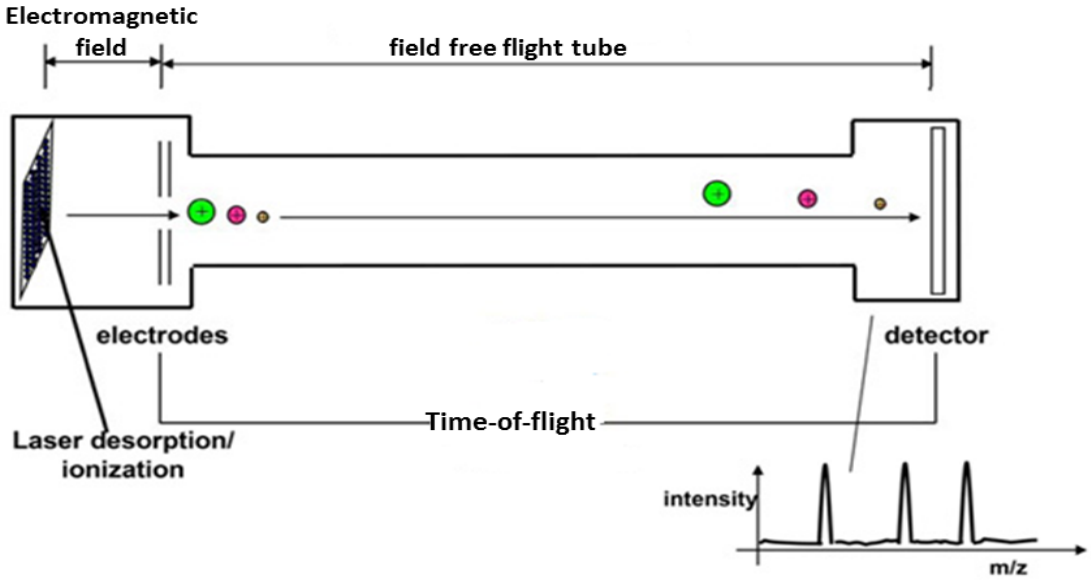

Fig.2.8 Schematic MS: a vaporised sample is ionised. These ions are then forced to pass through a field free flight tube and then separated according to their mass-to-charge ratio, typically by accelerating them and subjecting them to an electric or magnetic field. At the end, different ions were detected and plotted by intensity against m/z (Adapted from www.benthamopen.com).

In this work, the produced molecules were characterised by electrospray/ionisation time of flight (ESI-TOF MS) (Bruker microTOF) following a standard method. The different molecules were dissolved in methanol and pumped into a capillary. In order to allow samples to disperse into a chamber of highly charged droplets, a high voltage of 4kV was applied to the capillary. This process was possible using a nebulising nitrogen gas flowing around the capillary at 0.4 Bar. The charged droplets were then divided through a series decreasing pressure steps and canalised them to form a batch of different products including positive ions. The batch of ions corresponding to each specific compound was then analysed and converts to a molecular weight by a detector system (Fig.2.11). Measurements were performed between 200-3000 Da to be referred to mass-to-charge ratio (m/z). The mass spectrum plots the relative intensity of each compound against the observed m/z ratio. Indeed, each molecular weight is represented by a peak.

2.2.3.3 FOURIER TRANSFORM INFRARED SPECTROSCOPY (FT-IR)

Fourier transform infrared spectroscopy (FT-IR) is a technique which is used to obtain an infrared spectrum of absorption or emission of a solid, liquid or gas sample. An FTIR spectrometer simultaneously collects high spectral resolution data over a wide spectral range. This confers a significant advantage over a dispersive spectrometer which measures intensity over a narrow range of wavelengths at a time (Haris, 1995). The goal of any absorption spectroscopy (e.g. FTIR, ultraviolet-visible ("UV-Vis") spectroscopy) is to measure how well a sample absorbs light at each wavelength. The most straightforward way to do this, the "dispersive spectroscopy" technique, is to shine a monochromatic light beam at a sample, measure how much of the light is absorbed, and repeat for each different wavelength (Haris, 1995).

Rather than shining a monochromatic beam of light at the sample, Fourier transform spectroscopy shines a beam containing many frequencies of light at once, and measures how much of that beam is absorbed by the sample. Next, the beam is modified to contain a different combination of frequencies giving a second data point (Kong, 2007). This process is repeated many times. Afterwards, a computer takes all these data and works backwards to infer what the absorption is at each wavelength. The beam described above is generated by starting with a broadband light source containing the full spectrum of wavelengths to be measured. The light shines into a Michelson interferometer, an array of mirrors, one of which is moved by a motor. As this mirror moves, each wavelength of light in the beam is periodically blocked and transmitted by the interferometer due to wave interference.

Different wavelengths are modulated at different rates so that, at each moment, the beam coming out of the interferometer has a different spectrum (Fig.2.9) (Haris, 1995).

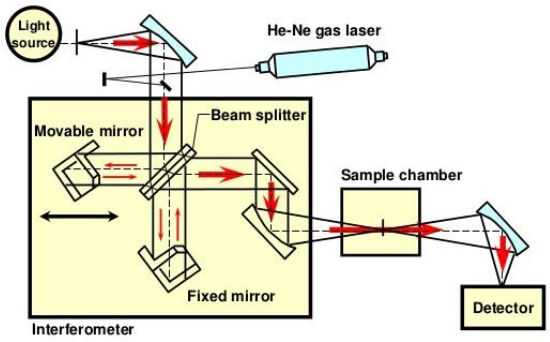

Fig.2.9Mechanism of FTIR operation mode: A beam is generated through a light source in order to have the full spectrum of wavelengths. Then, the light shines into an interferometer in which each wavelength is sequentially blocked and transmitted. Therefore, different wavelengths are processed at different rates and the beam coming out from the interferometer has a peculiar spectrum (Adapted from http://www.slideshare.net/bhavanavedantam/dispersive-ftir).

A data-processing technique called Fourier transform turns this raw data into the desired result (the sample's spectrum): Light output as a function of infrared wavelength (or equivalently, wavenumber). As described above, the sample spectrum is always compared to a reference. Indeed, IR spectroscopy is often used to identify structures because functional groups give rise to characteristic bands both in terms of intensity and position (frequency). The positions of these bands are summarized in correlation tables as shown below.

Table 2.9 Infrared spectroscopy correlation table: each wavenumber corresponds to a particular chemical group. The outcome is the fingerprint of the sample given by the different wavenumber showed in the spectrum that highlights the presence of specific groups (Jackson, 1995).

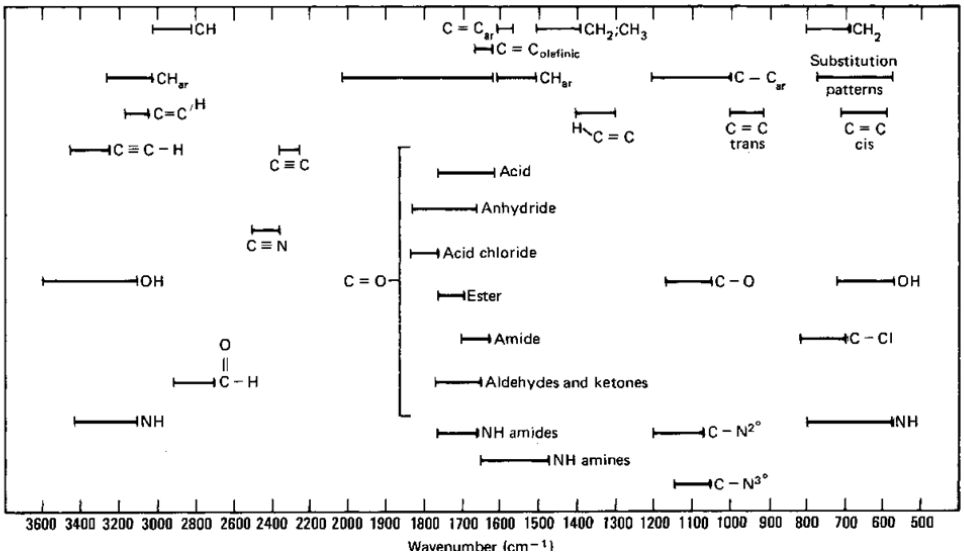

In this work, dendrons and dendrons tethered with bioactive linear angiogenic peptide were analysed using a Perkin Elmer Spectrum 65 FTIR spectrophotometer, fitted with an attenuated total reflectance (ATR) attachment. Each sample was analysed from 4000-650 cm^{-1} for 8 scans at room temperature.

2.3 RESULTS

Several batches of dendrons and dendrons tethered with bioactive linear angiogenic peptide have been produced during the project using a Fmoc SPPS manual mode peptide synthesis (Table 2.10).

*Table 2.10 Summary of the production of dendrons and dendrons tethered bioactive linear angiogenic peptide during PhD project. *The unsuccessful batches refer to those batches where the cleavage solution 1 was used or that were contaminated.*

Poly (Ɛ-lysine) dendron	NUMBER OF BATCHES	NUMBER OF CLEAVAGE	SUCCESSFUL BATCHES	UNSUCCESSFUL BATCHES*	YIELD PER SUCCESSFUL BATCHES (Mean of batches in mg)
FFgen0K	**7**	**21**	**5**	**2**	**100 ± 3.7**
FFgen1K	**4**	**12**	**3**	**1**	**104 ± 2.8**
FFgen2K	**4**	**12**	**3**	**1**	**98 ± 1.7**
FFgen0K(QHREDGS)$_2$	**5**	**15**	**3**	**2**	**101 ± 1.9**
FFgen1K(QHREDGS)$_4$	**4**	**12**	**4**	**0**	**102 ± 2.4**
FFgen2K(QHREDGS)$_8$	**4**	**12**	**4**	**0**	**100 ± 2.6**
FFgen0K(WQELYQLKY)$_2$	**5**	**15**	**4**	**1**	**104 ± 2.1**
FFgen0K(RKIEIVRKK)$_2$	**5**	**15**	**3**	**2**	**97 ± 1.5**

This method has been demonstrated to be an efficient approach for the production of hyperbranched structures, including dendrons. Indeed, FFgen0K, FFgen1K and FFgen2K have been synthesised and efficiently analysed.

Firstly, it is important to address that in the very beginning of the experimental work, the use of a mixture of TFA and water (95:5) as cleavage solution (cleavage solution 1) led to the production of highly impure dendrons.

HPLC chromatograms plotted several elution peaks and showed the existence of multiple impurities, for example in the analysis of FFgen2K (Fig.2.10). Indeed, it is not possible to identify a single predominant peak that represents the produced dendron because it is masked by peaks due to the presence of several impurities.

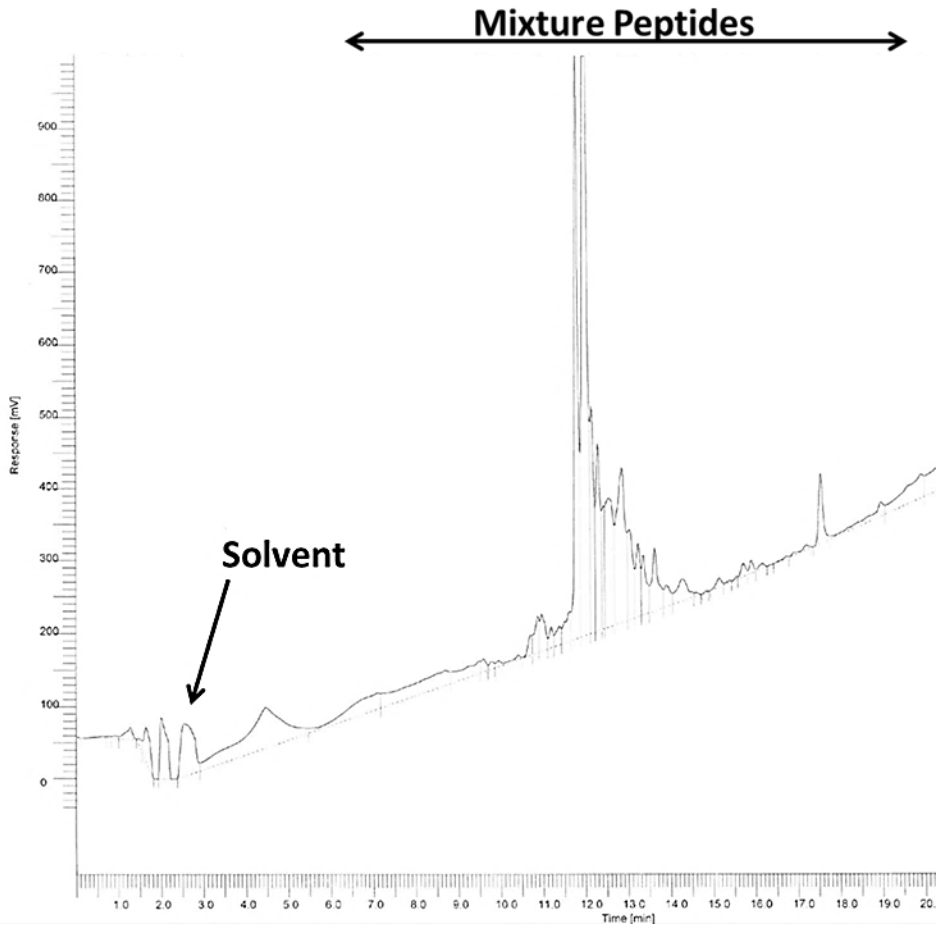

Fig.2.10 Representative HPLC chromatogram of FFgen2K cleaved with cleavage solution 1 (TFA/Water). The presence of several different peaks eluted between 10 and 17 minutes demonstrates the poor purity of the produced dendron limiting the detection of the desired product.

The presence of several impurities when the dendron is cleaved with cleavage solution 1 is confirmed by the MS analysis. Indeed, FFgen2K with a theoretical molecular weight of 1209.7 g/mol is not comparable with just one the peaks produced by MS. Moreover, the peak with the higher relative intensity (745.54 m/z), that frequently in a MS spectrum is representative of the molecule analysed, is characterised by an increased molecular weight of 1026 g/mol compared to that of FFgen2K (Fig.2.11).

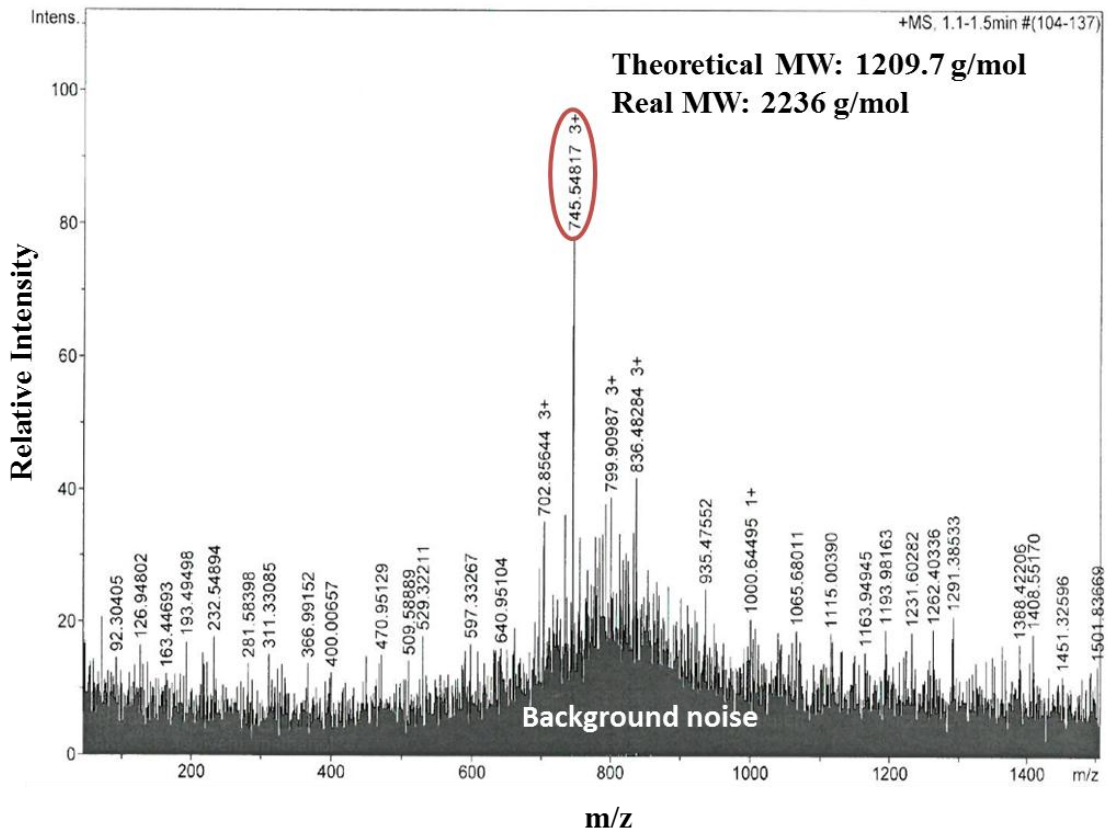

Fig. 2.11 MS spectrum of FFgen2K cleaved with cleavage solution 1 (TFA/Water). The spectrum revealed the presence of a high background noise that make impossible the recognition and so the characterisation of FFgen2K.

It is possible that the use of cleavage solution 1 (95% TFA- 5% Water) did not block side reactions that could occur during the synthesis process, creating aggregates and unwanted molecules. Moreover, the presence of such fragments and impurities leads to a less precise characterisation when using mass spectrometry due to the fact that these artefacts generate much more background noise.

To overcome problems related to the formation of impurity and aggregates a different cleavage solution was therefore used to cleave the dendrons and the dendrons tethered with bioactive linear angiogenic peptide. The new cleavage solution (cleavage solution 2) is composed of 95% TFA + 2.5% Water + 2.5% TIPS. The addition of triisopropylsilane (TIPS) as a scavenger in the cleavage solution stops side chemical reactions, leading to the formation of fewer impurities and to a better characterisation.

The different batches cleaved with the cleavage solution 2 have generated comparable results confirming the reproducibility of molecules synthesis using the SPPS method. For this reason, in the following sections representative results of a single batch of different dendron generations and dendrons tethered with bioactive linear angiogenic peptide obtained with cleavage solution 2 will be reported.

2.3.1 HPLC CHARACTERISATION OF FFgen0K, FFgen1K and FFgen2K

FFgen0K, FFgen1K and FFgen2K were analysed with analytical HPLC. These results of the HPLC analysis demonstrate the effective production of FFgen0K, FFgen1K and FFgen2K, as indicated by a decrease in peak retention time as the molecular weight increases.

Firstly, a single HPLC run with methanol alone (dendrons eluent) (Fig.2.12) was performed in order to distinguish in the following chromatograms peaks generated by the solvent and those related to the molecule being analysed.

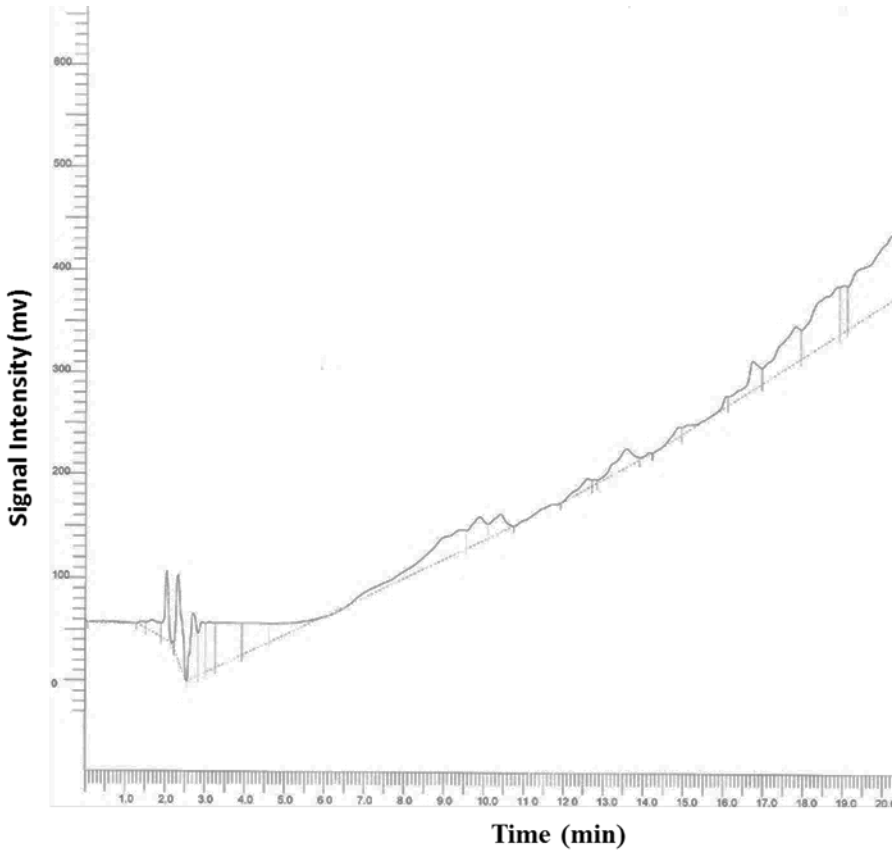

Fig.2.12 Chromatogram of methanol used as a blank being the solvent in which dendrons and dendrons tethered with bioactive linear angiogenic peptide have been dissolved.

Fig. 2.13 shows a chromatogram of FFgen0K. Peaks before 4 minutes are not considered because they represent the solvent peaks (i.e. methanol) (Fig. 2.13) in which the dendrons were dissolved. As can be seen, there is only one predominant peak in the chromatogram with an elution time of approximately eleven minutes. The other smaller peaks can be referred to as some irrelevant impurities that can be found in the methanol chromatogram and so not related to the molecule but instead to the HPLC background readings. However, these small peaks do not overlap at a significant level with the FFgen0K peak.

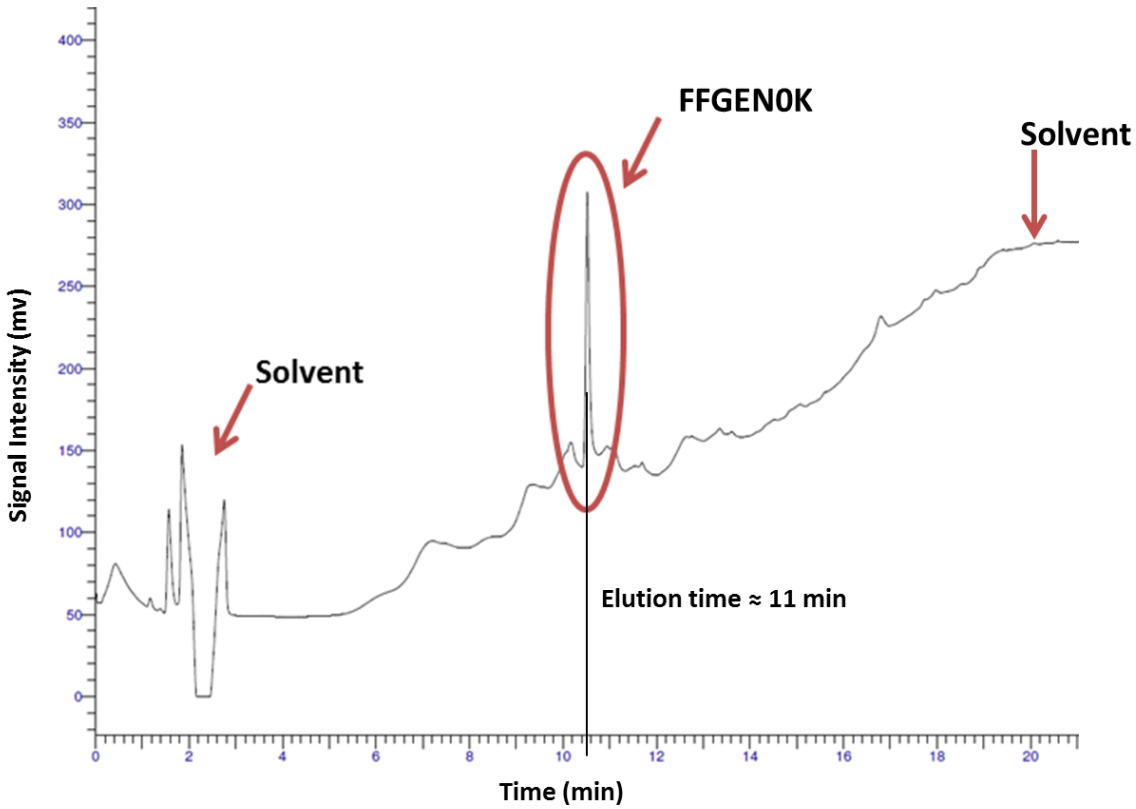

Fig. 2.13 Chromatogram of FFgen0K showing a predominant peak at 11 minutes after sample injection.

The same result has been obtained through the analysis of FFgen1K. Indeed, as for FFgen0K, the first series of peaks were assigned to the solvent, as well as the smaller peaks were linked either to the presence of impurities and/or to the roll-over of the dendrimer repeatidly interacting with the chromatographic medium through the hydrophobic FF root and/or to the possible aggregation of dendrons. The peak assigned to the pure macromolecule was once again well separated by the remaining peaks (Fig. 2.14, Circle). This peak is observed at an elution time of nine minutes because of the larger size of the FFgen1K when compared to that of the FFgen0K where a reduced hydrophobic interaction with the columns solid phase is likely to take place thus taking less time to be eluted from the HPLC column.

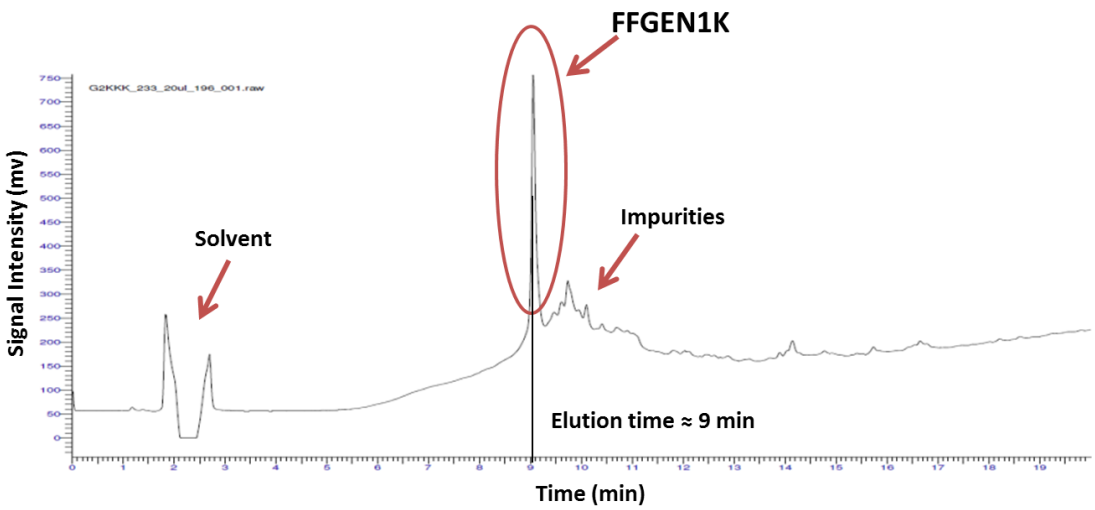

Fig. 2.14 Chromatogram of FFgen1K showing a predominant peak at 9 minutes after sample injection indicating a bigger molecular weight than FFgen0K.

Lastly, FFgen2K has been characterised by HPLC. In Fig. 2.15 it is possible to recognise the same characteristic peak attributable to the solvent. FFgen2K appeared to contain an increased amount of impurities when compared with the previous two chromatograms. This appearance is supported by the relative intensity of these minor peaks that have a higher intensity (Fig. 2.15) if compared to the ones of FFgen0K (Fig. 2.13). However, the main peak with an elution time of approximately nine minutes demonstrated the presence of FFgen2K molecule with a larger molecular weight than FFgen1K (elution time of 11 minutes; Fig 2.15).

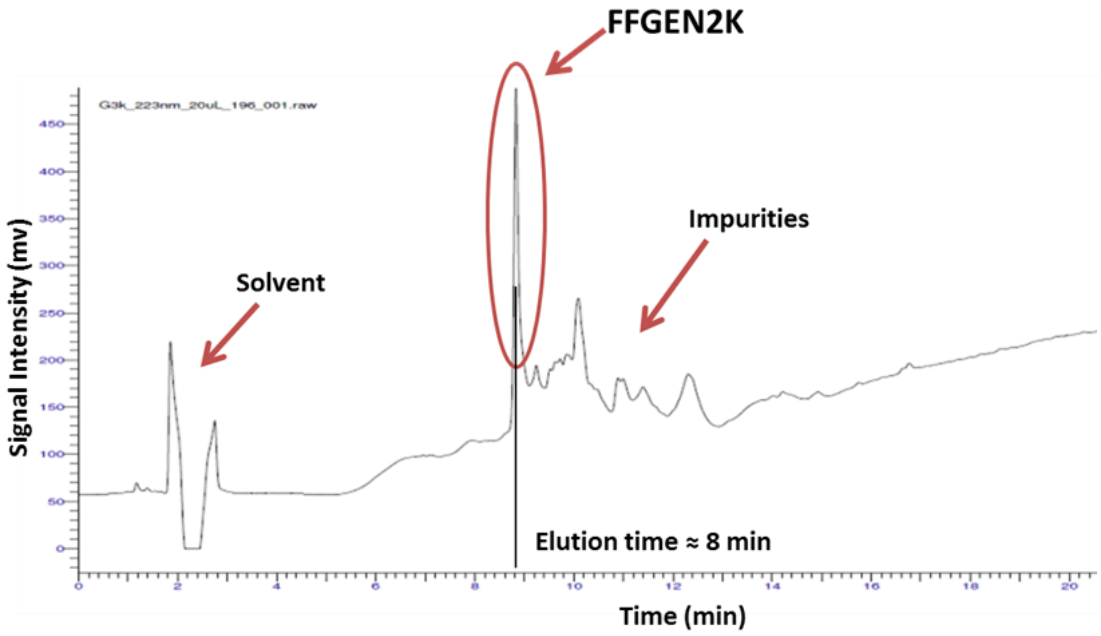

Fig. 2.15 Chromatogram of FFgen2K showing a predominant peak at 8 minutes after sample injection indicating a bigger molecular weight than FFgen1K and FFgen0K.

It is important to note that during the SPPS process, dendrons of higher branching generation are likely to be subject to the production of more impurities. This effect is due to the molar excess of the reagents that must be used in a SPPS divergent method of synthesis and that is accumulated during the synthesis process. For this reason, the presence of the TIPS (scavenger) in the cleavage solution is important.

2.3.2 MS ANALYSIS

Further investigation with MS revealed that the HPLC peaks were generated by different products having an increasing molecular weight. Indeed, Fig. 2.16 shows the mass spectra obtained from the analysis of FFgen0K. As explained previously, a mass spectrum gives a series of mass/charge peaks that can be referred to the analysed molecular weight compound or to some of its fragments. Indeed, the peak with m/z 440.25 (Fig.2.16) corresponds to the $FFgen0K^{+}$ ion; in fact the theoretical molecular weight of FFgen0K is exactly 440.25 g/mol, the m/z ratio that characterised the predominant peak of FFgen0K spectrum. The other two peaks, with a relative intensity much lower than the FFgen0K peak can be referred to some molecule fragment that has been produced during the synthesis process and to the formation of some aggregates of the dendrimer. Indeed, the peak with an m/z of 879.52 almost doubled FFgen0K molecular weight, indicating the aggregation of two FFgen0K molecules and the 276.16 m/z correspond to the root fragment (F-F).

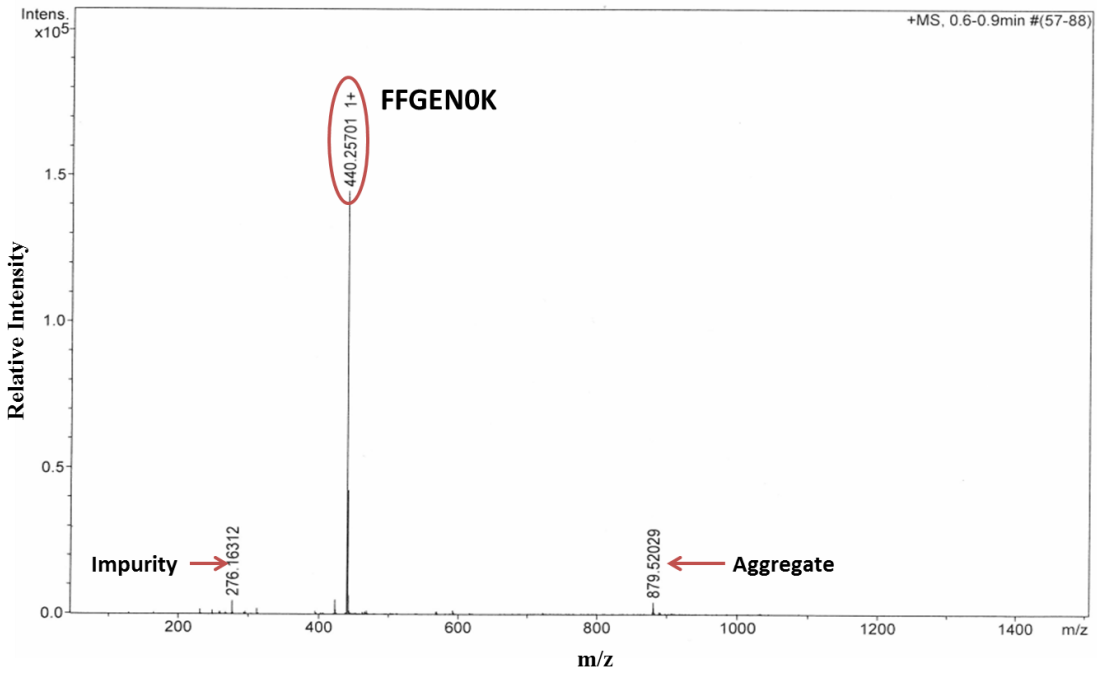

Fig. 2.16 Mass spectra obtained from the analysis of FFgen0K (MW: 440.25 g/mol).

The theoretical molecular weight of FFgen1K is 550.76 g/mol. Regarding FFgen1K mass spectrum, many peaks have been generated through MS analysis (Fig.2.17) symptomatic that some aggregation occurred during the analysis. Indeed, there are peaks with m/z values bigger than the one corresponding to FFgen1K's theoretical molecular weight, for example the 1080.75 m/z peak that corresponds to an aggregate formed of two FFgen1K molecules. Despite this outcome it is still possible to identify the presence of FFgen1K with the 540.87 m/z peak (circled in Fig.2.17) and that is in good agreement with the FFgen1K theoretical molecular weight.

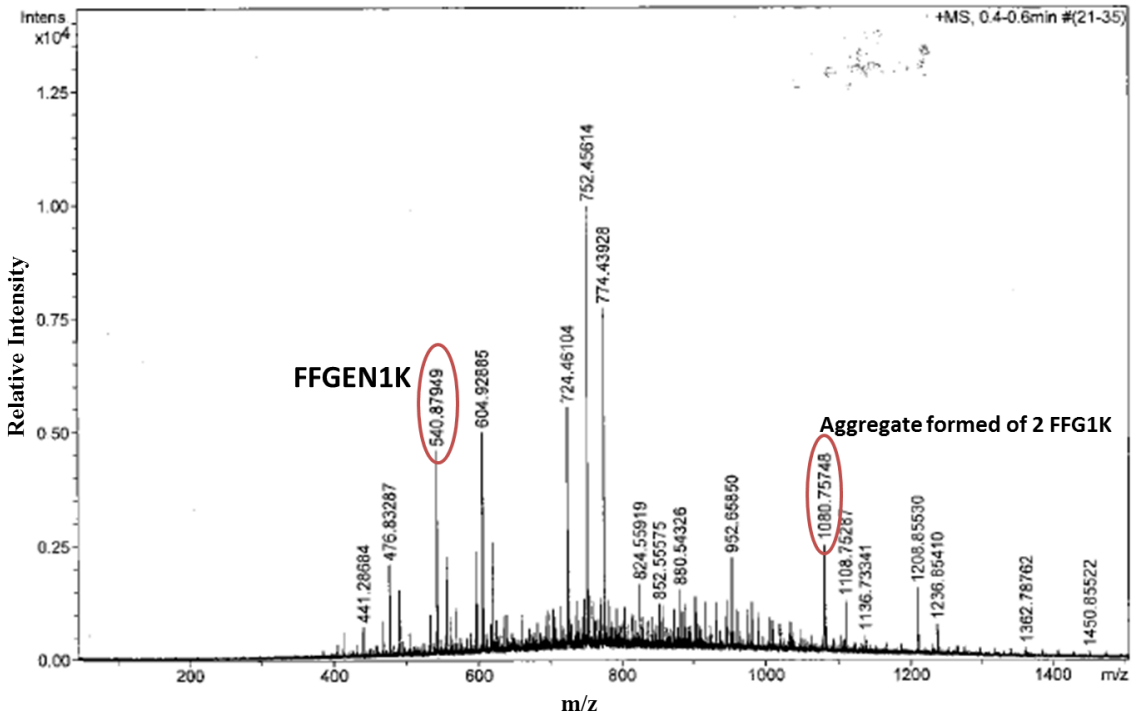

Fig. 2.17 Mass spectra obtained from the analysis of FFgen1K (MW: 550.76 g/mol).

As for FFgen1K, the FFgen2K mass spectrum is composed of several peaks that make the recognition of the FFgen2K peak more difficult (Fig.2.18). In addition is not possible to identify a direct correspondence between one of the generated peaks and FFgen2K.

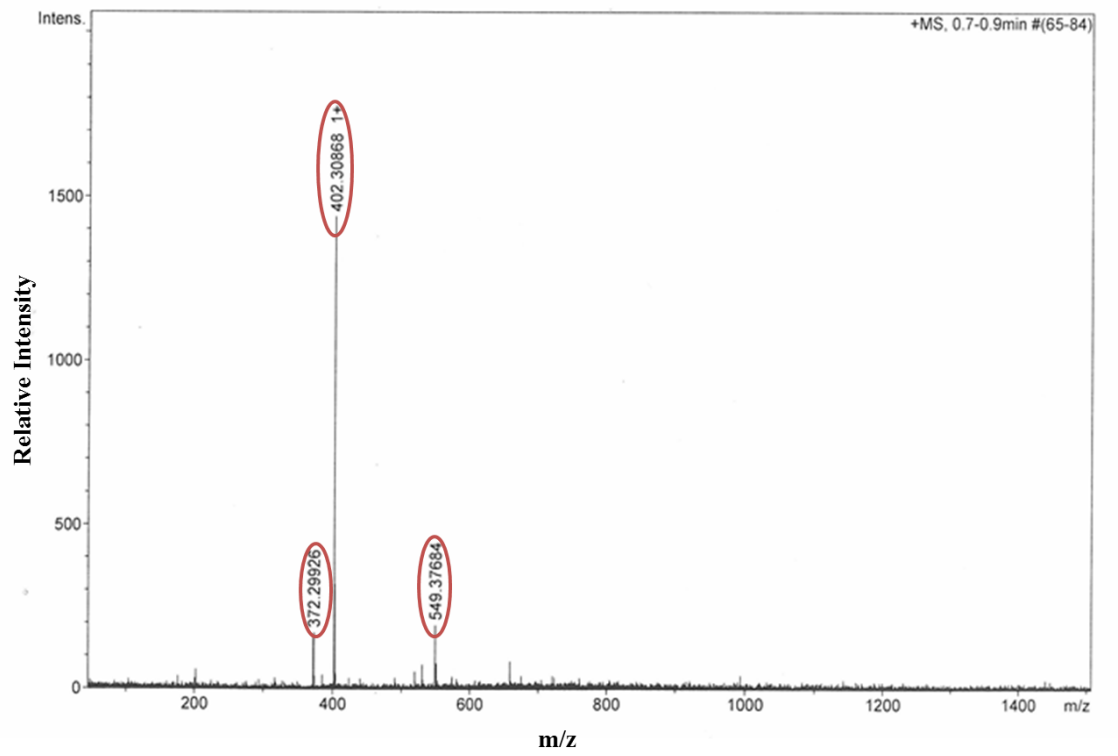

Fig. 2.18 Mass spectra obtained from the analysis of FFgen2K (MW: 1209.7 g/mol).

For this reason, the Protein Prospector Software (PPS) (http://prospector.ucsf.edu/prospector/mshome.htm) has been used to find a direct correspondence of the peaks generated through the mass spectra and the analysed molecule. Indeed, PPS software can analyse the different peaks generated through MS and attribute them to specific linear fragments of the sample. PPS software has classified 372.29 m/z, 402.30 m/z and 549.37 m/z peaks as consequential fragments of FFgen2K (Fig. 2.19). Indeed, the presence of the three peaks shows that the analysed molecule is the one wanted. Indeed, 372.29 m/z peak identify the root of the molecule (F-F-K), 402.30 m/z identify a first fragment (K-K-K) and 549.37 m/z a second fragment (F-K-K-K).

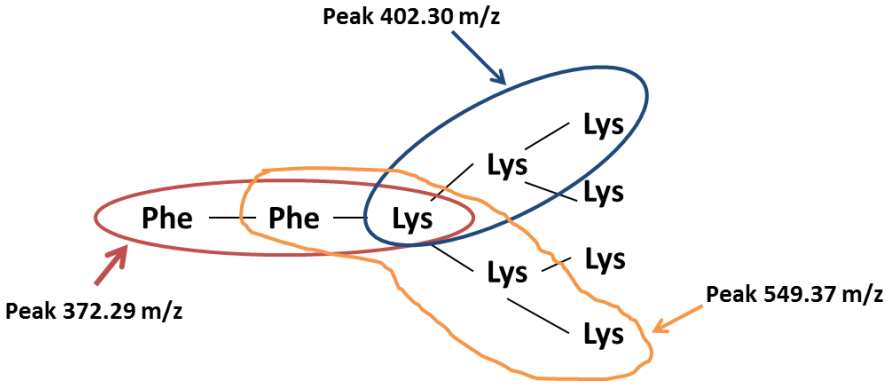

Fig. 2.19 Results of the PPS fragmentation: FFgen2K has been fragmented into three regions (red, blue and orange) to which correspond the three different peaks generated though MS.

MS analysis has also been used for the first validation of the functionalisation of the different dendron generations with the bioactive linear angiogenic peptide. Due to the increase in the molecular weight of these molecules caused by the addition of the bioactive linear peptide every mass spectra has shown the presence of several peaks and so the fragmentation of the analysed molecule. For this reason, PPS software has been used to analyse peaks of each of the following mass spectra.

Fig. 2.20 shows FFgen0K $(QHREDGS)_2$ mass spectrum. In this case, the peaks outlined by PPS software are 402.29 m/z and 731.88 m/z. Indeed, the first peak (402.29 m/z) identify a fragment of the root and the second (731.88 m/z) the consequential ion fragment of the sequence K-Q-H-R-E-D proving the successful occurred synthesis of FFgen0K $(QHREDGS)_2$ as the two peaks correspond to sequential molecule fragments.

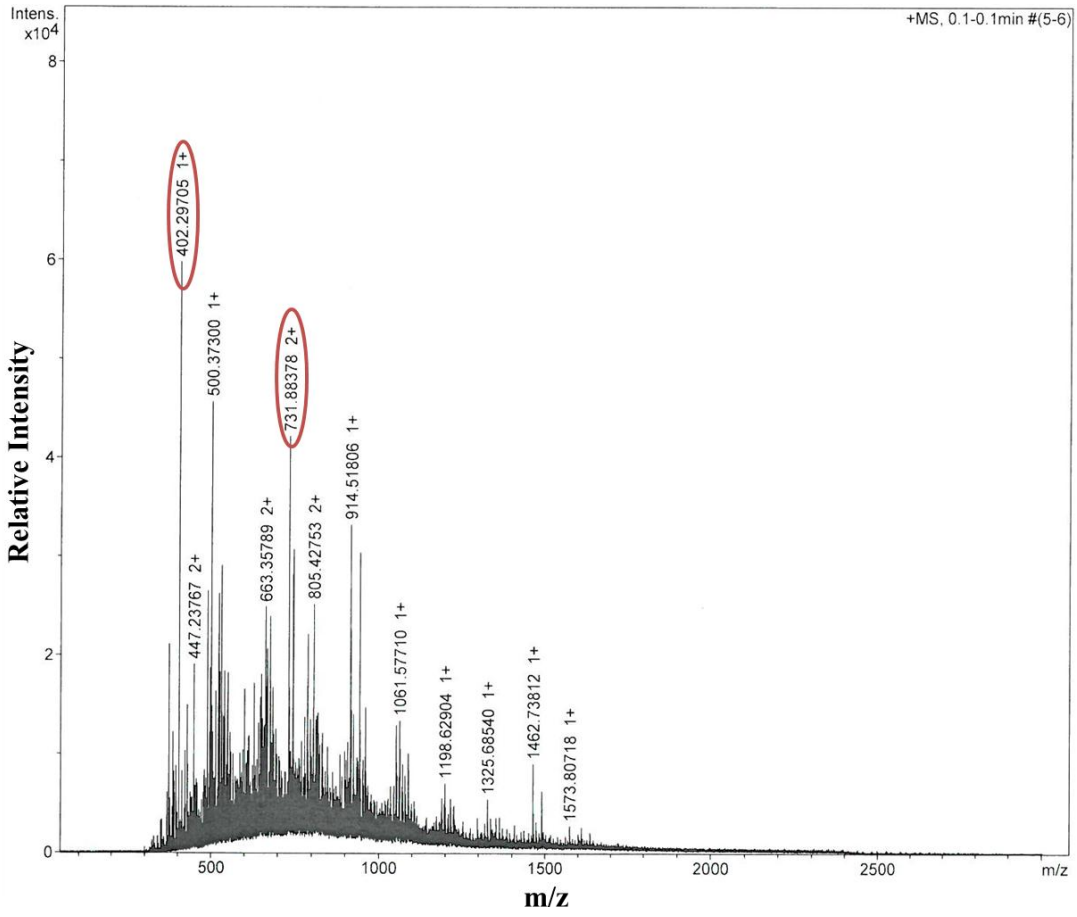

Fig.2.20 Mass spectra obtained from the analysis of FFgen0K(QHREDGS)$_2$ (MW: 1807.87 g/mol).

The same method has been used for the interpretation of FFgen1K$(QHREDGS)_4$ mass spectrum (Fig.2.21).

The peaks corresponding to precise fragments of FFgen1K$(QHREDGS)_4$ outlined by PPS software are: 625.31 m/z, 772.38 m/z, 859.41 m/z and 974.45 m/z.

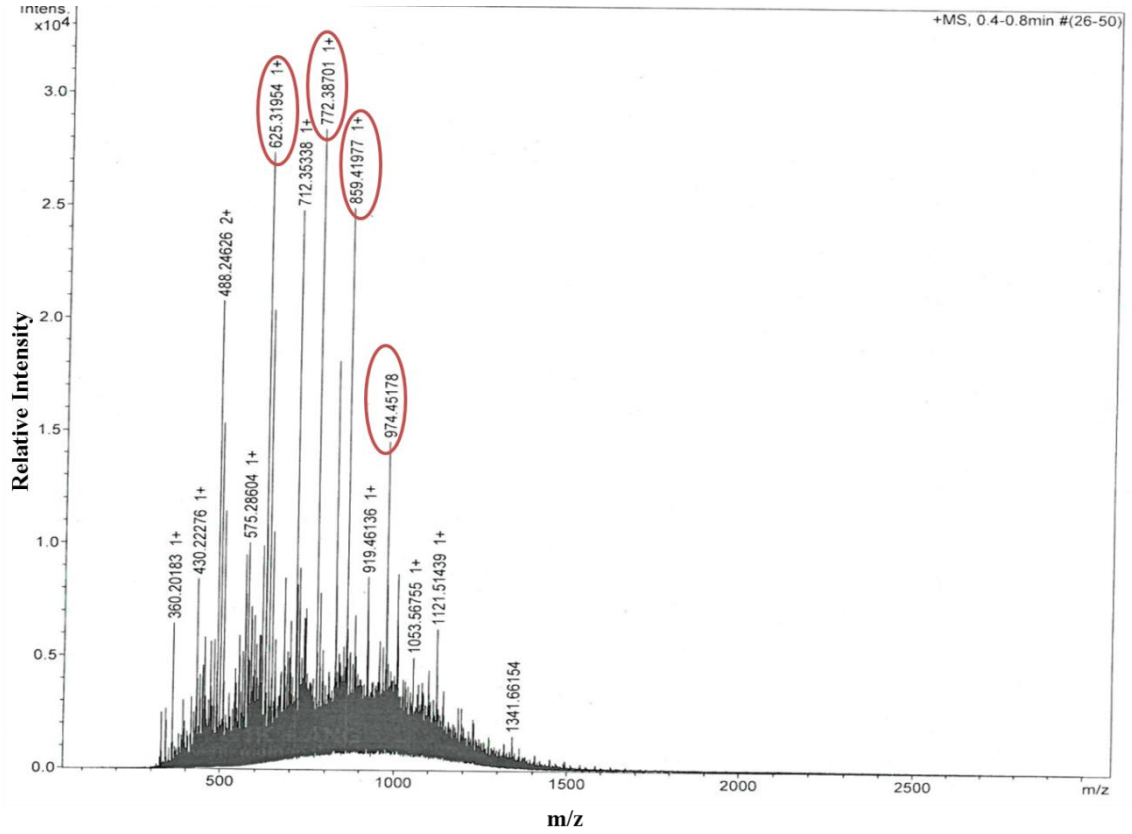

Fig. 2.21 Mass spectra obtained from the analysis of FFgen1K(QHREDGS)$_4$ (MW: 3286 g/mol).

Moreover, the peak that proves the functionalisation of FFgen1K with the peptide is seen at 974.45 m/z: this peak identifies a fragment composed by the bioactive linear angiogenic peptide and two consecutive lysine residues confirming the on-going synthesis (Fig. 2.22).

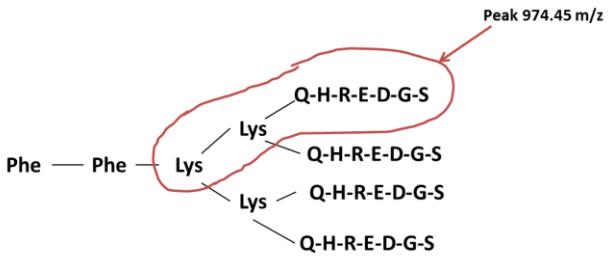

Fig. 2.22 Results of the PPS fragmentation of FFgen1K(QHREDGS)$_4$: the fragment that validates the occurred synthesis is the one composed by the bioactive linear angiogenic peptide and two consecutive lysine residues, that correspond to peak 974.45 m/z generated though MS analysis.

The last dendron generation that has been functionalised with the bioactive linear mimicking peptide of Ang-1 is FFgen2K.

This molecule has a theoretical molecular weight of 6680.98 g/mol, much bigger than the molecules analysed above. Of course, this is due to the higher generation of the dendron

used that exposed eight amino groups and so potentially contains eight bioactive linear angiogenic peptide sequences when functionalised. Despite the good characterisation results obtained for the previous molecules with the MS, the characterisation of FFgen2K(QHREDGS)$_8$ with MS becomes more problematic due to the ionisation techniques (electrospray ionisation) used to volatilise the molecule. Therefore, when molecules with such a high level of ramification, like FFgen2K(QHREDGS)$_8$, are analysed with electrospray ionisation techniques, zones of the molecule could not be ionised and so not detected. Therefore, in the FFgen2K(QHREDGS)$_8$ mass spectra (Fig.2.23) it is possible to identify some fragments, with the help of PSS software, which can be attributed to molecule fragmentations but not to the whole molecule.

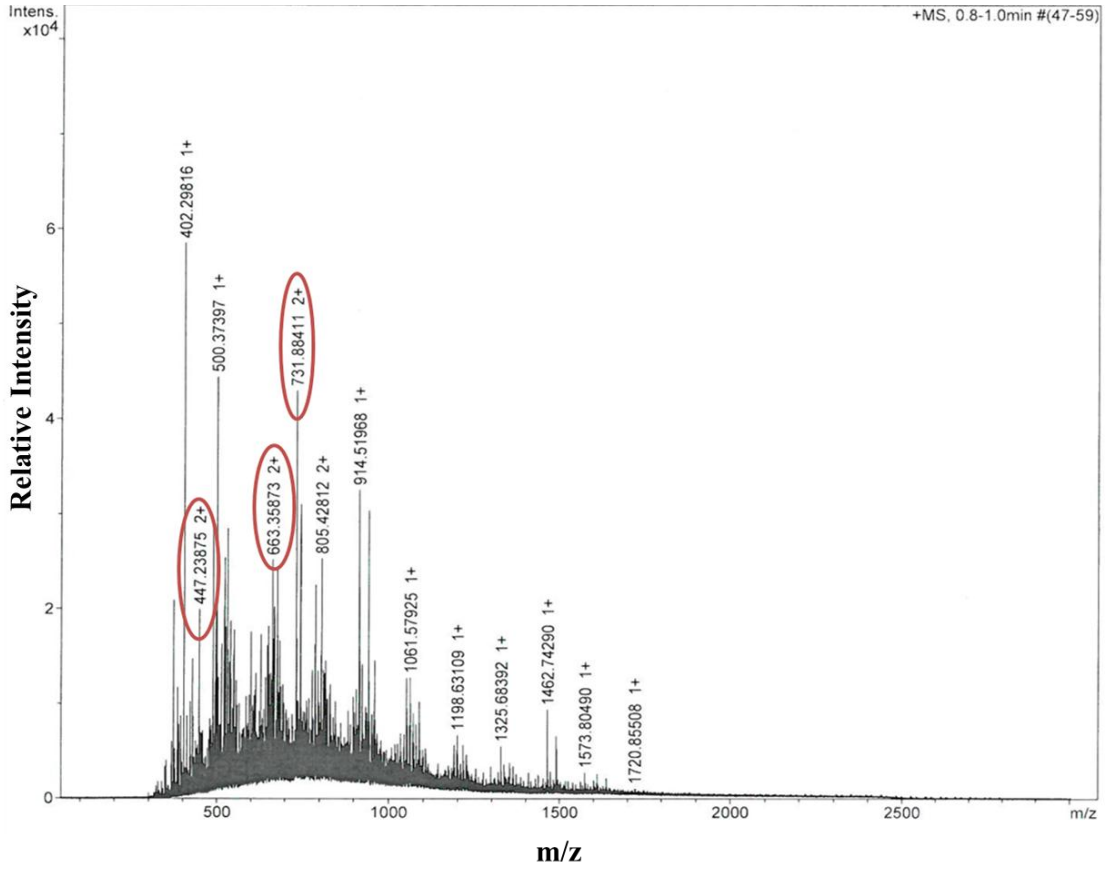

Fig. 2.23 Mass spectra obtained from the analysis of FFgen2K(QHREDGS)$_8$ (MW:6680.98 g/mol). It is possible to identify some peaks that correspond to molecule fragments but not all of them due to the ionisation technique limitations.

The next molecule analysed by MS analysis is FFgen0K(WQELYQLKY)$_2$ (VEGF peptide analogue). Fig. 2.24 shows its mass spectrum. PPS software has highlighted two fragments that correspond to FFgen0K(WQELYQLKY)$_2$, which are 534.77 m/z and 1060.54 m/z. These two peaks identify to distinct fragments of the molecule: 534.77 m/z identifies a fragment composed by Q-L-K-Y sequence that correspond to the last part of the molecule; 1060.54 m/z identifies W-Q-E-L-Y-Q-L-K-Y fragment that correspond to the sequence of

VEGF mimicking peptide confirming the occurred synthesis of FFgen0K(WQELYQLKY)$_2$.

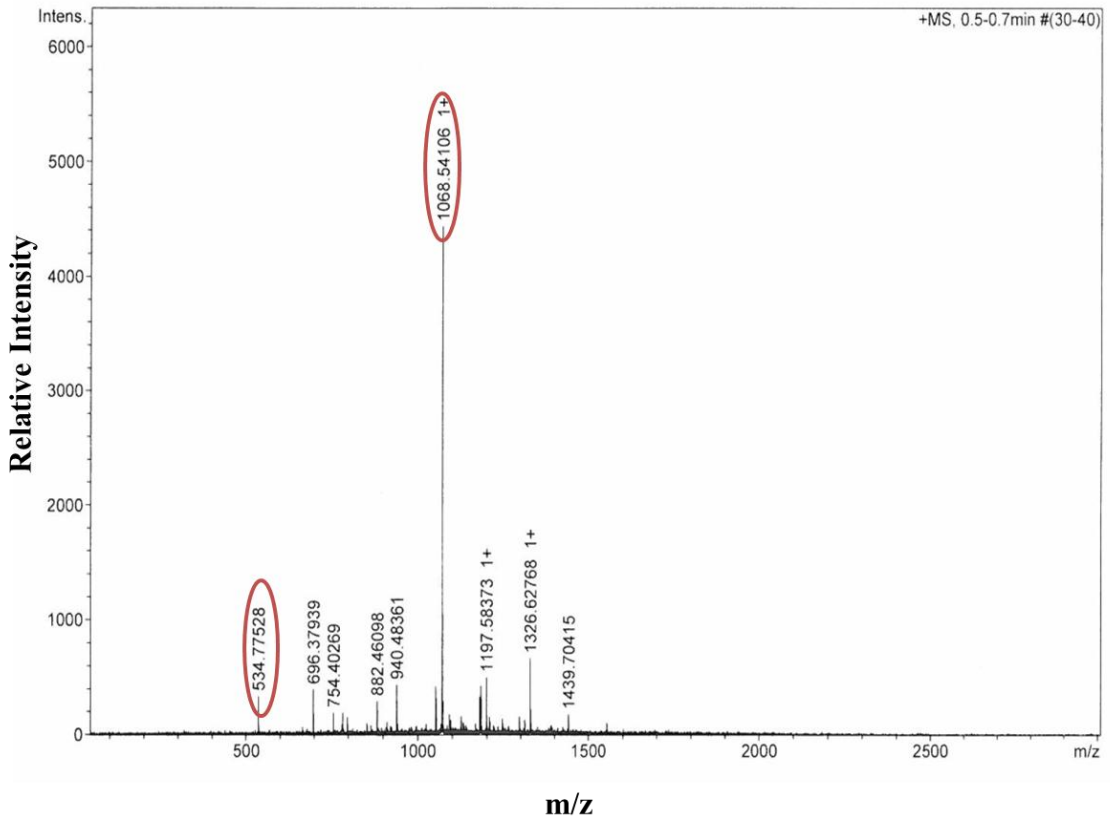

Fig. 2.24 Mass spectra obtained from the analysis of FFgen0K(WQELYQLKY)$_2$ (MW: 2622.93 g/mol).

Lastly, FFgen0K has been functionalised with a PDGF-BB peptide analogue, -RKIEIVRKK and characterised through MS. Fig. 2.25 shows FFgen0K(RKIEIVRKK)$_2$ mass spectra. As already pointed out, when a direct correspondence is not shown in the mass spectra, PPS can be used to identify peaks corresponding to molecule fragments. In this case, the peaks highlighted by PPS correspond to precise consequential fragments of FFgen0K(RKIEIVRKK)$_2$. Indeed, 544.36 m/z identifies the fragment F-F-K-R, which includes the root, and 696.46 m/z that identifies part of the bioactive linear sequences of PDGF-BB that is I-V-R-K-K.

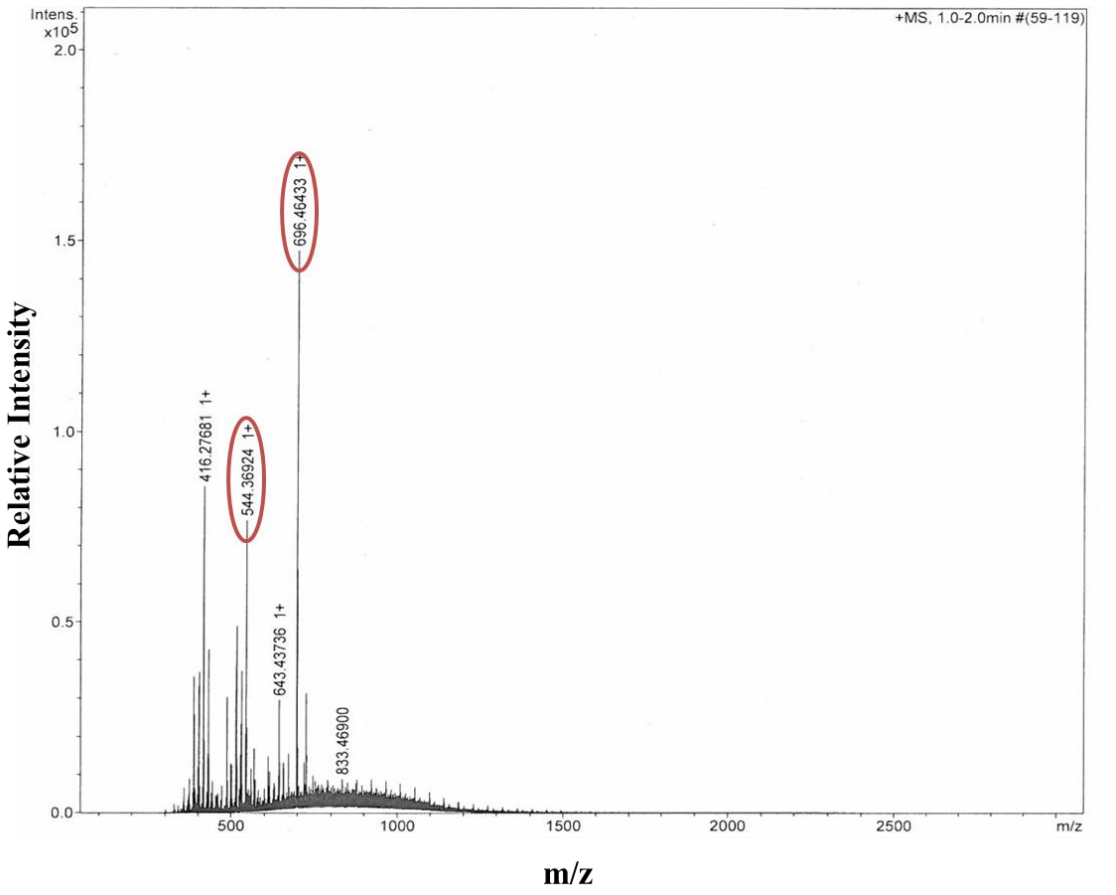

Fig. 2.25 Mass spectra obtained from the analysis of FFgen0K(RKIEIVRKK)$_2$ (MW: 1380.76 *g/mol).*

2.3.3 FT-IR ANALYSIS

FT-IR analysis was used as further confirmation of the results obtained with HPLC and MS regarding dendrons and dendrons tethered with bioactive linear angiogenic peptides. The analysis was conducted comparing dendrons' FT-IR spectra to those obtained from dendrons with tethered bioactive linear angiogenic peptides.

The analysis has been performed in a range of 4000-650 cm^{-1}, however the characterisation results are presented as a zoom of the spectrum from 650 cm^{-1} to 2000 cm^{-1} in order to highlight the fingerprint of each molecule analysed. As already stated in the materials and methods paragraph (Section 2.2.3.3, Table 2.10) the sample spectrum is always compared to a reference.

Starting from the FT-IR analysis of FFgen0K(QHREDGS)$_2$, FFgen1K(QHREDGS)$_4$ and FFgen2K(QHREDGS)$_8$, these three different molecules differ for the branched generation from which the bioactive linear angiogenic peptide, mimicking Ang-1, is attached. Hence, it is easy to state that the occurred functionalisation of dendrons with the bioactive linear Ang-1 peptide is found in the fingerprint of the linear peptide. Therefore, Fig. 2.26, 2.27

and 2.28 show FT-IR spectra of FFgen0K(QHREDGS)$_2$, FFgen1K(QHREDGS)$_4$ and FFgen2K(QHREDGS)$_8$, respectively, where FT-IR spectrum of dendron almost overlaps those of dendrons tethered with the bioactive linear peptide except for the peaks highlighted on the graphs. These peaks are the fingerprint of the presence of –QHREDGS sequence thus confirming functionalisation. Indeed, peaks 873.61 cm^{-1} (Fig.2.26), 879.07 cm^{-1} (Fig.2.27) and 879.07 cm^{-1} (Fig.2.28) can be referred to an alcohol group (-OH) (Fig.2.27) exposed from a serine residue of the Ang-1 peptide analogue that is not present in the FFgen0K, FFgen1K and FFgen2K spectra; peaks 1350 cm^{-1} (Fig. 2.26), 1349 cm^{-1} (Fig.2.27) and 1351 cm^{-1} (Fig. 2.28) identify the presence of an Alkene (C=C) group that correspond to the side group exposed from the histidine residue present in the QHREDGS sequence.

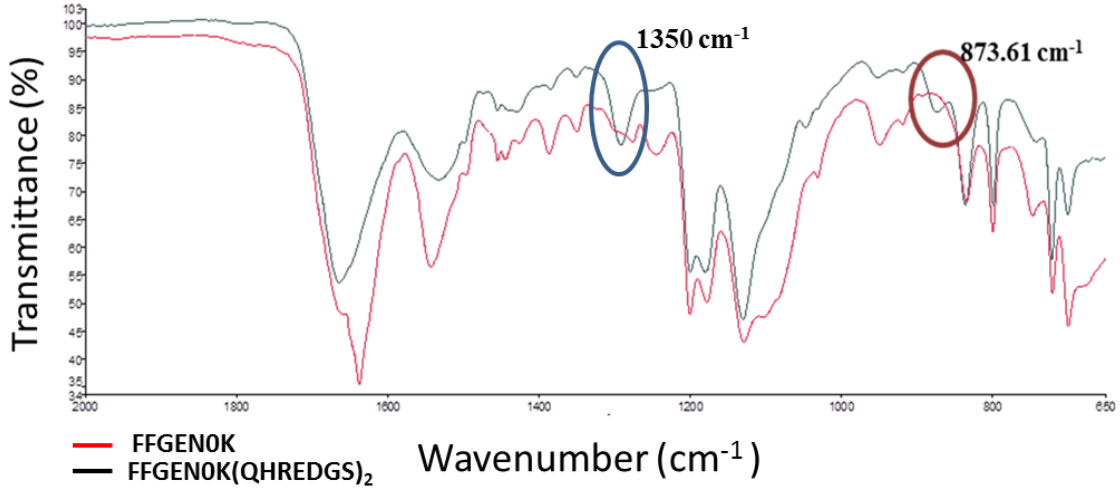

Fig. Fig. 2.26 Fingerprint region of FT-IR spectra of FFGEN0K (red line) and FFgen0K(QHREDGS)$_2$ (black line).

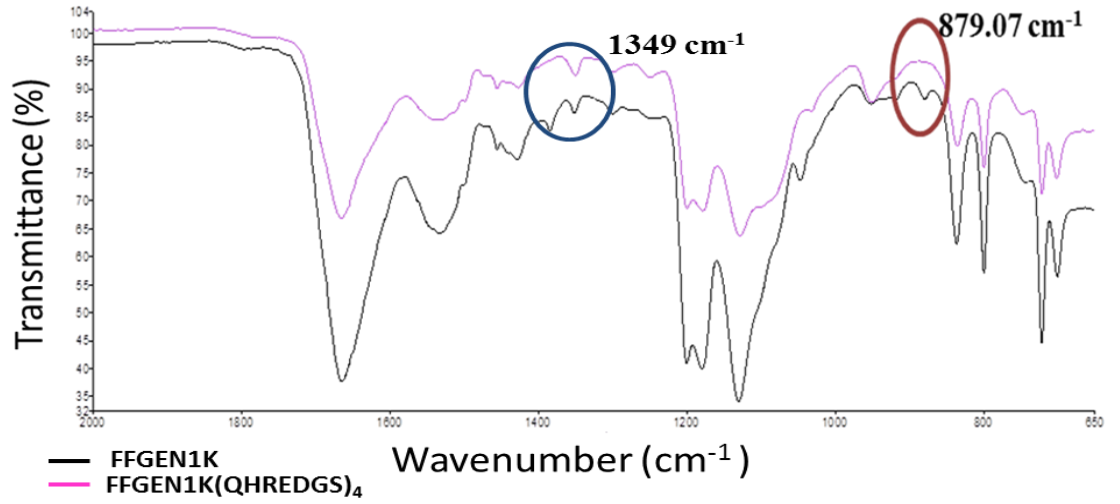

Fig. 2.27 Fingerprint region of FT-IR spectra of FFgen1K (black line) and FFGEN1K(QHREDGS)$_4$ (pink line).

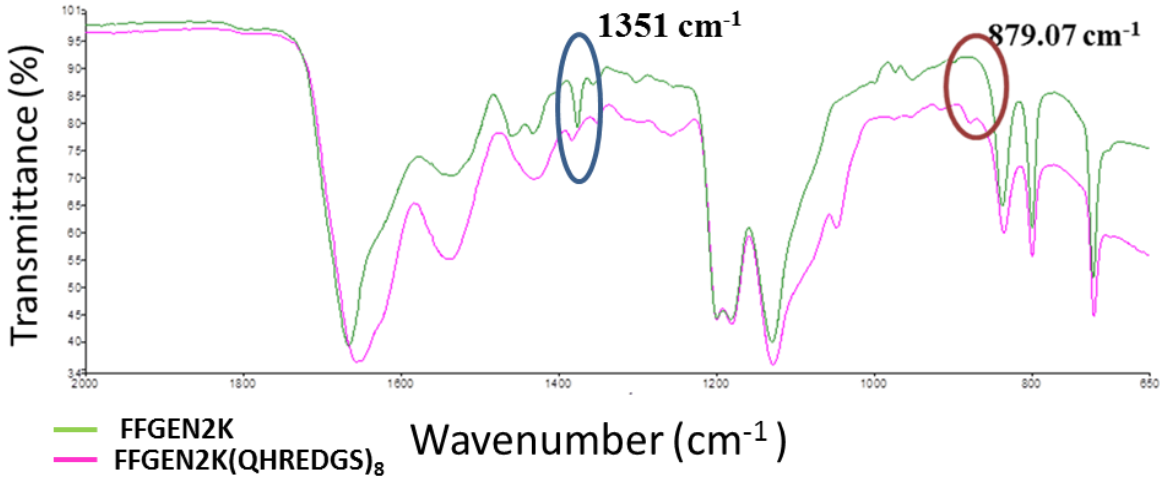

Fig. 2.28 Fingerprint region of FT-IR spectra of FFgen2K (green line) and FFgen2K(QHREDGS)$_8$ (pink line).

The presence of these two peaks, that is not recognisable in the dendrons spectra, supported the occurred synthesis of the bioactive linear peptide sequence of Ang-1 on the different dendron generations. Moreover, the serine residue that exposes the alcohol group is the last one of the linear peptide sequence. Therefore, FT-IR analysis confirms and validates the synthesis of dendrons with tethered Ang-1 bioactive linear peptide.

FT-IR analysis has also been used also to verify the functionalisation of FFgen0K with the -WQELYQLKY bioactive peptide. Spectra of FFgen0K (Fig.2.29, pink line) and of FFgen0K(WQELYQLKY)$_2$ (Fig.2.29, purple line) differ from each other by the presence of a peak at 1454.96 cm^{-1} in the FFgen0K(WQELYQLKY)$_2$ sample due to the presence of an amide group that belongs to the glutamine residue present in the VEGF bioactive peptide, proving the functionalisation of FFgen0K with the peptide.

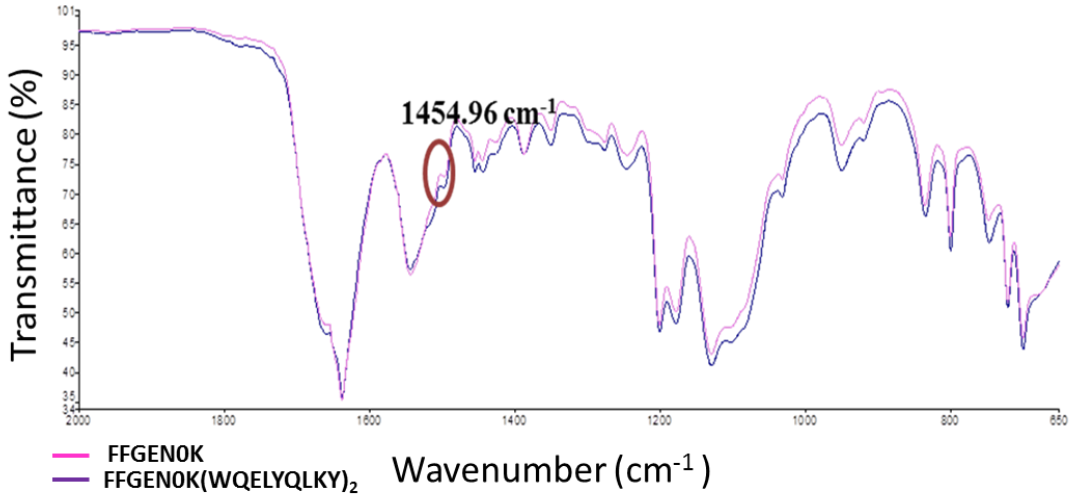

Fig. 2.29 Fingerprint region of FT-IR spectra of FFgen0K (pink line) and FFgen0K(WQELYQLKY)$_2$ (purple line).

The last molecule analysed by FT-IR analysis is FFgen0K(RKIEIVRKK)$_2$. Fig. 2.30 shows the spectrum of FFgen0K (orange line) and of FFgen0K(RKIEIVRKK)$_2$ (green line). In this case, the fingerprint of FFgen0K(RKIEIVRKK)$_2$ that makes it different from FFgen0K, proving that the functionalisation has occurred is the amide group. This group is a side group of a valine residue that is one of the amino acids present in the PDGF-BB peptide analogue.

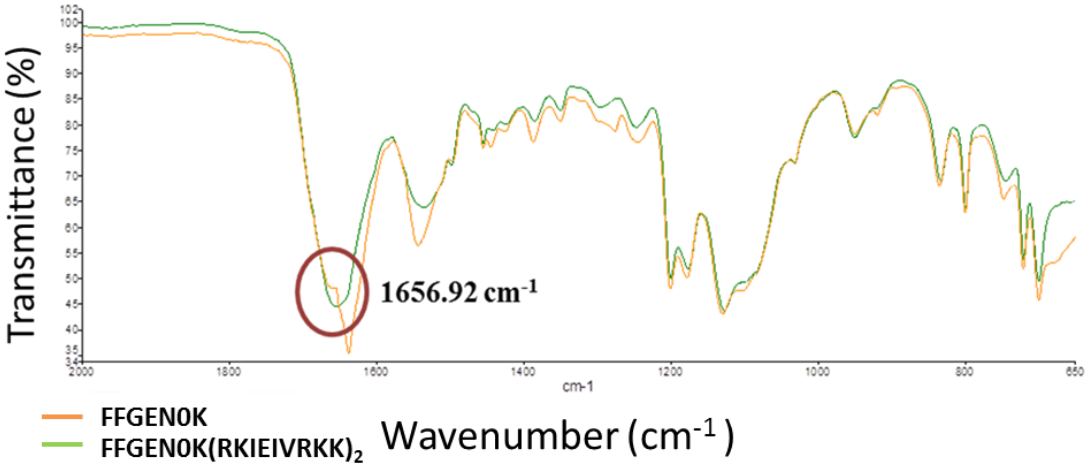

Fig. 2.30 Fingerprint region of FT-IR spectra of FFgen0K (orange line) and FFgen0K(RKIEIVRKK)$_2$ (green line).

2.4 DISCUSSION AND CONCLUSIONS

The aim of this chapter was to explain the methodology used to design, synthesise dendrons and angiogenic linear bioactive peptides and to present the experimental results obtained for the synthesis, functionalisation and characterisation of a well-defined class of poly (ε-lysine) dendrons of different generations.

Dendrons have been used in regenerative medicine applications as carriers or delivery system for decades (Bosman, 1998). The main features that make this a class of macromolecules of great pharmaceutical interest are their capability to be functionalised with a range of different bioactive moieties, from growth factors to drugs (Crampton, 2007) and the ability to give a spatial organisation to these bioactive molecules in order to achieve their improved interaction with the target site (e.g. a cell receptor). Indeed, several dendritic molecules can be designed and produced having peculiar physiochemical and biological properties to be specific for individual clinical applications (Oliveira, 2010). Therefore, generation three dendrons have been used to tether phosphoserine and create a biomimetic coating on titanium surfaces to induce biomineralisation and bone regeneration (Meikle, 2014). Another application includes dendrimers combined with cisplatin, an antitumor drug, as a novel approach to cancer chemotherapy (Malik, 1999; Kesavan,2015; Nguyen, 2015) and there are a large number of reviews regarding the production of dendrimers for various clinical applications (Crampton, 2007; Svenson, 2012; Lee, 2005). It is clear that the design of the branched molecule and the synthesis method have a central role when related to the final application.

The synthesis of dendrimers and dendrons had to face a series of problems when precise nanoscale shape and chemical properties were required in medical applications like gene therapy and drug delivery (Bai, 2006). Indeed, during the synthesis process the risk of side reactions, formation of impurities and molecules folding was so high that it prevented dendrimers and dendrons from being successfully synthesised and finally commercialised (Kandhare, 2012). Many attempts have been made to overcome these problems, like the use of an alternative synthesis method that is the solid-phase peptide synthesis (SPPS) (Zhang, 2008). SPPS gives the possibility to build either linear or branched molecules starting from a solid support (resin) and attach N-α- derivatives amino acids via a linker (Mitchell, 2008). For this reason, SPPS has proven to be the method of choice for producing peptides and small proteins of specific sequences (Bosman, 1998). However, disadvantages related to incomplete reactions, side products, steric hindrance and long reactions time persist (Shin, 2005).

In this work, in order to overcome the above-mentioned problems related to the use of SPPS method, a manual mode has been used to synthesise dendrons and dendrons tethered with bioactive linear angiogenic peptides. Effectively, a manual SPPS method allows the productions of different batches simultaneously and direct control over all the reaction steps and reproducibility resulting in a significant manufacturing advantage for future industrial applications in terms of simultaneous synthesis of different molecules.

The great potential of solid-phase peptide synthesis method is to allow any kind of design and so to produce molecules with a high level of specificity for the final clinical application. The benefit of dendrons is in their precise design: the root can be produced to be suitable to grafting on biomaterial surfaces like polymeric, metallic or ceramic or to have a biological cue and so able to interact with biological structures such as those of macromolecules of the ECM; the end groups can work as a platform for exposing specific moieties, like drugs and bioactive peptide sequences in an orderly spaced manner.

In this work, for the first time, different poly (ε-lysine) dendrons have been designed specifically to target myocardial ischemic tissue presenting a dual functionality (Fig. 2.31). Firstly, the root has been designed to expose di-phenylalanine residues capable of interacting with the ECM by a physical interaction: these residues have the characteristics to be relatively hydrophobic thus increasing the retention in the ECM favouring the interaction with some of its specific components positively charged (i.e. collagen,) (Perugini, 2011). Indeed, the aim of using di-phenylalanine residues is to simulate the in vivo conditions: the majority of the ECM and basement membrane protein (i.e. laminin) forming the blood vessels wall are highly hydrophobic thus more stable to enhance (i) biomolecular recognition between dendritic angiogenic peptides and endothelial cells and (ii) a more controlled release of the bioactive molecule (Karuppuswamy, 2014).

As ECM has a fundamental role in the earliest events that leads to the interactions between synthetic molecules and host tissue (Daley, 2008), the production of molecules able to interact with this structure and mimic it have the potential to improve the therapeutic efficacy of any novel bioactive compound.

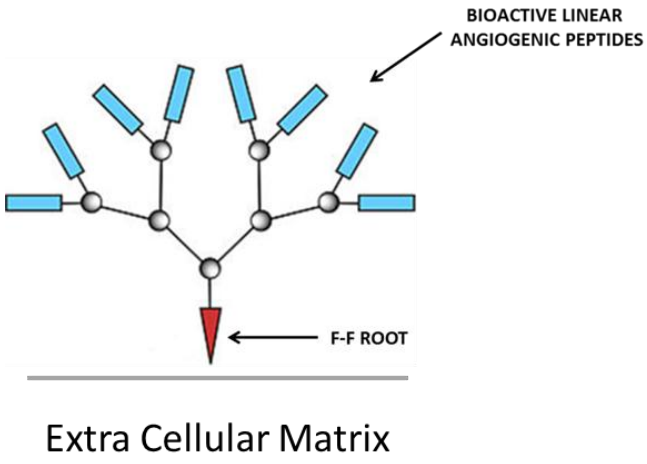

Fig. 2.31 Schematic representation of a poly (ε-lysine) dendron designed starting from a root able to interact with tissue ECM and that exposes bioactive linear angiogenic peptide specific for myocardial ischemic tissue regeneration.

Secondly, as the peripheral dendrons surface allows the attachment of a wide range of moieties it can act as a platform to present specific physicochemical and biological cues. Indeed, in this project dendrons have been used as protein scaffolds to expose bioactive linear angiogenic peptide capable of inducing a precise biological response on targeting cells. Additionally, every dendron generation has been designed and produced in order to maximise the interaction between the growth factor analogue and their receptors as it occurs for the natural growth factors. This means that FFgen0K has been synthesised to provide a bulk support to VEGF and PDGF-BB peptide analogues because FFgen0K exposes two amino groups that can be functionalised with the relative growth factor analogues and enhance the interaction with their relative receptors through their dimerization within the cell membrane (Fig 2.32). For example, VEGF binds to two different receptors (Kinase dependent receptors (KDR) and Flt-1) dimerising them within the plasmalemma and leading to the formation of the complete and functional VEGF receptor, VEGFR (Ferrara, 2003).

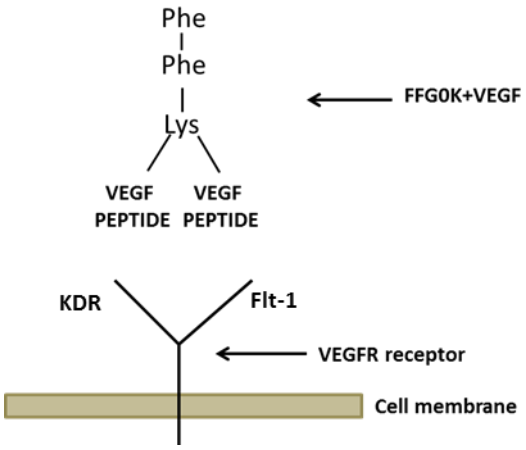

Fig. 2.32 Schematic representation of the theoretical interaction between VEGFR1 receptor and generation zero dendron tethered with a bioactive linear peptide sequence mimicking the natural VEGF.

Regarding the exposure of the Ang-1 peptide analogue, a different approach was adopted as Tie-2 and Ang-1 receptor do not dimerise so the selection of the best dendron generation to be used has been thoroughly investigated through *in vitro* testing (Refer to Chapter 5). Therefore, different dendron generations (FFgen0K, FFgen1K and FFgen2K) have been functionalised to present the Ang-1 peptide analogue to the cells at different degrees of local density and spacing.

Subsequently, the molecules produced have been characterised to prove that the synthesis occurred giving the desire products. Indeed, HPLC, MS and FT-IR have been used as characterisation technique.

Several characterisation techniques have been used in the past decades in order to analyse proteins: one of the most commonly used is gel filtration in combination with high concentrations of organic acids or denaturants (Gibbs, 2004). Despite the wide use of this technique the employment of acid solution makes it less accurate for the detection of peptides because these solutions are not transparent when analysed at the wavelength of peptide detection. Therefore, HPLC has become the separation method of choice in the protein chemistry field (Mahoney, 1980). Indeed, a considerable number of studies have included HPLC analysis for the identification and isolation of proteins and small peptide (Girgin, 2013; Gibbs, 2004). For this reason, a reverse phase HPLC method has been used as a method of choice for the characterisation of dendrons (Kantchev, 2008). Comparing HPLC results (Section 2.3.1), it is apparent how an increase in the molecular weight of the different molecules (from FFgen0K to FFgen2K) led to a decrease in peak retention time from ≈11 min to ≈8 min. This behaviour is due to the hydrophobic interaction that occurs

between the stationary phase and the sample: the stationary phase provides the hydrophobic surface that retains the molecule depending on its relative hydrophobicity: the more the molecule presents a hydrophobic nature the longer it will take to pass though the column. In addition, HPLC analysis suggest the presence of either contaminants or of aggregates of dendrimers or single dendrimers rolling on the HPLC column. The results obtained in this work regarding the characterisation of dendrons by HPLC analysis are in agreement with what has been published in the literature. Indeed, polylysine dendrons of higher generations (gen4 and gen5) have been characterised trough HPLC analysis showing a decrease in peak retention time while the generation increase (Kantchev, 2008); polyamine dendrons have been functionalised with class II hydrophobin protein and then analysed with a semi-preparative HPLC (Kostiainen, 2006).

The second characterisation method used to validate the successful synthesis of the peptides was MS. The analysis of protein and peptides by mass spectrometry takes advantage of the wide and constantly updating of the protein database. The outcome produced by MS, plot a series of peaks identified by intensity and mass-to-charge (m/z) values. These m/z values can be manipulated and compared with a list of theoretical peaks generated from peptide fragmentation that can be found in the above-mentioned database in which one of the most employed is Protein Prospector Software (PPS). Peptides identification by mass spectroscopy is conducted by the simultaneous operation of MS equipment and gas-phase peptide chemistry (Wysocki, 2005). The MS instrumentation used in this project for the characterisation of dendrons and dendrons tethered with bioactive linear angiogenic peptide is formed by an electrospray ionisation (ESI) support that allows peptide to be fragmented and ionised in order to be analysed and detected. It is important to consider that the molecules analysed in this work are branched molecules that can be affected by some characterisation problem if compared to the same types of characterisation techniques applied to linear peptides. For this reason, even if the MS instrumentation fits all the parameters needed to analyse the peptide, the characterisation of branched molecules can be more cumbersome. During the ionisation step a linear peptide is positively charged and move towards a negative pole; when a branched molecule is ionised there could be the chance that not all the molecule fragments are ionised resulting in a less accurate analysis. Moreover, one potential cause of less precise analysis with MS can be found in the presence of residual TFA in the peptide that could lead to peak suppression and result in the appearance of low intensities peaks in the MS spectrum (Annesley, 2003). Despite these disadvantages, MS has been proven to be an efficient characterisation method for branched molecules as demonstrated by previous work

(Kantchev, 2008; Grayson, 2001). Indeed, peaks generated through MS analysis for the characterisation of different dendron generations are in complete agreement with the HPLC analysis results.

Finally, in order to verify the functionalisation of dendrons with bioactive linear angiogenic peptides and make a further validation of the previous obtained results, FT-IR spectroscopy was performed. This technique provides a basis for comparison between the different chemical groups present in the analysed sample and allows the comparison of a sample with another by the presence or absence of specific chemical groups. Indeed, FT-IR is widely used when there is the need to test the functionalisation of a biomaterial (Gupta, 2004; Jiang, 2007) and to check if a drug is successfully coupled to a drug delivery carrier (Horcajada, 2007). Therefore, it represents a reliable method when two different samples show clear chemical differences like in the case of FFgen0K and the QHREDGS sequence where there is no correspondence between amino acids and specific FT-IR peaks are by unique moieties for each molecule. The situation changes when two samples have chemical similarity, such as in FFgen0K and RKIEIVRKK where the presence of lysine is observed in both molecules making the FT-IR spectra interpretation more difficult. To overcome this problem an improvement could be made subtracting the FT-IR spectra of the linear peptide sequence in order to have further basis for comparison. Consequently, FT-IR analysis is really necessary in the last validation of the results obtained previously for the dendritic angiogenic peptides characterisation, highlighting the presence of the bioactive linear angiogenic peptide proving the occurred synthesis of the final molecule.

2.5 CONCLUSION

In conclusion it can be stated that:

1) Dendrons (FFgen0K, FFgen1K and FFgen2K) and dendrons tethered with angiogenic bioactive linear peptides ($FFgen0K(QHREDGS)_{2,}$ $FFgen1K(QHREDGS)_4$, $FFgen2K(QHREDGS)_{4,}$ $FFgen0K(WQELYQLKY)_2$ and $FFgen0K(RKIEIVRKK)_2$) have been designed for the first time specifically to target cells relevant to the treatment of myocardial ischemic tissue. Their molecular design includes a FF root capable of interacting with the tissue ECM through hydrophobic interactions that enhance retention into the tissue and terminal molecular branches exposing angiogenic bioactive linear peptide to enhance angiogenesis *in vitro*.
2) The novel molecules have been synthesised through a manual SPPS method and characterised successfully though HPLC, MS and FT-IR where all the results obtained in this project are in agreement with each other and with the literature.

The further step, aim of the following chapter, will be to test the biological efficacy of these novel molecules in inducing a specific response on human umbilical vein endothelial cells (HUVECs) *in vitro*.

3. SYNTHESIS OF COLLAGEN TYPE I BEADS AS A DELIVERY SYSTEM FOR DENDRITIC ANGIOGENIC PEPTIDE

3.1 INTRODUCTION

The common biomaterial approach to treat MI can be divided into three categories: (i) left ventricular (LV) restraints, (ii) cardiac patches and (iii) injectable strategy (Leor, 2005). Over the last ten years, there was an increase in the number of the clinical trials with cardiac patches and, most recently, with injectable biomaterials, proving that the tissue engineering approach to treat MI is becoming increasingly relevant (Grover, 2015, O'Neill,2018). In this chapter, the attention is focused on injectable biomaterials and in particular on engineered collagen beads.

3.1.1 INJECTABLE BIOMATERIALS FOR THE TREATMENT OF MI INJURY

Recently, the field of injectable biomaterial has become wider and has taken a predominant role in the treatment of MI injury. Both synthetic and natural biomaterial can be injected alone or as supporting system for the delivery of cells, bioactive molecules or biological cues (Fig.3.1).

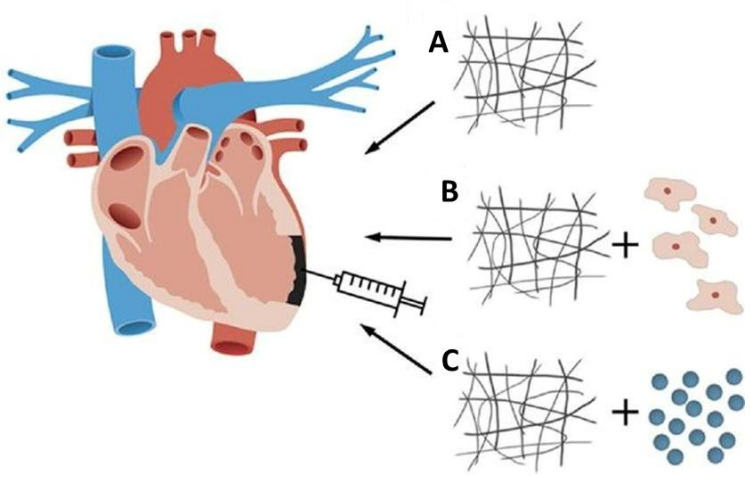

Fig. 3.1 Injectable biomaterial approaches for the treatment of MI injury: (A) Injectable biomaterials can be used as they are produced, (B) with the addition of cells or/and (C) with bioactive and biological moieties. (Adapted from Rane, 2011).

The promising results (increase in the neovascularisation, reduction of the infarcted area and progress in cardiac function), obtained in the early stage of the use of injectable biomaterials for the treatment of MI, have encouraged researchers to extend their studies to large animal pre-clinical models and even early clinical trials stage (Ruvinov,2016). Outstanding biomaterials for this specific application are those materials (alginate, chitosan, collagen type I, myocardial matrix, etc.) who have gelation properties that enhance percutaneous delivery into the myocardium, reducing the need of invasive procedures required for cardiac patches (Singelyn, 2011). The first worth mentioning study that has proven the feasibility of injectable biomaterials for the treatment of MI tests fibrin

in a rat ischemia-reperfusion model: fibrin was loaded with skeletal myoblasts preserving cardiac function post MI and improving cell transplant survival (Christman, 2004). From that study different cell sources have been investigated such as bone marrow stem cells (Nakamuta, 2009), marrow-derived cardiac stem cells (Guo, 2011) and adipose-derived stem cells (Zhang, 2010) demonstrating that cells may improve tissue regeneration when compared with acellular implants. However, many studies show similar improvements in cardiac function also with just the biomaterial: fibrin-alginate composite materials have been injected in a pig model after 1 week post MI maintaining wall thickness and making the infarcted area expansion smaller 7 days post-injection (Mukherjee, 2008). Alginate was injected also 8 weeks later the infarct event showing, after 2 months of injection, improvement in the cardiac function and reduction in scar tissue formation thus proving that this polysaccharide alone is a good candidate to enhance tissue regeneration following MI (Landa, 2008). Further studies have been made using alginate as platform for the delivery of bioactive molecules such as VEGF or PDGF. Indeed, the delivery of these growth factors alone or in a sequential delivery in alginate showed an improvement in left ventricular remodelling if compared to alginate alone in a rat MI model (Hao, 2007) meaning that the addition of bioactive molecules may improve the outcome of the treatment. Other natural materials have been inspected for treating MI such as: (i) chitosan injected with undifferentiated embryonic stem cells 1 week post MI in a rodent MI model resulting in an improvement of cardiac function and remodelling compared to the acellular scaffold (Lue, 2010); (ii) chitosan functionalised with bFGF improve arteriole density and decrease infarct size and fibrotic area if compared with the injection of bFGF alone after 4 weeks in a rodent MI model (Wang,2010); (iii) gelatine loaded with bFGF has shown enhancement in cardiac function when injected in small animals (Shao, 2006) and large animals (Liu, 2006); (iv) Matrigel was injected right after the infarct event resulting in a decrease of the infarct wall thickness when compared with saline injection in a rat MI model (Ou, 2011).

3.1.2 ENGINEERING OF COLLAGEN INTO BEADS

Collagen is the most abundant protein present in the ECM of several tissues. Because of its intrinsic biocompatibility, it has a great potential as a biomaterial for many regenerative medicine applications. Collagen-based biomaterials for tissue regeneration are widely used especially in cardiovascular, orthopedic and dental applications (Sheehy,2018). Collagen can be produced in different shapes (scaffold, fibers, spheres) regarding its final application. When the damaged tissue is anatomically difficult to reach by surgical

intervention or it has an irregular shape (i.e. multiple openings, branched sections), it is preferable to use biomaterial formulations like spheres that can infiltrate easily the target site (Keshaw, 2007). In the literature, it is possible to find a wide selection of different production methods for the creation of collagen spheres. Microspheres composed by a combination of hydroxyapatites and collagen type I were prepared with a water-in-oil emulsion technique: hydroxyapatites and collagen type I solution was emulsified into olive oil in order to form droplets; successively, collagen was reconstituted into hydroxyapatites at 37°C (Hsu, 1999). Another manufacturing collagen beads method is the dispersion of a collagen solution in water-immiscible organic solvents at 0-25°C: regenerated collagen fibrils are assembled into beads by dispersing drop by drop the acidic aqueous collagen solution in a water-immiscible organic solvent and stabilising the formed droplets by the addition of a water-miscible organic solvent or by raising the temperature to 30-40°C (Miyata, 1986). Some alternative methods that do not include the use of oily or solvents solution is the thermally-induced phase separation (TIPS). This method considers the delivery of collagen solution droplets into liquid nitrogen followed by freeze-drying. The stabilisation of collagen spheres is reached when cross-linked by glutaraldehyde vapour that prevents the relatively fast collagen spheres degradation in aqueous solution and reduces the presence of unreacted glutaraldehyde species or their self-polymerisation (Keshaw, 2009; Onder,2016). Furthermore, it is possible to produce collagen spheres taking advantage of ionic interactions. Indeed, collagen spheres can be assembled through an ionic gelation method: the formation of the collagen spheres is obtained as a results of the interaction between sodium tri-polyphosphate (TPP) negative chemical groups and the positively charged amino groups of collagen (Moeini,2018). Finally, it is possible to produce collagen beads enriched with cell by a self-assembling technique where the cells are directly included during the manufacturing process; liquid droplets of collagen/cells solution can be dispensed onto a non-adhesive surface and incubate at 37°C in order to induce gelation (Li,2016).

The above-described techniques to produce engineered collagen beads may be applied to several tissue engineering applications. Many studies are reported in the literature about the use of collagen in combination with hydroxyapatite as potential platform delivery for bone regeneration applications. A collagen/hydroxyapatite composite was assembled into microspheres for the treatment of skeletal defects where nanocomposite microspheres have been shown to favour the recruitment, adhesion and growth of rat bone marrow derived stem cells (BMDSC). Furthermore, rat BMDSCs, supported by the microspheres implant, encourage the expression of specific bone-associated genes as well as osteogenic marker

more than single cells injection, suggesting that collagen microspheres act as a suitable substrate for the cells thus showing a high potential in bone regeneration applications (Kim, 2007). In another study, the composite collagen/ hydroxyapatite microspheres served as a platform to immobilise bone morphogenetic proteins (BMPs): the results achieved unveiled the capacity of collagen/ hydroxyapatite microspheres to support osteoblast proliferation and to increase the alkaline phosphatase activity, sign that the implant may be used in filling bone defects (Hsu, 1999). Collagen spheres can be used also in wound healing applications. Microporous collagen spheres have been used in fistulae wound healing applications where spheres cultured with myofibroblast have enhanced significantly the secretion of VEGF *in vitro* (if compared with cells alone) and the formation of blood vessels in a CAM assay model. The above-mentioned results suggest collagen spheres as novel substrate biomaterials for those tissue where regeneration is pursued in difficult anatomical areas (Keshaw, 2009). Finally, collagen spheres can be used also as means of encapsulation for cells delivery. Indeed, collagen spheres have been used to carry and deliver Mesenchimal stem cells (MSCs) cells for various applications like musculoskeletal (Pittenger, 2007) or cardiovascular (Helm, 2005) regeneration. MSCs can be encapsulated into collagen spheres by a self-assembling process. This system provided support to growth and migration of cells due to collagen spheres specific properties of stability, injectability and protective support to cells. Furthermore, MSCs is demonstrated to preserve their stem cell nature also after encapsulation (Chan, 2007). Ultimately, the use of collagen beads delivering bioactive molecules or cells can be made available as injectable formulations enabling minimally-invasive intervention.

3.1.3 AIM OF THE CHAPTER

The aim of this chapter is to produce collagen type I beads and modify them with dendritic angiogenic peptides in order to assess, in the following chapters, their potential to induce angiogenesis *in vitro*. In order to verify the occurred functionalisation with the three different dendritic angiogenic peptides, collagen beads and collagen beads tethered with dendritic angiogenic peptides have been synthesised through the gelation crosslinking of collagen derivatised by succinylation. Later, the derivatised collagen was tethered with the dendrimeric angiogenic peptides and characterised trough Scanning Electron Microscopy (SEM), Fourier Transform Infrared Spectroscopy (FT-IR) and Dinamic Light Scattering (DLS).

3.2 MATERIALS and METHODS

3.2.1 Materials

Table 3.1 Materials used during the experimental process of collagen type I synthesis

Product	***Supplier***	***Code No***
Collagen, type I solution from rat tail	Sigma-Aldrich	9007-34-5
Acetic acid (diluted to 1% v/v)	Sigma-Aldrich	320099
Methanol (HPLC grade)	Fisher Scientific	M/4056/17
Succinic anhydride	Sigma-Aldrich	239690
Acetone	Sigma-Aldrich	34850
Sodium tripolyphosphate (TPP)	Fisher Scientific	218675000
N-(3-Dimethylaminopropyl)-N′-ethylcarbodiimide hydrochloride or EDC	Sigma-Aldrich	03450
N-Hydroxysuccinimide or NHS	Sigma-Aldrich	130672
MES	Sigma-Aldrich	M3671

3.2.2 Synthesis of Collagen Type I beads

3.2.2.1 N-succinylation of collagen Type I

Synthesis of collagen beads started from the succinylation of the collagen itself. First of all, collagen Type I (60 mg) was dissolved as a 1% (w/v) solution in 1% (v/v) acetic acid under magnetic stirring. When the solution resulted homogeneous, succinic anhydride was added to the solution at 4% (w/v) of collagen-acetic acid solution only. Therefore, succinic anhydride has been dissolved in acetone in order to obtain a 14% (w/v) solution and added drop by drop into a stirring collagen solution. After an overnight incubation under magnetic stirring, collagen solution was ready for dialysis: N-succinylated collagen solution was transferred into the wet dialysis tube via a funnel and the tube was secured on its extremities and placed in clean dH_2O for 48 hours, with fresh dH_2O changed 2-3 times per day. Once, acetone and acetic acid have diffused out to be replaced by fresh dH_2O, N-succinylated collagen was visible as white precipitate inside the dialysis tubing. Dialysis tubing was emptied into 75ml falcon tube for direct lyophilisation at 0.1mbar/ -70°C.

When lyophilised, N-succinylated collagen was weighted out resulting in 58.4 mg of collected material.

3.2.2.2 Bead synthesis

Thirty milligrams of N-succinylated collagen were used for beads synthesis. N-succinylated collagen was dissolved in fresh dH_2O to make a 1mg/ml solution under stirring conditions. Once the N-succinylated collagen was completely dissolved in dH_2O, 2mg/ml solution of sodium tri-polyphosphate (TPP) was added to the main solution dropwise while considering that the required volume of TPP solution had to be equal to one quarter of the N-succinylated collagen solution volume.The final step of the synthesis included the desalting of the beads solution using dialysis and lyophilisation, performed as reported in Section 3.2.2.1.

3.2.2.3 Dendritic angiogenic peptides functionalisation

Dendritic angiogenic peptides [FFgen0K$(QHREDGS)_2$, FFgen0K$(WQELYQLKY)_2$ and FFgen0K$(RKIEIVRKK)_2$] were covalently bonded to collagen beads by carbodiimide reaction using the carboxyl groups exposed by dendritic angiogenic peptides root and the collagen free amino groups. Therefore, collagen beads were dissolved in 2ml MES buffer to obtain a 1mg/ml concentration (w/v). The carboxyl groups from dendritic angiogenic peptides were then activated by addition of EDC (4mM) and NHS (10 mM) where the activation reaction was allowed to proceed at room temperature for 30 minutes. At this stage dendritic angiogenic peptides were dissolved in MES buffer (1mg/ml) and added to collagen beads solution at a volume ratio of 1:1. The conjugation reaction was allowed to proceed under magnetic stirring condition overnight at room temperature. The obtained three modified collagen beads with dendritic angiogenic peptides were then lyophilised and stored at -20°C.

3.2.3 Sterilisation

The different obtained biomaterials (collagen beads functionalised with the three different dendritic angiogenic peptides) were sterilised directly after lyophilisation by UV. UV sterilisation techniques is widely used to sterilise biodegradable scaffolds where the time of sterilisation is crucial to preserve biomaterial properties (Dai,2016). Studies reported that up to two hours no significant differences in biodegradable material properties are reported (Baume,2016). In this study a UV lamp has been used on samples in a fume hood for one hour (Fig.3.2).

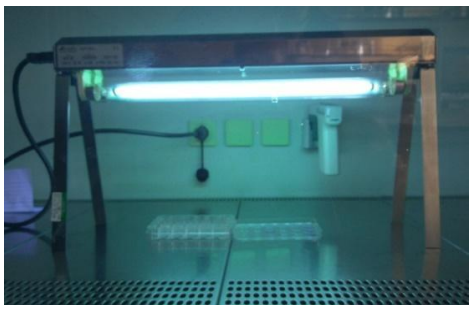

Fig. 3.2 Representative image of samples in a 24 well plate under UV sterilisation.

3.2.4 Characterisation of Collagen beads functionalised with dendritic angiogenic peptides by FT-IR, SEM and DLS

Collagen beads functionalised with FFgen0K$(QHREDGS)_2$, FFgen0K$(WQELYQLKY)_2$ and FFgen0K$(RKIEIVRKK)_2$ respectively were characterised using a Scanning Electron Microscopy (SEM), Fourier Trasform Infrared Spectroscopy (FT-IR) and Dinamic Light Scattering (DLS).

3.2.4.1 Fourier Trasform Infrared Spectroscopy (FT-IR)

FT-IR has been widely explained in Chapter 2, Section 2.2.3.3.

For the results obtained in this chapter, samples have been analysed over the range of 4000-650 cm^{-1} in triplicates for 8 scans at room temperature.

3.2.4.2 Scanning Electron Microscopy (SEM)

Scanning electron microscopy (SEM) is composed by an electron source with a suitable intensity (generally is an incandescent filament that emits electrons through thermo-ionic effect) and by a device that accelerates the emitted electron beam. Moreover, this device submits a high tension in a range of 20-100.00 Volt.

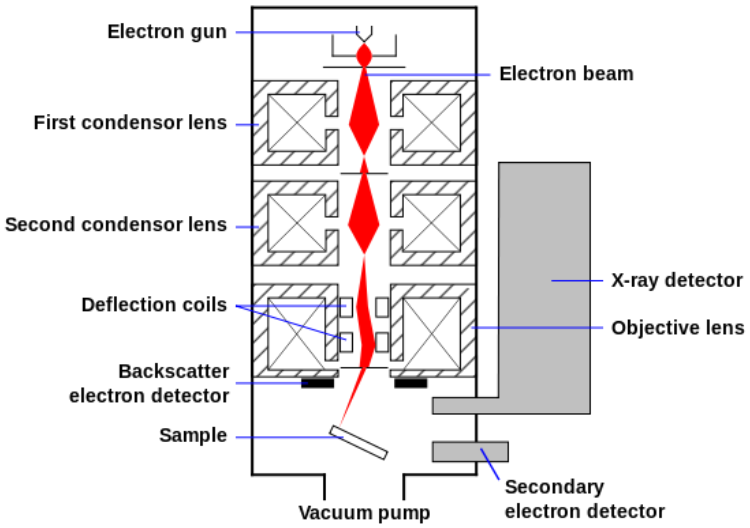

Fig. 3.3. SEM schematic operation system (Adapted from Kang, 2009).

The accelerated electron beam passes through a capacitor (electrostatic or magnetic) and hits the sample. After that, the beam is collected on a lens (electrostatic or magnetic) and, passing through an eyepiece, it hits a fluorescent screen or a plate forming the picture. All this process is conducted in high vacuum ensured by a proper pump system. In these conditions, the electron wavelength goes from 0.1 to 0.005 Å, ten of a thousand times smaller than the visible light with a power resolution of the nanometer.

Scanning electron microscopy (SEM) gives information about the appearance, the nature and the superficial property of solid samples; also the sample's underlying layers could be investigated.

This information is given with an average resolution of 2 to 5 nm, referring to the secondary electron signal generated. The types of signals produced by a SEM include secondary electrons (SE), back-scattered electrons (BSE), characteristic X-rays, light (cathodoluminescence) (CL), specimen current and transmitted electrons. When SEM is equipped with an X-ray detector (EDS: energy-dispersive X-ray spectroscopy) elemental analysis or chemical characterisation of a sample could be done (Kang, 2009).

In this study, collagen beads functionalised with dendritic angiogenic peptides have been sputter-coated with a thin gold layer before placing them in the vacuum SEM sample chamber and analysed at 2.0 kV with different magnification.

3.2.4.3 Dinamic Light Scattering (DLS)

The dynamic light scattering technique is a non-disruptive technique to determine the size of small particles (from 1 nm to 5 μm) present in a suspension under Brownian motion [ref]. If the particles or molecules are detected by a laser, the intensity of the scattered light varies at a rate that is dependent on the size of the particles: smaller particles are "kicked" ahead by the solvent molecules and move more rapidly. Analysis of these intensity variation yield the velocity of the Brownian motion and hence the particle size using the Stokes-Einstein relationship:

$$d(H) = kT / 3\pi\eta D \qquad \text{(Stokes-Einstein equation)}$$

where
d(H): hydrodynamic diameter
k = Boltzmann's constant
T = Absolute temperature
η = Viscosity

The hydrodynamic diameter is the diameter of a hard sphere that diffuses at the same speed as the particle or molecule being measured. It depends not only on the size of the particle

"core" but also on any surface structure, as well as the type and concentration of any ions in the medium.

In order to investigate collagen beads size, a Malvern Zetasizer nano ZS90 was employed. Collagen beads have been dissolved in dH_2O at 5mg/ml concentration, sonicated in order to fully disperse the material in the solvent and loaded into a disposable sizing cuvette. Sample were analysed setting the instrument with 3 measurements of 50 runs for each sample with 120 seconds of equilibration time at room temperature.

3.3 RESULTS

The results showed in this section are referred to the synthesis, functionalisation with dendritic angiogenic peptides and characterisation of both non-functionalised and dendron-functionalised collagen Type I beads.

3.3.1 Fourier Trasform Infrared Spectroscopy (FT-IR)

Collagen Type I beads synthesis has been monitored and recorded trough FT-IR analysis (Fig. 3.4). Firstly, characteristic peaks of collagen Type I have been collected resulting in four major peaks: 1658 cm^{-1} that identifies α-like helix of collagen type I, 1555 cm^{-1} correlated to the presence of II amide, 1403 cm^{-1} that marks the presence of $\delta(CH_3)$ groups and finally 1238 cm^{-1} the presence of δ(C-N) groups (Fig. 3.4, graph A). Going ahead with the synthesis, collagen Type I has been succinylated as confirmed by FT-IR spectrum where it is possible to notice a transmittance reduction of the 10% on the 3307 cm^{-1} peak (proof of the presence of free amino groups) and a shift of peak (1451 cm^{-1}) related to $\delta(CH_3)$ groups if compared to the control collagen Type I spectrum (Fig, 3.4, graph B). When the formation of the collagen Type I beads finally occurs, the spectrum of succinylated collagen Type I beads is comparable to succinylated collagen Type I spectrum unless for two peaks, 1035 cm^{-1} and 887 cm^{-1}, present there because of the formation of alkene groups and methylene groups (CH_2) as a result of the natural crosslinking occurred during the beads formation (Fig.3.4, graph C, peaks n. 1 and 2).

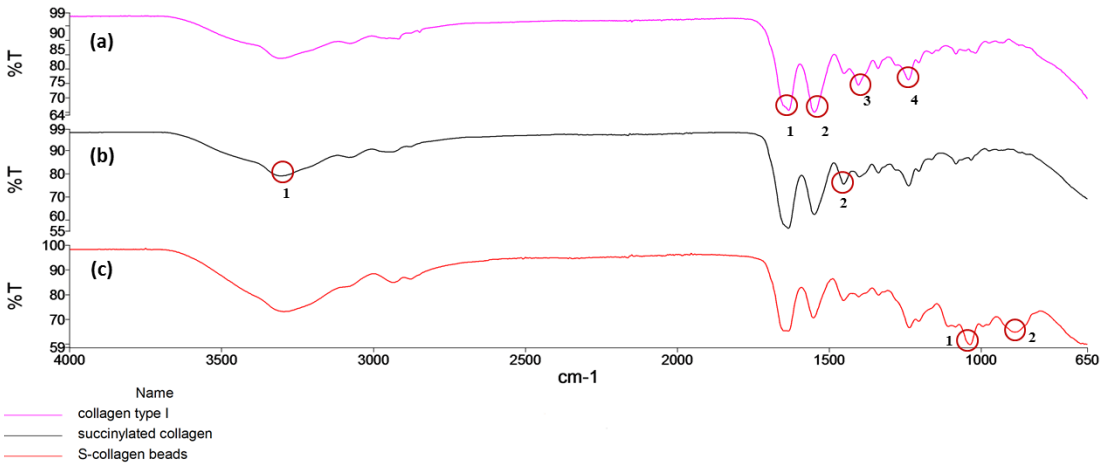

Fig. 3.4 FT-IR Spectra of a) collagen type I where circles indicate peaks: 1-1658 cm^{-1} ,2-1555 cm^{-1} 3- 1403 cm^{-1} ,4-1238 cm^{-1}; b) succinylated collagen where circles indicate peaks: 1-3307 cm^{-1} , 2-1451 cm^{-1} and c) S-collagen beads where circles indicate peaks: 1-1035 cm^{-1} ad 2- 887 cm^{-1}.

Table 3.2 Relevant peaks involved in the characterisation of collagen type I beads synthesis.

Relevant peaks	
Collagen type I	1) 1658 cm^{-1} 2) 1555 cm^{-1} 3) 1403 cm^{-1} 4) 1238 cm^{-1}
Succinylated collagen	1) 3307 cm^{-1} 2) 1451 cm^{-1}
S-collagen beads	1) 1035 cm^{-1} 2) 887 cm^{-1}

Later, collagen type I beads have been functionalised with dendritic angiogenic peptides by carbodiimide reaction and characterised by FT-IR to prove the modification occurred.

Collagen Type I beads have been functionalised with FFgen0K$(QHREDGS)_2$ and analysed in comparison with FFgen0K$(QHREDGS)_2$ crude spectrum (Fig. 3.5). From spectra it is possible to recognise the footprint of collagen Type I that is the 1658 cm^{-1} peak that identifies α-like helix of collagen type I (Fig. 3.5, green line). Regarding the beads+FFgen0K$(QHREDGS)_2$ it is possible to highlight the fingerprint of FFgen0K$(QHREDGS)_2$ (Fig. 3.5, black line) that has been already recognised in Chapter 2, Section 2.3.3: peaks 873 cm^{-1} and 1350 cm^{-1} are the fingerprint of the presence of –QHREDGS sequence thus confirming functionalisation. These peaks are: (i) peak 873.61

cm^{-1} that can be referred to an alcohol group (-OH) exposed from a serine residue of the Ang-1 peptide analogue that is not present in the beads+FFgen0K$(QHREDGS)_2$ spectrum and (ii) peak 1350 cm^{-1} that identifies the presence of an Alkene (C=C) group that corresponds to the side group exposed from the histidine residue present in the QHREDGS sequence.

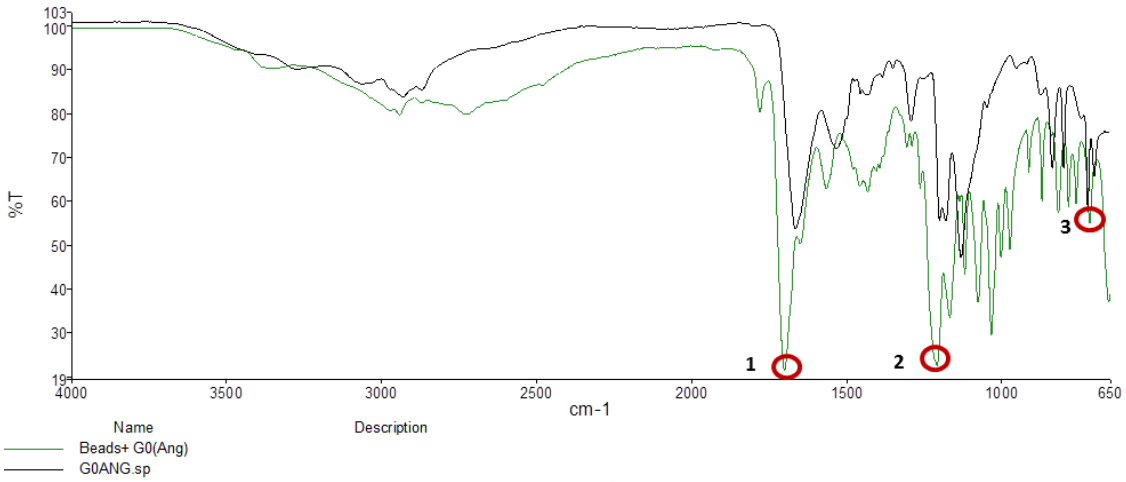

Fig. 3.5 FT-IR Spectra of S-Collagen Beads functionalised with FFgen0K$(QHREDGS)_2$ (green line where the circles indicate peaks 1-1658 cm^{-1} 2-1350 cm^{-1} and 3-873 cm^{-1}) and of FFgen0K$(QHREDGS)_2$ (black line where the circle indicates 1-873 cm^{-1}).

Table 3.3 Relevant peaks involved in the characterisation of collagen type I beads functionalisation with FFgen0K$(QHREDGS)_2$.

Relevant peaks	
S-collagen beads + FFgen0K$(QHREDGS)_2$	1) 1658 cm^{-1} 2) 1350 cm^{-1} 3) 873 cm^{-1}
FFgen0K$(QHREDGS)_2$	1) 873 cm^{-1}

FT-IR analysis has also been used also to verify the functionalisation of collagen Type I beads with the -WQELYQLKY bioactive dendritic peptide. Spectra of collagen Type I beads functionalised with FFgen0K$(WQELYQLKY)_2$ (Fig.3.6, yellow line) and of FFgen0K$(WQELYQLKY)_2$ (Fig.3.6, black line) differ from each other by the presence of a peak at 1658 cm^{-1} in the collagen Type I beads functionalised with FFgen0K$(WQELYQLKY)_2$ sample due to the presence of α-like helix of collagen type I and by the presence of peak at 1087 cm^{-1} due to the increase of secondary amide. Moreover, it is possible to notice a correspondence between the two different spectra in

peaks 1454 cm^{-1} and 782 cm^{-1} fingerprints of FFgen0K(WQELYQLKY)$_2$ where the first peak identifies an amide group that belongs to the glutamine residue present in the VEGF bioactive peptide and the second one highlights the presence of an aromatic groups derived from the tyrosine residue of VEGF bioactive peptide. Overall, these peaks prove the successful functionalisation of collagen Type I beads with the dendritic angiogenic peptide.

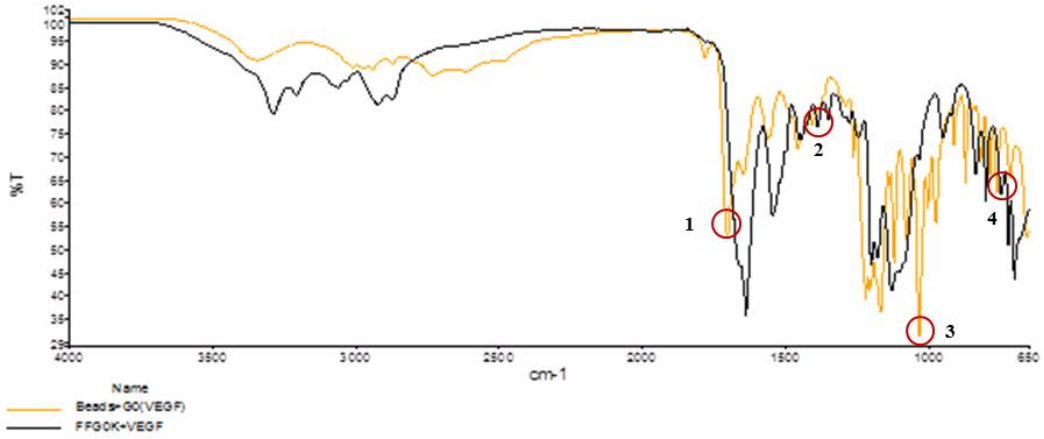

Fig. 3.6 FT-IR Spectra of S-Collagen Beads functionalised with FFgen0K(WQELYQLKY)$_2$ (Orange line where the circles indicate peaks 1-1658 cm^{-1} 2-1545 cm^{-1} 3-1087 cm^{-1} and 4-782 cm^{-1}) and of FFgen0K(WQELYQLKY)$_2$ (black line where the circles indicate peaks 2-1454 cm^{-1} and 4-782 cm^{-1}).

Table 3.4 Relevant peaks involved in the characterisation of collagen type I beads functionalisation with FFgen0K(WQELYQLKY)$_2$.

Relevant peaks	
S-collagen beads + FFgen0K(WQELYQLKY)$_2$	1) 1658 cm^{-1} 2) 1454 cm^{-1} 3) 1087 cm^{-1} 4) 782 cm^{-1}
FFgen0K(WQELYQLKY)$_2$	2) 1454 cm^{-1} 4) 782 cm^{-1}

The last material analysed by FT-IR analysis is collagen type I beads+FFgen0K(RKIEIVRKK)$_2$. Fig. 3.7 shows the spectrum of collagen type I beads+FFgen0K(RKIEIVRKK)$_2$F (purple line) and of FFgen0K(RKIEIVRKK)$_2$ (black line). In this case, the fingerprint of FFgen0K(RKIEIVRKK)$_2$, proving that the functionalisation has occurred, is the increase of the transmittance of peak at 1656 cm^{-1} that corresponds to the presence of amide groups: this group is also a side group of a valine

residue that is one of the amino acids present in the PDGF-BB peptide analogue. Peak at 740 cm^{-1} that identifies the presence of alcohol groups derived from PDGF-BB bioactive peptide residues. Moreover, it is possible to notice the presence of a peak at 1357 cm^{-1} in both spectra but with different transmittance intensity.

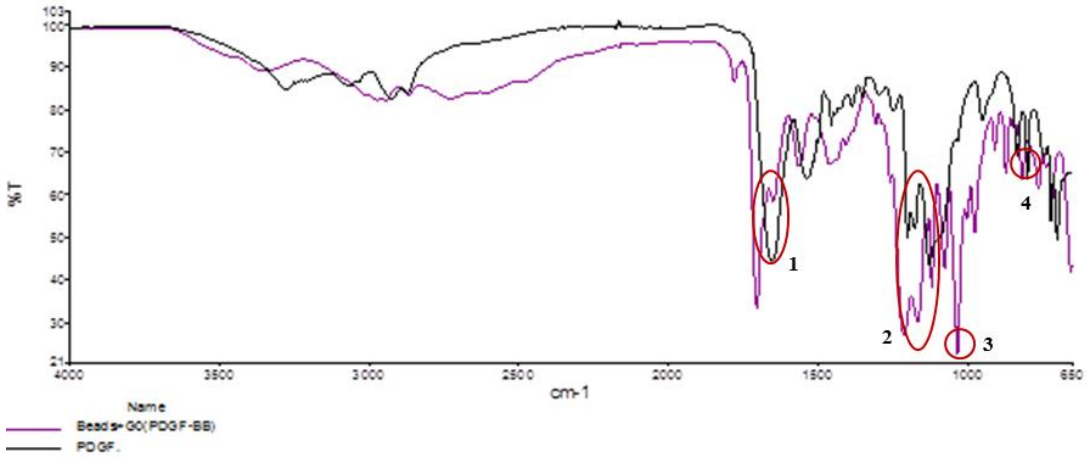

Fig. 3.7 FT-IR Spectra of S-Collagen Beads functionalised with FFgen0K(RKIEIVRKK)$_2$ (purple line where circles indicate peaks 1- 1656 cm^{-1} 2-1357 cm^{-1} 3-1087 cm^{-1} and 4- 740 cm^{-1}) and of FFgen0K(RKIEIVRKK)$_2$ (black line where the circles indicate peaks 1- 1656 cm^{-1} 2-1357 cm^{-1} and 4- 740 cm^{-1}).

Table 3.5 Relevant peaks involved in the characterisation of collagen type I beads functionalisation with FFgen0K(RKIEIVRKK)$_2$.

Relevant peaks	
S-collagen beads + FFgen0K(RKIEIVRKK)$_2$	1) 1656cm^{-1} 2) 1357 cm^{-1} 3) 1087 cm^{-1} 4) 740 cm^{-1}
FFgen0K(RKIEIVRKK)$_2$	1) 1656cm^{-1} 2) 1357 cm^{-1} 4) 740 cm^{-1}

3.3.2 Morphological analysis of functionalised collagen beads

SEM analysis has been used to assess the morphology of collagen Type I beads compared to collagen type I morphology. Image of collagen Type I (Fig. 3.8) shows the combination of fibres forming the typical foamy structure of collagen Type I before the beads formation, whereas higher magnification images (130.00K x) show the relatively smooth surface of the fibre surface (Fig. 3.8).

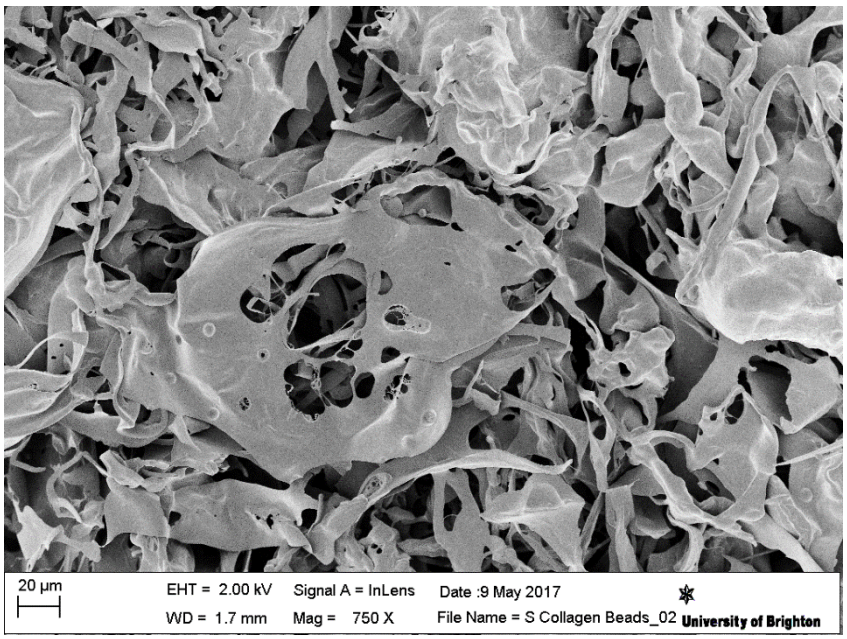

Fig. 3.8 SEM morphological analysis of S-collagen type I at 750x magnification showing the combination of fibers and foamy structure,typical appearance of collagen type I.

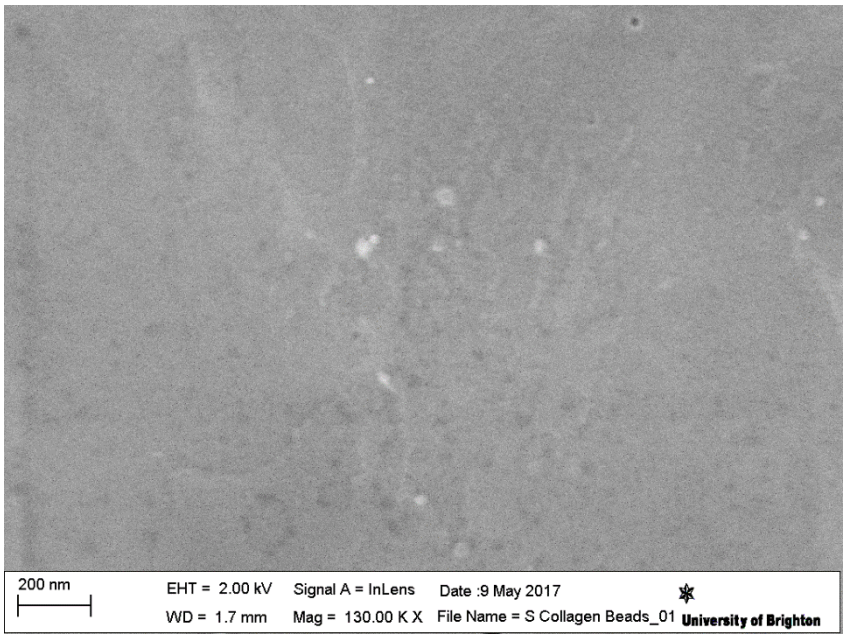

Fig. 3.9 SEM morphological analysis of S-collagen type I at 130K x: higher magnification shows a smooth collagen type I appereance.

When functionalised collagen beads are analysed by SEM at the same magnification of the S-collagen Type I used as control (130.00K x), a significantly different morphology can be observed (Fig.3.10). Indeed, it is possible to observe a structure where there is the

prevalence of beads that are likely to be aggregated by the process of drying required by the sample preparation procedure.

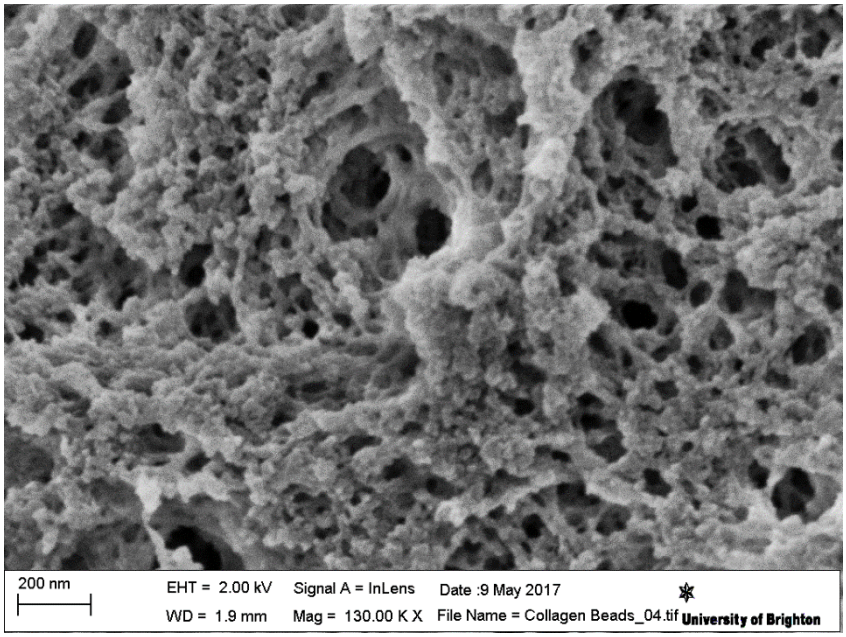

Fig. 3.10 SEM morphological analysis of functionalised S-collagen type I beads at 130K x, where it is possible to observe structure resembling beads aggregates.

Due to the SEM results showing the formation of collagen type I beads aggregates, further macroscopically investigation have been made in order to assess the nature of these beads aggregates. When S-collagen Type I, S-collagen beads and dendron-functionalised S-collagen beads were lyophilysed they seem to acquire different structures (Fig. 3.11). Indeed, S-collagen type I has a textured morphology (Fig.3.11, panel A) whereas S-collagen beads and functionalised S-collagen beads have a wool-like structure (Fig. 3.11, panel B and C).

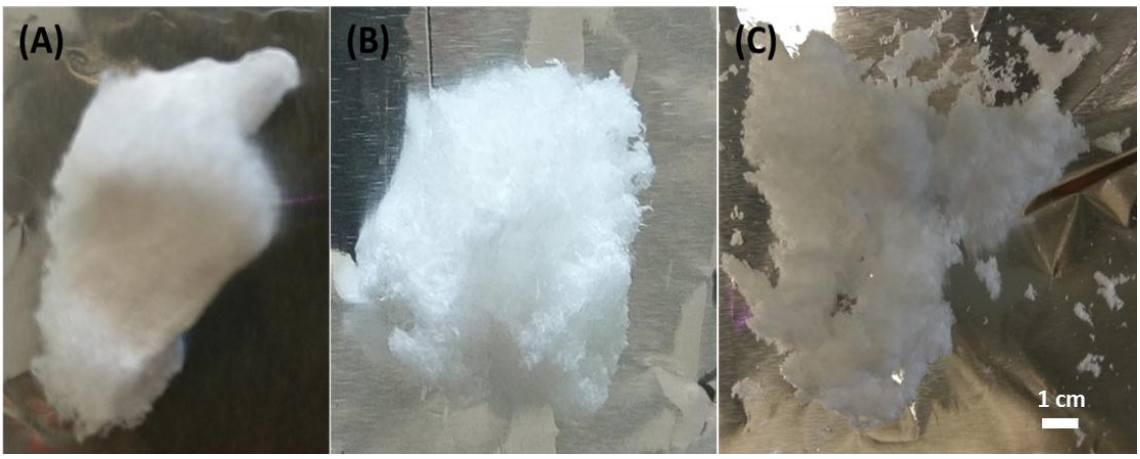

Fig.3.11: Appearance of A) N-succinylated Collagen type I, B) S-Collagen Beads, C) dendron-functionalised S-Collagen Beads after lyophilisation.

When dried S-collagen beads are dissolved in water at room temperature and at neutral pH it is possible to observe a turbid solution after 24h incubation that become completely clear after 48h (Fig.3.12) incubation.

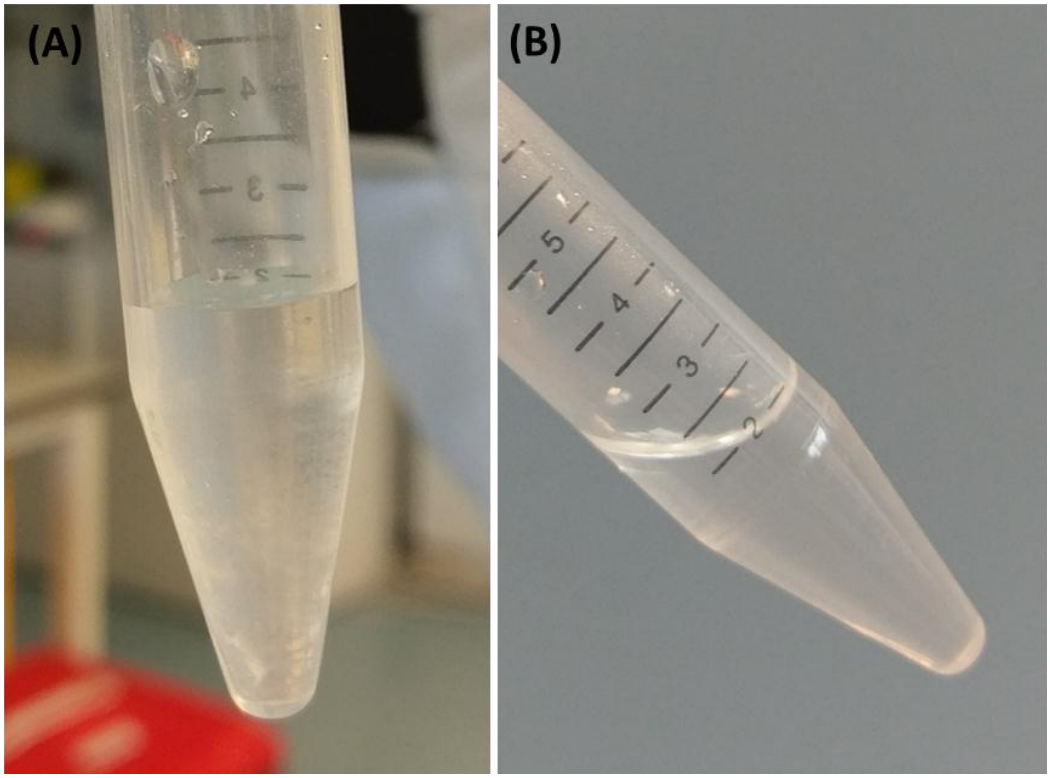

Fig. 3.12 Appearance of S-collagen beads in dH_2O after A) 24h and B) 48h incubation at neutral pH and room temperature.

On the contrary, dendron-functionalised S-collagen beads were resuspended in dH_2O and after 24h they dissolved (Fig. 3.12) resulting in a clear and homogeneous suspension.

Fig. 3.12: Appearance of a suspension of S-collagen beads functionalised with dendritic angiogenic peptide in dH_2O solution after 24h.

3.3.3 Dynamic Light Scattering (DLS)

Due to the results obtained from the macroscopically analysis DLS characterisation has been performed in order to estimate the diameter of the s-collagen beads aggregates after 24 h in dH_2O and the functionalised collagen beads size after 24h in dH_2O (Fig.3.13). The results obtained show a diameter of 90 nm for the S-collagen beads (Fig.3.14) and 178 nm for the aggregates (Fig.3.15) with a polydispersity index of 0.423 and 0.385, respectively. Moreover, DLS results of the dendron-functionalised S-collagen beads show only 1 peak of reduced size indicating smaller and mono-dispersed beads.

DLS results confirm that the production of functionalised collagen beads has been successfully.

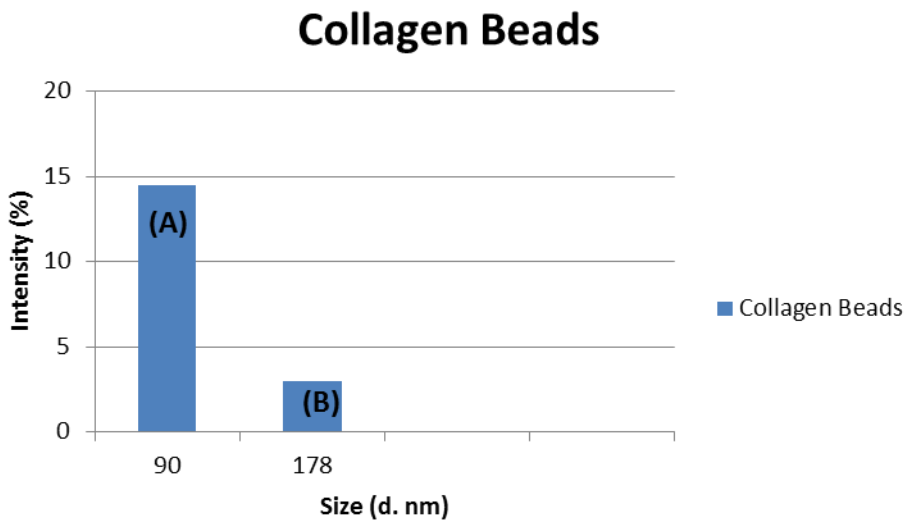

Fig. 3.13 Beads diameter when beads are in dH_2O solution. (A) Collagen Beads (B) Collagen Beads Aggregates.

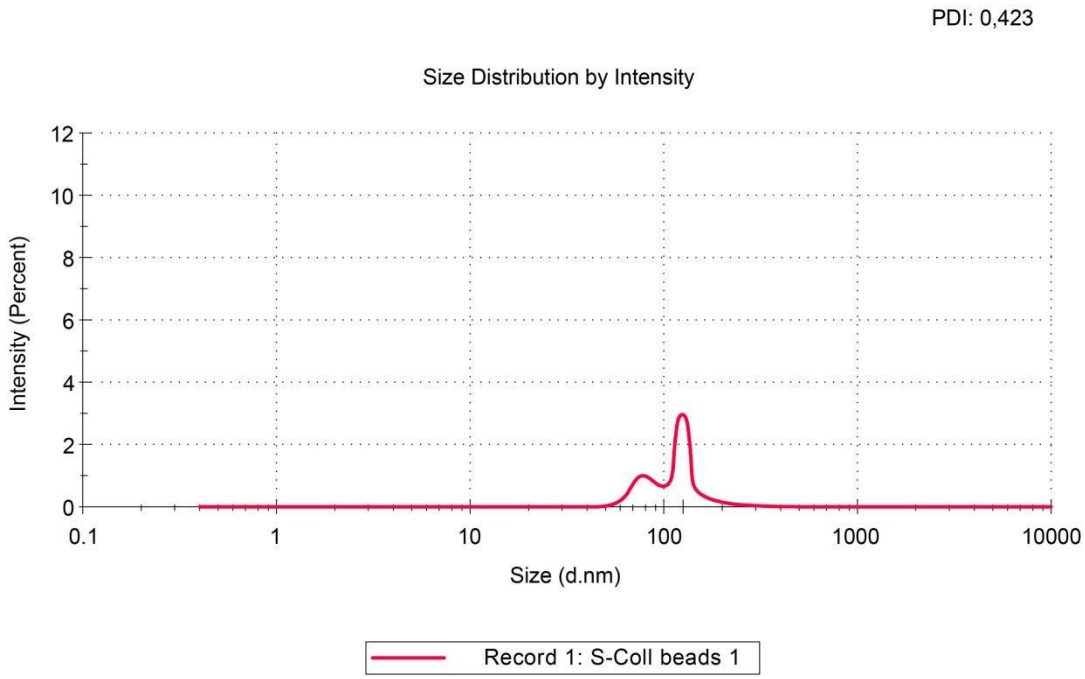

Fig. 3.14 Size distribution of S-collagen beads aggregates after 24h incubation in dH_2O solution.

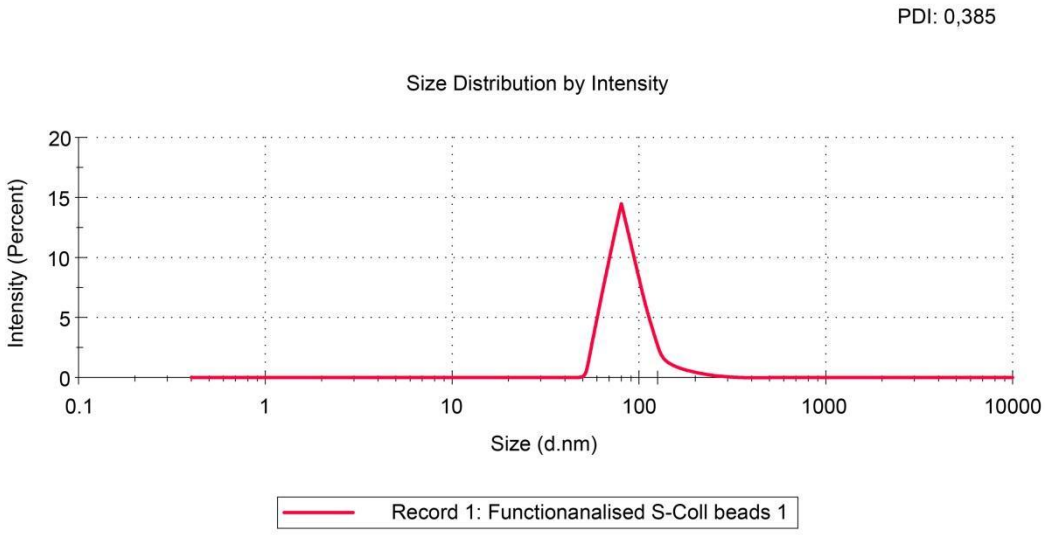

Fig. 3.15 Size distribution of dendron-functionalised S-collagen beads after 24h incubation in dH_2O solution.

3.4 DISCUSSION

The common tissue engineering approach for the treatment of MI injury considers the use of a "support system" capable of delivering bioactive and/or biological factors and/or cells as well as acting alone as scaffold to support tissue regeneration (Novosel, 2011). This "support system" can be either injectable or a patch where obviously the main difference between these two approaches is the ease with injectable materials can be used as they do not require invasive surgery procedure. Indeed, in the last 5 years injectable materials had a predominant role in the treatment of MI injury (O'Neill,2018). For this reason, the general hypothesis behind the development of this chapter is: is it possible to design, produce and characterise collagen type I beads as a delivery system for dendritic angiogenic peptide?

The answer to this question has been achieved through the flourish of sequential objective:

1) Design and synthesis of collagen type I beads
2) Functionalisation of beads with dendritic angiogenic peptides
3) Characterisation of the obtained novel biomaterial with FT-IR, SEM and DLS

Starting from the design of the beads, the choice of the material to be used relapses on collagen type I. This material is the most abundant protein that is possible to find in native blood vessel and in ECM (Buttafoco, 2006). Collagen type I has acceptable biocompatibility and capable of providing biological signal to the targeting cells; moreover, this biopolymer is resorbable and highly hydrophilic (Kolacna, 2007). For these characteristics, collagen type I has been chosen to be the material for the synthesis of beads as platform for the spaced presentation of dendritic angiogenic peptides.

The experimental method used to produce collagen type I beads is an already established method, where firstly collagen type I is succinylated in order to transform ε-amino groups of lysine and other reactive groups of the amino acid residues to –COOH groups in order to increase collagen type I negative charge and hydrophilicity at physiological pH. This modification allows better cell adhesion and their proliferation as well as compromised bacterial adhesion as their surface is also negatively charged (Kumar, 2011). After the succinylation of collagen type I, beads where produced using an ionic gelation method with sodium tri-polyphosphate (TPP) as polyanionic crosslinker. Literature reports several methods for the production of collagen beads: (i) water-in-oil emulsion technique (Hsu, 1999), (ii) dispersion of collagen solution in water-immiscible organic solvents and solidification of the spheres under a thermal gradient (Miyata, 1986) and (iii) thermally-induced phase separation (Keshaw, 2009). Methods (i) and (ii) have been set aside for medical application due to their problems related to the incomplete removal of oil or

solvent residual that could lead to a cytotoxic final product (Hsu, 1999). These methods have been replaced by thermally induced phase separation: this method does not include the use of oil or solvent being more feasible for clinical application but it involves glutaraldehyde as crosslinking agent, well known to be cytotoxic when not completely removed (Keshaw, 2009). Moreover, the above mentioned methods are complicated for repeatable production and with spheres subjected to a too long exposure to an aqueous continuous phase (Blaker, 2008). For these reasons, the ionic gelation method is considered to be the golden method for the production of beads for drug delivery or cell encapsulation (Moeini, 2018). Ionic gelation method for the production of beads involves just physical interaction that is positive/negative charge interactions. In this particular case, sodium tri-polyphosphate (TPP) has been used, due to its native negative charge, to interact with collagen (rich in positive charge groups) in order to form spherical structure without the introduction of any chemical agent. This is a great advantage when the final application of this material required an high level of biocompatibility. Indeed, ionic gelation is an extraordinarily mild process that brings to controllable size beads and adequate encapsulation capacity for bioactive or biological cues (Papadimitriou, 2007).

Regarding the functionalisation of the produced collagen type I beads with dendritic angiogenic peptides, a carbodiimide reaction process has been used with NHS/EDC compounds in order to create a covalent bond between the amino groups exposed by collagen type I beads and the carboxyl group exposed by the dendritic angiogenic peptides root. Carbodiimide functionality (EDC) is often used to activate carboxylic acid towards amide (Fig.3.16): this is indeed the chemical reactions that let the dendritic angiogenic peptides to be covalent bonded to collagen type I beads (Mojarradi, 2010).

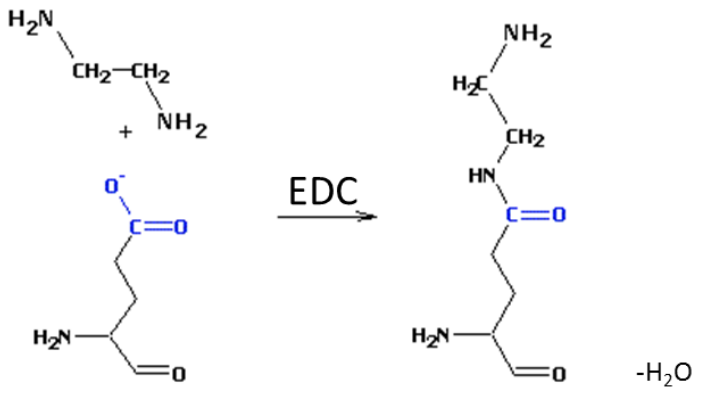

Fig. 3.16 Chemical scheme of the reaction between a carboxylic acid (blue labeled) and an amine group (black labeled) through a carbodiimide reaction and the resulting loss of a water molecule (Adapted from Proteinchemist, 2003).

The last objective to develop, in order to answer to the general hypothesis of the chapter, is the characterisation of the produced collagen type I beads functionalised with dendritic angiogenic peptides. A good validation starting point is the analysis of the FT-IR peaks collected for collagen type I. Indeed, peaks reported previously in this chapter (section 3.3.1, Fig. 3.3, panel A) related to the characterisation of collagen type I have been compared to the ones already published in literature: Belbachir *et al*. in 2009 have analysed the FT-IR spectra of several collagen type. Spectrum of collagen type I is identifiable by the presence of peculiar peaks that demonstrate the presence of α-like helix structure, secondary amide groups, $\delta(CH_3)$ and δ(C-N) making collagen type I spectra unique. Experimental results of this chapter for the characterisation of collagen type I are in complete agreement with the results collected by Belbachir group. Succinylation of collagen has been proven to occur through a reduction of the 10% in peak that identify the presence of free amino groups on collagen and by a shift in the peak related to the presence of carboxyl groups. Indeed, succinylation reaction substitutes free amino groups with carboxyl groups (Kumar, 2011) justifying the 10% reduction of the peak related to the presence of free amino groups on collagen. Finally, the FT-IR spectrum of collagen type I beads shows the formation of beads by the presence of peaks that identify alkene groups and methylene groups (CH_2) as a result of the natural crosslinking occurred during the beads formation between collagen and TPP. FT-IR has been used also to characterised the functionalisation of collagen type I beads with dendritic angiogenic peptides. Functionalised collagen type I beads spectrum is compared with single dendritic angiogenic peptide in order to verify the presence of the peculiar fingerprint of FFgen0K$(QHREDGS)_2$, FFgen0K$(WQELYQLKY)_2$ and FFgen0K$(RKIEIVRKK)_2$ in the functionalised beads spectrum. It is important to outline and highlight that fingerprints of dendritic angiogenic peptides that has been collected in this chapter are present in both spectra and are in total agreement with the ones obtained in chapter 2 (section 2.3.3), a proof of the occurred functionalisation.

When beads are morphologically analysed by SEM images and macroscopical analysis, it is possible to notice the presence of functionalised collagen beads and functionalised collagen beads aggregates. Indeed, comparing SEM images of S-collagen with the ones of collagen beads functionalised with dendritic angiogenic peptides is clear that the ionic gelation has occurred forming collagen beads but SEM images reveal also the presence of aggregates. This behaviour is most probably due to the lyophilisation process occurred just before taking the images. Macroscopical analysis of the S-collagen beads and functionalised collagen beads with dendritic angiogenic peptides have shown different

behaviour when incubate at neutral pH and at room temperature for a different holding time. S-collagen beads, after 24h incubation, are still not completely dispersed in water where actually the complete dispersion took place after 48h. On the contrary, dendron-functionalised collagen beads disperse completely in water only after 24h incubation. Different resuspension capacity is related to free amino groups concentration: these groups are positively charged making molecules more hydrophilic than other molecules. Dendritic angiogenic peptides are rich in free amino groups explaining why functionalised collagen beads are more dispersed in water than S-collagen beads. Moreover, the different suspension rate of collagen beads and functionalised collagen beads is another proof of the occurred functionalisation of collagen beads with dendritic angiogenic peptides. DLS analysis is in complete agreement with the results obtained with the morphological characterisation. In particular, the different polydispersity index obtained for S-collagen beads and functionalised collagen beads after 24h provides the idea of the beads size distribution: S-collagen beads, after 24h suspension in water, are still under aggregates shape and the polydispersity index (PDI:0.423) is higher than the one of functionalised collagen beads (PDI: 0.385) meaning that there is a wider size beads distribution related to the not yet complete resuspension of the s-collagen beads into water. In any case, both materials exhibited relatively narrow beads size distribution, meaning that the results are consistent with the measurement. Moreover, the functionalisation with dendritic angiogenic peptides not only adds a new bio functionality to the collagen, but improves the quality of the beads that become mono-disperse and smaller.

In order to make the collagen type I beads suitable for clinical application they have been sterilise by UV irradiation. Collagen type I is a polymer that is susceptible to denaturation and cross-linking if undergoes to high temperature . For this reason, sterilisation method such as autoclave or gamma irradiation, that needs high temperature (Allcock, 2011) to be performed were excluded for this project. Indeed, UV sterilisation permits to eliminate microbial agent at low temperature, low cost and without toxic residual but as already explained before, the exposure time should not exceed two hours in order to not have side effects (i.e. changes in biochemical properties) (Dai,2016).

When the damaged tissue is difficult to reach for regeneration and has an irregular shape, as it is likely to be the case for myocardial injuries, it is preferable to use formulations like beads that can infiltrate easily the target tissue (Keshaw, 2007). Results collected in this chapter regarding the functionalisation of collagen type I beads with dendritic angiogenic peptides reveal a new suitable system to be injected for myocardial repair that are likely to be able to remain entrapped in the clot or in the tissue extracellular matrix due to their

shape while providing biocues for angiogenesis. Moreover, it is important to highlight that this new technology offers the option to deliver a mix of beads containing different types of angiogenic factors or to deliver the peptides in a chronological order that is tuned with tissue regeneration.

3.5 CONCLUSION

In conclusion it can be stated that:

1) Collagen type I beads have been designed and synthesised successfully
2) The functionalisation of beads with dendritic angiogenic peptides [FFgen0K$(QHREDGS)_2$, FFgen0K$(WQELYQLKY)_2$ and FFgen0K$(RKIEIVRKK)_2$] has occurred as assessed by FT-IR analysis
3) Beads functionalised with dendritic angiogenic peptides have been characterised successfully showing an improved in monodispersity that is an important property for the material handling and injection.

The achievement of the main objectives of this chapter paves the way towards the main hypothesis of the chapter that is to find out whether Collagen type I beads can act as a supporting and delivery system for dendritic angiogenic peptides. This is the focus of later chapters and encourages the development of patches with same functionalisation properties as described in Chapter 4.

4. FUNCTIONALISATION OF ULTRAFOAM^{TM} SCAFFOLDS WITH DENDRITIC ANGIOGENIC PEPTIDES AS CARDIAC PATCHES WITH ANGIOGENIC PROPERTIES

4.1 INTRODUCTION

4.1.1 PATCHES FOR THE TREATMENT OF MI INJURY

In the past, cardiac patches have been used in the research field as delivery platform for cells, bioactive and biological moieties; only recently cardiac patches have been used in the treatment of myocardium ischemic disease as an acellular therapy (Aboli, 2011). Indeed, there are scientific evidences that scaffolds used as cardiac patches can provide a specific microenvironment and architecture capable to support cellular differentiation and organisation (Sarig, 2011). Currently, it is possible to identify three categories of approach for the treatment of myocardium infarction: (i) narrowing left ventricle with polymeric material for preventing heart failure; (ii) *in vitro*-growth of engineered cardiac tissue consequently implanted *in vivo* and (iii) the use of biomaterials, with or without cells, into/on the myocardium to create an *in situ*-engineered cardiac tissue (Venugopal, 2014).

Taking into consideration the third approach, the selection of the biomaterials scaffold has a key role in tissue regeneration: the scaffold should guide the organisation, growth and differentiation of cells in the engineered implant (Langer, 2004). In order to fulfil these requirements, scaffolds for myocardium regeneration must have precise mechanical, chemical and biological properties. An ideal scaffold for tissue engineering must be biocompatible, non-immunogenic, structurally stable and elastic to support stress and strain, sterilisable and mechanical properties comparable to the tissue it is replacing. Scaffold degradation and resorption are other characteristics needed to achieve the goal of tissue regeneration (Park, 2005). From a physicochemical point of view, the scaffold should be hydrophilic to enhance cells attachment and porous with interconnected structures capable of allowing cell penetration and colonisation throughout the scaffold. Vascularisation is enhanced when pore size is at least 50 μm, size that allows cells to receive nutrients and to remove secretions (Chachques, 2007).

Of course, cardiac patches have to provide specific chemical and biological cues essential for the formation of new healthy tissue. In particular, the device should be able to interact, at molecular level, with cells in a manner similar to the natural interactions occurring between cells and the native ECM (Leor, 2005). During the last 10 years, several cardiac patches have been investigated *in vivo* for the treatment of ischemic disease (O'Neill,2018). Literature reports the use of different biomaterials starting from biologically-derived materials such as collagen (Lambert,2017), a combination of collagen and laminin (i.e. Matrigel, Tao,2014), fibrin (Chrobak, 2016) and alginate (Ruvinov,2016) or alternatively with synthetic materials like elastic biodegradable polyester urethane urea

(Jamadi, 2016), high porous polyurethane (D'Amore, 2016) or biodegradable poly(glycolic-co-caprolactone) (Sugiura, 2016). In addition, decellularised organs for the production of cardiac patches have been investigated and used in *in vivo* studies. Godier-Furnemont (2011), for instance, has seeded human mesenchymal progenitor cells in fibrin on a decellularised human myocardial sheet and implanted the scaffold in a rat MI model resulting in an improvement of the vascular network and cell migration into the damaged tissue. Decellularised small intestinal submucosa (SIS) alone or seeded with MSCs was implanted in a rabbit MI model and led to an improvement in left ventricle remodelling (Chang,2016). Recently, the focus has moved to bioactive materials, that are biomaterials having from one side the appropriate physical strength and degradation rate of synthetic materials and from the other side the biological cues of the most important component of ECM (collagen, fibronectin and laminin) (Weber,2015). A further step ahead is to create bioactive materials: biomaterials modified with bioactive molecules. The main advantage of these novel biomimetic materials is that the bulk materials are known materials, widely reported in literature and proven to be safe for clinical use (Chachques, 2015), while the surface functionalisation with bioactive can add new biological properties enhancing the tissue regeneration properties of the implant. These bioactive molecules could be either whole ECM molecules as well as "cell-binding" domain sequences identified within the whole protein that have the advantages outlined throughout this thesis.

4.1.2 AVITENE ULTRAFOAM™ AS TREATMENT FOR MI INJURY

Avitene Ultrafoam™ sponge is composed by microfibrillar collagen type I and consists of a sheet that can be cut to any shape or size (Fig.4.1).

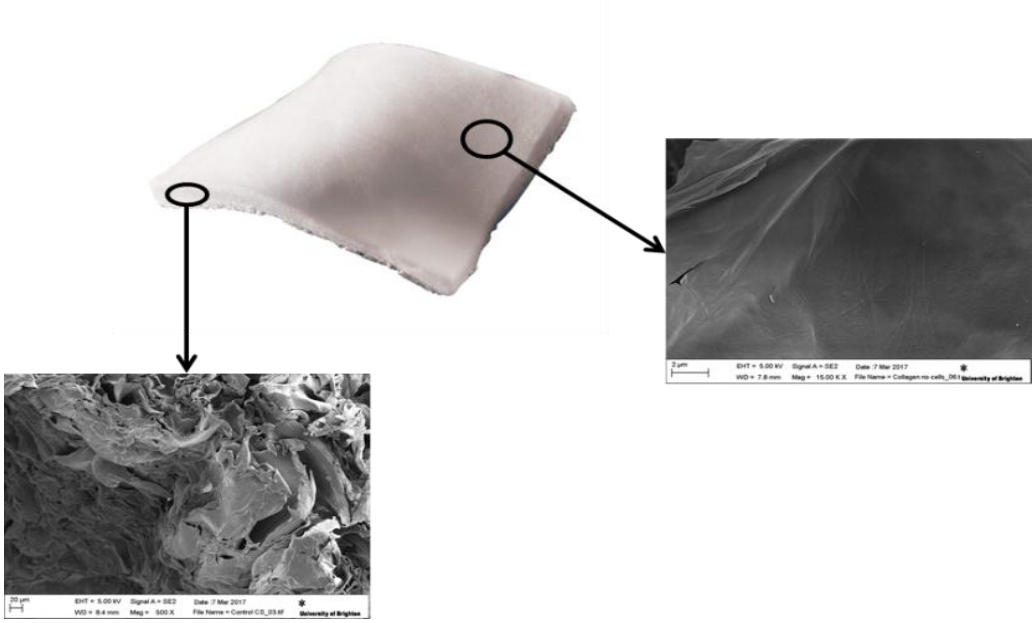

Fig.4.1 Morphological appearance of Avitene ultrafoam™ sponge sheet: when the sponge is microscopically analysed it is possible to distinguish a smooth surface whereas the inside shows the tipical fibrils-like structure derived from collagen type I entanglement.

Avitene microfibrillar collagen is derived from bovine corium and it is provided as a formulation of wool consistency that can be shaped based on the clinical needs as it adapts well to irregular surfaces (Low, 2003). Ultrafoam™ has been developed as an active absorbable collagen with haemostatic properties as it has been shown to accelerate clot formation (Achneck, 2010). This collagen sponge has been studied in more than 200 published papers and it is widely used in surgical procedures for its efficacy and safety. Avitene Ultrafoam™ sponge has been on the market from over 40 years and indeed is a well-known material: it does not swell significantly and is absorbed in approximately 8 weeks (Wagner, 1996); it is a really suitable material for surgeons who can use it in minimally-invasive laparoscopic procedures (Low, 2003). Regarding its use in the research field, Ultrafoam™ sponge has been used in studies focussing on the understanding of the inflammatory process occurring after a tissue injury. In particular, Ultrafoam™ sponge has been used as a scaffold *in vivo* in mice in order to test the vascularisation of the scaffold itself by the recruitment and activation of a specific macrophages phenotype that enhances angiogenesis (Spiller, 2014). Due to its morphological properties (interconnected microfibrils), Avitene UltrafoamTM has been used as a 3D growth platform for the hepatic

differentiation of pluripotent human liver stem cells (HLSCs) for liver regeneration: results show that HLSCs infiltrate the sponge, form clusters and change their phenotype into a mature hepatic population (Carraro, 2010). In clinics, Avitene Ultrafoam™ is widely used as haemostatic agent as well as for periodontal reconstruction (Achneck, 2010). This material is able to enhance the coagulation process: when Avitene ultrafoam™ is in contact with blood, it enhances platelets aggregation. These platelet aggregates degranulate and deliver factors able to induce clot formation (Andreoli, 2000). Regarding its dental applications, when bone is in contact directly with Avitene Ultrafoam™ it interpenetrates into the material pores and this entanglement of the sponge with the tissue creates a perfect "material with osteoconductive properties" (Bosshardt, 2009). Not many studies have been published with Avitene Ultrafoam™ sponge for myocardium tissue regeneration as well as Avitene Ultrafoam™ sponge modified with biological cues. However, remarkable examples of the use of Avitene Ultrafoam™ sponge in this application field are reported hereinafter.

In order to slow down the effect of heart failure due to ischemic event, the use of cell therapy with hematopoietic and peripheral blood-derived stem/progenitor cells could have beneficial effects. For this reason Avitene Ultrafoam™ sponge has been used as a scaffold for the *in vivo* delivery of bone marrow cells. Results show that cells are not able to differentiate just only with the help of the scaffold but that the combination of cells and collagen scaffold enhances angiogenesis and vasculogenesis in injured hearts of rats (Pozzobon, 2010).

A scaffold produced with biological-derived materials tethering biological cues forms the ideal platform for cardiac tissue engineering. Indeed, Avitene Ultrafoam™ collagen sponge functionalised with specific peptides sequence could improve cells viability and differentiation. For this reason, Ultrafoam™ sponge has been covalently functionalised with –RGDS sequences that have a crucial role during fetal cardiac development and with –RGD that acts as a ligand for integrins that promote cardiac healing (Lee,2016). The new functionalised Ultrafoam™ sponge was used then *in vitro* to test the improvement that such biomaterials could bring to contractile properties of cardiomyocytes. Results demonstrate that cardiomyocytes enhance their contractile behaviour and increase their viability and differentiation when seeded on functionalised Ultrafoam™ sponge and cultured *in vitro* (Shimazaki, 2008).

4.1.3 AIM OF THE CHAPTER

The aim of this chapter is to functionalise and characterise an already existing commercial product, Aviten Ultrafoam^{TM} collagen type I sponge, with the dendritic angiogenic peptides developed in Chapter 2 and to assess the potential of the obtained innovative device as a cardiac patch with angiogenic properties in the treatment of myocardial infarction. Likewise Chapter 3, the functionalisation of the collagen scaffold with the three different dendritic angiogenic peptides was examined by SEM and FT-IR.

4.2 MATERIALS and METHODS

4.2.1 Materials

Table 4.1 Materials used during the experimental process of Ultrafoam™ functionalisation with dendritic angiogenic peptides.

Product	***Supplier***	***Code No***
Avitene UltrafoamTM Collagen type I sponge	Bard	1050050
N-(3-Dimethylaminopropyl)-N′-ethylcarbodiimide hydrochloride or EDC	Sigma-Aldrich	03450
N-Hydroxysuccinimide or NHS	Sigma-Aldrich	130672
MES	Sigma-Aldrich	M3671

4.2.2 Ultrafoam™ sponge scaffold preparation

Collagen Type I scaffold have been obtained from a Ultrafoam™ collagen type I sponge sheet using a biopsy punch able to cut scaffold of approximately 5x4 mm dimensions (Fig. 4.2).

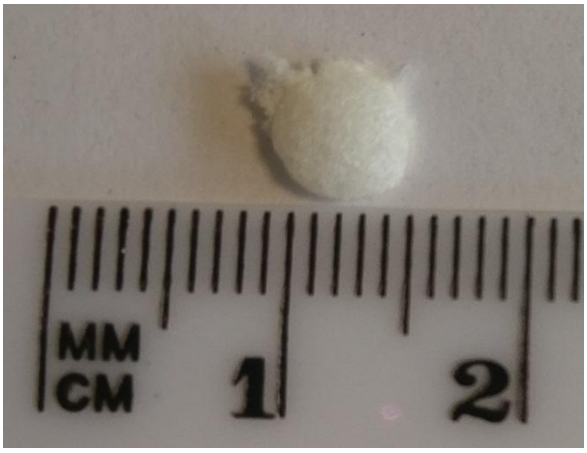

Fig. 4.2 Ultrafoam™ Scaffold obtained by cutting the sponge with a punch with dimensions of approximately 5x4 mm.

4.2.3 Functionalisation of Collagen type I scaffold

Dendritic angiogenic peptides [FFgen0K$(QHREDGS)_2$, FFgen0K$(WQELYQLKY)_2$ and FFgen0K$(RKIEIVRKK)_2$], as synthesised in Chapter 2, were covalently bound to collagen scaffolds by carbodiimide reaction using the carboxyl groups exposed by dendritic angiogenic peptides root and the collagen's free amino groups. Therefore, collagen scaffolds were gently placed in a 24 well plate and soaked in 1mL 0.1M MES buffer at pH 6.5. The carboxyl groups from dendritic angiogenic peptides were then activated by

addition of EDC (4mM) and NHS (10 mM) where the activation reaction was allowed to proceed at room temperature for 30 minutes. At this stage dendritic angiogenic peptides were dissolved in MES buffer (1mg/mL) and pipetted onto collagen scaffolds. The conjugation reaction took place overnight at room temperature under agitation. The obtained three modified collagen scaffolds with dendritic angiogenic peptides were then lyophilised and stored at -20°C.

4.2.4 Characterisation of Collagen scaffold embedded dendritic angiogenic peptides by SEM and FT-IR

Collagen scaffolds functionalised with FFgen0K$(QHREDGS)_2$, FFgen0K$(WQELYQLKY)_2$ and FFgen0K$(RKIEIVRKK)_2$ respectively were characterised using a SEM and FT-IR.

4.2.4.1 FT-IR

FT-IR method has been described in Chapter 2, Section 2.2.3.3.

For the results obtained in this chapter, collagen scaffolds functionalised with dendritic angiogenic peptides have been analysed over the range of 4000-650 cm^{-1} in triplicates for 8 scans at room temperature.

4.2.4.2 SEM

SEM method has been described in Chapter 3, Section 3.2.4.1.

In this study, collagen scaffolds have been coated with a thin gold layer before placing them in the vacuum SEM sample chamber and analysed at 5.0 kV at different magnifications.

4.3 RESULTS

4.3.1 FT-IR

Avitene Ultrafoam™ scaffolds have been functionalised with dendritic angiogenic peptides trough a carbodiimide reaction and characterised by FT-IR analysis. As a control FT-IR spectrum of Ultrafoam™ has been recorded in order to have a comparison with spectra obtained from the scaffolds functionalised with the dendritic angiogenic peptides. Ultrafoam™ collagen Type I scaffold spectrum (Fig. 4.3) shows the typical peaks already observed in Chapter 3 (Section 3.3.1, Fig. 3.4, peaks n.1, 2, 3 and 4). Indeed, it is possible to recognize a peak at 1658 cm^{-1} that identifies α-like helix of collagen type I, a peak at 1555 cm^{-1} correlated to the presence of II amide, a peak at 1403 cm^{-1} that marks the presence of $\delta(CH_3)$ groups and the last one at 1238 cm^{-1} related to the presence of δ(C-N) groups.

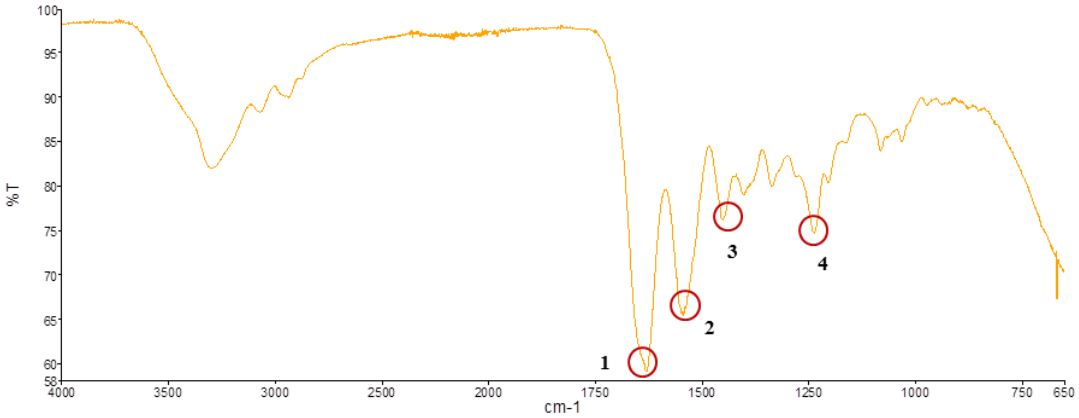

Fig. 4.3 FT-IR Spectrum of Avitene Ultrafoam™ collagen (type I) sponge where circles indicate peaks: 1-1658 cm^{-1} ,2- 1555 cm^{-1} 3- 1403 cm^{-1} ,4-1238 cm^{-1}.

Table 4.2 *Relevant peaks involved in the characterisation of Avitene Ultrafoam™ collagen (type I) sponge.*

Relevant peaks		Identified Groups
Avitene Ultrafoam™	1) 1658 cm^{-1} 2) 1555 cm^{-1} 3) 1403 cm^{-1} 4) 1238 cm^{-1}	1) α-like helix 2) $-CONH_2$ 3) $-CH_3$ 4) -C-N

Avitene Ultrafoam™ scaffolds have been functionalised with the three different angiogenic peptides, that are FFgen0K$(QHREDGS)_2$, FFgen0K$(WQELYQLKY)_2$ and

FFgen0K(RKIEIVRKK)$_2$ and FT-IR performed again to verify the occurred functionalisation of the Ultrafoam^{TM} scaffold. Therefore, Fig. 4.4 shows the spectrum obtained from the characterisation of scaffold+FFgen0K(QHREDGS)$_2$ (green line) in comparison with Ultrafoam^{TM} scaffold spectrum (red line): it is possible to highlight the fingerprint of FFgen0K(QHREDGS)$_2$ (Fig. 4.4, green line) that has already been identified in Chapter 2, Section 2.3.3: peaks 873 cm^{-1} and 1350 cm^{-1} are the fingerprint of the presence of –QHREDGS sequence and so confirm functionalisation. These peaks are indeed, peak 874 cm^{-1} can be referred to an alcohol group (-OH) exposed from a serine residue of the Ang-1 peptide analogue that is not present in the Ultrafoam^{TM} scaffold spectrum and peak 1350 cm^{-1} that identifies the presence of an alkene (C=C) group that corresponds to the side group exposed from the histidine residue present in the QHREDGS sequence. Moreover, scaffold+FFgen0K(QHREDGS)$_2$ peak at 3337 cm^{-1} indicates a decrease in the quantity of free NH_2 groups, a further proof of the occurred functionalisation.

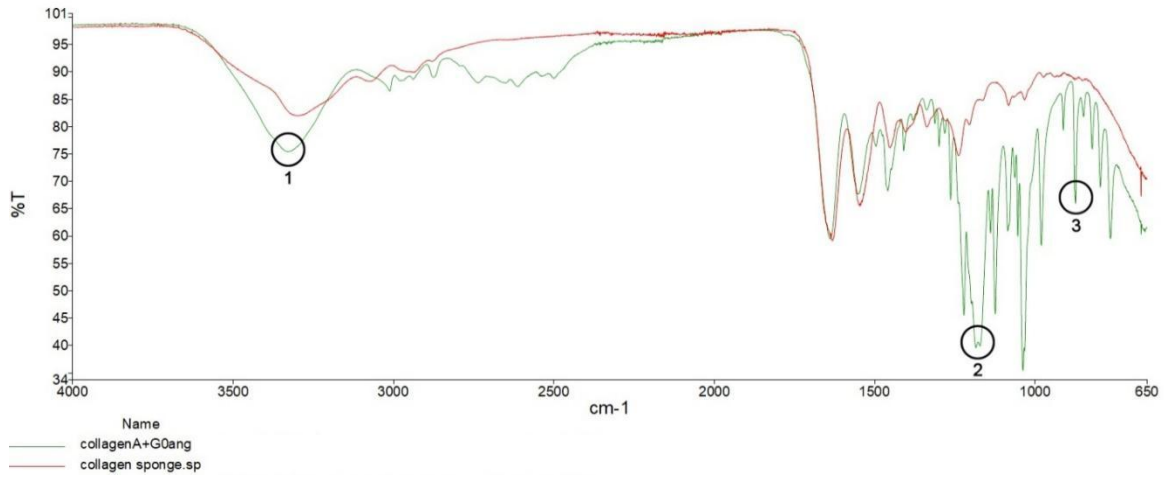

Fig.4.4 FT-IR Spectra of Ultrafoam^{TM} sponge functionalised with FFgen0K(QHREDGS)$_2$ (green line where circles indicate peaks: 1-3337 cm^{-1} ,2- 1350 cm^{-1} 3- 874cm^{-1}) and of Avitene Ultrafoam^{TM} collagen (type I) sponge (red line).

Table 4.3 *Relevant peaks involved in the characterisation of Avitene Ultrafoam^{TM} collagen (type I) scaffold functionalised with FFgen0K(QHREDGS)$_2$.*

Relevant peaks		Identified Groups
Ultrafoam^{TM}+ FFgen0K(QHREDGS)$_2$	1) 3337 cm^{-1} 2) 1350 cm^{-1} 3) 874 cm^{-1}	1) NH_2 2) CH_2=CH_2 3) -OH

FT-IR analysis has also been used to verify the functionalisation of Ultrafoam^{TM} scaffold with the –WQELYQLKY- bioactive dendritic peptide. Spectra of Ultrafoam^{TM} scaffold functionalised with FFgen0K(WQELYQLKY)$_2$ (Fig.4.5, purple line) and of FFgen0K(WQELYQLKY)$_2$ (Fig. 4.5, black line) differ from each other for the presence of a peak at 780 cm^{-1} fingerprints of FFgen0K(WQELYQLKY)$_2$ that highlight the presence of an aromatic groups derived from the tyrosine residue of VEGF bioactive peptide, proving the functionalisation of the Ultrafoam collagen type I with the dendritic angiogenic peptide. Moreover, FT-IR analysis detected also a decrease in transmittance intensity of the peak related to the presence of free NH_2 (peak 3350 cm^{-1}).

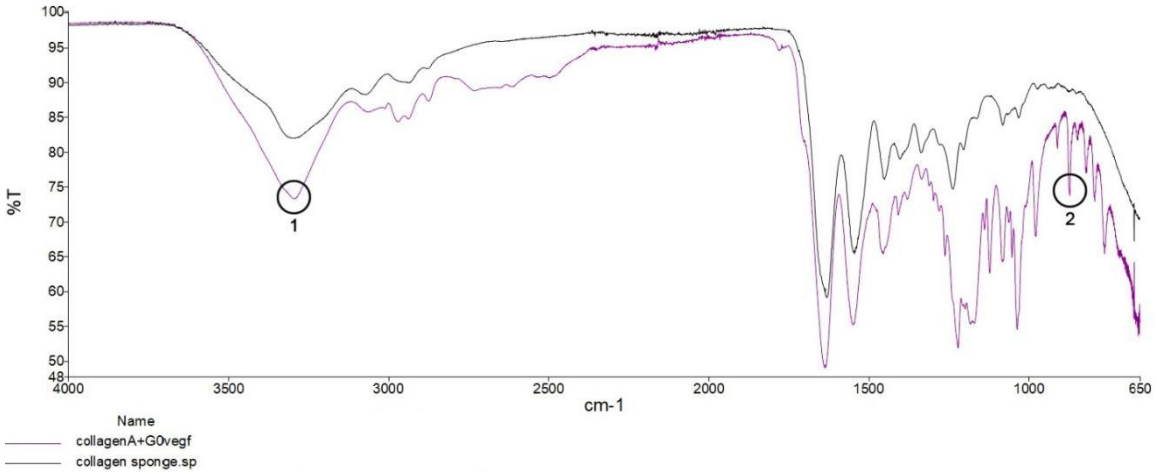

Fig. 4.5 FT-IR Spectra of Ultrafoam^{TM} sponge functionalised with FFgen0K(WQELYQLKY)$_2$ (purple line where circles indicate peaks: 1-3350 cm^{-1} ,2- 780 cm^{-1}) and of Avitene Ultrafoam^{TM} collagen (type I) sponge (black line).

Table 4.4 *Relevant peaks involved in the characterisation of Avitene Ultrafoam^{TM} collagen (type I) scaffold functionalised with FFgen0K(WQELYQLKY)$_2$.*

Relevant peaks		Identified Groups
Ultrafoam^{TM}+ FFgen0K(WQELYQLKY)$_2$	1) 3350cm^{-1} 2) 780 cm^{-1}	1) Aromatic Group 2) NH_2

The last material analysed by FT-IR analysis is Ultrafoam^{TM}+FFgen0K(RKIEIVRKK)$_2$. Fig. 4.6 shows the spectrum of Ultrafoam^{TM}+FFgen0K(RKIEIVRKK)$_2$ (grey line) and of FFgen0K(RKIEIVRKK)$_2$ (black line). In this case, the fingerprint of FFgen0K(RKIEIVRKK)$_2$ proving that the functionalisation has occurred is the peak at 790 cm^{-1} that identifies the presence of alcohol groups derived from PDGF-BB bioactive peptide residues.

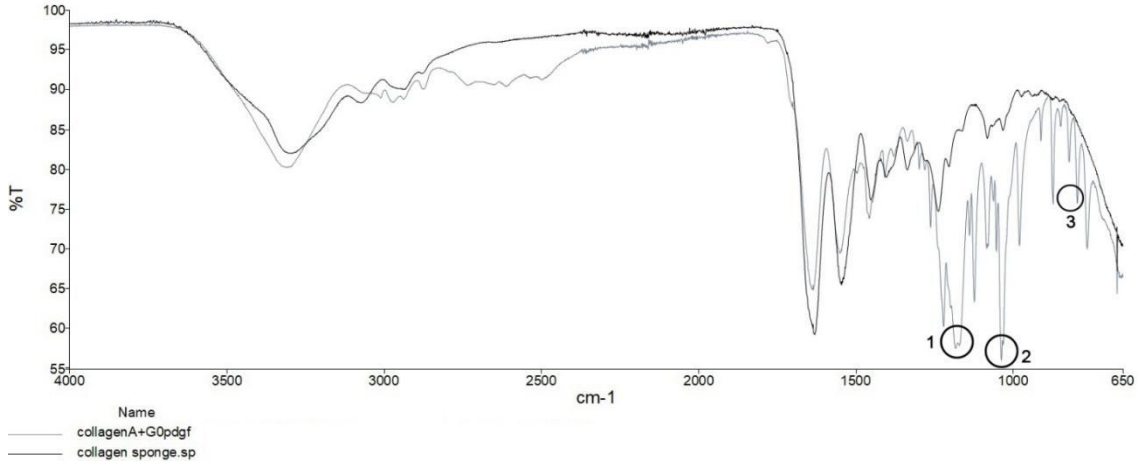

Fig. 4.6 FT-IR Spectra of Ultrafoam™ sponge functionalised with FFgen0K(RKIEIVRKK)$_2$ (grey line where circles indicate peaks: 1-1348 cm^{-1} ,2- 1085 cm^{-1} 3- 790 cm^{-1}) and of Avitene Ultrafoam™ collagen (type I) sponge (black line).

Table 4.5 *Relevant peaks involved in the characterisation of Avitene Ultrafoam™ collagen (type I) scaffold functionalised with FFgen0K(RKIEIVRKK)$_2$.*

Relevant peaks	
Ultrafoam™+ FFgen0K(RKIEIVRKK)$_2$	1) 1348 cm^{-1} 2) 1085 cm^{-1} 3) 790 cm^{-1}

4.3.2 SEM

SEM microscopy analysis has been used to investigate the morphology of Ultrafoam™ collagen sponge before (Fig. 4.7, panel A) and after (Fig.4.7, panel B) functionalisation with dendritic angiogenic peptides. The resulting images show a smooth surface structure when Ultrafoam™ sponge sheet is analysed before cutting it to form the cylindrical scaffold. On the contrary, SEM image of fucntionalised Ultrafoam™ scaffold with dendritic angiogenic peptides reveals a different morphological structure: the surface became characterised by a relatively rough topography probably attributable to the presence of the grafted dendritic angiogenic peptides.

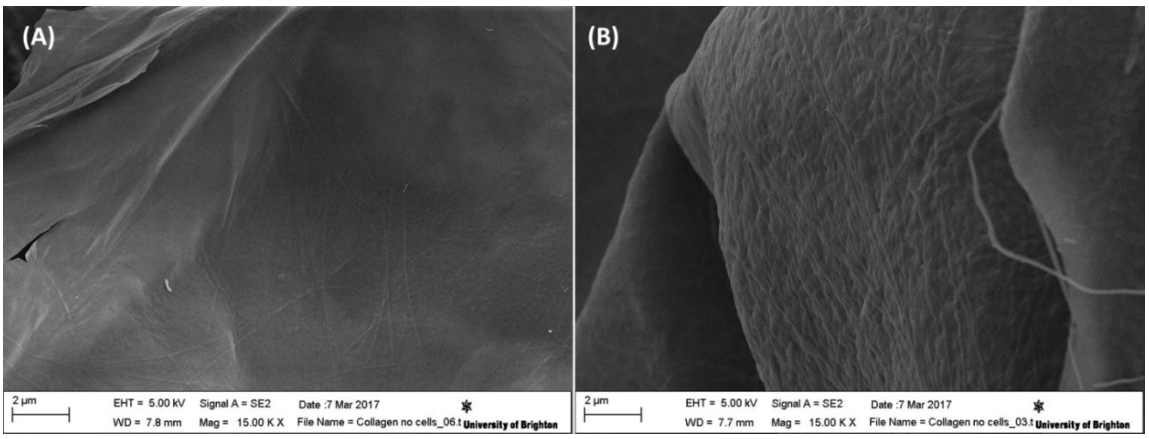

Fig. 4.7 Morphological SEM analysis of A)Ultrafoam^{TM} collagen type I scaffold surface and B) functionalised Ultrafoam^{TM} collagen with FFgen0K(WQELYQLKY)$_2$ scaffold surface as representative image of a functionalised scaffold. .

4.4 DISCUSSION

In the last years, cardiac patches have been always used as delivery platform for cells, bioactive factors and biological cues. Recently, cardiac patches have been used as acellular matrices for the regeneration of the myocardium after ischemic event (O'Neill,2016). This new approach in the treatment of MI injury is due to the intrinsic characteristics of the patch that can create an advantageous environment capable of supporting tissue regeneration (Aboli, 2011). Dendritic angiogenic peptides, as assessed in the previous chapters of this thesis, are high versatile molecules that can be used as free drugs, as functionalisation moieties for injectable materials as well as to functionalise scaffolds. Whereas, in the last few years, investigators have pointed out the need to produce biomimetic materials: the combination of natural polymeric patches and bioactive molecules gains great relevance in the research field (Spiller, 2014). Indeed, in this chapter the focus was on the improvement of an already existing product on the market, Avitene Ultrafoam^{TM} sponge with dendritic angiogenic peptides. Therefore, the main hypothesis of this chapter was to ascertain whether dendritic angiogenic peptides can be used as functionalisation moieties for cardiac patches.

The objectives pursued to reach the answer to this hypothesis were:

1) Cut Ultrafoam^{TM} sponge into reproducible cylindric patches
2) Perform the functionalisation of the scaffolds with dendritic angiogenic peptide
3) Characterise the scaffolds by FT-IR and SEM analysis to prove the efficacy of the coupling reaction.

Scaffolds were obtained from a collagen type I sponge, where the characteristic of collagen type I has been widely explained in the previous chapter. Scaffold where cut into cylinder of 5x4 mm in order to have a suitable size for implantation for further *in vivo* studies. Avitene Ultrafoam^{TM} sponge has been chosen as cardiac patch for the treatment of ischemic myocardium for specific reasons: (i) it is available in dry woolly form that can be assembled in different shapes based on the needs of the specific clinical application; (ii) it is adaptable to irregular surfaces as well as on large surface areas as those observed in myocardial injuries; (iii) its proven use in clinics is as haemostatic plug, is advantageous in the treatment of myocardial injury as it helps reducing bleeding since clotting is achieved within 2 to 5 minutes (Baker, 1999); (iv) it does not swell significantly since it has been treated with ethyl alcohol during the manufacturing process in order to prevent that the swallowed patch constricts other adjacent healthy areas (Spotnitz, 2012); (v) it is absorbed in 8-10 weeks proving good support to tissue regeneration and tuned resorption of the

patch; (vi) it is well-known to be easy to handle; (vii) it can be used in laparoscopic procedures and (viii) it is an FDA approved product (Wagner, 1996). All these characteristics make Avitene Ultrafoam™ a suitable candidate as scaffold for myocardium regeneration. In addition, Avitene Ultrafoam™ sponge has been widely used in different studies as, for example, to investigate the inflammatory process, as a 3D cell growth platform, as a haemostatic agent and in periodontal reconstruction. On the other hand, little is known about the use of Avitene Ultrafoam™ for myocardium regeneration and in particular for its angiogenic properties. These knowledge gaps prompted the present study aiming at unveiling the properties of this material in this specific application.

In this study, in order to improve and make Avitene Ultrafoam™ sponge patch suitable for myocardium regeneration after ischemic event, a carbodiimmide reaction has been used to functionalise the collagenic scaffold with dendritic angiogenic peptide. FT-IR demonstrated the successful functionalisation of the scaffold surface. Moreover, all the peaks extract from FT-IR spectrum listed in this chapter and used to characterise the functionalised patches are in agreement with the ones collected in the previous chapter of this thesis where the peptides were coupled to collagen beads. SEM analysis has shown the typical structure of Avitene Ultrafoam™ sponge and the modified morphology after covalent attachment of dendritic angiogenic peptides, further demonstration of the successful functionalisation process.

The most significant achievement was that the functionalisation of Avitene Ultrafoam™ sponge with dendritic angiogenic peptides created an interface between patch and cells where cells could recognise both specific signals together with the relatively rough topography known to encourage cell colonisation on biomaterials organisation (Bettinger, 2009) (Fig.4.8).

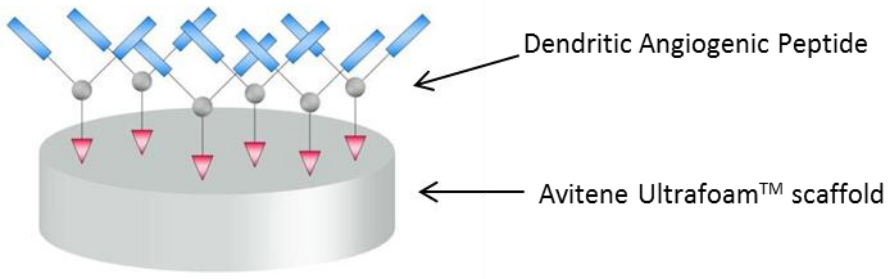

Fig. 4.8 Scheme of Avitene Ultrafoam™ sponge functionalised with dendritic angiogenic peptides showing the dendritic angiogenic peptide spacial orientation on the scaffold.

Dendritic angiogenic peptides are covalently bond to both beads and Ultrafoam^{TM} scaffold by a peptide bond. Peptide bond is the reason of the dendritic angiogenic peptides orientation shown in Figure 4.8. This type of bond has the peculiarity to have the four bonding atoms and the two α carbons on the same plane (Brown, 2002). Moreover, the bond angles around the carbonyl groups and amide groups are approximately 120° (Morrison, 1997).This geometry is given by the representation of the peptide bond as an resonance hybrid of two structure: the first has a double bond between carbon and oxygen and the second has a double bond between the carbon and the nitrogen. Indeed, in the real structure, C-N bond is mainly a double bond (Fig. 4.9) (Morrison, 1997).

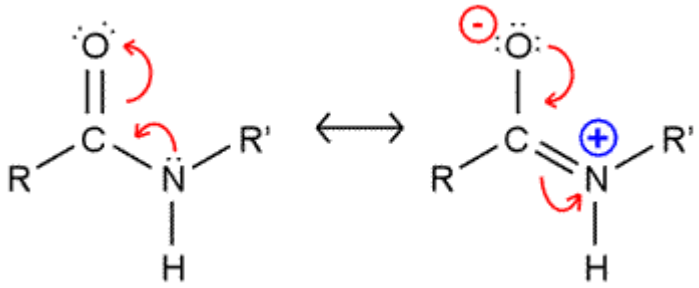

Fig.4.9 Chemical representation of the resonance hybrid of peptide bond (Adapted from www.quora.com).

The preferred configuration of the peptide bond atoms is the one in which the two α carbons are in the trans position. In this way, peptide bond become rigid and planar. Indeed, the rigid geometry and the limit to rotational changes confer to peptide bond and thus to structure formed by this bond defined and precise form and spatial orientation (Brown, 2002).

4.5 CONCLUSION

In conclusion it is possible to state that:

1) Cardiac patches can be produced from Ultrafoam^{TM} collagen type I sponge
2) Ultrafoam^{TM} scaffold have been functionalised successfully with dendritic angiogenic peptides as proven by FT-IR and SEM analysis

The functionalisation of cardiac patches with dendritic angiogenic peptides has occurred successfully and the angiogenic potential of this new biomaterial will be tested in Chapter 6. This assessment will need to be preceded by a study of cytotoxicity and bioactive properties of the dendrimeric peptides when used as soluble angiogenic factors. This was the focus of Chapter 5.

5. ASSESSMENT OF THE CYTOTOXICITY AND ANGIOGENIC POTENTIAL OF POLY (ϵ-LYSINE) DENDRONS TETHERED WITH ANGIOGENIC PEPTIDES BY A 2D CULTURE MODEL

5.1 INTRODUCTION

Angiogenesis is the process from which new blood vessels are developed starting from pre-existing ones (Adams, 2007). For this reason, therapeutic angiogenesis has been widely investigated in regenerative medicine in order to restore the functionality of damaged myocardium through the formation of new blood vessels (Nakamura, 2009).

5.1.1 BLOOD VESSELS FORMATION: FROM ANGIOBLAST TO VASCULAR NETWORK

During the embryo development, blood vessels start to assembly from the angioblast, endothelial precursor of the mesoderm, which differentiates into a basic vascular tangle through the vasculogenesis process (Swift, 2009). Hereafter, the primitive vasculature is subjected to angiogenesis by vessel sprouting creating a labyrinth of arteries and veins (Fig.3.1) (Adams, 2007).

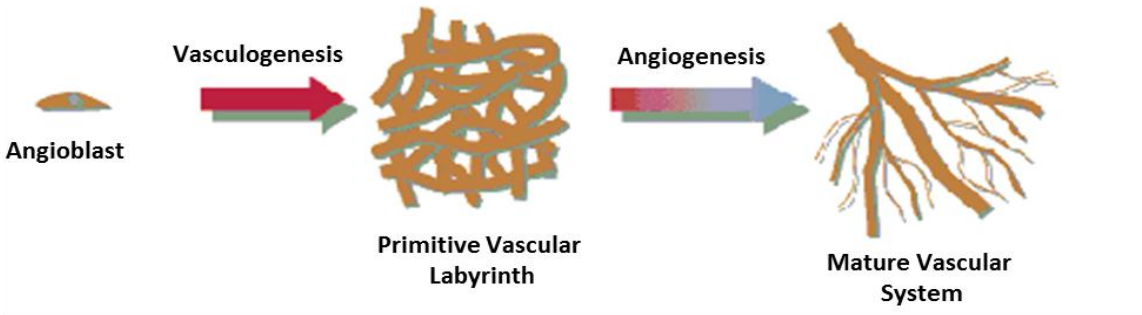

Fig. 5.1 Vasculogenesis process allows the angioblast to differentiate into a primitive vascular network. Subsequently, vessel sprouting (angiogenesis) constitute a mature vascular system formed by arteries and veins (Adapted from www.unifr.ch).

Finally, pericytes and vascular smooth muscle cells are recruited to provide stability to the newly formed vessels and regulate perfusion during the arteriogenesis (Jain, 2003). In the adult, the formed vessels are quiescent and infrequently form new branches but endothelial cells still have high ductility in perceiving and responding to angiogenic signals (Potente, 2001). The newly formed blood vessel system would be responsible of essential roles such as transporting oxygenated blood, removing waste products, working as a connection system for hormonal communication inside the human body and enhancing fast deployment of the immune response (Swift, 2009).

The mature vascular system is divided into three categories (as widely discussed in Chapter 1, Section 1.1) of blood vessels: arteries, veins and capillaries.

All of these three categories share the same basic structure (Saladin, 2012) (Fig. 3.2) composed of three different layers:

- Tunica intima: the inner layer of a blood vessel is composed of endothelial cells immersed in a polysaccharide intercellular matrix. This layer is capable of absorbing fluids that flow through the lumen vessel and transferring cells from the lumen to the tissues.
- Tunica media: is the thickest layer in arteries and is composed by circular elastic fibres, connective tissue and polysaccharide substances. The tunica media may be abundant of vascular smooth muscle cells which guide the contraction of the vessel.
- Tunica adventitia: layer of connective tissue which contains the nerves that serve the muscle layer and the capillaries for the transport of nutrients in the larger vessels.

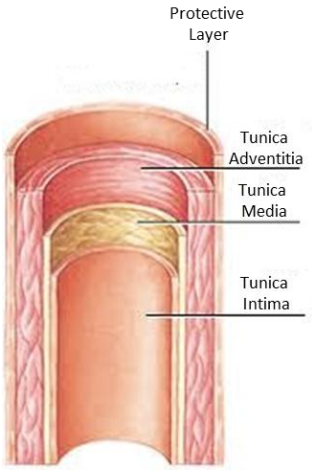

Fig. 5.2: Schematic representation of basic blood vessels structure (Adapted from www.aviva.co.uk).

5.1.2 ENDOTHELIAL CELLS

Endothelial cells form the continuous lining of blood vessels and they have a considerable capacity to adapt their number and arrangement according to the local need (Saladin, 2012). Almost all tissues depend on a blood supply and this is ultimately related to the role of endothelial cells, which create an adaptable life support system by branching into an intricate vasculature system throughout the body (Asahara, 2009). Growth and tissue repair would not be possible without the ability of the endothelial cells to extend and remodel the network of blood vessels. Indeed, if the amount of connective tissue, smooth muscle cells and elastic fibres could vary in the blood vessels structure, the endothelial lining is always present (Moon, 2010). Endothelial cells cover the inner surface of the entire vascular system, from the heart to the smaller capillary, and control the flow of nutrients as well as the transit of white blood cells across the blood vessel wall into the surrounding tissues in the case of immune reactions (Sanvicens, 2013). In adults, endothelial cells retain the

ability to proliferate and migrate. For instance, if an area of the aorta wall is damaged and deprived of its endothelial cells, those that remain in the surrounding areas are capable of proliferate and migrate in order to cover the damaged surface (Jain, 2003). In conclusion, endothelial cells not only repair the inner lining of existing blood vessels but are also able to create new blood vessels through the angiogenesis process (Clapp, 2009).

Indeed, endothelial cells have been used widely *in vitro* to test different biomaterials. Confluent adult bovine aortic endothelial cells (ABAE) have been used to investigate their response when treated with collagen gel loaded with Ang-1 growth factor for therapeutic angiogenesis application: cells grown on the gel, migrate into it and form capillary-like tubules (Miklas, 2013). Human umbilical vein endothelial cells (HUVEC) were used to elucidate the role of Ang-1 in promoting stabilisation of vascular networks and branching morphogenesis *in vivo* and *in vitro* (Reis, 2011). Moreover, HUVECs were treated with a 3D gel composed of Type I collagen functionalised with VEGF and bFGF in order to test the enhancement of the scaffold after the functionalisation to induce angiogenesis *in vitro* (Shen, 2008). Lastly, neonatal rat cardiomyocytes were co-cultured with adult cardiac endothelial cells to test the ability of endothelial cells to protect cardiomyocytes from injury (Rask, 2010).

5.1.3 ANGIOGENIC BIOACTIVE PEPTIDES

To overcome problems related to protein therapy (widely explained in Chapter 1), peptide fragments from the ECM growth factors have been demonstrated to have a role in the angiogenic process rather than the full proteins (Post, 2001).

5.1.3.1 Vascular Endothelial Growth Factor Analogue

D'Andrea's group (2005) discovered that a synthetic version of a VEGF-mimicking peptide (QK) would activate receptors responsible for the onset of angiogenesis. Their studies indicated that QK peptide could stimulate proliferation and sprouting of endothelial cell. D'Andrea's results were confirmed by Leslie-Barbicks (2011) studies using a poly (ethylene glycol) hydrogel scaffold functionalised with the QK peptide. According to Leslie-Barbick, endothelial cells migrate, form tubule-like structures and make cell-cell contacts in response to the functionalisation with QK peptide of the hydrogel scaffold, demonstrating the scaffolds ability to promote angiogenesis *in vitro*. Moreover, Leslie-Barbick's study demonstrated the ease with which VEGF mimicking-peptide can be incorporated into a hydrogel, compared to the whole protein. Chan (2011) restated the same concept of D'Andrea and Leslie-Barbick: sequences derived from VEGF have a role

in the angiogenic process, even if they are small. Furthermore, linear peptides have a poor stability and their potential could be improved by integrating them with protein scaffolds. Indeed, Chan's studies reported that 'grafting' QK peptide to cyclic peptide scaffolds makes them more stable in human serum compared to the 'non-grafted' peptide. Indeed, QK peptide grafted to cyclic peptide scaffolds was shown to affect angiogenesis *in vivo* at nanomolar concentrations (Chan, 2011).

5.1.3.2 Angiopoietin-1 Analogue

The Ang-1 mimicking peptide, QHREDGS, promotes cardiomyocyte elongation and assembly of contractile structure and reduced cardiomyocyte apoptosis (Reis, 2013). Different strategies have been developed to use this peptide to promote angiogenesis, both *in vitro* and *in vivo*, and to test its potential in cardiac tissue regeneration. Rask et al. (2010) produced a new hydrogel scaffold composed of a photo-crosslinkable chitosan functionalised with –QHREDGS-NH_2 peptide. Attachment and viability of neonatal rat heart cells was shown to be higher on chitosan-QHREDGS scaffold compared to cells seeded on other hydrogel scaffold. Thus, chitosan-QHREDGS scaffold may support adhesion and survival of cells (Rask, 2010). Another approach could be the use of a chitosan-collagen scaffold still functionalised with QHREGDS peptide sequence. Even if the scaffold material composition is changed, results confirm that neonatal rat heart cells adhere and spread on the functionalised scaffold (Miklas, 2013). Furthermore, long-term angiogenic effects were investigated in a porcine myocardial ischemia model. This study demonstrated that Ang-1 enhances improvement of ventricular perfusion, which accelerates recovery of ischemic myocardium via arteriogenesis (Shim, 2006).

5.1.3.3 Platelet Derived Growth Factors Analogue

Identification of the PDGF-BB peptide analogue has been performed testing the agonist/antagonist properties of several peptides corresponding to residues in loops I and III of PDGF-BB using human dermal fibroblast: -RKIEIVRKK-NH_2 peptide induced stimulatory signals on these cells proving its capability of mimicking PDGF-BB role (Brennand, 1997). However, little is known in literature about the effects of this peptide analogue on the angiogenesis process.

The use of peptide analogue represents a great novelty in the treatment of ischemic disease by therapeutic angiogenesis, but these molecules have some disadvantages including poor stability, limited targeting of the precise tissue area and the controlled release over time. For these reasons, this peptide analogue has been used in combination with biomaterials in

order to achieve conformational stability, to enhance receptor interaction through precise spatial orientation and to prolong peptides efficiency (Deli, 2013).

5.1.4 AIMS OF THE CHAPTER

The aim of this chapter is to assess the bioactivity of dendritic angiogenic peptides as " free drugs" that have been designed and synthesised as illustrated in Chapter 2. The rationale in the design of this type of dendron was to have a precise number of angiogenic peptide analogue moieties capable of interacting with their receptors in the regenerating tissue microenvironment. For this reason, an assessment of the bioactivity of the different produced molecules was performed *in vitro* on human umbilical endothelial cells (HUVECs) where 2D test evaluated both cell viability and morphology. This assay offered an insight into the efficacy of the dendritic angiogenic peptides to induce angiogenesis *in vitro*.

5.2 MATERIALS and METHODS

5.2.1 Materials

Table 5.1 Materials used during the experimental process of in vitro assessment of dendritic angiogenic peptides influence on HUVECs and 3T3.

Product	***Supplier***	***Code No***
Human umbilical vein endothelial cells (HUVECs)	American Type Culture Collection (ATTC)	CRL-1730
Primary mouse embryonic fibroblast cells (3T3)	American Type Culture Collection (ATTC)	CL-173
Endothelial basal medium (F12K medium)	PAA	
Endothelial cell growth supplement (ECGS)	Sigma-Aldrich	E2759
Heparin	Fisher	9041-08-1
Foetal bovine serum (FBS)	PAA	30-20202
Dulbecco's Modified Eagle Medium (DMEM)	PAA	30-2002
Trypsin 0.05% EDTA(1x)	Fisher	25300
CytoTox 96 Non-radioactive Cytotoxivity (LDH) assay	Promega	G1780
ANTI CD-31 antibody HEC7	ABCAM LTD	ab119339
Donkey anti-mouse igG H&L (Alexa fluor 488)	ABCAM LTD	ab150105
Phalloidine-Rhodamine (TRICT)	Sigma-Aldrich	P2141

5.2.2 Methods

5.2.2.1 Cell Culture

This section is referred to the tissue culture techniques and the biological assays performed on dendritic angiogenic peptides. In particular, the molecules that have been tested in this chapter are shown in Table 5.2.

Table 5.2. Molecules tested on HUVECs by a 2D in vitro model.

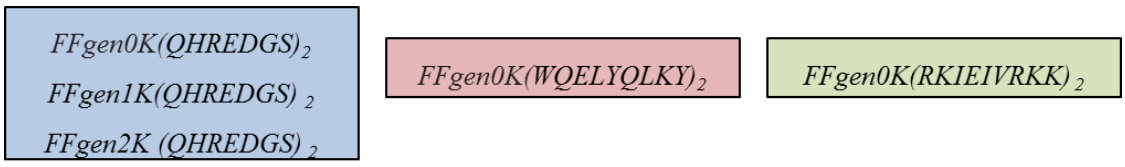

5.2.2.2 Sample Treatments, Sterilisation and Controls

All the above-mentioned samples were dissolved in phosphate-buffered saline (PBS,Fisher Scientific, UK) solution and filtered for sterilisation with a plastic syringe equipped with a 0.22 µm filter. Tissue culture plastic multi-well was used as negative, non-toxic control for biological response assessment as well as linear angiogenic peptide and non-functionalised dendrons.

5.2.2.3 Cells And Medium

In this project two different cell lines were used:

- HUVECs, human umbilical vein endothelial cells
- 3T3, derived from the primary mouse embryonic fibroblast cells.

All procedures described below were performed under standard sterile conditions. HUVECs were cultured in endothelial basal medium (F12 K) supplemented with 10 % (v/v) of foetal bovine serum, 0.05 $g \cdot mL^{-1}$ heparin and 0.1 $g \cdot mL^{-1}$ of endothelial cell growth supplement (ECG). 3T3 cells were cultured in Dulbecco's Modified Eagle Medium (DMEM) containing high glucose concentration and 10% (v/v) of fetal bovine serum (FBS).

5.2.2.4 Passaging of Confluent Cells

Both cell populations were maintained by routinely growing cell monolayer stocks in 75cm^2 plastic flasks at 37˚C in a humidified incubator with 5% CO_2 in air. When confluence was reached, both cell lines were ready for passaging. Medium was removed from the flask and replace with 2 mL of trypsin. The flask was placed back in the incubator for 5 minutes. A centrifuge tube was filled with 4 mL of medium to neutralise the trypsin. Cells were checked with the optical microscope and when they were freely floating in the trypsin, they were transferred in the centrifuge tube. Cells were centrifuged for 5 min at 1500 rpm and the supernatant removed using the vacuum line to leave a cell pellet. The cell pellet was resuspended in 1 mL of fresh medium and cells counted using a haemocytometer.

5.2.2.5 Counting by Haemocytometer

Cell suspension (8-10 µL) was applied to the edge of the cover slip and drawn into the haemocytometer by capillary action. Using the microscope, cells were then counted in the four outer corner counting squares. The average number of the cells counted in the four different areas x 10^4 represents the cells per mL of suspension.

5.2.2.6 Cell Seeding

When cells were needed for experiments, they were generally seeded into 24-well plate format for repetitions of experimental parameters. HUVECs density for *in vitro* test has been choosen based on previuos studies (Meikle,2011; Senturk, 2016). Cells were suspended in fresh medium counting with haemocytometer 30000 cells/mL 3T3 and 22000 cells/mL HUVECs. Cell-specific media were used to resuspend the cells (30000 3T3 and 20000 HUVECs) that were seeded in the wells. After seeding, different dendrons solutions were used to spike the cells. The experiments were performed in triplicate as detailed on Table 5.3.

Table 5.3 Functionalised and non-functionalised dendrons applied to HUVECS and 3T3 cell culture.

Cell line	**Material**	**Material Concentration (µM)**
HUVECs/3T3	*FFgen0K(QHREDGS)$_2$*	(50, 10, 1)
HUVECs/3T3	*FFgen1K(QHREDGS)$_4$*	(100, 50, 10, 1)
HUVECs/3T3	*FFgen2K(QHREDGS)$_8$*	(50, 10, 1)
HUVECs/3T3	*FFgen0K(WQELYQLKY)$_2$*	(10, 1)
HUVECs/3T3	*FFgen0K(RKIEIVRKK)$_2$*	(100, 10, 1)
HUVECs/3T3	*QHREDGS*	(50, 10, 1)
HUVECs/3T3	*WQELYQLKY*	(10, 1)
HUVECs/3T3	*RKIEIVRKK*	(100, 10, 1)
HUVECs/3T3	*FFgen0K*	(50, 10, 1)
HUVECs/3T3	*FFgen1K*	(100, 50, 10, 1)
HUVECs/3T3	*FFgen2K*	(50, 10, 1)

5.2.1.7 LDH Cellular Toxicity Test

LDH assay was performed on media removed from each samples (see Section 5.2.2.6). Media was centrifuged at 500g for 5 min to remove any cells in the media. Then media were removed and centrifuged at 500g for 5 min to remove cells and the supernatant was stored at -20°C. Released LDH in culture supernatants was measured using the Promega CytoTox96 Non-Radioactive Cytotoxicity Assay. The kit was used following a protocol from the Promega technical bulletin.

Lysis solution was used as positive control, indicating 100% LDH release for the analysis. This was obtained by diluting 1:10 the lysis solution in fresh media and added 100µL of the lysis solution in two control wells (cells seeded on plastic plate). LDH substrate mix was produced adding 12mL of assay buffer to a bottle of substrate. Fifty microliters of the reconstituted buffer was transferred to every well of a 96 well plate and 50 µL of sample supernatant from all wells was then added to the corresponding position in the same 96 well plate.

The plate was covered with foil to protect it from light, incubated at room temperature for 30 minutes, then 50 µl of stop solution was added to each well. The absorbance was measured at 490 nm within one hour after the addition of stop solution. The obtained absorbance values were converted into a measurement of toxicity based upon the LDH released from lysed cells, using the following equation:

$$\frac{Sample\ absorption}{Lysis\ absorption} * 100 = \%Cytotoxicity$$

5.2.1.8 HPI Staining

The aim of this test was to examine viable, apoptotic and necrotic cell. This staining is based on a combined action of Hoechst 33342 and propidium iodide.

The binding of the dye Hoechst 33342 to the cell DNA is possible because of the ability of the dye to penetrate freely both the plasmalemma and the nuclear membrane of living cells and to stain their DNA. Living cells with an intact DNA appear as an intense blue colour at the fluorescent microscope light. Propidium Iodide (red dye) does not enter the living cells but is able to penetrate the membrane of the dead and apoptotic ones. Thus, by fluorescent microscopy, these two types of cells assumed a red and pink colour, respectively.

HPI staining must be used in darkness to avoid fluorescence emission quenching of the dye. For this reason all plates were wrapped in foil while transferred from hood to the microscope unit and kept in a dark room throughout their processing and analyis.

HPI staining (500 µL) was prepared by mixing 20 µL of Hoechst 33342 solution (10 µg/mL) with 20 µL of propidium iodide solution (10 µg/mL) in 460 µL of growth medium. A duplicate of samples was used for HPI study. Media was taken off and stored for the following LDH test and 100 µL of HPI staining was dropped in a new 24-well plate. The samples were observed as soon as possible because cells rapidly die in these conditions and the assessment of their viability can be compromised by artefacts due to long permanence of cells in dry environment. The samples were analysed under fluorescent microscope

using a broad-band filtre at excitation wavelength of 365 nm and an emission wavelength of 397 nm.

Living cells were blue, apoptotic ones were pink or white and the dead cells appeared red. Magnification was kept constant for all the investigation at 40x. Both HUVECs and 3T3 were analysed taking six images per well.

5.2.1.9 Phalloidine-Rhodamine Assay

Phalloidine-Rhodamine is usually used to study the organisation of actin filaments inside the cells (Adami, 1999). Phalloidine is a fungal toxin. Its toxicity is attributed to the ability of this molecule to bind F-actin in the liver and the muscles cells. Thus, fluorescent conjugates of the Phalloidine are used to bind actin filaments for histological applications.

Phalloidine (100 mg) was dissolved in 0.1 mL of pure methanol. Final dilution was made by adding 1.9 mL sterile PBS to the first solution. A 2mL aliquot of the final fluorescent Phalloidine conjugate solution in PBS with a final concentration of 50 µg/mL was obtained and stored at 4˚C. The media was removed from the seeded cells using the vacuum line and 1mL of pure methanol was added to wells with the samples in order to fix cells. After washing with PBS for 30 seconds, 100 µL of stain solution was dropped in the different wells. The samples were observed thanks to the inverted fluorescence microscope using a red filter (540 nm).

5.2.1.10 Immunostaining of HUVEC

HUVECs were stained using CD31 antibody. CD31 is an integral membrane protein that mediates cell-to-cell adhesion. Moreover, CD31 is expressed on the surface of endothelial cells and mediates endothelial cell-cell interaction and angiogenesis.

For this reason, HUVECs spiked with dendrons functionalised with the Ang-1 mimicking peptide were immunostained and analysed using confocal microscope.

Primary antibody (anti CD31 antibody) was diluted 1:100 in 1% (w/v) BSA-PBS and incubated for two hours at room temperature. After three washes with PBS, the secondary antibody was added. This antibody is a donkey anti-mouse IgG labelled with alexa fluor 488 that is the fluorophore able to highlight the presence of CD31 protein on the HUVECs surface. The secondary antibody was diluted 1:200 in 1% (w/v) BSA-PBS and left incubated at room temperature for one hour. At the end of the incubation time, a drop of DAPI was added to the sample in order to stain cells nuclei. As a negative control the secondary antibody was conjugated directly without the use of the primary one.

5.2.1.11 Statistical Analysis

All cell culture experiments were conducted in triplicate. Results were statistically analysed using one-way ANOVA tests. Collected data were considered significantly different at $p \leq 0.05\%$. Error bars represent standard deviation. Different n values have been reported in the legends of the figures relative to each experiment.

5.3 RESULTS

This section reports the results obtained by a 2D culture model to test dendritic angiogenic peptides on HUVECs and 3T3 fibroblast.

5.3.1 2D culture model of 3T3 Fibroblast treated with dendritic angiogenic peptides

3T3 Fibroblast have been used as control cell line and to test the effect of dendritic angiogenic peptides.

5.3.1.1 HPI Staining

As expected different non-functionalised dendron generation, FFgen0K$(QHREDGS)_2$ and FFgen0K$(WQELYQLKY)_2$ have no effect on 3T3 and the number of viable cells is comparable to the one of the control (3T3) (fig.5.3, fig.5.4 and fig.5.5).Different Poly (ε-Lysine) dendrons generation (Fig.5.3), FFgen0K$(QHREDGS)_2$ and FFgen0K$(WQELYQLKY)_2$ resulted to be non significantly different when compared within the same time point (p value $\geq 0.05\%$).

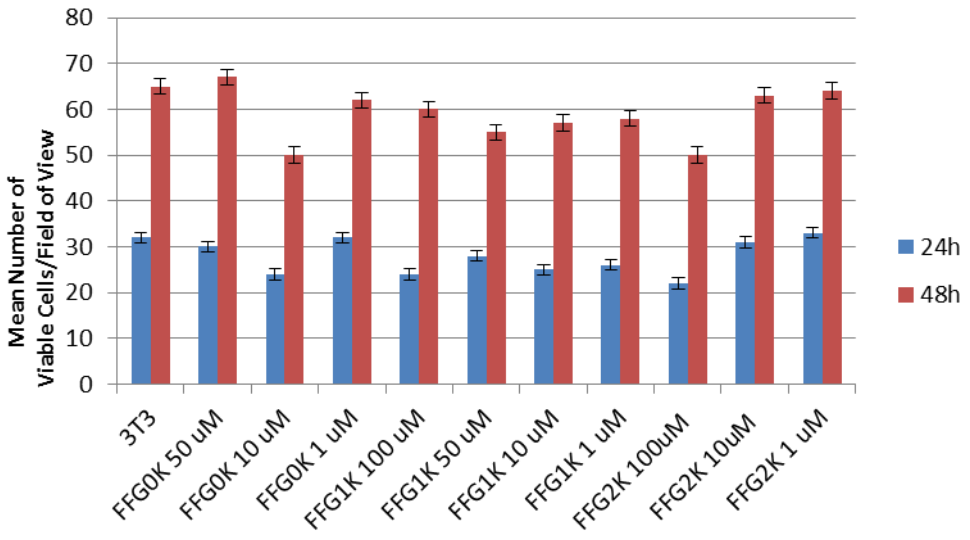

Fig. 5.3 Effects of different Poly (ϵ-lysine) dendrons generation on 3T3 Fibroblast at 24 and 48 hours of incubation. Mean value plotted, error bars indicate standard deviation, n=3, p-value within the same time point $\geq 0.05\%$.

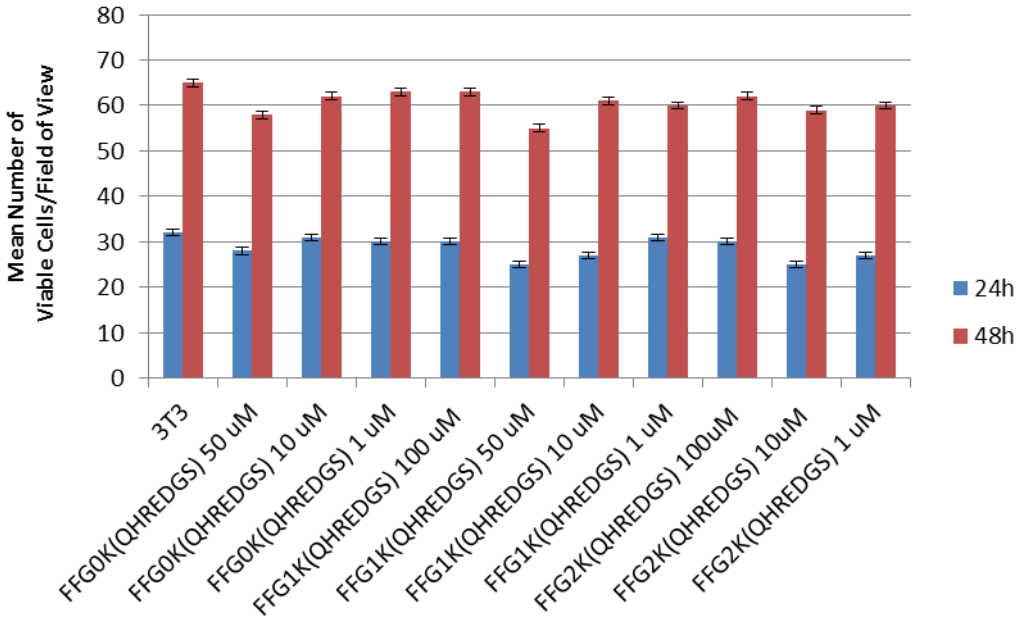

Fig. 5.4 Effects of different Poly (ϵ-lysine) dendrons generation functionalised with Ang-1 mimicking peptide on 3T3 Fibroblast at 24 and 48 hours of incubation. Mean value plotted, error bars indicate standard deviation, n=3, p-value within the same time point ≥ 0.05%.

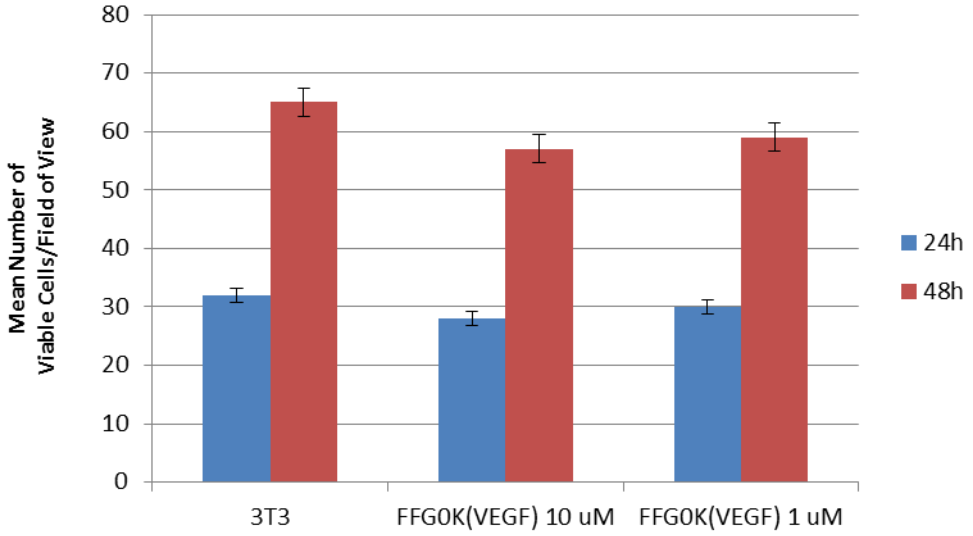

Fig. 5.5 Effects of FFgen0K(WQELYQLKY)$_2$ on 3T3 Fibroblast at 24 and 48 hours of incubation. Mean value plotted, three replicates performed, error bars indicate standard deviation, n=3, p-value within the same time point ≥ 0.05%.

Regarding results obtained for the viability of 3T3 Fibroblast when treated with FFgen0K(RKIEIVRKK)$_2$ it is possible to notice how PDGF-BB dendritic peptide is able to enhance fibroblast proliferation especially at 10μM concentration (Fig.5.6) manifestation of the bioactivity of FFgen0K(RKIEIVRKK)$_2$. Indeed, FFgen0K(RKIEIVRKK)$_2$ at 10μM concentration resulted to be significantly different if compared to other concentration at 48 hours (p-value ≤ 0,05%).

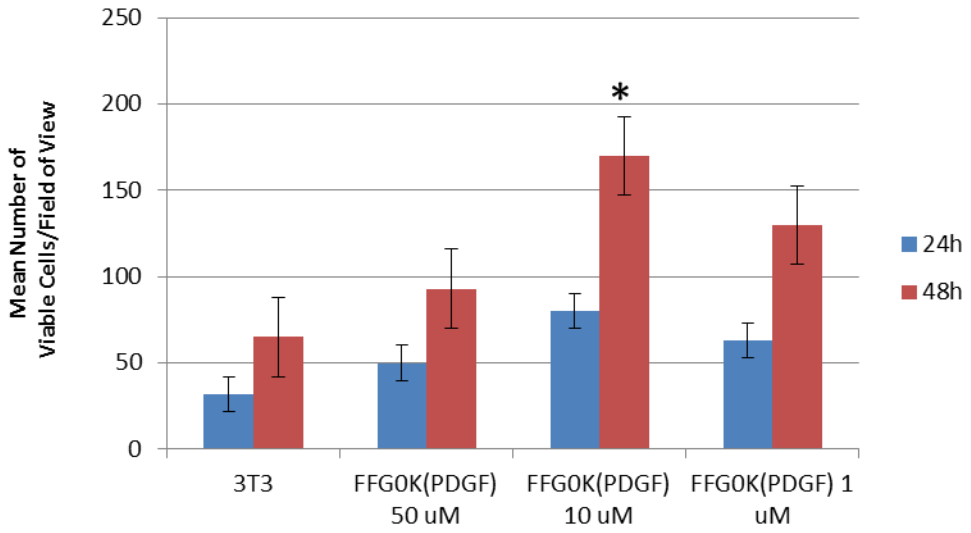

Fig. 5.6 Effects of FFgen0K(RKIEIVRKK)$_2$ on 3T3 Fibroblast at 24 and 48 hours of incubation. Mean value plotted, error bars indicate standard deviation, n=3, p-value ≥ 0,05% for different FFgen0K(RKIEIVRKK)$_2$ concentration at 48 hours.

5.3.2 2D culture model of HUVECs treated with dendritic angiogenic peptides

5.3.2.1 HPI Staining

HPI staining has been used to evaluate HUVECs viability at 24h and 48h of incubation. This coloration (Fig.5.7) allows the investigator to discriminate between living (Fig.5.8, panel C, intense blue), apoptotic (Fig.5.8, panel B, bright blue) and necrotic (Fig.5.8, panel A, pink) cells.

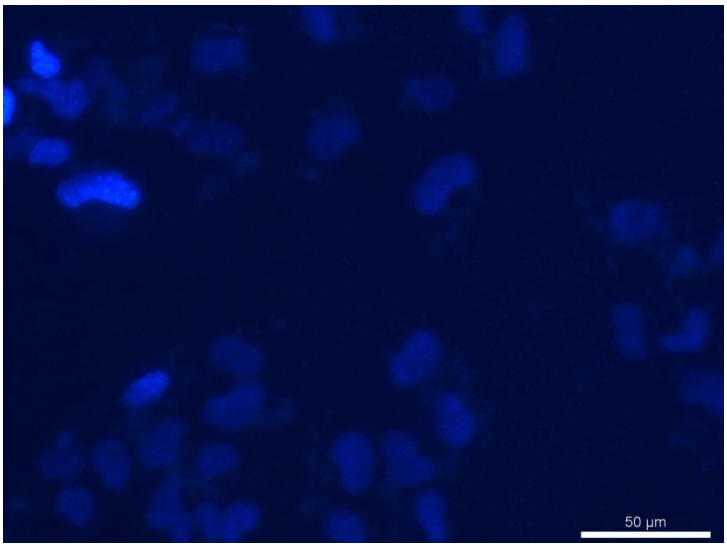

Fig.5.7: Representative image of cell viability test with HPI staining on HUVECs after 24h.

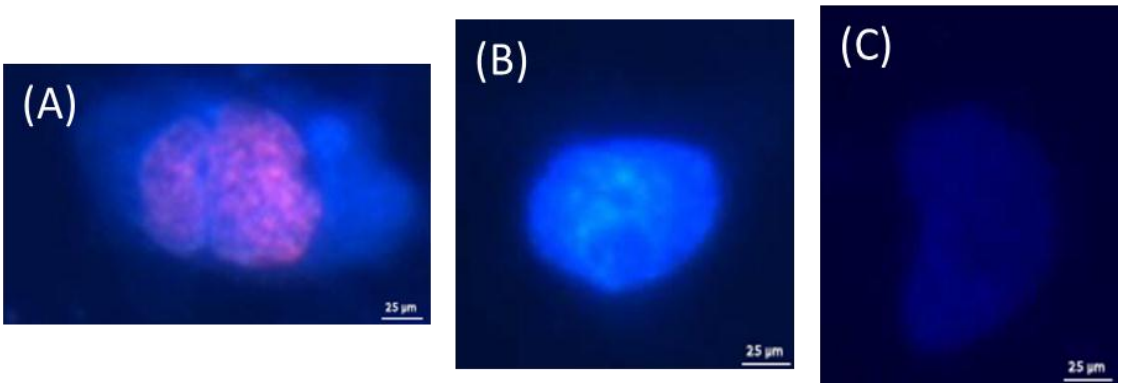

Fig. 5.8 Flourescence microscope images of a) necrotic, b) apoptotic and c) live HUVECs cell when stained with propidium iodide for viability test.

Results obtained from the analysis of the images taken with the fluorescent microscope have been plotted into graphs representing the mean number of viable cells/field of view. Firstly, the influence of different dendron generations on HUVECs has been tested (Fig.5.9): the number of viable cells increases as the dendrons generation and dose decrease having the best combination with generation zero dendron at 10µM concentration (Fig. 5.9, panel C) with a significant difference (p-value ≤0,05%) within the different concentration at 48 hours. The number of apoptotic and necrotic cells were not significant in comparison with living cells (data not shown). Moreover, it is possible to notice how bigger Dendron generation has a negative impact on HUVECs (Fig.5.9, panel A) with a significant difference both at 24 and 48 hours.

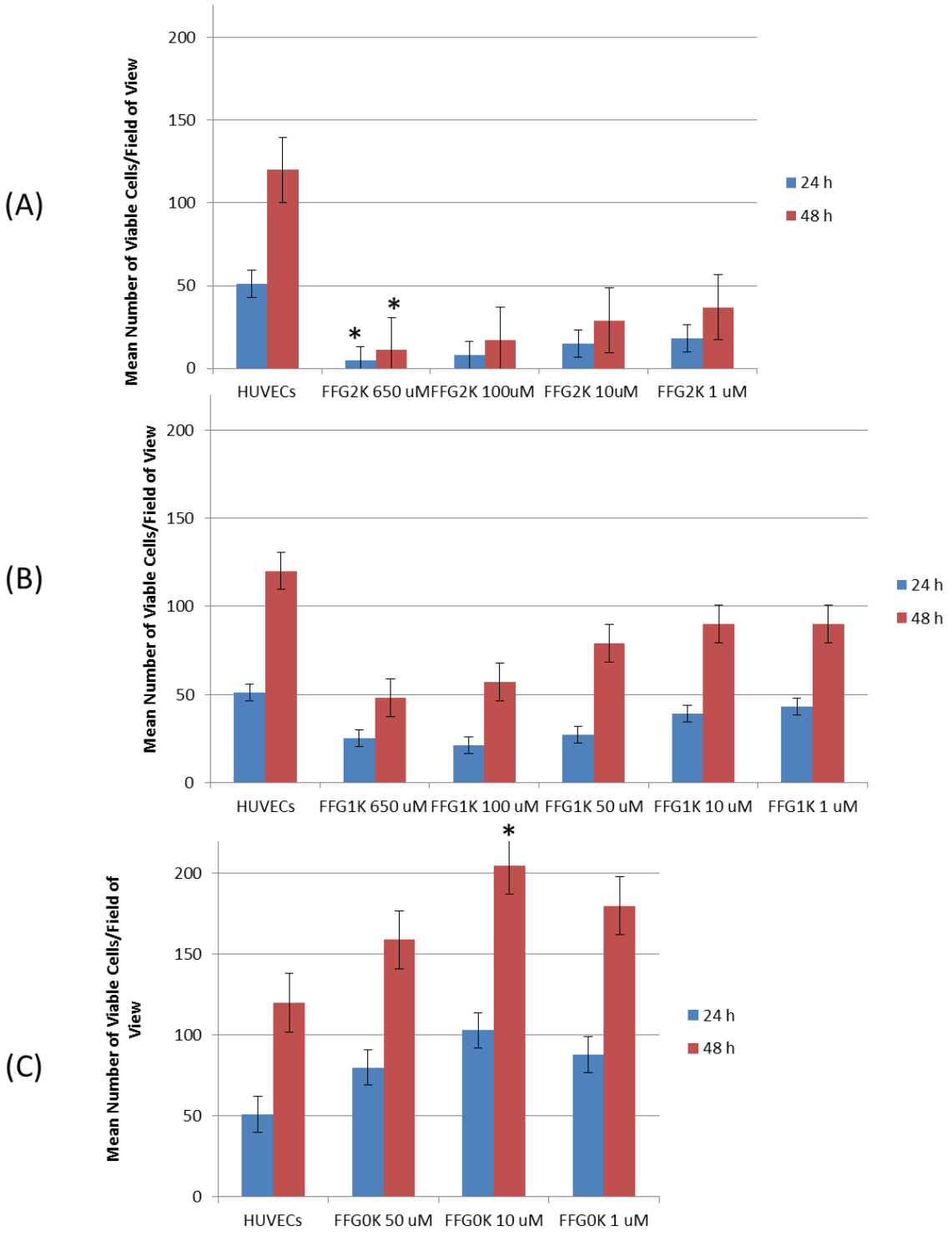

Fig. 5.9 Effects of different Poly (ϵ-lysine) dendrons generation on HUVECs at 24 and 48 hours of incubation. (A) FFgen2K, (B) FFgen1K and (C) FFgen0K. Mean value plotted, error bars indicate standard deviation, n=3, stars indicate when population is statistically different from other within the same time point.

Moving then forward on the analysis of viable cells, HUVECs treated with different dendron generations functionalised with Angiopoietin-1 bioactive peptide (-QHREDGS) have been investigated. As mentioned above, HUVECs viability is influenced by dendrons in a generation and dose dependent manner: the same behaviour was also observed when

different dendron generations act as protein scaffold for the –QHREDGS bioactive peptide. Indeed, Fig. 5.10 shows that the best HUVECs performance is obtained when cells are treated with FFgen0K(QHREDGS)$_2$ at 1 µM concentration (Fig. 5.10, panel C). Statistical analysis shows a significant difference of FFgen0K(QHREDGS)$_2$ at 650 µM if compared to other concentrations at the same time point confirming the influence of dose and dendron concentration on HUVECs.

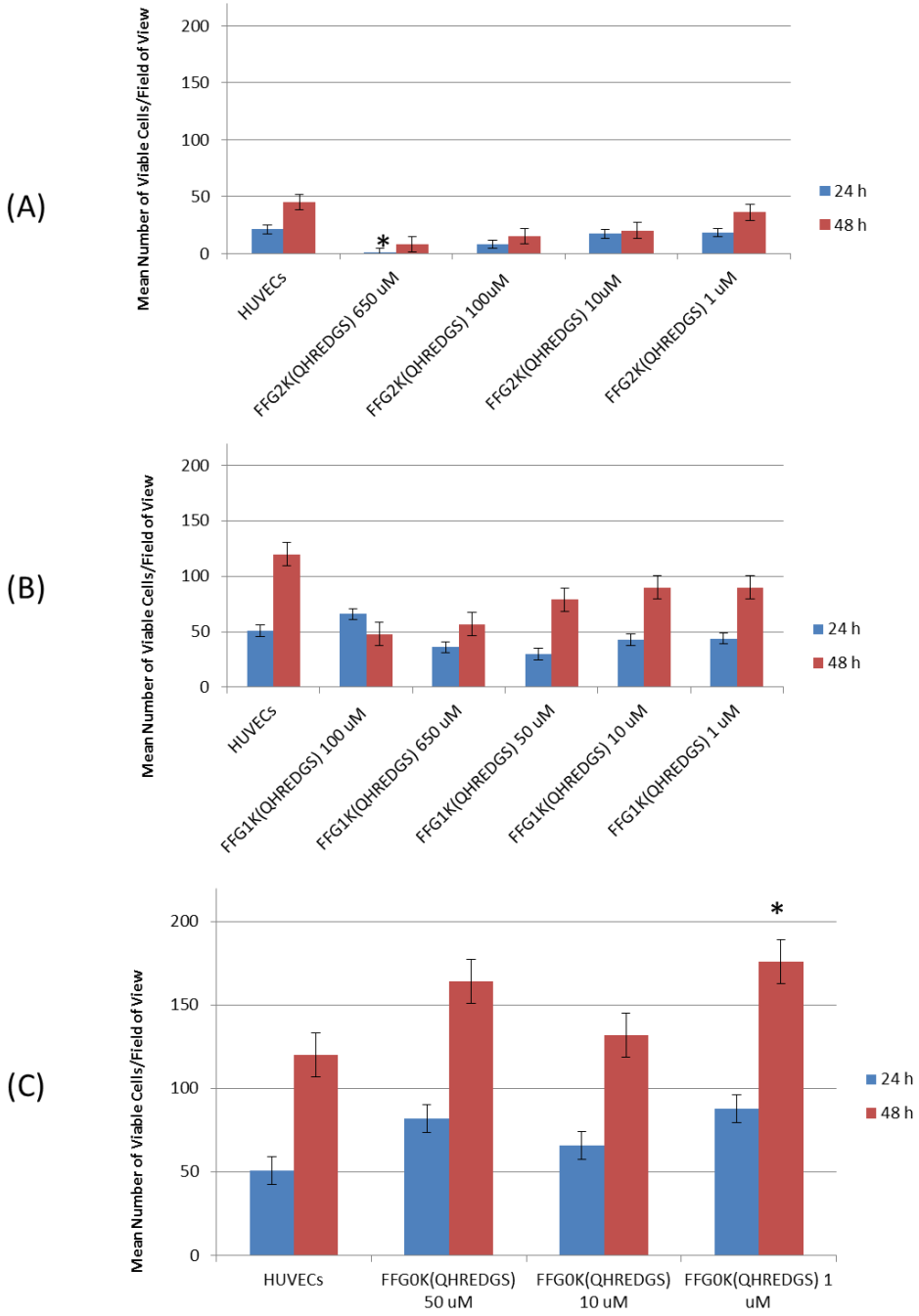

Fig. 5.10 Effects of different Poly (ϵ-lysine) dendrons generation functionalised with Ang-1 mimicking peptide on HUVECs at 24 and 48 hours of incubation. (A) FFgen2K(QHREDGS)$_8$, (B) FFgen1K(QHREDGS)$_4$ and (C) FFgen0K(QHREDGS)$_2$. Mean value plotted, error bars indicate standard deviation, n=3.

Results obtained for HUVECs treated with FFgen0K(WQELYQLKY)$_2$ are in agreement with the results showed above: FFgen0K(WQELYQLKY)$_2$ influences HUVECs viability in a dose dependent manner (Fig.5.11) where the optimal result is at 10µM concentration. No statistically significant difference is observed between different concentration at the same time point.

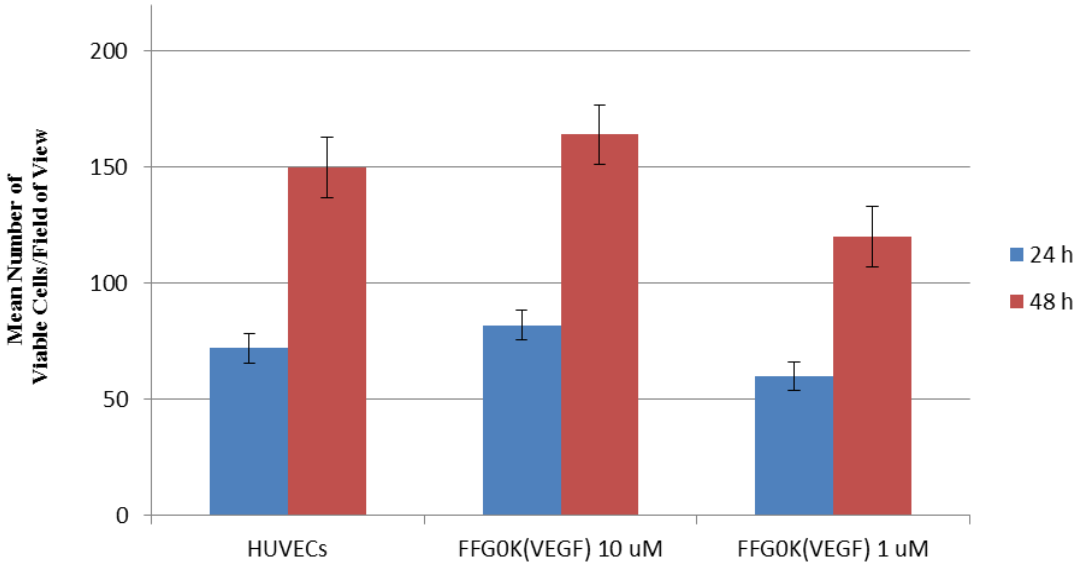

Fig. 5.11 Effects of dendritic angiogenic peptide FFgen0K(WQELYQLKY)$_2$ on HUVECs at 24 and 48 hours of incubation. Mean value plotted, error bars indicate standard deviation,n=3.

Finally, the last dendritic angiogenic peptide tested on HUVECs was FFgen0K(RKIEIVRKK)$_2$ where the number of viable cells were comparable to the control, resulting in a lack of influence of the molecule on cells (Fig.5.12). No statistically significant difference is observed between different concentration at the same time point.

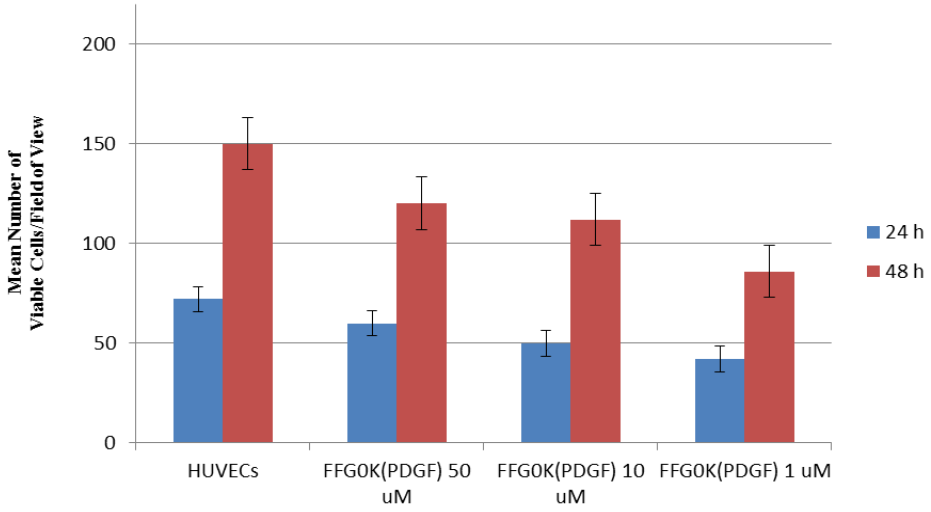

Fig. 5.12 Effects of FFgen0K(RKIEIVRKK)$_2$ on HUVECs at 24 and 48 hours of incubation. Mean value plotted, error bars indicate standard deviation, n=3.

5.3.2.2 LDH Assay

Regarding the LDH assay, the final absorbance value to be taken into consideration as an evaluation of cytotoxicity is obtained as follow:

$$\frac{SAMPLE\ ABSORBANCE\ (Sample - Medium - Cells)}{LYSATE\ ABSORBANCE} * 100 = \%\ Cytotoxicity$$

The values resulting from this equation are all negative or very close to zero as shown in Table 5.4, evidence of non citotoxicity of the dendritic angiogenic peptides on HUVECs.

Table 5.4: Elaboration data of LDH measurement on HUVECs supernatants samples after 48h of incubation.

Samples	Ab Average	Ab Average- Medium-Well
FFgen2K	0.13	-0.14
FFgen1K	0.12	-0.15
FFgen0K	0.12	-0.15
FFgen2K(QHREDGS)$_8$	0.24	-0.03
FFgen1K(QHREDGS)$_4$	0.21	-0.06
FFgen0K(QHREDGS)$_2$	0.22	-0.05
FFgen0K(WQELYQLKY)$_2$	0.22	-0.05
FFgen0K(RKIEIVRKK)$_2$	0.21	-0.06
QHREDGS	0.11	-0.16
WQELYQLKY	0.10	-0.17
RKIEIVRKK	0.11	-0.16
Cells	0.14	
Lysate	0.32	

5.3.2.3 PHALLOIDINE-RHODAMINE Assay

Phalloidin-Rhodamine staining shows the effect of different branched Ang-1-mimicking peptide concentrations in the induction of endothelial cell sprouting. Indeed, while in the control cells (HUVECs) grew as a monolayer, FFgen0K(QHREDGS)$_2$ and

FFgen1K(QHREDGS)$_4$ clearly induce the formation of a network of endothelial sprouting where cells appeared to establish connection (Fig.5.13). In particular, endothelial sprouting is induced more clearly with FFgen0K(QHREDGS)$_2$ and FFgen1K(QHREDGS)$_4$ dendrons at 10µM and 1µM, respectively. On the contrary, FFgen2K(QHREDGS)$_8$ seems to have no influence on HUVECs spatial organisation.

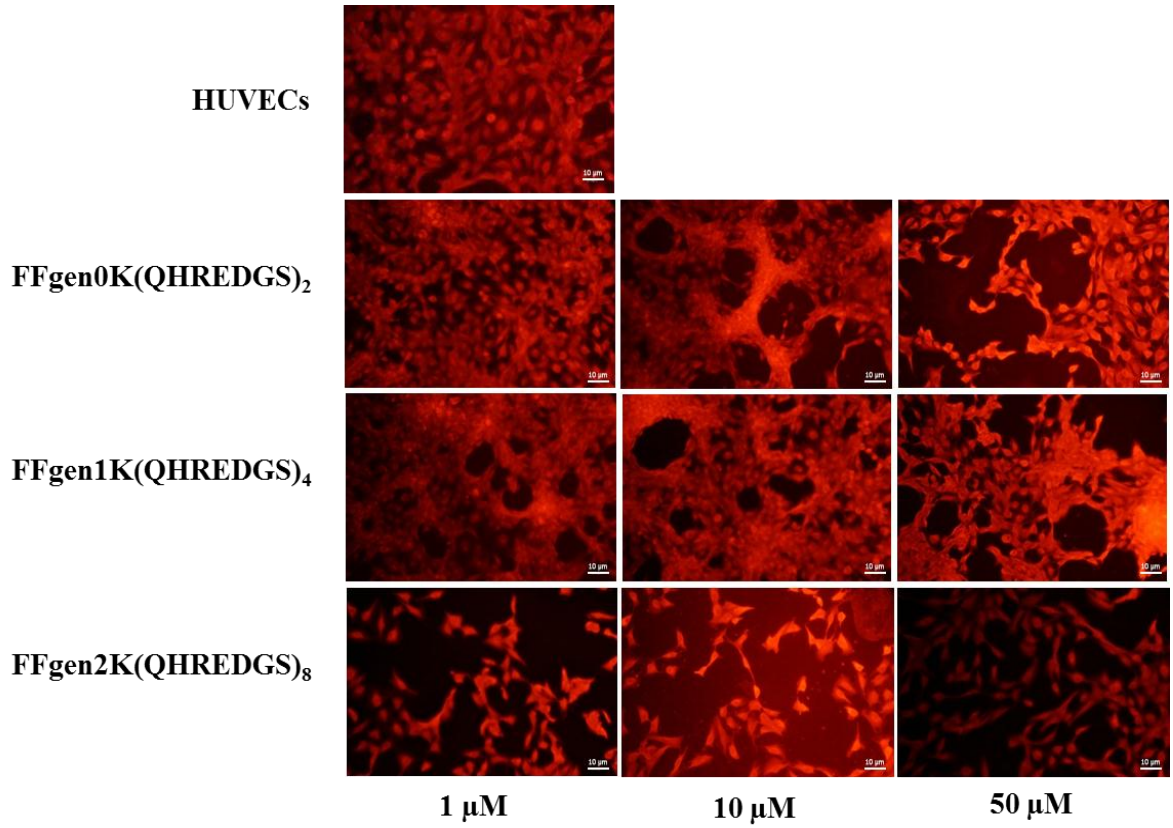

Fig. 5.13 Induction of HUVECs sprouting by different dendritic angiogenic peptide after 6 days of incubation;HUVECs spiked with different dendritic angiogenic peptides and different dose are compared.

Laser confocal images with Phalloidin-Rhodamine staining show the effect of the linear and branched Ang-1-mimicking peptides (-QHREDGS). Indeed, while in the control cells grew as a monolayer (Fig. 5.14, panel A), the QHREDGS linear peptide appeared to induce HUVECs organisation into 2D branched patterns (Fig. 5.14, panel B). The spiking with FFgen0K dendron generated more dense branched 2D patterns (Fig. 5.14, panel C), but FFgen0K(QHREDGS)$_2$ clearly induces the formation of a network of endothelial sprouting where cells appeared to establish connections also in a 3D fashion (Fig. 5.14 panel D). Therefore, the results shown in Fig. 5.14 panel C and D seem to demonstrate the synergistic action played by the dendron branched structure and by the -QHREDGS sequence in guiding the 3D organisation of the endothelial sprouting.

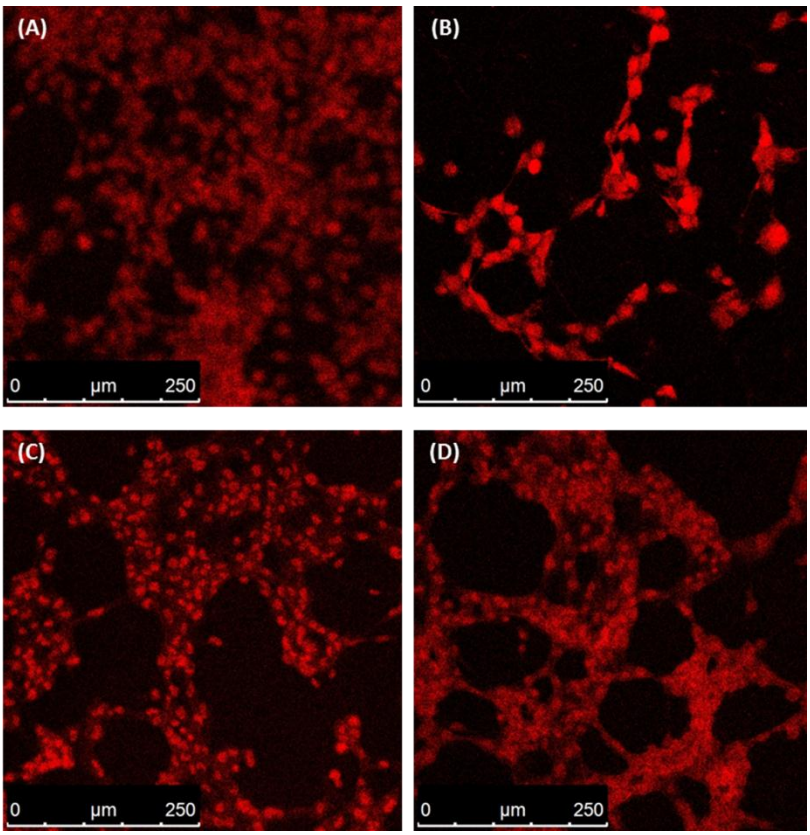

Fig. 5.14 Effect of linear Ang-1 peptide and FFgen0K(QHREDGS)$_2$ on HUVEC in a 2D model at 24h. A) Control; B) linear QHREDGS peptide; C)FFG0K and D) FFgen0K(QHREDGS)$_2$.

Laser confocal images with CD31 immunostaining show the presence of this specific integral membrane protein when HUVECs are spiked with FFgen0K(QHREDGS)$_2$ (Fig.5.15,panel B) while there is no presence or at least a quantity non sufficiently high to be detected of that protein in the control (tissue plastic plate) (Fig.5.15, panel A).

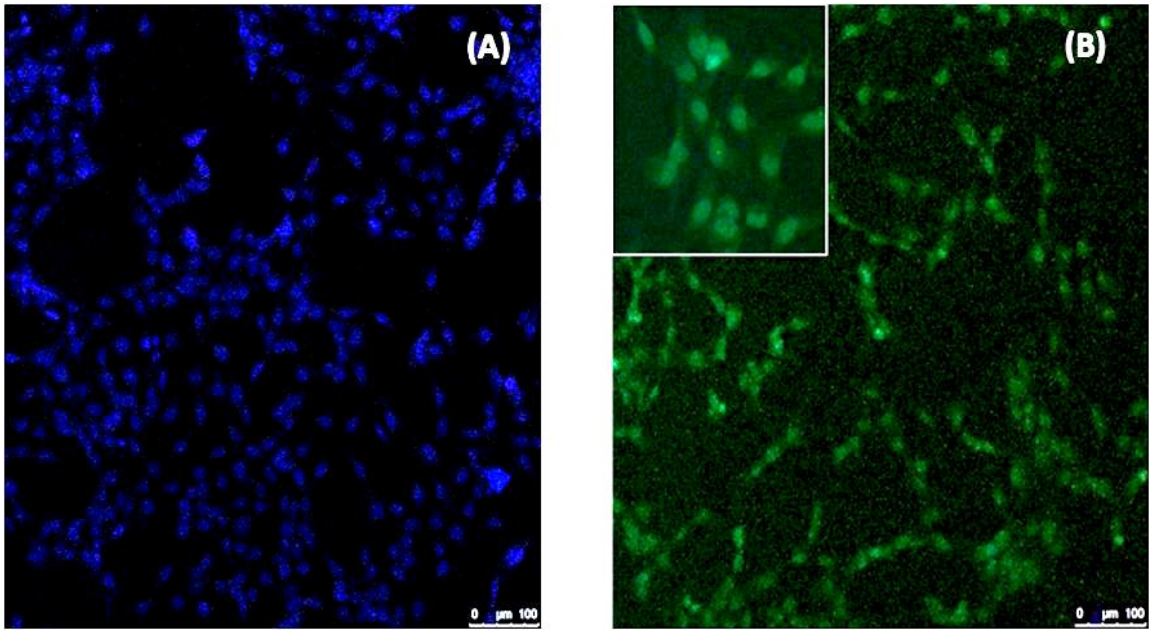

Fig. 5.15 Immunofluoresce of CD31 protein on HUVECs spiked with FFgen0K(QHREDGS)$_2$ solution. (A) tissue culture plate control,(B) FFgen0K(QHREDGS)$_2$.

Laser confocal images with Phalloidin-Rhodamine staining of FFgen0K(WQELYQLKY)$_2$ detected through MS and HPLC, induce a specific response in HUVEC resulting in the formation of endothelial sprouting (Fig.5.16, panel D) whereas is not possible to identify such structure when HUVECs are treated just with linear VEGF peptide or FFgen0K (Fig.5.16, panel B and C).

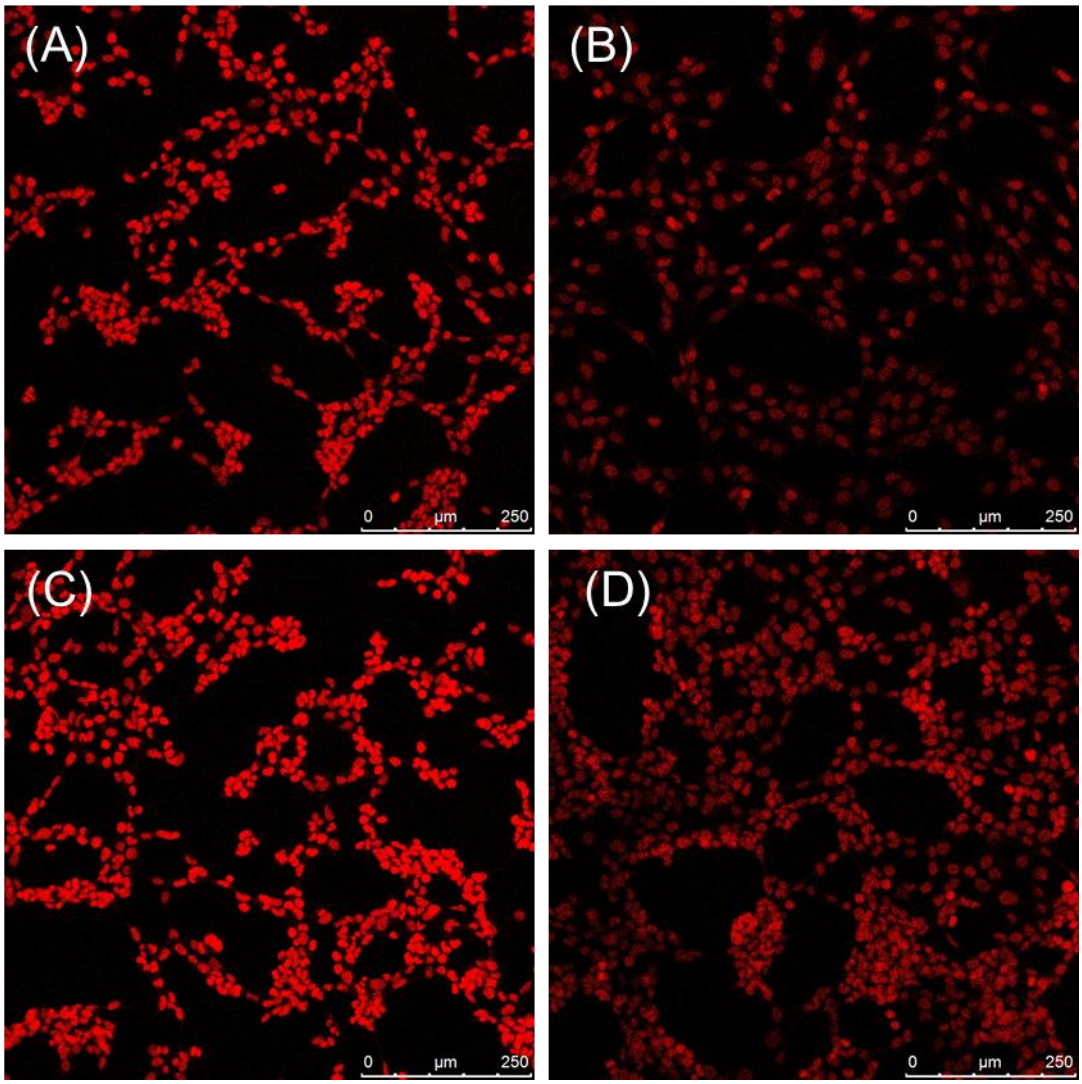

Fig. 5.16 Effect of linear VEGF peptide and FFgen0K(WQELYQLKY)$_2$ on HUVEC in a 2D model at 48h. A) Control; B) linear VEGF peptide; C)FFgen0K; D) FFgen0K(WQELYQLKY)$_2$.

5.4 DISCUSSION

Coronary heart disease and stroke are leading causes of mortality in Europe, resulting in a loss of function of the affected tissue (Nichols, 2014). The challenge is to restore the tissue functionality using dendritic angiogenic peptides to stimulate the development of pre-existing blood vessels and enhance myocardium tissue regeneration.

Dendrons can act as protein scaffold for the bioactive peptides and provide them define spatial organisation given by the branched structure. Indeed, dendrons act as structure used to present peptide analogue preserving their bioactivity and making them capable of interacting with cells. Moreover, dendrons provide conformational stability to bioactive peptides, precise spatial orientation to enhance receptor interaction and capacity to prolong peptides efficiency. The use of these branched structures prompts tissue regeneration by controlled growth factors delivery. It is already established in the literature that the use of the whole growth factor molecules is limited by their susceptibility to denaturation, uncontrolled retention in the target tissue and their bioavailability (Lee, 2010). Therefore, to overcome the disadvantages related to the use of growth factors, peptide analogues have been used in this study.

Indeed, the focus of this chapter was the validation of poly (ε-lysine) dendrons as protein scaffolds for the spaced exposure of angiogenic bioactive peptides. The main hypothesis behind the experimental work of this chapter was to test if dendritic angiogenic peptides were capable of induce angiogenesis *in vitro* in a 2D culture model when used as "free drugs"

The objectives to answer this hypothesis were:

1) To assess dendritic angiogenic peptides cytotoxicity
2) To evaluate dendritic angiogenic peptides potential on inducing HUVECs proliferation
3) To validate dendritic angiogenic peptides capacity of inducing angiogenesis in vitro in form of endothelial sprouting when used to spike HUVECs

Different dendritic angiogenic peptides concentrations as well as different dendrons generations have been tested in order to find the optimal balance to induce the better cell response. A first analysis of cell proliferation seems to indicate an adverse effect of most of the tested peptides. However, LDH assays and sprouting tests showed opposite results suggesting that the arrangement of cells into tubule-like structures led to an underestimate of their numbers when stained by HPI and counted by fluorescent microscopy. Indeed, the majority of the cells appeared viable by this method.

The Angiopoietin-1 peptide analogue has been used to functionalise different dendron generations, starting from generation zero up to generation two. This choice was made according to the type of interaction that the natural growth factor has with its specific receptors. Tie-2 receptor is capable of autophosphorylation after binding with the growth factor and can be ascribed to a linear receptors whereas VEGF and PDGF-BB receptors are composed by two fragments that dymerised after binding (Deli, 2013). For this reason there was the need to test different dendron generations and concentrations in order to find the most suitable combination for Angiopoietin-1 peptide analogue. Cytotoxicity tests of FFgen2K(QHREDGS)$_8$, FFgen2K(QHREDGS)$_4$ and FFgen2K(QHREDGS)$_2$ show how all these materials has no cytotoxic effect on HUVECs even when higher dendron generation is reached. This outcome is in agreement with the results obtained for the HPI staining: when HUVECs are spiked with FFgen2K(QHREDGS)$_8$, FFgen2K(QHREDGS)$_4$ and FFgen2K(QHREDGS)$_2$ it is possible to state that the number of viable cells is comparable with the one of the control even if it is important to notice that the best response is obtained when HUVECs are treated with FFgen2K(QHREDGS)$_2$ where the number of viable cells is significantly increased (Fig. 5.10). Such results find confirmation within the literature where it is clearly stated that Angiopoietin-1 has no effect on cells proliferation but is indispensable for the survival of endothelial cells and capillary tube formation (Falkman, 1996). Consequently, Phalloidin-Rhodamine staining of FFgen2K(QHREDGS)$_8$, FFgen2K(QHREDGS)$_4$ and FFgen2K(QHREDGS)$_2$ gives a morphological validation to the numerical results obtained for HUVECs viability and cytotoxicity: FFgen2K(QHREDGS)$_2$ induce the formation of a network of endothelial sprouting (Fig.5.13). To assess the functional role of FFgen2K(QHREDGS)$_2$ on HUVECs, light microscope image was analysed with imageJ angiogenesis analyser, where the number of sprouts and segment length were significantly higher than the other conditions analysed (data not shown) where mostly the angiogenesis analyser could not be used due to the absence of sprouting. Moreover, another confirmation of the induction of endothelial sprouting by FFgen2K(QHREDGS)$_2$ has been given by immunostaining of HUVECs treated with FFgen2K(QHREDGS)$_2$: the expression of CD31 protein is a clear sign of the interactions between HUVECs and dendritic angiogenic peptide in forming tubular-like structure because this protein participates in the regulation of angiogenesis (Yang, 1999). Induction of endothelial sprouting by FFgen2K(QHREDGS)$_2$, could be attributing to the natural interaction that occurs between the whole angiopoietin-1 and its receptors, Tie-2. Even if Tie-2 receptor does not undergo dimerisation, too high dendron generation and so too high exposure and concentration of Ang-1 peptide analogue could lead to a saturation

of the binding site preventing an interaction between dendritic angiogenic peptides and HUVECs (Reis, 2011). Another reason why FFgen2K(QHREDGS)$_8$ does not produce the expected response on HUVECs could be due to the molecule chemical structure. Indeed, generation two has more branched unit than lower generation resulting in a bigger steric effect that appears to obstruct the interaction between the Ang-1 peptide analogue and its receptor Tie-2.

In conclusion, it is necessary to outline the great potential of the combination of dendron and peptide analogue: confocal images of FFgen2K, - QHREDGS and FFgen2K(QHREDGS)$_2$ show how the synergic action of dendron and linear peptide is responsible for the induction of endothelial sprouting. For this reason this study helps to make a step ahead in the knowledge of induction of angiogenesis *in vitro*, overcoming all the problems related to the use of this two single structures separately (Rask, 2010; Lee, 2005).

VEGF peptide analogue (-WQELYQLKY), used to functionalised generation zero dendron, induces a specific response on HUVECs: endothelial cells migrate and make cell to cell interactions in response to the VEGF dendritic peptide treatment resulting in the formation of endothelial sprouting. Moreover, is important to outline how important is the use of peptides analogue instead of the whole natural growth factors. Several studies have pointed out the capability of small peptide to promote angiogenesis more consistently than whole growth factors (Leslie-Barbick, 2001; Webber, 2010). This outcome is due to the possibility to overcome the disadvantages related to the use of whole growth factors molecules: growth factors are susceptible of denaturation loosing consequently their bioactivity whereas the VEGF peptide analogue, being a linear peptide, is not susceptible to denaturation (D'Andrea, 2006); the retention in the target tissue is difficult to reach because relatively large molecules such as growth factors may not penetrate the tissue adequately upon administration and finally the costs of production and batch-to-batch variability in a situation where VEGF peptide analogue could be produced in a very reproducible manner at a large scale (Rask, 2010). Moreover, it is important to outline how VEGF dendritic peptide has specific influence on HUVECs if compared to the linear peptide and to the non-functionalised dendron: it clearly appears how the response given by the single linear peptide and the generation zero is present when HUVECs are treated with FFgen0K(WQELYQLKY)$_2$ resulting in a synergic action of the two materials.

Regarding PDGF-BB peptide analogue little is known in literature about its influence on mural cells and the consequent role in the stabilisation of blood vessels. For this reason, the validation of this peptide analogue has been starting from cytotoxicity assay. Results

showed how FFgen0K(RKIEIVRKK)$_2$ have no toxic effect on 3T3 if compared to the control. Moreover, the peptide had a clear stimulatory effect on this type of fibroblasts that have a phenotype similar to the mural cells of the blood vessels.

5.5 CONCLUSION

In conclusion it can be stated that all the novel macromolecules that have been synthesised have produced the expected results:

- Angiopoietin-1 is involved in the regulation of capillary tube formation and is indispensable for endothelial cells survival (Dallabrida, 2005). Accordingly, the same role has been performed by dendron functionalised with the Ang-1 peptide analogue when the molecule is used to spike HUVECs cells in a 2D model *in vitro* resulting in the formation of structures typical of the endothelial sprouting process. Moreover, the collected results have shown how Poly (ε-Lysine) dendrons tethered with an Angiopoietin-1-peptide analogue (-QHREDGS) induces endothelial sprouting in a dendron generation- and dose-dependent manner.

- VEGF is the crucial regulator of angiogenesis and is clear how FFgen0K(WQELYQLKY)$_2$ is able to mimic the same behaviour of the natural growth factor.

For this reason the evaluation of the efficacy of the new molecules to modulate angiogenic stimuli *in vitro* as free drugs through a 2D model *in vitro* has been successfully achieved, proving that dendrons used as protein scaffold for the exposure of angiogenic peptide are really promising molecules to be used in the regeneration of myocardial ischemic tissue.

6. *IN VITRO* ANALYSIS OF FUNCTIONALISED ULTRAFOAM^{TM} SCAFFOLD AS PROMOTER OF ANGIOGENESIS *IN VITRO*

6.1 INTRODUCTION

6.1.1 Strategies for biomaterial presentation of bioactive molecules

Two different approaches can be used in tissue engineering to present bioactive molecules, in this particular case growth factors and bioactive peptides: (i) chemical interaction and bond of the bioactive molecules either loaded in the device bulk or grafted on its surface; (ii) physical encapsulation of the free bioactive molecules in a specific delivery system. The first strategy consists in a chemical binding or affinity communication between the biomaterial functionalised with the bioactive molecules and a cell population or tissue whereas the second strategy consists in the encapsulation and controlled diffusion of the bioactive molecules in the surrounding tissue (Lee, 2010). In this chapter, only the chemical immobilisation will be discussed and in relation to the Ultrafoam-based cardiac patches. Indeed, the testing of the collagen beads by the adopted 2D in vitro model proved to be unreliable because of the tendency of the beads to float in the tissue culture medium. As in both the beads and patch cases the angiogenic dendrons were covalently grafted on collagen-based material, the scope of this chapter was to see if angiogenesis could be induced on the modified collagenic surface irrespective of its formulation.

6.1.1.1 Chemical immobilisation of growth factors to biomaterials

Several techniques can be used to immobilise growth factors to naturally-derived or synthetic biomaterials. The addition of such macromolecules on matrices provide a direct interaction between cells and biomaterial and a restrict area where the signal could act and control cell behaviour (stem cell differentiation, cell proliferation) (Dawson, 2008). Growth factors or bioactive peptides may have influence on the surrounding environment in the bound state or be switched on into a soluble form by the cleavage of their bond from the biomaterial to which they are coupled. There are two separate approaches for the presentation of growth factors on ECM: (i) non-covalent strategy: physical interaction like protein-protein hydrogen bonding or hydrophobic interactions with bioactive molecules acting as a molecular chaperone; (ii) covalent strategy: covalent bonding of growth factors to the biomaterials (Lee, 2011). Whatever technique is used to immobilise growth factors, it makes the scaffold adhesive to cells and helps in bringing the cells into close contact to each other (Cross, 2003).

Non-covalent incorporation of growth factors is mainly driven by electrostatic and/or hydrophobic interactions between the biomaterial surface and the bioactive molecules or indirect interaction trough proteins or other biological molecules (Li, 2009). Natural

polymeric materials (fibronectin, laminin, collagen, elastin) or several synthetic hydrogels have been used as ECM-mimicking biomaterials to present bioactive moieties (Lee, 2010). Fibrin, for example, has been used to present and deliver the β-nerve growth factor (NGF) that is released by the protolithic activity of plasmin, enhancing nerve regeneration (Sakiyama-Elbert, 2001); likewise BMP-2 has been used to functionalise fibrin resulting in induced bone defect healing (Schmoekel, 2001) and finally a VEGF mimicking peptide incorporates into fibrin induces angiogenesis when released (Zisch, 2001).

Covalent attachment of growth factors to biomaterials can contribute to a more prolonged release that the one achieved through non-covalent bonding. Moreover, growth factors remain bioactive even if they degrade more slowly (Lee, 2010). The functional groups available both on the material surface and in the natural growth factor or its analogue have a key role in this strategy as they allow the coupling. For example, epidermal growth factor (EGF) has been covalently bound to amino-silane glass trough PEO resulting more effective in promoting hepatocytes proliferation than the non-covalent EGF (Kuhl, 1996). Likewise, TGF-β1, covalently attached to poly(ethylene glycol) (PEG), improves ECM production and has the same effect of RGD peptide absorbed to the same PEG (Mann, 2001).

In conclusion, chemical immobilisation approach for growth factors and bioactive peptides delivery provides a robust method to present bioactive molecules to various tissues and cell populations. Improvement in this field could be achieved finding the right balance between the growth factors dose, the physio-chemical properties of the scaffold as well as the precise orientation of the bioactive moieties to the surrounding biological environment.

6.1.1.2 Immobilisation of small peptides mimicking natural proteins

The functionalisation of biomaterials with small peptides capable of mimicking the cell adhesion properties of large matrix molecules can enhance the effective response by a combined delivery of growth factors (Lin, 2009). For example, macroporous scaffolds presenting an -RGD sequence on their surface have been used for the transplant of myoblast as well as a platform for the delivery of hepatocyte growth factor (HGF) and fibroblast growth factor-2 (FGF-2) to regenerate muscle laceration (Hill, 2006). Results show how the combined action of scaffold, cells and growth factors aid the survival and migration of the myoblast cells enhancing muscle regeneration that would otherwise not be achieved with any of these components in isolation (Hill, 2006). Similarly, a macroporous alginate scaffold able to release VEGF and functionalised by the covalent grafting of cell-adhesion peptides, significantly increased the survival of endothelial progenitor cells

injected into the body and enhanced blood reperfusion in ischaemic tissue (Silva, 2008). The use of small peptides to functionalise scaffolds could be used also as a platform for immune-modulating function: -YCWSQYLCY peptide, mimicking of tumour necrosis factor-a (TNF-a) recognition loop, has been used to functionalise a PEG hydrogel supporting the survival and bioactivity of encapsulated cells (Lin, 2009). Moreover, literature reports the use of an amphiphilic peptide used to form self-assembled factor delivery platform: the self-assembled peptide is composed of alternating hydrophilic and hydrophobic amino acids as building blocks. At the end of the blocks sequence a biotin molecules is attached in order to let the incorporation of biotinylated IGF-1 (insulin-like growth factor) in the attempt to prolong the growth factor delivery (Lee, 2011).

6.1.1.3 Variables affecting growth factor interaction

The last response of a target cell to a specific growth factor could be regulated by different external factors, such as the capacity to bind the ECM, the degradation rate of the ECM as well as the growth factors concentration and the cell target location (Lee, 2009). Indeed, the ECM is able to regulate the spatial presentation of growth factors by controlling the presentation of these factors to the matrix: Some growth factor molecules, for instance, have heparin-binding domains that are essential for the intervention of specific interactions with the ECM (Lee, 2011). In addition, if there is the presence of specific domains in the molecules to be delivered, such as heparin-binding domains, specific interaction with ECM is easier to achieve and can provide a specific cellular response whereas growth factors without ECM binding cues can diffuse more in tissues (Cao, 2007).

The concentration of the growth factor is another variable that can affect growth factor-ECM interaction and consequently cells response: growth factor concentration could impact on cadherin-mediated cell-cell contact, where if the concentration of the growth factor is below the threshold level, cell proliferation is blocked (Kim, 2009). The same problem can occur during angiogenesis as stimulated by VEGF: this process is controlled by notch signalling, capable of stopping the uptake of VEGF (Cao, 2009).
A wide range of growth factors and growth factor-mimicking peptides have been used for different applications, like bone regeneration and regeneration of ischaemic tissues. Several studies have been published on the ability of angiogenic factors to treat ischaemic diseases but all of them with non-satisfactory clinical results (Freedman, 2002; Takeshita 2000; Rosengart, 2000). This lack of success was mainly due to the formulation, the dose and the presentation of the growth factors used: too high doses of growth factors directly

injected into the body do not let target tissue to sense the growth factor bioactivity and moreover could lead to pathological angiogenesis (Simons, 2003).

6.1.2 AIM OF THE CHAPTER

The aim of this chapter is to assess the bioactivity of dendritic angiogenic peptides, as functionalisation moieties on cardiac patches, which have been designed and synthesised as illustrated in Chapter 4. The rationale in the design of this new biomaterial-based approach was to have a precise spatial orientation of dendritic angiogenic peptides at the implant surface in order to drive a physiological interaction with relevant cell receptors in the regenerating tissue microenvironment. For this reason, an assessment of the bioactivity of produced biomaterial (Ultrafoam^{TM} collagen type I scaffold functionalised with dendritic angiogenic peptides) was performed *in vitro* on human umbilical endothelial cells (HUVECs) where morphology and immunofluorescence were tested. This assay offered an insight into the efficacy of the dendritic angiogenic peptides to induce angiogenesis *in vitro* when grafted on a scaffold.

6.2 MATERIALS AND METHODS

6.2.1 Materials

Table 6.1 materials used during the experimental process of in vitro assessment of functionalised Ultrafoam^{TM} scaffold with dendritic angiogenic peptides.

Product	***Supplier***	***Code No***
Human umbilical vein endothelial cells (HUVECs)	American Type Culture Collection (ATTC)	CRL-1730
Endothelial basal medium (F12K medium)	PAA	
Endothelial cell growth supplement (ECGS)	Sigma-Aldrich	E2759
Heparin	Fisher	9041-08-1
Foetal bovine serum (FBS)	PAA	30-20202
Trypsin 0.05% EDTA(1x)	Fisher	25300
CytoTox 96 Non-radioactive Cytotoxivity (LDH) assay	Promega	G1780
ANTI CD-31 antibody HEC7	ABCAM LTD	ab119339
Donkey anti-mouse igG H&L (Alexa fluor 488)	ABCAM LTD	ab150105
Phalloidine-Rhodamine (TRICT)	Sigma-Aldrich	P2141
Avitene UltrafoamTM Collagen type I sponge	Bard	1050050

6.2.2 Methods

6.2.2.1 sterilisation of Ultrafoam^{TM} scaffold functionalised with dendritic angiogenic peptides

Scaffold functionalised with FFgen0K$(QHREDGS)_2$, FFgen0K$(WQELYQLKY)_2$ and FFgen0K$(RKIEIVRKK)_2$ were placed in a 24-well plastic plate in triplicate and sterilised under an UV lamp for 1hour.

6.2.2.2 HUVECs seeding on scaffolds

HUVECs were suspended in fresh medium and counted by haemocytometer. Cell suspension in relevant medium (22000 cells/ml) was used to seed cells on the surface of the functionalised scaffold previously equilibrated with the same medium and positioned in the wells. The seeded scaffolds were incubated for 6 days at 37 ^{o}C, 95% air, 5% CO_2 at static conditions. Each type of scaffold was tested in triplicate.

6.2.2.3 Preparation and paraffin embedded scaffold for further immufluorescence analysis

After 6 days of incubation, scaffolds seeded with HUVECs were fixed with 4% (v/v) paraformaldehyde for 4 hours at room temperature. Samples were then dehydrated through a series of increasing ethanol concentrations for 2 hours and placed in a plastic mould in order to be embedded into paraffin using a specialised automated processing system. Paraffin scaffold blocks where then allowed to cool for 2 hours and then precisely sliced into 6μm section using a rotary microtome. Sections were then mounted onto gelatine-coated histological slides, dried overnight in an hoven at 60 °C and stored at 2 °C. Sections coming from the middle of the scaffold were analysed to test HUVECs migration throughout the 3D scaffold core.

6.2.2.4 Fluorescent staining of Paraffin-embedded sections

Scaffold sections were rehydrated starting with two washes in xylene, then through a series of washes in increasing ethanol concentrations and finally rinsed in PBS. At this point, the process of immunostaining and analysis of sections was the same used in Chapter 5, Section 5.2.1.9.

6.2.2.5 HUVECs fixation for SEM Imaging

Cell morphology for each different functionalised Ultrafoam^{TM} scaffold was analysed using SEM. HUVECs were seeded as explained in Section 6.2.2.2 and incubated for 6 days. After incubation, scaffolds seeded with cells were fixed with 2% (v/v) glutaraldehyde in 0.05 M sodium cacodylate buffer for 1 hours before dehydration using a series of increasing ethanol concentrations. Prior to analysis, samples were coated with a thin gold layer before placing them in the vacuum SEM sample chamber and analysed at 5.0 kV at different magnifications.

6.3 RESULTS

This section reports the data obtained from the analysis of HUVECs seeded on functionalised Ultraofam™ scaffold.

6.3.1 *In vitro* test of HUVECs seeded on Ultrafoam™ scaffolds functionalised with dendritic angiogenic peptide

6.3.1.1 SEM Morphological analysis

HUVECs morphology on Ultrafoam™ scaffold functionalised with dendritic angiogenic peptides were verified trough SEM analysis of the different scaffold surfaces and cross-section (Fig. 6.1). Starting from the comparison between SEM images of a control Ultrafoam™ scaffold and the same unmodified Ultrafoam™ scaffold but seeded with HUVECs (Fig. 6.1, HUVECs), it is possible to notice how cells occupy both the surface and cross-section of the collagen scaffold affecting its surface morphology. Moreover, it is possible to see single adhering cells. Subsequently, Ultrafoam™ scaffold functionalised with FFgen0K(QHREDGS)$_2$ and FFgen0K(WQELYQLKY)$_2$ clearly induced a precise response on the spatial orientation of HUVECs both on the surface and in the cross-section of the scaffold [Fig.6.1, FFgen0K(QHREDGS)$_2$ cross-section] where cells appear to be interconnected and form elongated structures resembling vessel-like structures. The same outcome is achieved when HUVECs were seeded on scaffold functionalised with FFgen0K(WQELYQLKY)$_2$: HUVECs arranged themselves in elongated structures, forming a network that can be ascribed to a sprouting process [Fig. 6.1, FFgen0K(WQELYQLKY)$_2$ surface and cross-section]. No effect can be observed when HUVECs are seeded on Ultrafoam™ scaffold functionalised with FFgen0K(RKIEIVRKK)$_2$ both on surface and cross-section of the scaffold [Fig. 6.1, FFgen0K(RKIEIVRKK)$_2$ surface and cross-section].

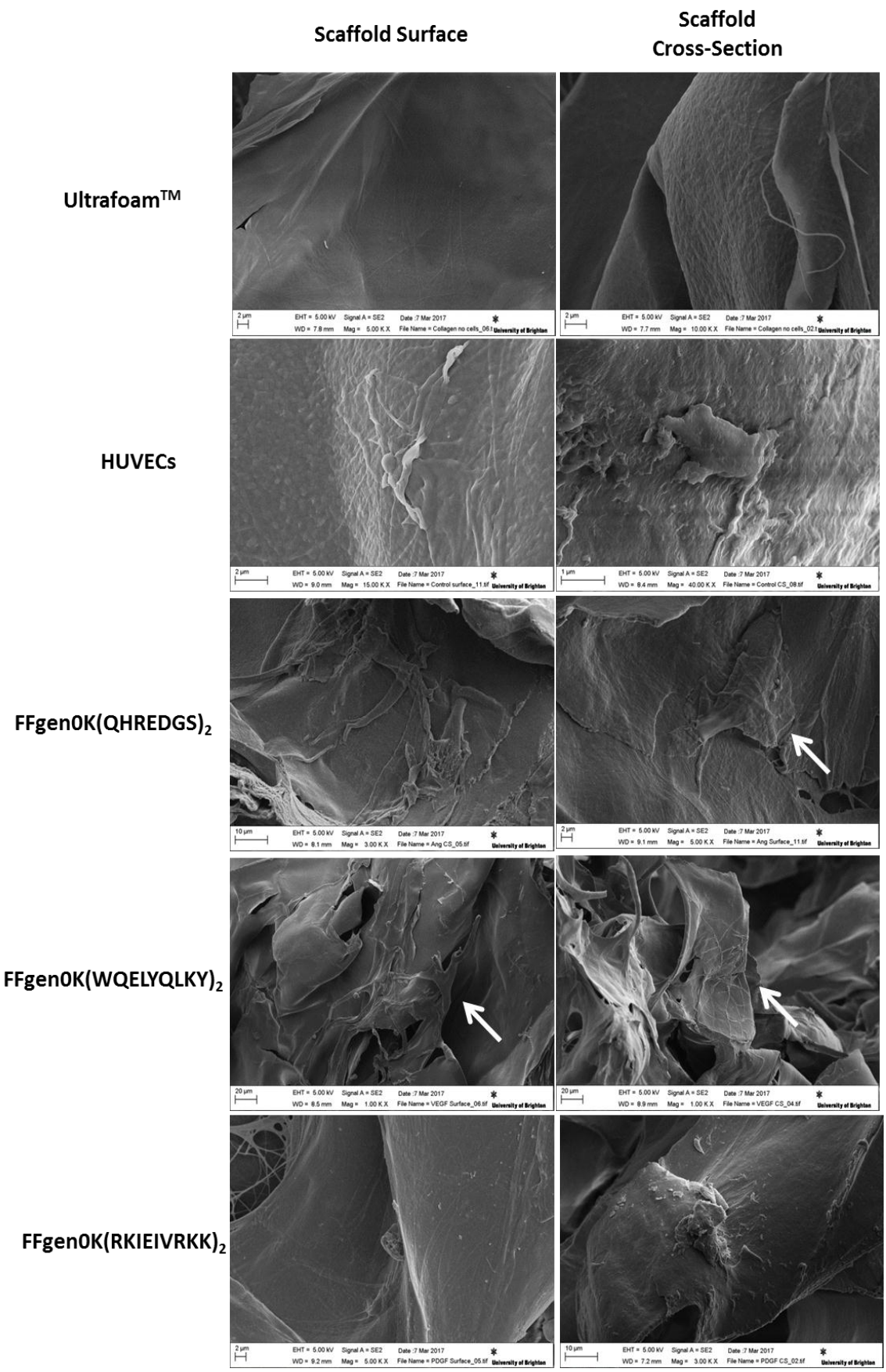

Fig. 6.1 Evaluation of the sprouting potential of dendritic angiogenic peptides on HUVECs when seeded on Ultrafoam™ scaffold after 6 days of incubation.Arrows highlighted those pictures where vessel-like structure are observed.

6.3.3.2 Immunofluorescence of HUVECs on Ultrafoam™ scaffold functionalised with dendritic angiogenic peptides

Results obtained with SEM analysis were confirmed by the Immunofluorescence of CD31 and by Rhodamine-Phalloidin staining. Slides where taken from the middle region of the scaffold as shown in Fig. 6.2.

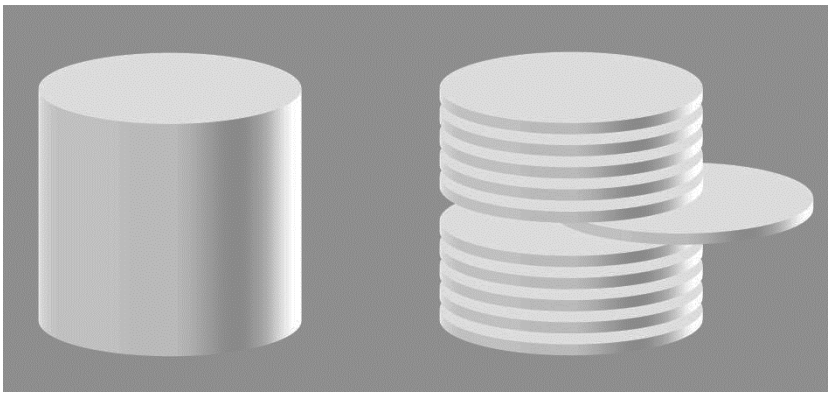

Fig. 6.2 schematic procedure of slicing Ultrafoam™ patch into 6µm section: slices coming from the middle zone were analysed.

Indeed, Fig. 6.3 reports images taken with the confocal microscope highlighting the influence that dendritic angiogenic peptides have on HUVECs. The spatial organisation that HUVECs acquire when seeded on scaffold functionalised with FFgen0K$(WQELYQLKY)_2$ is striking: cells organised themselves in a vessel-like network, where the correspondence between phalloidin staining and CD31 expression is higher, meaning that dendritic angiogenic peptide potentially induce interconnection between HUVECs leading to the formation of a network of endothelial sprouting. The same result can be found also when HUVECs are treated with FFgen0K$(QHREDGS)_2$ as a further confirmation of the angiogenic potential of dendritic angiogenic peptides.

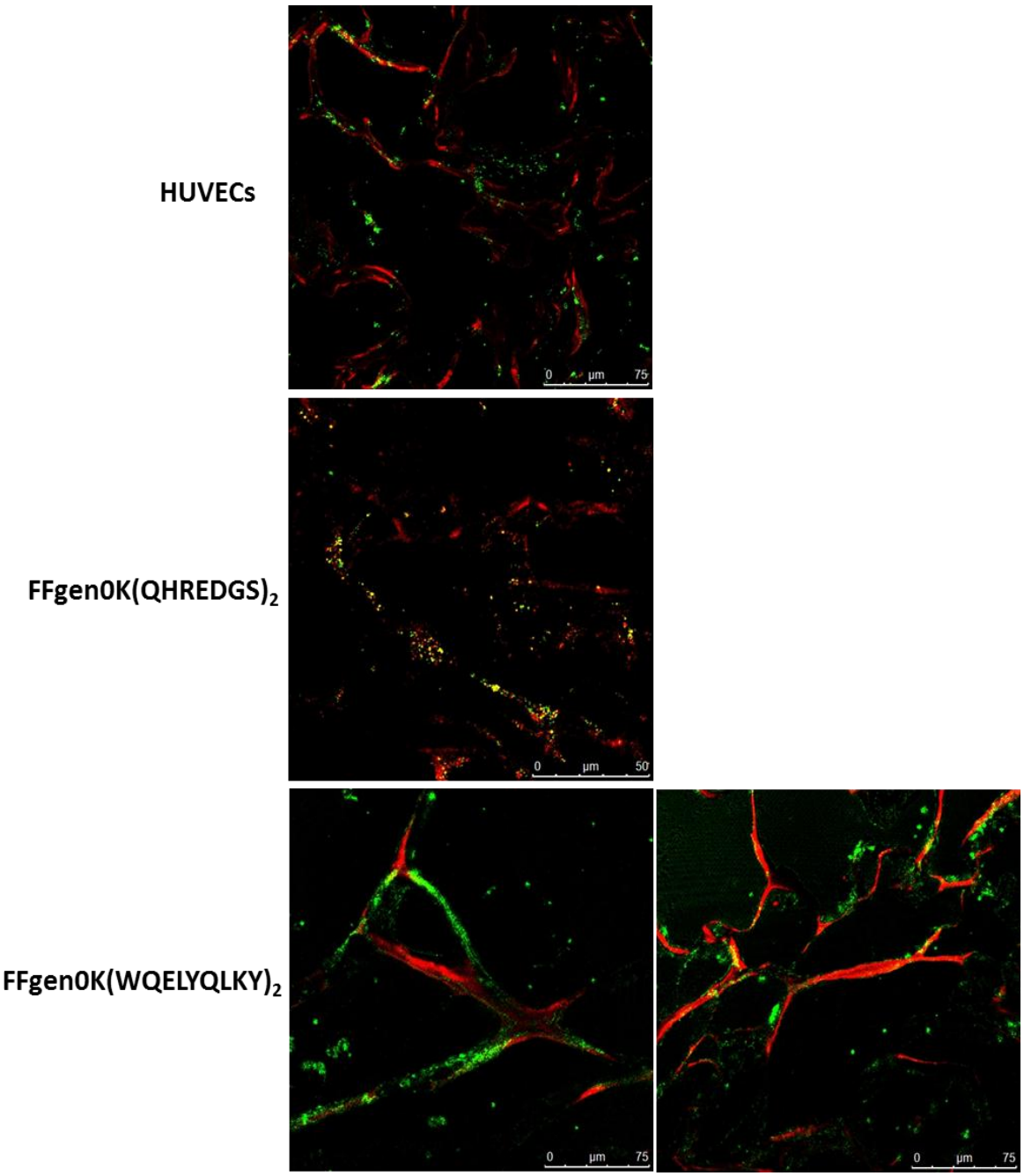

Fig. 6.3 Sprouting Effects of dendritic angiogenic peptides on HUVECs stained with CD31 antibody and Rhodamine-Phalloidin where it is possible to observe a potential network of endothelial sprouting especially when ultrafoam scaffold is functionalised with FFgen0K(WQELYQLKY)$_2$.

6.4 DISCUSSION

Both injectable materials and patches have been widely used *in vitro* to assess their potential in the treatment of MI injury. In this project only Ultrafoam™ functionalised with dendritic angiogenic peptides has been used to treat HUVECs. This choice has been made for various reasons. Firstly, the chemistry and the functionalisation procedure behind the production of Ultrafoam™ scaffold functionalised with dendritic angiogenic peptides and collagen type I beads functionalised with dendritic angiogenic peptides were the same: the starting material was for both of the devices collagen type I even if in different formulations; dendritic angiogenic peptides were designed and synthesised in the same way for both scaffold and beads and the covalent chemical reaction to bind dendritic angiogenic peptides to the materials (carbodiimide reaction) was exactly the same. Secondly, there were experimental limits linked to the *in vitro* test of collagen type I beads functionalised with dendritic angiogenic peptides with HUVECs: when the cells suspension was added, beads started to float making impossible the control over the experimental procedure and consequently its characterisation.

Therefore, the main hypothesis behind the development of this chapter was to verify if it is possible to improve a commercially-available biomaterial with dendritic angiogenic peptide in order to enhance its angiogenesis potential *in vitro* in the view of its use as a cardiac patch for MI injury repair.

Ultrafoam™ scaffold have been seeded with HUVECs and incubated for 6 days in order to see if any structure resembling a sprouting process could be observed. The results obtained with SEM morphological analysis indicated that scaffold functionalised with dendritic angiogenic peptides clearly enhance the formation of elongated structures, that are vessel-like structures similar to those observed at the beginning of a sprouting process. These structures were not observed in control Ultrafoam™ scaffolds where a good adhesion of cells was not followed by their organisation into vessel-like structures. Moreover, HUVECs penetrated inside the scaffold, as the SEM cross-section images suggest, proving that the porosity of the scaffold was encouraging cell penetration and was not affected by the chemical modification performed to couple the angiogenic peptides to its surface. SEM morphological analysis were corroborated by the results obtained by immunofluorescence and morphological analysis of HUVECs. CD31-positive cells organised themselves in a network of endothelial sprouting, developing elongated structure that looks like a vessel-shaped structure. The sprouting process of HUVECs clearly started and was enhanced by the presence of the dendritic angiogenic peptides. These results were confirmed by the

expression of CD31 protein, while phalloidin stained the overall cytoskeleton, allowing the determination of the CD31 marker location in proximity of the cell-to-cell contacts. This results suggest that dendritic angiogenic peptides aid angiogenesis *in vitro* giving a precise signalling to the HUVECs that, in response, organised themselves in tubular–like structures. This outcome was not found when Ultrafoam^{TM} alone was seeded with HUVECs indicating that the angiogenic potential of the tested dendritic angiogenic peptides is significant and can really be considered for future treatments of MI injury.

The achievement of such results was unexpected. Indeed, if the outcome obtained from dendritic angiogenic peptides used as "free drugs" could be expected (results showed in Chapter 5) because of their mimicking role of growth factors acting as soluble molecules (Reis, 2013), the results obtained from dendritic angiogenic peptides grafted on Ultrafoam^{TM} scaffold are surprising. This means that even when dendritic angiogenic peptides are grafted onto biomaterials they preserve their bioactivity making their own bioavailability accessible to cells receptors. Moreover, dendritic angiogenic peptides organisation on the biomaterial creates the perfect stimulating environment to enhance angiogenesis. This could be stimulated also by the changed topography of the modified scaffolds that appeared to be relatively rougher than the control material.

From the beginning of this experimental work was clearly stated that the presentation of this new molecules to the biological environment was essential to induce a specific response on HUVECs. Indeed, when dendritic angiogenic peptides are used as functionalisation moieties on injectable materials (beads) and on cardiac patches (Ultrafoam^{TM} scaffold) they are likely to assemble on the materials in a different way as shown in Fig. 6.4, but in both cases the dendritic angiogenic peptides covers all the surfaces with a correct orientation maximising the ordered presentation of the biocues.

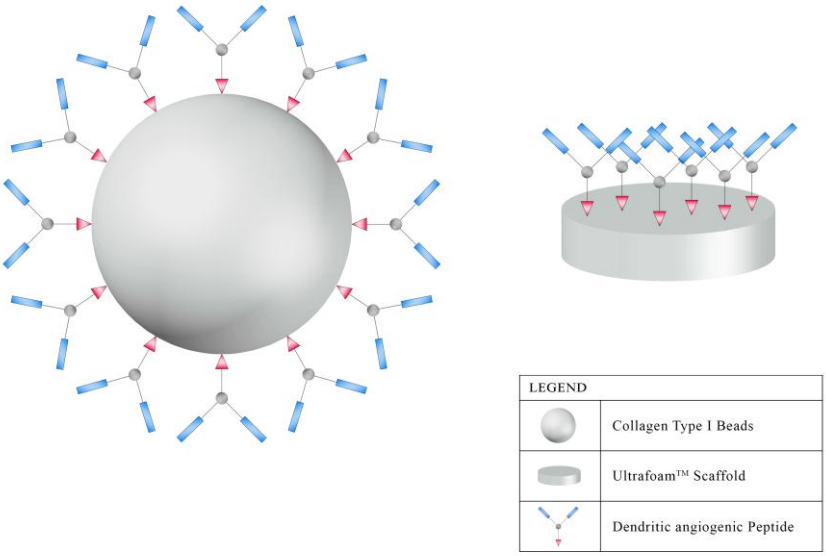

Fig. 6.4. Graphical representation of the spatial orientation of dendritic angiogenic peptides when used to functionalised collagen type I beads and Ultrafoam^{TM} scaffold.

Results obtained in this part of the project highlight how the efficacy of dendritic angiogenic peptides presentation could be enhanced by "3D patterning" of the moieties on scaffold (Lee, 2010). Most probably, the spatial orientation of dendritic angiogenic peptides used to functionalise Ultrafoam^{TM} scaffold induces a specific response by the HUVECs that enter a sprouting process to organise themselves in tube-like structures.

6.5 CONCLUSION

In conclusion it is possible to state that:

1) Ultrafoam^{TM} scaffold angiogenic potential has been enhanced by the presence of dendritic angiogenic peptides *in vitro*.
2) HUVECs organised themselves in a network of endothelial cell tubes that is the typical consequence of an active sprouting process
3) Although no experiment has been performed with linear peptides, the spatial orientation acquired by the relevant sequences when integrated in dendritic macromolecules appears to be crucial to dictate cell behaviour.

This chapter has presented a novel biomaterial-based approach to stimulate angiogenesis through nano-structured biomaterials emphasising the need for a finely spaced presentation of the relevant biocues in combination with optimal porosity to obtain endothelial sprouting throughout the implanted cardiac patch.

7. DISCUSSION AND FUTURE WORK

7.1 OVERALL DISCUSSION

Ischemia of the myocardium can be pharmaceutically treated by inducing the revascularisation of tissue through the formation of new blood vessels from the existing vasculature, a process known as angiogenesis (Ahrendt, 1998). Therapeutic angiogenesis takes advantage of specific biomolecules that have angiogenic potential (typical growth factors such as VEGF, Ang-1 and PDGF-BB) to enhance the formation of new blood vessels in the damaged tissue and support the viability and physiological function of the myocardium not yet compromised by necrosis. There are many problems related with the use of these particular angiogenic growth factors and they include: (i) targeting and controlled release of the specific biomolecules to the damaged tissue, (ii) susceptibility to denaturation both under storage and *in vivo* as well as bioavailability, (ii) adequate tissue retention in the damaged tissue (Post, 2001). Therefore, the use of peptide analogues able to mimic the behaviour and the function of the whole growth factor has been gaining interest as a suitable therapeutic approach, particularly due to their batch-to-batch reproducibility and costs of manufacturing. They have been proposed as therapeutics in several clinical applications, including bone regeneration, cancer therapy and ischemic disease treatments (Post, 2011). However, the use of peptide analogues is not free from drawbacks, related to their storage conditions (i.e. refrigeration), limited *in vivo* half-life and like for natural growth factors, lack of specific targeting and controlled release in the tissue (Miklas, 2012). Indeed, there is the need for new formulations that could provide conformational stability to bioactive peptides, improve their retention in the body and make them more efficacious in terms of activation of specific cell pathways of tissue regeneration; biomolecules of this kind have not yet been reported in literature.

Based on the previous considerations, the rationale behind this project was to pave the way towards novel angiogenic biomaterials by designing and producing novel synthetic morphogens capable of guiding angiogenesis in the tissue affected by ischemia. In the first place, it is important to state that from the very beginning of the project the main goal was focused on the need to find an alternative feasible solution to the treatments of myocardium ischemic disease, able to overcome the limits found in current care and, above all, pave the way to a new field of research for the treatment of this widespread disease.

Therefore, the first novelty of this project was the synthesis of short amino acid sequences, known to have a bioactivity analogue to that of specific growth factors involved in the angiogenesis process, into a hyperbranched peptide molecular scaffold capable of:

1. stabilising their structure

2. presenting them to cells in a spacely-ordered and high density manner
3. favouring their retention within the target tissue through a specific hydrophobic interactions when used as soluble molecules
4. Make them suitable as surface functionalisation moieties of conventional biomaterials to make them acquiring new tissue integration properties through specific biointeractions.

These peptide analogues are capable of exerting a bioactivity similar to that of the natural growth factors and, moreover, they are less susceptible to conformational changes, they have an inherent biocompatibility and biodegradability and finally they have higher affinity/specificity to the target tissue when compared to the whole growth factor molecule (Miklas, 2012).

As mentioned above, another novelty of this project is in the use of a system, a so-called protein scaffold (Meikle, 2011), capable of enhancing the stability of peptide analogues, enhancing their bioactivity and improving their controlled delivery. One of these systems are the dendrons; they have the great potential of stabilising the bioactive peptide sequence and give it precise spatial orientation as they mimic the secondary structure of natural proteins (Grayson, 2001) and they offer the opportunity of controlling the clustering of the relative cell receptors (Perugini, 2018), the local density of the bioactive molecules as well as the retention within the targeted tissue~~,~~ through the exposure of ECM-anchoring moieties.

In this work, a manual SPPS protocol was used to synthesise *ad hoc*-designed dendrons presenting peptide sequences with known angiogenic properties. The successful synthesis of dendrons, linear peptide sequences and dendritic angiogenic peptide analogues was a crucial step in the project. Indeed, this method fulfills the need to achieve precise nanoscale structures and chemical properties. Even if incomplete reactions, side products, steric hindrance and long reaction time could result from using the SPPS method, this method offers the possibility of building successfully synthesised linear or branched molecules with high reproducibility, a feature of significant commercial value. Indeed, a manual SPPS method allows the production of various batches simultaneously resulting in a time-effective manufacturing process, direct control over all the reaction steps and reproducibility. Moreover, the great potential of the SPPS method is that it permits most types of molecular design, thus it is possible to produce molecules with a high level of specificity for the final clinical application: a fundamental requirement for an application such as ischemia that was the focus of this project. A first attempt to scale up the SPPS

method, remaining however within the context of experimental research, is in the use of a manifold device able to house multiple syringes for the SPPS method, where synthesis of different molecules can be driven forward simultaneously. The use of the manifold represents a step forward in the scaled-up synthesis of the dendrimeric analogues for future commercial production.

Preclinical and clinical studies of "therapeutic angiogenesis", defined as the treatment of helping the body conduct its natural purpose of creating a vascular structure from an existing one, have pointed out the need for the continued delivery of low doses of angiogenic moieties to produce functional vasculature at the target site (Zisch, 2003). This requirement is possible only when angiogenic molecules are presented by a specific structure capable of increasing the retention time at the disease sites in order to enhance their bioactivity to a target region and ruling out the occurrence of angiogenesis in other tissues. Different poly (ε-lysine) dendrons have been designed in this project to target specifically cells relevant to the process of angiogenesis in ischemic tissues and ability to be retained by them for longer periods of. Firstly, the root was designed to expose di-phenylalanine residues capable of interacting with the tissue ECM (Mann, 1989). As ECM has a fundamental role in the earliest events that characterise the interaction between synthetic molecules and host tissue (Daley, 2008), the production of molecules able to interact with this structure have great potential. Secondly, as the peripheral dendron surface allows the attachment of any kind of moieties it can act as a platform to present specific physiochemical and biological cues. Indeed, in this project, dendrons were used as protein scaffolds to expose bioactive linear angiogenic peptides capable of inducing a precise biological response on targeting cells. Moreover, it is a great challenge to create a system capable of releasing angiogenic activity in tune with the real healing process because the quantity and kinetics of the release must be synchronised with cell demand and response at the disease treatment site (Zisch, 2003). Dendritic angiogenic peptides thus have been created in order to maximise the interaction between the growth factor analogue and their receptors as it occurs for natural growth factors. This means that FFgen0K has been synthesised to provide bulk support to VEGF and PDGF-BB peptide analogues because FFgen0K exposes two amino groups that can be functionalised with the relative growth factor analogues and can enhance interaction with their relative receptors through their dimerisation within the cell membrane (Ferrara, 2003). Regarding the exposure of the Ang-1 peptide analogue, a different approach was adopted as the Tie-2, Ang-1 receptor, does not dimerise. Therefore, different dendron generations (FFgen0K, FFgen1K and FFgen2K) were functionalised to present the Ang-1 peptide analogue to the cells at different degrees

of local density and spacing. Keeping in mind all the above-mentioned considerations that lead to the final design of the dendritic angiogenic peptides, it was possible to move ahead and characterise the newly produced molecules.

Methods used for the characterisation of dendritic angiogenic peptides in each step of the production process (HPLC, MS, FT-IR, SEM) are reliable and well established methods for peptides and dendrimers (Islam, 2005; Wysocki, 2005). For this reason, throughout the development of the project, characterisation methods able to return unequivocal and reliable results that could support the experimental process step by step were used. This guaranteed a degree of purity of the bioactive peptides (> 95%) acceptable for future clinical use. Moreover, it is important to highlight that throughout the experimental process the characterisation data of the dendritic angiogenic peptides were obtained from different techniques all in agreement with each other and therefore potentially adoptable as quality controls of future manufacturing processes. In this project, this robust characterisation was the starting point for a reliable assessment of dendritic angiogenic peptides by *in vitro* studies.

Therefore, dendritic angiogenic peptides were used as "free drugs" on HUVECs: FFgen0K$(QHREDGS)_2$, FFgen0K$(WQELYQLKY)_2$ and FFgen0K$(RKIEIVRKK)_2$ were spiked on cells in an *in vitro* 2D model, respectively. At the same time, their testing on fibroblasts, cells that have no specific receptors for the relative growth factors, had the dual benefit of showing both their cytotoxicity thresholds and of representing a negative control to prove their biospecific action on HUVECs.

The use of these new molecules highlighted, at the same time, how the combination of a structure capable of presenting and supporting bioactive analouges and peptide sequences capable of mimicking the functions of growth factor creates a favourable environment for the regeneration of blood vessel in a ischemic tissue such as the damaged myocardium. In fact, problems found in literature regarding the direct use of growth factors and problems such as control over their denaturation, variable shelf-life, inactivation or blocking of the active sites due to covalent of physical binding (Miklas, 2013), were not observed during the assessment of poly (ϵ-lysine) dendrons as protein scaffolds for the spaced exposure of angiogenic bioactive peptides. Indeed, the results collected during the *in vitro* 2D tests have shown thatthe molecules produced do not create cytotoxicity issues when in contact with cells, as demonstrated by the tests carried out on 3T3 Fibroblast and more importantly, how they are able to drive cellular behaviour when spiked on HUVECs.

From a literature review, it is possible to summarise VEGF and Ang-1 as the two main growth factors involved in the angiogenesis process, capable of triggering the cascade that

lead to the formation of new blood vessels, enhance cell survival and preserve endothelial cell functionality, respectively (Reis, 2012; Porter, 2010). Results collected during the *in vitro* studies with dendritic angiogenic peptides confirm what has been reported in literature: VEGF and Ang-1 mimicking peptides are able to induce a specific response on HUVECs, resulting in the formation of structures that can be referred to a sprouting process, even if they are just linear amino acid sequences. Those results would not have been achieved without the use of poly (ϵ-lysine) dendrons as protein scaffolds because the use of just linear peptides would not have enabled the formation of new vessels in a precise tissue area, due to the lack of a supporting structure capable of immobilising the peptide and addressing it to the precise targeted tissue (Chapter 5, Section 5.3.2.3). Moreover, to ensure the precise regeneration of the tissue it is important to take the retention capacity and the concentration of the molecule in the tissue that needs to be treated into consideration. The retention capacity and the concentration should not be too short, as the bioactive signal would not be sufficient to induce a cellular response, nor too long because it would create an undesired reaction, such as the formation of abnormal vessels (Ferrara, 1999). Therefore, the choice to create branched structures able to mimic the natural interaction as much as possible between the growth factor and receptor to have the best response from cells becomes obvious. In this way, issues such as the saturation of the binding site generated by high exposure and concentration or the relevant steric effect capable of preventing interaction between dendritic angiogenic peptides and HUVECs (Reis, 2011) were not detected.

The assessment of the angiogenic potential of poly (ϵ-lysine) dendrons as protein scaffolds for the spaced exposure of angiogenic bioactive peptides in a 2D culture model *in vitro* unveil the potential of dendritic angiogenic peptides to induce precise responses on HUVECs and in particular, points out the importance of the role of each part of the molecules and that without the combination of the dendron with the linear angiogenic peptide analogue, it would not have been possible to achieve the same biological effects.

Dendritic angiogenic peptides can be used not only as soluble drugs but also as functionalisation moieties for both injectable materials and patches. Cardiac patches are used in situations where tissue regeneration needs to be supported by a microenvironment and architecture able to promote cellular differentiation, organisation and to prevent anoikis (Sarig, 2011). Even if these medical devices require a more invasive surgical procedure than ~~the~~ injectable biomaterials, they are necessary in clinical conditions where spontaneous healing is not achievable. Collagen type I biomaterial used in this project can be processed either as porous scaffolds that provide mechanical support or as beads for

injection (Zisch, 2003). Regardless of the collagen type I formulation, this material provides suitable features to present dendritic angiogenic peptides to the surrounding tissue aiming at the formation of new blood vessels. Moreover, the functionalisation of Ultrafoam^{TM} scaffolds with short peptides, in particular with the dendritic angiogenic peptides of this project, provides higher stability to conformational changes, control over surface density and peptide orientation that is more favourable for ligand–receptor interaction and cell adhesion (Chung, 2007). In the present dissertation, reference has often been made to the use of peptide analogues to overcome problems related to the use of whole growth factors, at the same time brought other disadvantages: including, among others, short *in vivo* lifespan. When growth factors or peptide analogues are used as functionalisation moieties for scaffolds, the scaffolds need to be modified grafting docking sites for the growth factors. For instance, scaffolds could be pre-treated with heparin in order to enhance the release of bFGF, being molecules with high affinity (Yoon, 2006). Another study demonstrated how functionalisation with a polydopamine (pDA) layer onto the polymer scaffolds enhances the immobilisation of peptides derived from an osteogenic growth factor via catechol chemistry for bone regeneration (Ko, 2013).

Therefore, it is necessary to underline how, in this project, results collected from an analysis of HUVECs seeded onto an Ultrafoam^{TM} scaffold functionalised with dendritic angiogenic peptides were obtained creating a simple peptide bond between the active amino groups exposed by the scaffold and the carboxyl root group of dendritic angiogenic peptides. This method, for the production of this novel biomaterial, proved to be a great advantage in terms of timesaving, production costs and general industrial feasibility. Moreover, the peptide bond that immobilise dendritic angiogenic peptides onto Ultrafoam^{TM} scaffolds gives also the certainty that dendritic angiogenic peptides are exposed in a precise manner to HUVECs because of the spaced distance between dendrimeric branches. It can also be speculated that the rotational limit of the peptide bond contributes to a specific spatial orientation of the dendritic angiogenic peptide and thus a specific presentation to cells (Fig.7.1).

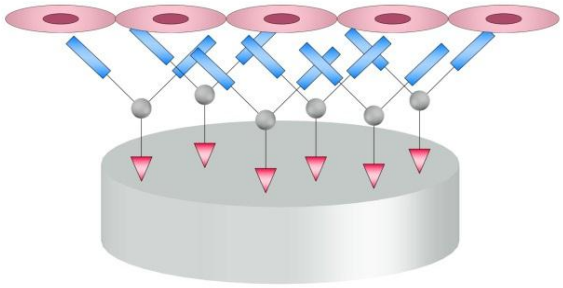

Fig.7.1 Schematic representation of the first interaction between an Ultrafoam^{TM} scaffold functionalised with dendritic angiogenic peptides and HUVECs.

When then dendritic angiogenic peptides are used as functionalisation moieties, it becomes clear how important the spatial presentation of these dendritic angiogenic peptides to HUVECs is. As a matter of fact, dendritic angiogenic peptides preserve their bioactivity even if they are covalently attached to a scaffold, creating a new potential set of different applications.

In conclusion, it can be stated that dendritic angiogenic peptides induce angiogenesis *in vitro* when used as both free drugs and as functionalisation moieties. Moreover, the results collected during this experimental study suggests a novel biomaterial-based approach to stimulate angiogenesis through nano-structured biomaterials and emphasises the need for a finely spaced presentation of the relevant peptide sequence to obtain established endothelial sprouting.

7.2 FUTURE WORK

The present project, as has been proven by the results collected and presented in this thesis, has been able to move a step forward in the development of synthetic, highly-efficient morphogens for guided angiogenesis. Surely, a lot more could be done in improving this particular method of treatment for the regeneration of myocardium after an ischemic event. The peculiarity of the synthesis method of dendrons and consequently dendritic angiogenic peptides makes the production of such molecules on a large scale possible, keeping in mind a future inclusion on the market as a pharmaceutical product. Considering the commercial aspect of the matter, it is important to investigate the most adequate method of administration of these dendritic angiogenic peptides when used as soluble drugs. The oral administration of this drug is not suitable due to the physicochemical properties of the dendritic angiogenic peptides: size, short half-life and enzymatic degradation added to aggregation behaviour, adsorption and denaturation make this method of administration unreliable for patients (Patole, 2008). Other routes of administration have been tested in order to allow the drug to move directly into the systemic circulatory system thus bypassing the gastrointestinal tract where the drug would be easily metabolised but plasma protease could lead to the same degradation (Soltero, 2000). In contrast with the two above-mentioned methods there are local administration and intramuscular/intravenous injection. Studies in animal models have demonstrated the feasibility of these two methods, especially for the delivery of VEGF (Talwar, 2014; Venugopal, 2001; Rane, 2001). For the dendrimers here produced, the most suitable administration route would be a local injection of either the free molecules of proven bioactivity or as molecules grafted to injectable micro-beads.

The difficulties observed in setting a valuable in vitro model for the assessment of the collagen type I bead bioactivity prevented the study of this second formulation. A specific in vitro model should be developed to overcome the limitations of a conventional cell culture method by entrapping the beads in a hydrogel mimicking the natural tissue. For instance, collagen type I beads, non-functionalised and functionalised with dendritic angiogenic peptides could be entrapped in a Matrigel matrix that could be further seeded with HUVECs to assess their migration towards the beads. Using this system, it might also be possible to perform degradation studies where the real potential of dendritic angiogenic peptides could emerge.

After the assessment of the beads' angiogenic potential, a combined use of both a scaffold and beads could be a possibility: scaffold functionalised with dendritic angiogenic peptides

would be used as support for the tissue growth whereas collagen type I beads could be injected at different stages of the regeneration process, mimicking the angiogenesis process through time as well. Indeed, better knowledge of the various steps of the angiogenesis process and the specific growth factors involved would allow the participation of complementary factors capable of ensuring sprouting and the final maturation of the newly formed vessel network.
Finally, the validation of the technology should undergo *in vivo* studies in recognised animal models for cardiac ischaemia (Sarig, 2011).

At the conclusion of this thesis, it is clear that a lot more could be done to regenerate myocardium after an ischemic event but is equally clear how this project has moved the experimental knowledge on the use of synthetic peptides in regenerative medicine forward, disclosing future prospects of dendritic angiogenic peptides used as a realistic and effective treatment for the regeneration of myocardium.

REFERENCES

Ahmed, Z., & Bicknell, R. (2009). Angiogenesis Protocols, *467*. https://doi.org/10.1007/978-1-59745-241-0

Ahrendt, G, Chickering, DE, Ranieri, JP. Angiogenic growth factors: a review for tissue engineering. Tissue Eng.1998; 2: 117–30

Allen, G. C., Sorbello, F., Altavilla, C., Castorina, A., & Ciliberto, E. (2005). Macro-, micro- and nano-investigations on 3-aminopropyltrimethoxysilane self-assembly-monolayers. *Thin Solid Films*, *483*(1–2), 306–311. https://doi.org/10.1016/j.tsf.2004.12.062

Annesley, T. M. (2003). Ion suppression in mass spectrometry. *Clinical Chemistry*, *49*(7), 1041–1044. https://doi.org/10.1373/49.7.1041

Asahara, T., Murohara, T., Sullivan, A., Silver, M., Van Der Zee, R., Li, T., … Isner, J. M. (1997). Isolation of putative progenitor endothelial cells for angiogenesis. *Science*, *275*(5302), 964–967. https://doi.org/10.1126/science.275.5302.964

Bacakova, L., Filova, E., Parizek, M., Ruml, T., & Svorcik, V. (2011). Modulation of cell adhesion, proliferation and differentiation on materials designed for body implants. *Biotechnology Advances*, *29*(6), 739–767. https://doi.org/10.1016/j.biotechadv.2011.06.004

Bell, B. F., Schuler, M., Tosatti, S., Textor, M., Schwartz, Z., & Boyan, B. D. (2011). Osteoblast response to titanium surfaces functionalized with extracellular matrix peptide biomimetics. *Clinical Oral Implants Research*, *22*(8), 865–872. https://doi.org/10.1111/j.1600-0501.2010.02074.x

Bettinger, C. J., Langer, R., & Borenstein, J. T. (2009). Engineering substrate topography at the Micro- and nanoscale to control cell function. *Angewandte Chemie - International Edition*, *48*(30), 5406–5415. https://doi.org/10.1002/anie.200805179

Bird, I. N., Taylor, V., Newton, J. P., Spragg, J. H., Simmons, D. L., Salmon, M., & Buckley, C. D. (1999). Homophilic PECAM-1(CD31) interactions prevent endothelial cell apoptosis but do not support cell spreading or migration. *Journal of Cell Science*, *112 (Pt 1*, 1989–1997.

Blaker, J. J., Knowles, J. C., & Day, R. M. (2008). Novel fabrication techniques to produce microspheres by thermally induced phase separation for tissue engineering and drug delivery. *Acta Biomaterialia*, *4*(2), 264–272. https://doi.org/10.1016/j.actbio.2007.09.011

Blumenthal, J. A., Sherwood, A., Babyak, M. A., Watkins, L. L., Smith, P. J., Hoffman, B. M., … Hinderliter, A. L. (2012). Exercise and pharmacological treatment of depressive symptoms in patients with coronary heart disease: Results from the UPBEAT (understanding the prognostic benefits of exercise and antidepressant therapy) study. *Journal of the American College of Cardiology*, *60*(12), 1053–1063. https://doi.org/10.1016/j.jacc.2012.04.040

Bosman, A. W., Janssen, H. M., & Meijer, E. W. (1999). About Dendrimers : Structure , Physical Properties , and Applications. https://doi.org/10.1021/cr970069y

Bosshardt, D. D., & Sculean, A. (2009). Does periodontal tissue regeneration really work? *Periodontol 2000*, *51*(ii), 208–219. https://doi.org/PRD317 [pii]\n10.1111/j.1600-0757.2009.00317.x

Boyan, B. D., Hummert, T. W., Dean, D. D., & Schwartz, Z. (1996). Role of material surfaces in regulating bone and cartilage cell response. *Biomaterials*, *17*(2), 137–146. Retrieved from http://www.ncbi.nlm.nih.gov/pubmed/8624390

Bracci, L., Falciani, C., Lelli, B., Lozzi, L., Runci, Y., Pini, A., … Neri, P. (2003). Synthetic Peptides in the Form of Dendrimers Become Resistant to Protease Activity. *Journal of Biological Chemistry*, *278*(47), 46590–46595. https://doi.org/10.1074/jbc.M308615200

Brinker, C. J., Frye, G. C., Hurd, A. J., Ashley, C. S., Laboratories, S. N., & Introduction, I. (1991). 97 f u n d a m e n t a l s of s o l - g e l dip coating, *201*, 97–108.

Brown, W. H., & Foote, C. S. (2002). Organic chemistry. Forth Worth: Harcourt College Publishers

Cao, L., & Mooney, D. J. (2007). Spatiotemporal control over growth factor signaling for therapeutic neovascularization. *Advanced Drug Delivery Reviews*, *59*(13), 1340–1350. https://doi.org/10.1016/j.addr.2007.08.012

Carmeliet, P. (2003). Angiogenesis in Health and Disease : Therapeutic Opportunities. *Nature Medicine*, *9*(6), 653–660. https://doi.org/10.1038/nm0603-653

Carraro, A., Flaibani, M., Ph, D., Cillo, U., Michelotto, L., Sc, D., … Zavan, B. (2010). A Combining Method to Enhance the In Vitro Differentiation of Hepatic Precursor Cells. *Tissue Engineering Part C*, *0*(0), 1–10. https://doi.org/10.1089/ten.tec.2009.0795

Ceylan, H., Kocabey, S., Tekinay, A. B., & Guler, M. O. (2012). Surface-adhesive and osteogenic self-assembled peptide nanofibers for bioinspired functionalization of titanium surfaces. *Soft Matter*, *8*(14), 3929. https://doi.org/10.1039/c2sm25127b

Chachques, J. C., Trainini, J. C., Lago, N., Herreros, J., Schussler, O., & Carpentier, A. F. (2010). Myocardial Assistance by Grafting a New Upgraded bioartificial Myocardium (MAGNUM Trial): Clinical results at 2 years. *European Heart Journal*, *13*, S48. https://doi.org/10.1016/j.athoracsur.2007.10.052

Chan, B. P., Hui, T. Y., Yeung, C. W., Li, J., Mo, I., & Chan, G. C. F. (2007). Self-assembled collagen-human mesenchymal stem cell microspheres for regenerative medicine. *Biomaterials*, *28*(31), 4652–4666. https://doi.org/10.1016/j.biomaterials.2007.07.041

Chang, C. W., Petrie, T., Clark, A., Lin, X., Sondergaard, C. S., & Griffiths, L. G. (2016). Mesenchymal stem cell seeding of porcine small intestinal submucosal extracellular matrix for cardiovascular applications. *PLoS ONE*, *11*(4), 1–19. https://doi.org/10.1371/journal.pone.0153412

Chen, R. R., Silva, E. A., Yuen, W. W., Brock, A. A., Fischbach, C., Lin, A. S., … Mooney, D. J. (2007). Integrated approach to designing growth factor delivery systems. *The FASEB Journal*, *21*(14), 3896–3903. https://doi.org/10.1096/fj.06-7873com

Christman, K. L., & Lee, R. J. (2006). Biomaterials for the Treatment of Myocardial Infarction. *Journal of the American College of Cardiology*, *48*(5), 907–913. https://doi.org/10.1016/j.jacc.2006.06.005

Chrobak, M. O., Hansen, K. J., Gershlak, J. R., Vratsanos, M., Kanellias, M., Gaudette, G. R., & Pins, G. D. (2017). Design of a Fibrin Microthread-Based Composite Layer for Use in a Cardiac Patch. *ACS Biomaterials Science and Engineering*, *3*(7), 1394–1403. https://doi.org/10.1021/acsbiomaterials.6b00547

Chung, H. J., & Park, T. G. (2007). Surface engineered and drug releasing pre-fabricated scaffolds for tissue engineering. *Advanced Drug Delivery Reviews*, *59*(4–5), 249–262. https://doi.org/10.1016/j.addr.2007.03.015

Clapp, C., Thebault, S., Jeziorski, M. C., & Martinez De La Escalera, G. (2009). Peptide Hormone Regulation of Angiogenesis. *Physiological Reviews*, *89*(4), 1177–1215. https://doi.org/10.1152/physrev.00024.2009.

Cloninger, M. J. (2002). Biological applications of dendrimers, (Figure 2), 742–748.

Cook, a D., Hrkach, J. S., Gao, N. N., Johnson, I. M., Pajvani, U. B., Cannizzaro, S. M., & Langer, R. (1997). Characterization and development of RGD-peptide-modified poly(lactic acid-co-lysine) as an interactive, resorbable biomaterial. *Journal of Biomedical Materials Research*, *35*(4), 513–523. Retrieved from http://www.ncbi.nlm.nih.gov/pubmed/9189829

Coradin, T., Boissière, M., & Livage, J. (2006). Sol-gel chemistry in medicinal science. *Current Medicinal Chemistry*, *13*(1), 99–108. Retrieved from http://www.ncbi.nlm.nih.gov/pubmed/16457642

Crampton, H. L., & Simanek, E. E. (2007). Dendrimers as drug delivery vehicles: non-covalent interactions of bioactive compounds with dendrimers. *Polymer International*, *56*(4), 489–496. https://doi.org/10.1002/pi.2230

D'Amore, A., Yoshizumi, T., Luketich, S. K., Wolf, M. T., Gu, X., Cammarata, M., … Wagner, W. R. (2016). Bi-layered polyurethane – Extracellular matrix cardiac patch improves ischemic ventricular wall remodeling in a rat model. *Biomaterials*, *107*, 1–14. https://doi.org/10.1016/j.biomaterials.2016.07.039

D'Andrea, L. D., Iaccarino, G., Fattorusso, R., Sorriento, D., Carannante, C., Capasso, D., … Pedone, C. (2005). Targeting angiogenesis: Structural characterization and biological properties of a de novo engineered VEGF mimicking peptide. *Proceedings of the National Academy of Sciences*, *102*(40), 14215–14220. https://doi.org/10.1073/pnas.0505047102

Dai, Z., Ronholm, J., Tian, Y., Sethi, B., & Cao, X. (2016). Sterilization techniques for biodegradable scaffolds in tissue engineering applications. *Journal of Tissue Engineering*, *7*, 204173141664881. https://doi.org/10.1177/2041731416648810

Daley, W. P., Peters, S. B., & Larsen, M. (2008). Extracellular matrix dynamics in development and regenerative medicine. *Journal of Cell Science*, *121*(Pt 3), 255–264. https://doi.org/10.1242/jcs.006064

Dallabrida, S. M. (2005). Angiopoietin-1 Promotes Cardiac and Skeletal Myocyte Survival Through Integrins. *Circulation Research*, *96*(4), e8–e24. https://doi.org/10.1161/01.RES.0000158285.57191.60

Dangas, G. D., Farkouh, M. E., Sleeper, L. A., Yang, M., Schoos, M. M., Macaya, C., … Fuster, V. (2014). Long-term outcome of PCI versus CABG in insulin and non-insulin-treated diabetic patients: Results from the FREEDOM trial. *Journal of the American College of Cardiology*, *64*(12), 1189–1197. https://doi.org/10.1016/j.jacc.2014.06.1182

De Campos, A. M., Sanchez, A., & Alonso, M. J. (2001). Chitosan nanoparticles: a new vehicle for the improvement of the delivery of drugs to the ocular surface. Application to cyclosporin A. *International Journal of Pharmaceutics*, *224*(1–2), 159–168. https://doi.org/10.1016/S0378-5173(01)00760-8

Deligianni, D. D., Katsala, N., Ladas, S., Sotiropoulou, D., Amedee, J., & Missirlis, Y. F. (2001). Effect of surface roughness of the titanium alloy Ti-6Al-4V on human bone marrow cell response and on protein adsorption. *Biomaterials*, *22*(11), 1241–1251. Retrieved from http://www.ncbi.nlm.nih.gov/pubmed/11336296

Des Rieux, A., Ucakar, B., Mupendwa, B. P. K., Colau, D., Feron, O., Carmeliet, P., & Préat, V. (2011). 3D systems delivering VEGF to promote angiogenesis for tissue engineering. *Journal of Controlled Release*, *150*(3), 272–278. https://doi.org/10.1016/j.jconrel.2010.11.028

Esfand, R., & Tomalia, D. a. (2001). Poly(amidoamine) (PAMAM) dendrimers: from biomimicry to drug delivery and biomedical applications. *Drug Discovery Today*, *6*(8), 427–436. Retrieved from http://www.ncbi.nlm.nih.gov/pubmed/11301287

European Cardiovascular Disease Statistics. (2012).

Explorer, I., & Lioy, A. (2008). Un po’ di storia. *Informatica*, 1–8.

Ferrara, N., & Kerbel, R. S. (2005). Angiogenesis as a therapeutic target. *Nature*, *438*(7070), 967–974. https://doi.org/10.1038/nature04483

Ferrara, N., Gerber, H. P., & LeCouter, J. (2003). The biology of VEGF and its receptors. *Nat Med*, *9*(6), 669–676. https://doi.org/10.1038/nm0603-669

Ferris, D. M., Moodie, G. D., Dimond, P. M., Gioranni, C. W., Ehrlich, M. G., & Valentini, R. F. (1999). RGD-coated titanium implants stimulate increased bone formation in vivo. *Biomaterials*, *20*(23–24), 2323–2331. Retrieved from http://www.ncbi.nlm.nih.gov/pubmed/10614938

Folkman, J., & D’Amore, P. A. (1996). Blood vessel formation: What is its molecular basis? *Cell*, *87*(7), 1153–1155. https://doi.org/10.1016/S0092-8674(00)81810-3

Forget, G., Latxague, L., Héroguez, V., Labrugère, C., & Durrieu, M. C. (2007). RGD nanodomains grafting onto titanium surface. *Conference Proceedings : ... Annual International Conference of the IEEE Engineering in Medicine and Biology Society. IEEE Engineering in Medicine and Biology Society. Conference*, *2007*, 5107–5110. https://doi.org/10.1109/IEMBS.2007.4353489

Galli, C., Piemontese, M., Meikle, S. T., Santin, M., Macaluso, G. M., & Passeri, G. (2012). Biomimetic coating with phosphoserine-tethered poly(epsilon-lysine) dendrons on titanium surfaces enhances Wnt and osteoblastic differentiation. *Clinical Oral Implants Research*, 1–7. https://doi.org/10.1111/clr.12075

Gamble, J. R., Drew, J., Trezise, L., Underwood, A., Parsons, M., Kasminkas, L., … Vadas, M. A. (2016). Cell Junctions.

Garcia, a. J., & Reyes, C. D. (2005). Bio-adhesive Surfaces to Promote Osteoblast Differentiation and Bone Formation. *Journal of Dental Research*, *84*(5), 407–413. https://doi.org/10.1177/154405910508400502

García, J. R., Clark, A. Y., & García, A. J. (2016). Integrin-specific hydrogels functionalized with VEGF for vascularization and bone regeneration of critical-size bone defects. *Journal of Biomedical Materials Research - Part A*, *104*(4), 889–900. https://doi.org/10.1002/jbm.a.35626

Gautam, S., Chou, C. F., Dinda, A. K., Potdar, P. D., & Mishra, N. C. (2014). Surface modification of nanofibrous polycaprolactone/gelatin composite scaffold by collagen type i grafting for skin tissue engineering. *Materials Science and Engineering C*, *34*(1), 402–409. https://doi.org/10.1016/j.msec.2013.09.043

Graf, J., Ogle, R. C., Robey, F. a, Sasaki, M., Martin, G. R., Yamada, Y., & Kleinman, H. K. (1987). A pentapeptide from the laminin B1 chain mediates cell adhesion and binds the 67,000 laminin receptor. *Biochemistry*, *26*(22), 6896–6900. Retrieved from http://www.ncbi.nlm.nih.gov/pubmed/2962631

Grant, D. S., Kinsella, J. L., Fridman, R., Auerbach, R., Piasecki, B. A., Yamada, Y., … Kleinman, H. K. (1992). Interaction of Endothelial-Cells With a Laminin-a Chain Peptide (Sikvav) Invitro and Induction of Angiogenic Behavior Invivo. *Journal of Cellular Physiology*, *153*(3), 614–625. https://doi.org/10.1002/jcp.1041530324

Grayson, S. M., & Fréchet, J. M. J. (2001). Convergent dendrons and dendrimers: From synthesis to applications. *Chemical Reviews*, *101*(12), 3819–3867. https://doi.org/10.1021/cr990116h

Grover, G. N., & Christman, K. L. (2016). Injectable Hydrogels for Cardiac Tissue Regeneration Post-Myocardial Infarction. *Injectable Hydrogels for Regenerative Engineering*, 377–414. https://doi.org/10.1142/9781783267477_0010

Gurunathan, S., Han, J. W., Dayem, A. A., Eppakayala, V., & Kim, J. H. (2012). Oxidative stress-mediated antibacterial activity of graphene oxide and reduced graphene oxide in Pseudomonas aeruginosa. *International Journal of Nanomedicine*, *7*, 5901–5914. https://doi.org/10.2147/IJN.S37397

Haddow, D. B., Hadfield, S. R., Street, M., & Crescent, C. (1996). Characterization of sol-gel surfaces for biomedical applications, *7*, 255–260.

Harbers, G. M., & Healy, K. E. (2005). The effect of ligand type and density on osteoblast adhesion , proliferation , and matrix mineralization. https://doi.org/10.1002/jbm.a.30482

Haris, P. I., & Severcan, F. (1999). FTIR spectroscopic characterization of protein structure in aqueous and non-aqueous media. *Journal of Molecular Catalysis - B Enzymatic*, *7*(1–4), 207–221. https://doi.org/10.1016/S1381-1177(99)00030-2

Helm, G. a, & Gazit, Z. (2005). Future uses of mesenchymal stem cells in spine surgery. *Neurosurgical Focus*, *19*(6), E13. https://doi.org/190613 [pii]

Hendriks, J., Riesle, J., & Blitterswijk, C. A. van. (2010). Co-culture in cartilage tissue engineering. *Journal of Tissue Engineering and Regenerative Medicine*, *4*(7), 524–531. https://doi.org/10.1002/term

Hill, E., Boontheekul, T., & Mooney, D. J. (2006). Regulating activation of transplanted cells controls tissue regeneration. *Proceedings of the National Academy of Sciences*, *103*(8), 2494–2499. https://doi.org/10.1073/pnas.0506004103

Hoffman, A. S. (1999). Non-Fouling Surface Technologies. *Journal of Biomaterials Science, Polymer Edition*, *10*(10), 1011–1014. https://doi.org/10.1163/156856299X00658

Huang, Y., Shan, J., Wang, C., Ma, J., Li, D., Li, L., … Li, Y. (2009). Can ischemic preconditioning alone really protect organs from ischemia reperfusion injury in transplantation. *Transplant Immunology*, *20*(3), 127–131. https://doi.org/10.1016/j.trim.2008.08.002

Hulkower, K. I., & Herber, R. L. (2011). Cell migration and invasion assays as tools for drug discovery. *Pharmaceutics*, *3*(1), 107–124. https://doi.org/10.3390/pharmaceutics3010107

Jamadi, E. S., Ghasemi-Mobarakeh, L., Morshed, M., Sadeghi, M., Prabhakaran, M. P., & Ramakrishna, S. (2016). Synthesis of polyester urethane urea and fabrication of elastomeric nanofibrous scaffolds for myocardial regeneration. *Materials Science and Engineering C*, *63*, 106–116. https://doi.org/10.1016/j.msec.2016.02.051

Jang, W., Selim, K. M. K., Lee, C., & Kang, I. (2009). Progress in Polymer Science Bioinspired application of dendrimers : From bio-mimicry to biomedical applications, *34*, 1–23. https://doi.org/10.1016/j.progpolymsci.2008.08.003

Jiang, G., Wang, L., & Chen, W. (2007). Studies on the preparation and characterization of gold nanoparticles protected by dendrons. *Materials Letters*, *61*(1), 278–283. https://doi.org/10.1016/j.matlet.2006.04.110

Jones, S. P., Gabrielson, N. P., Wong, C., Chow, H., Pack, D. W., Posocco, P., … Smith, D. K. (2011). Hydrophobically modified dendrons: Developing structure - Activity relationships for DNA binding and gene transfection. *Molecular Pharmaceutics*, *8*(2), 416–429.

Kaihara, S., Borenstein, J., Koka, R., Lalan, S., Ochoa, E. R., Ravens, M., … Vacanti, J. P. (2000). Silicon micromachining to tissue engineer branched vascular channels for liver fabrication. *Tissue Engineering*, *6*(2), 105–117. https://doi.org/10.1089/107632700320739

Kankuri, E., Cholujova, D., Comajova, M., Vaheri, A., & Bizik, J. (2005). Induction of hepatocyte growth factor/scatter factor by fibroblast clustering directly promotes tumor cell invasiveness. *Cancer Research*, *65*(21), 9914–9922. https://doi.org/10.1158/0008-5472.CAN-05-1559

Kantchev, E. A. B., Chang, C.-C., Cheng, S.-F., Roche, A.-C., & Chang, D.-K. (2008). Direct solid-phase synthesis and fluorescence labeling of large, monodisperse mannosylated dendrons in a peptide synthesizer. *Organic & Biomolecular Chemistry*, *6*(8), 1377–1385. https://doi.org/10.1039/b719737c

Karuppuswamy, P., Venugopal, J. R., Navaneethan, B., Laiva, A. L., Sridhar, S., & Ramakrishna, S. (2014). Functionalized hybrid nanofibers to mimic native ECM for tissue engineering applications. *Applied Surface Science*, *322*, 162–168. https://doi.org/10.1016/j.apsusc.2014.10.074

Keshaw, H., Georgiou, G., Blaker, J. J., Forbes, A., Knowles, J. C., & Day, R. M. (2009). Assessment of Polymer/Bioactive Glass-Composite Microporous Spheres for Tissue Regeneration Applications. *Tissue Engineering Part A*, *15*(7), 1451–1461. https://doi.org/10.1089/ten.tea.2008.0203

Keshaw, H., Thapar, N., Burns, A. J., Mordan, N., Knowles, J. C., Forbes, A., & Day, R. M. (2010). Microporous collagen spheres produced via thermally induced phase separation for tissue regeneration. *Acta Biomaterialia*, *6*(3), 1158–1166. https://doi.org/10.1016/j.actbio.2009.08.044

Kim, H.-W., Gu, H.-J., & Lee, H.-H. (2007). Microspheres of collagen-apatite nanocomposites with osteogenic potential for tissue engineering. *Tissue Engineering*, *13*(5), 965–973. https://doi.org/10.1089/ten.2006.0299

Kim, J.-H., Kushiro, K., Graham, N. a, & Asthagiri, A. R. (2009). Tunable interplay between epidermal growth factor and cell-cell contact governs the spatial dynamics of epithelial growth. *Proceedings of the National Academy of Sciences of the United States of America*, *106*(27), 11149–11153. https://doi.org/10.1073/pnas.0812651106

Kong, J., & Yu, S. (2007). Fourier transform infrared spectroscopic analysis of protein secondary structures. *Acta Biochimica et Biophysica Sinica*, *39*(8), 549–559. https://doi.org/10.1111/j.1745-7270.2007.00320.x

Kostiainen, M. A., Szilvay, G. R., Smith, D. K., Linder, M. B., & Ikkala, O. (2006). Multivalent dendrons for high-affinity adhesion of proteins to DNA. *Angewandte Chemie - International Edition*, *45*(21), 3538–3542. https://doi.org/10.1002/anie.200504540

Langer, R., & Tirrell, D. A. (2004). Designing materials for biology and medicine. *Nature*, *428*(6982), 487–492. https://doi.org/10.1038/nature02388

Lee, C. C., MacKay, J. a, Fréchet, J. M. J., & Szoka, F. C. (2005). Designing dendrimers for biological applications. *Nature Biotechnology*, *23*(12), 1517–1526. https://doi.org/10.1038/nbt1171

Lee, K., Silva, E. A., & Mooney, D. J. (2011). Growth factor delivery-based tissue engineering: general approaches and a review of recent developments. *Journal of The Royal Society Interface*, *8*(55), 153–170. https://doi.org/10.1098/rsif.2010.0223

Lee, M. S., Ahmad, T., Lee, J., Awada, H. K., Wang, Y., Kim, K., … Yang, H. S. (2017). Dual delivery of growth factors with coacervate-coated poly(lactic-co-glycolic acid) nanofiber improves neovascularization in a mouse skin flap model. *Biomaterials*, *124*, 65–77. https://doi.org/10.1016/j.biomaterials.2017.01.036

Lee, M. S., Park, H. S., Lee, B. C., Jung, J. H., Yoo, J. S., & Kim, S. E. (2016). Identification of Angiogenesis Rich-Viable Myocardium using RGD Dimer based SPECT after Myocardial Infarction. *Scientific Reports*, *6*(November 2015), 1–10. https://doi.org/10.1038/srep27520

Leslie-Barbick, J. E., Saik, J. E., Gould, D. J., Dickinson, M. E., & West, J. L. (2011). The promotion of microvasculature formation in poly(ethylene glycol) diacrylate hydrogels by an immobilized VEGF-mimetic peptide. *Biomaterials*, *32*(25), 5782–5789. https://doi.org/10.1016/j.biomaterials.2011.04.060

Li, X.-C., Wu, Y.-H., Bai, X.-D., Ji, W., Guo, Z.-M., Wang, C.-F., … Ruan, D. (2016). BMP7-Based Functionalized Self-Assembling Peptides Protect Nucleus Pulposus-Derived Stem Cells From Apoptosis *In Vitro*. *Tissue Engineering Part A*, *22*(19–20), 1218–1228. https://doi.org/10.1089/ten.tea.2016.0230

Lin, C. C., & Anseth, K. S. (2009). Controlling affinity binding with peptide-functionalized poly(ethylene glycol) hydrogels. *Advanced Functional Materials*, *19*(14), 2325–2331. https://doi.org/10.1002/adfm.200900107

Linkermann, A., Brasen, J. H., Darding, M., Jin, M. K., Sanz, A. B., Heller, J.-O., … Krautwald, S. (2013). Two independent pathways of regulated necrosis mediate ischemia-reperfusion injury. *Proceedings of the National Academy of Sciences*, *110*(29), 12024–12029. https://doi.org/10.1073/pnas.1305538110

Littauer, U. Z. (1998). Involvement of the YIGSR sequence of laminin in protein tyrosine phosphorylation, *424*, 243–247.

Liu, X., Chu, P., & Ding, C. (2004). Surface modification of titanium, titanium alloys, and related materials for biomedical applications. *Materials Science and Engineering: R: Reports*, *47*(3–4), 49–121. https://doi.org/10.1016/j.mser.2004.11.001

Mahla, E., Suarez, T. A., Bliden, K. P., Rehak, P., Metzler, H., Sequeira, A. J., … Gurbel, P. A. (2012). Platelet function measurement-based strategy to reduce bleeding and waiting time in clopidogrel-treated patients undergoing coronary artery bypass graft surgery: The timing based on platelet function strategy to reduce clopidogrel-associated bleeding rela. *Circulation: Cardiovascular Interventions*, *5*(2), 261–269. https://doi.org/10.1161/CIRCINTERVENTIONS.111.967208

Mahoney, W. C., & Hermodson, M. A. (1980). Separation of large denatured peptides by reverse phase high performance liquid chromatography. Trifluoroacetic acid as a peptide solvent. *Journal of Biological Chemistry*, *255*(23), 11199–11203.

Malinda, K. M., Nomizu, M., Chung, M., Delgado, M., Kuratomi, Y., Yamada, Y., … Ponce, M. L. (1999). Identification of laminin alpha1 and beta1 chain peptides active for endothelial cell adhesion, tube formation, and aortic sprouting. *FASEB Journal : Official Publication of the Federation of American Societies for Experimental Biology*, *13*(1), 53–62. Retrieved from http://www.ncbi.nlm.nih.gov/pubmed/9872929

Mann, D. L., Kent, R. L., & Iv, G. C. (2015). by Cellular Deformation.

Massiaso, S. P., & Hubbelloli, J. A. (1992). Immobilized Amines and Basic Amino Acids as Mimetic Heparin- binding Domains for Cell Surface Proteoglycan-mediated Adhesion *, *267*(14), 10133–10141.

Matthews, J. A., Wnek, G. E., Simpson, D. G., & Bowlin, G. L. (2002). Electrospinning of collagen nanofibers. *Biomacromolecules*, *3*(2), 232–238. https://doi.org/10.1021/bm015533u

Medina, S. H., & El-Sayed, M. E. H. (2009). Dendrimers as carriers for delivery of chemotherapeutic agents. *Chemical Reviews*, *109*(7), 3141–3157. https://doi.org/10.1021/cr900174j

Meikle, S. T., Bianchi, G., Olivier, G., & Santin, M. (2013). Osteoconductive phosphoserine-modified poly({varepsilon}-lysine) dendrons: synthesis, titanium oxide surface functionalization and response of osteoblast-like cell lines. *Journal of the Royal Society, Interface / the Royal Society*, *10*(79), 20120765. https://doi.org/10.1098/rsif.2012.0765

Meikle, S. T., Perugini, V., Guildford, A. L., & Santin, M. (2011). Synthesis, characterisation and in vitro anti-angiogenic potential of dendron VEGF blockers. *Macromolecular Bioscience*, *11*(12), 1761–1765. https://doi.org/10.1002/mabi.201100267

Mitchell, W. J., Ferguson, A. J., Kose, M. E., Rupert, B. L., Ginley, D. S., Rumbles, G., … Kopidakis, N. (2009). Structure-dependent photophysics of first-generation phenyl-cored thiophene dendrimers. *Chemistry of Materials*, *21*(2), 287–297. https://doi.org/10.1021/cm802410d

Miyata T., Namiki S., inventors; Koken Co., Ltd., assignee. Substrate consisting of regenerated collagen fibrils and method of manufacturing same United States patent US4565580 A. 21 Jen 1986.

Moheini, A. A., Cimmino, A., Dal, G., Biase, M. Di, Evidente, A., Lavermicocca, P., … Malinconico, M. (2018). Effect of pH and TPP concentration on chemico-physical properties, release kinetics and antifungal activity of Chitosan-TPP-Ungeremine microbeads. *Carbohydrate Polymers*. https://doi.org/10.1016/j.carbpol.2018.05.005

Molina, C. A., & Saver, J. L. (2005). Extending reperfusion therapy for acute ischemic stroke: Emerging pharmacological, mechanical, and imaging strategies. *Stroke*, *36*(10), 2311–2320. https://doi.org/10.1161/01.STR.0000182100.65262.46

Morrison R.T., Boyd R.N., (1997) Organic chemistry. CEA

Myocardial, E., Project, I., & Miocardico, I. (1995). Reperfusion injury after acute myocardial infarction Racial discri ination in efficine Equityforpatients is unlikely if we don â€™ t treat doctorsfairly, (February).

Nakamura, M., Yamaguchi, K., Mie, M., Nakamura, M., Akita, K., & Kobatake, E. (2009). Promotion of angiogenesis by an artificial extracellular matrix protein containing the laminin-1-derived IKVAV sequence. *Bioconjugate Chemistry*, *20*(9), 1759–1764. https://doi.org/10.1021/bc900126b

Nanci, a, Wuest, J. D., Peru, L., Brunet, P., Sharma, V., Zalzal, S., & McKee, M. D. (1998). Chemical modification of titanium surfaces for covalent attachment of biological molecules. *Journal of Biomedical Materials Research*, *40*(2), 324–335. Retrieved from http://www.ncbi.nlm.nih.gov/pubmed/9549628

Nguyen, H., Nguyen, N. H., Tran, N. Q., & Nguyen, C. K. (2015). Improved Method for Preparing Cisplatin-Dendrimer Nanocomplex and Its Behavior Against NCI-H460 Lung Cancer Cell. *Journal of Nanoscience and Nanotechnology*, *15*, 4106–4110. https://doi.org/10.1166/jnn.2015.9808

Novosel, E. C., Kleinhans, C., & Kluger, P. J. (2011). Vascularization is the key challenge in tissue engineering. *Advanced Drug Delivery Reviews*, *63*(4), 300–311. https://doi.org/10.1016/j.addr.2011.03.004

O'Neill, H. S., O'Sullivan, J., Porteous, N., Ruiz-Hernandez, E., Kelly, H. M., O'Brien, F. J., & Duffy, G. P. (2018). A collagen cardiac patch incorporating alginate microparticles permits the controlled release of hepatocyte growth factor and insulin-like growth factor-1 to enhance cardiac stem cell migration and proliferation. *Journal of Tissue Engineering and Regenerative Medicine*, *12*(1), e384–e394. https://doi.org/10.1002/term.2392

Önder, Ö. C., Yilgör, E., & Yilgör, I. (2016). Fabrication of rigid poly(lactic acid) foams via thermally induced phase separation. *Polymer (United Kingdom)*, *107*, 240–248. https://doi.org/10.1016/j.polymer.2016.11.025

Papadimitriou, S., Bikiaris, D., Avgoustakis, K., Karavas, E., & Georgarakis, M. (2008). Chitosan nanoparticles loaded with dorzolamide and pramipexole. *Carbohydrate Polymers*, *73*(1), 44–54. https://doi.org/10.1016/j.carbpol.2007.11.007

Park, H., Radisic, M., Lim, J. O., Chang, B. H., & Vunjak-Novakovic, G. (2005). A novel composite scaffold for cardiac tissue engineering. *In Vitro Cellular & Developmental Biology. Animal*, *41*(7), 188–196. https://doi.org/10.1290/0411071.1

Parody, R., Rabella, N., Martino, R., Otegui, M., del Cuerpo, M., Coll, P., & Sierra, J. (2007). Upper and lower respiratory tract infections by human enterovirus and rhinovirus in adult patients with hematological malignancies. *American Journal of Hematology*, *82*(9), 807–811. https://doi.org/10.1002/ajh

Perugini, V., Meikle, S. T., Guildford, A. L., & Santin, M. (2017). Hyperbranched poly(ϵ-lysine) substrate presenting the laminin sequence YIGSR induces the formation of

spheroids in adult bone marrow stem cells. *PLoS ONE*, *12*(12), 1–19. https://doi.org/10.1371/journal.pone.0187182

Petty, J. D., Huckins, J. N., & David, A. (2002). (12) Patent Application Publication (10) Pub . No .: US 2002/0187020 A1, *1*(19).

Phelps, E. A., Templeman, K. L., Thulé, P. M., & García, A. J. (2015). Engineered VEGF-releasing PEG–MAL hydrogel for pancreatic islet vascularization. *Drug Delivery and Translational Research*, *5*(2), 125–136. https://doi.org/10.1007/s13346-013-0142-2

Pierdomenico, S. D., Lapenna, D., Bucci, A., Di Tommaso, R., Di Mascio, R., Manente, B. M., … Mezzetti, A. (2005). Cardiovascular outcome in treated hypertensive patients with responder, masked, false resistant, and true resistant hypertension. *American Journal of Hypertension*, *18*(11), 1422–1428. https://doi.org/10.1016/j.amjhyper.2005.05.014

Pittenger, M. F., & Martin, B. J. (2004). Mesenchymal stem cells and their potential as cardiac therapeutics. *Circulation Research*, *95*(1), 9–20. https://doi.org/10.1161/01.RES.0000135902.99383.6f

Ponce, M. L. (2009). Angiogenesis Protocols, *467*, 183–188. https://doi.org/10.1007/978-1-59745-241-0

Porté-Durrieu, M. C., Labrugère, C., Villars, F., Lefebvre, F., Dutoya, S., Guette, a, … Baquey, C. (1999). Development of RGD peptides grafted onto silica surfaces: XPS characterization and human endothelial cell interactions. *Journal of Biomedical Materials Research*, *46*(3), 368–375. Retrieved from http://www.ncbi.nlm.nih.gov/pubmed/10397994

Pozzobon, M., Bollini, S., Iop, L., De Gaspari, P., Chiavegato, A., Rossi, C. A., … De Coppi, P. (2010). Human bone marrow-derived CD133+cells delivered to a collagen patch on cryoinjured rat heart promote angiogenesis and arteriogenesis. *Cell Transplantation*, *19*(10), 1247–1260. https://doi.org/10.3727/096368910X505864

Radin, S., Ducheyne, P., Kamplain, T., & Tan, B. H. (2001). Silica sol-gel for the controlled release of antibiotics. I. Synthesis, characterization, and in vitro release. *Journal of Biomedical Materials Research*, *57*(2), 313–320. Retrieved from http://www.ncbi.nlm.nih.gov/pubmed/11484196

Radisic, M., Euloth, M., Yang, L., Langer, R., Freed, L. E., & Vunjak-Novakovic, G. (2003). High-density seeding of myocyte cells for cardiac tissue engineering. *Biotechnology and Bioengineering*, *82*(4), 403–414. https://doi.org/10.1002/bit.10594

Rezania, a, & Healy, K. E. (1999). Integrin subunits responsible for adhesion of human osteoblast-like cells to biomimetic peptide surfaces. *Journal of Orthopaedic Research : Official Publication of the Orthopaedic Research Society*, *17*(4), 615–623. https://doi.org/10.1002/jor.1100170423

Rezania, A., Johnson, R., Lefkow, A. R., & Healy, K. E. (2006). Bioactivation of Metal Oxide Surfaces . 1 . Surface Characterization and Cell Response, (12), 6931–6939.

Ruvinov, E., & Cohen, S. (2016). Alginate biomaterial for the treatment of myocardial infarction: Progress, translational strategies, and clinical outlook. From ocean algae to patient bedside. *Advanced Drug Delivery Reviews*, *96*, 54–76. https://doi.org/10.1016/j.addr.2015.04.021

Sadler, K., & Tam, J. P. (2002). Peptide dendrimers: Applications and synthesis. *Reviews in Molecular Biotechnology*, *90*(3–4), 195–229. https://doi.org/10.1016/S1389-0352(01)00061-7

Sakai-Kato, K., & Ishikura, K. (2009). Integration of biomolecules into analytical systems by means of silica sol-gel technology. *Analytical Sciences : The International Journal of the Japan Society for Analytical Chemistry*, *25*(8), 969–978. Retrieved from http://www.ncbi.nlm.nih.gov/pubmed/19667472

Santos, E. M., Radin, S., & Ducheyne, P. (1999). Sol-gel derived carrier for the controlled release of proteins. *Biomaterials*, *20*(18), 1695–1700. Retrieved from http://www.ncbi.nlm.nih.gov/pubmed/10503970

Sarig, U., & Machluf, M. (2011). Engineering cell platforms for myocardial regeneration. *Expert Opinion on Biological Therapy*, *11*(8), 1055–1077. https://doi.org/10.1517/14712598.2011.578574

Sbai, M., Kallel, A., Ben Wafi, S., Ben Halima, M., Soussi, M., Baara, A., … Kaabachi, N. (2017). Paraoxonase 3 (PON3) polymorphisms, haplotypes and risk of myocardial infarction in the Tunisian population. *Archives of Cardiovascular Diseases Supplements*, *9*(1), 98. https://doi.org/10.1016/S1878-6480(17)30293-8

Schelbert, H. R. (2010). Anatomy and physiology of coronary blood flow. *Journal of Nuclear Cardiology*, *17*(4), 545–554. https://doi.org/10.1007/s12350-010-9255-x

Schneiders, W., Reinstorf, A., Pompe, W., Grass, R., Biewener, A., Holch, M., … Rammelt, S. (2007). Effect of modification of hydroxyapatite/collagen composites with sodium citrate, phosphoserine, phosphoserine/RGD-peptide and calcium carbonate on bone remodelling. *Bone*, *40*(4), 1048–1059. https://doi.org/10.1016/j.bone.2006.11.019

Schuler, M., Hamilton, D. W., Kunzler, T. P., Sprecher, C. M., Wild, M. De, Brunette, D. M., … Tosatti, S. G. P. (2009). Comparison of the Response of Cultured Osteoblasts and Osteoblasts Outgrown From Rat Calvarial Bone Chips to Nonfouling KRSR and FHRRIKA-Peptide Modified Rough Titanium Surfaces, 517–527. https://doi.org/10.1002/jbm.b.31425

Schuler, M., Owen, G. R., Hamilton, D. W., de Wild, M., Textor, M., Brunette, D. M., & Tosatti, S. G. P. (2006). Biomimetic modification of titanium dental implant model surfaces using the RGDSP-peptide sequence: a cell morphology study. *Biomaterials*, surgeon. *American Surgeon*, *78*(12), 1305–1321.

Schussler, O., Coirault, C., Louis-Tisserand, M., Al-Chare, W., Oliviero, P., Menard, C., … Lecarpentier, Y. (2009). Use of arginine-glycine-aspartic acid adhesion peptides coupled with a new collagen scaffold to engineer a myocardium-like tissue graft. *Nature Clinical Practice Cardiovascular Medicine*, *6*(3), 240–249. https://doi.org/10.1038/ncpcardio1451

Sell, S. A., McClure, M. J., Garg, K., Wolfe, P. S., & Bowlin, G. L. (2009). Electrospinning of collagen/biopolymers for regenerative medicine and cardiovascular tissue engineering. *Advanced Drug Delivery Reviews*, *61*(12), 1007–1019. https://doi.org/10.1016/j.addr.2009.07.012

Shen, Y. H., Shoichet, M. S., & Radisic, M. (2008). Vascular endothelial growth factor immobilized in collagen scaffold promotes penetration and proliferation of endothelial cells. *Acta Biomaterialia*, *4*(3), 477–489. https://doi.org/10.1016/j.actbio.2007.12.011

Shin, H., Jo, S., & Mikos, A. G. (2003). Biomimetic materials for tissue engineering, *24*, 4353–4364. https://doi.org/10.1016/S0142-9612(03)00339-9

Silva, E. a, & Mooney, D. J. (2007). Spatiotemporal control of vascular endothelial growth factor delivery from injectable hydrogels enhances angiogenesis. *Journal of Thrombosis and Haemostasis : JTH*, *5*(3), 590–598. https://doi.org/10.1111/j.1538-7836.2007.02386.x

Silva, E. A., Kim, E.-S., Kong, H. J., & Mooney, D. J. (2008). Material-based deployment enhances efficacy of endothelial progenitor cells. *Proceedings of the National Academy of Sciences*, *105*(38), 14347–14352. https://doi.org/10.1073/pnas.0803873105

Simon, a, Cohen-Bouhacina, T., Porté, M. C., Aimé, J. P., & Baquey, C. (2002). Study of two grafting methods for obtaining a 3-aminopropyltriethoxysilane monolayer on silica surface. *Journal of Colloid and Interface Science*, *251*(2), 278–283. https://doi.org/10.1006/jcis.2002.8385

Simon-Assmann, P., Orend, G., Mammadova-Bach, E., Spenlé, C., & Lefebvre, O. (2011). Role of laminins in physiological and pathological angiogenesis. *The International Journal of Developmental Biology*, *55*(4–5), 455–465. https://doi.org/10.1387/ijdb.103223ps

Soltero R. NE. The oral delivery of protein and peptide drugs. Innovations Pharm Technol. 2000;12 (3): 106-10

Spiller, K. L., Anfang, R. R., Spiller, K. J., Ng, J., Nakazawa, K. R., Daulton, J. W., & Vunjak-Novakovic, G. (2014). The role of macrophage phenotype in vascularization of tissue engineering scaffolds. *Biomaterials*, *35*(15), 4477–4488. https://doi.org/10.1016/j.biomaterials.2014.02.012

Spotnitz, W. D. (2012). Hemostats, sealants, and adhesives: A practical guide for the

Sugiura, T., Hibino, N., Breuer, C. K., & Shinoka, T. (2016). Tissue-engineered cardiac patch seeded with human induced pluripotent stem cell derived cardiomyocytes promoted the regeneration of host cardiomyocytes in a rat model. *Journal of Cardiothoracic Surgery*, *11*(1), 1–8. https://doi.org/10.1186/s13019-016-0559-z

Suwandi, J. S., Toes, R. E. M., Nikolic, T., & Roep, B. O. (2015). Inducing tissue specific tolerance in autoimmune disease with tolerogenic dendritic cells. *Clinical and Experimental Rheumatology*, *33*(March), 97–103. https://doi.org/10.1002/jbm.a

Svenson, S., & Tomalia, D. a. (2005). Dendrimers in biomedical applications--reflections on the field. *Advanced Drug Delivery Reviews*, *57*(15), 2106–2129. https://doi.org/10.1016/j.addr.2005.09.018

Svenson, S., & Tomalia, D. A. (2012). Dendrimers in biomedical applications-reflections on the field. *Advanced Drug Delivery Reviews*, *64*(SUPPL.), 102–115. https://doi.org/10.1016/j.addr.2012.09.030

Swift, M. R., & Weinstein, B. M. (2009). Arterial-venous specification during development. *Circulation Research*, *104*(5), 576–588. https://doi.org/10.1161/CIRCRESAHA.108.188805

Tao, Z., Chen, B., Tan, X., Zhao, Y., Wang, L., Zhu, T., … Su, H. (2011). Coexpression of VEGF and angiopoietin-1 promotes angiogenesis and cardiomyocyte proliferation reduces apoptosis in porcine myocardial infarction (MI) heart. *Proceedings of the National Academy of Sciences*, *108*(5), 2064–2069. https://doi.org/10.1073/pnas.1018925108

Tímár, J., Döme, B., Fazekas, K., Janovics, Á., & Paku, S. (2001). Angiogenesis-dependent diseases and angiogenesis therapy. *Pathology and Oncology Research*, *7*(2), 85–94. https://doi.org/10.1007/BF03032573

Tomalia, D. A., & Fr??chet, J. M. J. (2002). Discovery of dendrimers and dendritic polymers: A brief historical perspective. *Journal of Polymer Science, Part A: Polymer Chemistry*, *40*(16), 2719–2728. https://doi.org/10.1002/pola.10301

Tomalia, D. a., & Frechet, J. M. J. (2002). Discovery of dendrimers and dendritic polymers: A brief historical perspective. *Journal of Polymer Science Part A: Polymer Chemistry*, *40*(16), 2719–2728. https://doi.org/10.1002/pola.10301

Tomalia, D. A., Baker, H., Dewald, J., Hall, M., Kallos, G., Martin, S., … Smith, P. (1985). A New Class of Polymers: Starburst-Dendritic Macromolecules. *Polymer Journal*, *17*(1), 117–132. https://doi.org/10.1295/polymj.17.117

Tongers, J., Roncalli, J. G., & Losordo, D. W. (2008). Therapeutic angiogenesis for critical limb ischemia: Microvascular therapies coming of age. *Circulation*, *118*(1), 9–16. https://doi.org/10.1161/CIRCULATIONAHA.108.784371

Touzani, R. (2011). Dendrons, dendrimers new materials for environmental and science applications. *Journal of Materials and Environmental Science*, *2*(3), 201–214. https://doi.org/10.4161/onci.23245

Townsend, N., Nichols, M., Scarborough, P., & Rayner, M. (2015). Cardiovascular disease in Europe - Epidemiological update 2015. *European Heart Journal*, *36*(40), 2696–2705. https://doi.org/10.1093/eurheartj/ehv428

Tsiourvas, D., Tsetsekou, a, Arkas, M., Diplas, S., & Mastrogianni, E. (2011). Covalent attachment of a bioactive hyperbranched polymeric layer to titanium surface for the biomimetic growth of calcium phosphates. *Journal of Materials Science. Materials in Medicine*, *22*(1), 85–96. https://doi.org/10.1007/s10856-010-4181-7

Tully, D. C., & Fréchet, J. M. J. (2001). Dendrimers at surfaces and interfaces: chemistry and applications. *Chemical Communications*, *2*(14), 1229–1239. https://doi.org/10.1039/b104290b

V. Patole JS. Protein and Peptide Drug Delivery: Oral Approaches. Indian J Pharm Sci. 2008;70(3):269-77

Vacharathit, V., Silva, E. A., & Mooney, D. J. (2011). Viability and functionality of cells delivered from peptide conjugated scaffolds. *Biomaterials*, *32*(15), 3721–3728. https://doi.org/10.1016/j.biomaterials.2010.12.048

Venugopal, J. R., Prabhakaran, M. P., Mukherjee, S., Ravichandran, R., Dan, K., & Ramakrishna, S. (2012). Biomaterial strategies for alleviation of myocardial infarction. *Journal of The Royal Society Interface*, *9*(66), 1–19. https://doi.org/10.1098/rsif.2011.0301

Verma, S., Fedak, P. W. M., Weisel, R. D., Butany, J., Rao, V., Maitland, A., … Yau, T. M. (2002). Fundamentals of reperfusion injury for the clinical cardiologist. *Circulation*, *105*(20), 2332–2336. https://doi.org/10.1161/01.CIR.0000016602.96363.36

Waddell, T. G., Leyden, D. E., & DeBello, M. T. (1981). The nature of organosilane to silica-surface bonding. *Journal of the American Chemical Society*, *103*(18), 5303–5307. https://doi.org/10.1021/ja00408a005

Walker, J. M. (2009). *Cardiovascular Development Methods in Molecular Biology*. *Life Sciences* (Vol. 531). https://doi.org/10.1007/978-1-62703-239-1_1

Webber, M. J., Appel, E. A., Meijer, E. W., & Langer, R. (2015). Supramolecular biomaterials. *Nature Materials*, *15*(1), 13–26. https://doi.org/10.1038/nmat4474

Webber, M. J., Tongers, J., Newcomb, C. J., Marquardt, K.-T., Bauersachs, J., Losordo, D. W., & Stupp, S. I. (2011). Supramolecular nanostructures that mimic VEGF as a strategy for ischemic tissue repair. *Proceedings of the National Academy of Sciences*, *108*(33), 13438–13443. https://doi.org/10.1073/pnas.1016546108

Wysocki, V. H., Resing, K. a, Zhang, Q., & Cheng, G. (2005). Mass spectrometry of peptides and proteins. *Methods (San Diego, Calif.)*, *35*(3), 211–222. https://doi.org/10.1016/j.ymeth.2004.08.013

Yang, X., Hua, L., Gong, H., & Tan, S. N. (2003). Covalent immobilization of an enzyme (glucose oxidase) onto a carbon sol–gel silicate composite surface as a biosensing platform. *Analytica Chimica Acta*, *478*(1), 67–75. https://doi.org/10.1016/S0003-2670(02)01507-6

Yin Hsu, F., Chueh, S. C., & Jiin Wang, Y. (1999). Microspheres of hydroxyapatite/reconstituted collagen as supports for osteoblast cell growth. *Biomaterials*, *20*(20), 1931–1936. https://doi.org/10.1016/S0142-9612(99)00095-2

Zachary, I., & Morgan, R. D. (2011). Therapeutic angiogenesis for cardiovascular disease: Biological context, challenges, prospects. *Heart*, *97*(3), 181–189. https://doi.org/10.1136/hrt.2009.180414

Zhu, M., Lerum, M. Z., & Chen, W. (2012). How to prepare reproducible, homogeneous, and hydrolytically stable aminosilane-derived layers on silica. *Langmuir : The ACS Journal of Surfaces and Colloids*, *28*(1), 416–423. https://doi.org/10.1021/la203638g

Zisch, A. H., Lutolf, M. P., & Hubbell, J. A. (2003). Biopolymeric delivery matrices for angiogenic growth factors. *Cardiovascular Pathology*, *12*(6), 295–310. https://doi.org/10.1016/S1054-8807(03)00089-9